

**Neotectonic uplift and mountain building
in the Alpine-Himalayan Belt**

V.G. Trifonov, S.Yu. Sokolov and D.M. Bachmanov

The book describes neotectonic uplifts producing mountain building in the Alpine-Himalayan Belt. This process began in the Oligocene as formation of local uplifts in zones of concentration of collision compression and accelerated in the Pliocene and Quaternary as the isostatic effect of decrease of density of the uppermost mantle and the lower crust by partial replacing of the lithospheric mantle by the asthenosphere material and retrograde metamorphism of high-metamorphosed rocks by asthenosphere fluids. These changes were initiated and kept up by the sub-lithosphere upper mantle flows that spread, according to the seismic tomography data, from the Ethiopian-Afar superplume and were enriched by fluids, reworking the transitional mantle layer beneath the future mountain belt. The upper mantle flows not only move lithosphere plates with all plate-tectonic consequences of this process, but also initiate transformations of the lithosphere that results in vertical movements producing mountain building. The book is intended for wide circle of geoscientists.

Keywords: Oligocene to Quaternary, neotectonics, uplift, mountain building, molasses, seismic tomography, lithosphere, asthenosphere, mantle flows

Content

Introduction	5
Part 1. Neotectonic development of the central part of the Alpine-Himalayan Belt ..	9
1.1. Pre-history (<i>V.G. Trifonov</i>)	9
1.2. Neotectonic evolution of the Central Tien Shan (<i>V.G. Trifonov, D.M. Bachmanov</i>)	14
1.2.1. Changes in the regime of vertical movements during the neotectonic evolution	14
1.2.2. Horizontal shortening of the Earth's crust in the Oligocene-Quaternary ...	26
1.2.3. Contribution of compression to crustal thickening and uplift in the Central Tien Shan	31
1.2.4. The rise of the asthenosphere roof beneath the Central Tien Shan	33
1.2.5. Great thickness and density of the Central Tien Shan crust before its Cenozoic compression and possible transformation of the lower crust during the Quaternary uplift	34
1.2.6. Relative significance of different processes producing neotectonic uplift of the Central Tien Shan	35
1.3. Neotectonic evolution of the Pamirs and surrounding (<i>V.G. Trifonov, T.P. Ivanova</i>)	37
1.3.1. Mesozoic zoning and its deformation due to neotectonics	37
1.3.2. The Pamirs and Afghan–Tajik Basin	44
1.3.3. Recent geodynamics of the Pamir–Hindu Kush region	48
1.4. Neotectonic evolution of the Greater Caucasus (<i>V.G. Trifonov</i>)	53
1.5. Evolution of the Alpine-Himalayan Collision Belt in the Oligocene-Quaternary (<i>V.G. Trifonov, T.P. Ivanova, D.M. Bachmanov</i>)	57
1.5.1. Oligocene–Early Miocene (35–17 Ma)	57
1.5.2. Middle Miocene (16–11 Ma)	60
1.5.3. Late Miocene–Early Pliocene (10.0–3.6 Ma)	62
1.5.4. Late Pliocene–Quaternary (the last ~3.6 Ma)	63
1.5.5. Relationships between collision and tectonic uplift producing mountain building	72

1.5.5.1. Methodical Approach	72
1.5.5.2. Mountain building as a result of collision compression	73
1.5.5.3. Pliocene–Quaternary acceleration of tectonic uplift producing mountain building	76
1.5.6. Sources of neotectonic uplift in the Alpine-Himalayan Belt (<i>V.G. Trifonov</i>)	78
Part 2. Results of seismic tomography analysis of the mantle and deep sources of the Pliocene–Quaternary uplift	79
2.1. Seismic tomography profiling of the Alpine-Himalayan Belt (<i>S.Yu. Sokolov</i>)	79
2.2. A model of structural evolution of the mantle beneath the Tethys and Alpine-Himalayan Collision Belt in Mesozoic and Cenozoic and its geological consequences (<i>V.G. Trifonov, S.Yu. Sokolov</i>)	85
2.2.1. Ethiopian-Afar superplume and upper-mantle flows spreading away from it (<i>V.G. Trifonov, S.Yu. Sokolov</i>)	85
2.2.2. Cenozoic volcanism in the northern Arabian Plate and Arabian-Caucasus Segment of the Alpine-Himalayan Belt (<i>V.G. Trifonov, D.M. Bachmanov, T.P. Ivanova</i>)	93
2.2.2.1. Basaltic volcanism in the Arabian Plate	93
2.2.2.2. Correlation of the Cenozoic volcanism in the Arabian Plate and in the Arabian-Caucasus segment of the Alpine-Himalayan Belt	103
2.2.3. Intracontinental mantle seismic-focal zones in the Alpine-Himalayan Belt (<i>V.G. Trifonov, T.P. Ivanova, D.M. Bachmanov</i>)	107
2.2.3.1. The Pamir–Hindu Kush mantle seismic zone	107
2.2.3.2. The Vrancea mantle seismic megafocus	113
2.2.3.3. Origin of mantle seismicity	116
2.3. Plate tectonics and tectonics of mantle flows (<i>V.G. Trifonov, S.Yu. Sokolov</i>)	117
2.3.1. Development of plate tectonic theory	117
2.3.2. Tectonics of mantle flows	120
Conclusion	127
References	130

Introduction

Obruchev (1948), introducing the terms *neotectonics* and *neotectonic* epoch, applied them to the process leading to the formation of the present-day topography that is distinguished by high-mountain systems, which did not exist earlier in the Mesozoic and Cenozoic geological history. In this book, we consider the tectonic movements, which gave rise to the contemporary topography of the central Alpine–Himalayan Orogenic Belt between the Carpathians and Balkan–Aegean region in the west and the Tien Shan, Kunlun, Tibet, and Himalayas in the east (Fig. 1)¹.

In the first part of the book, we describe the history of neotectonic (Oligocene–Quaternary) movements that produced uplift of orogenic structures of the belt. Analyzing neotectonic evolution of the Central Tien Shan, Pamirs, Great Caucasus, and finally the orogenic belt as a whole, we show that their evolution includes two main stages. During the first long-time stage that lasted from Oligocene till the end of Miocene and even Pliocene in some regions, local uplifts formed. They were usually not higher than middle-level mountains (< 1500 m) and formed under collision compression as the results of isostatic compensation of thickening of the Earth's crust in zones of concentrated deformation. During the second Pliocene–Quaternary stage, the height of the mountains increased 2–3 times. This intensification of tectonic uplift producing mountain building can not be explained by effects of the collision compression. It was caused by a decrease in the density of the crust and upper mantle under the effect of the asthenosphere, which was activated by fluids.

The second part of the book is devoted to deep-seated sources of the neotectonic processes mentioned above. The analyzing seismic tomography data demonstrate two important features of the mantle. First, in the eastern (Indonesian) part of the Alpine–Himalayan Belt, where subduction has continued till now, the higher-velocity subducted slabs became approximately horizontal at the depths of about 400–700 km and these sub-horizontal lenses spread beneath the adjacent continental upper mantle. The same continuations of the subducted slabs are known in the North-Western Pacific, where they were termed as stagnant slabs (Fukao et al., 2001), or big mantle wedges (BMW) (Zhao, 2009; Zhao et al., 2010). Second, in the more western mountain part of the Alpine–Himalayan Belt, sub-lithosphere low-velocity (hot and lower-dense) mantle flows were identified. They begin in the Ethiopian–Afar superplume rising from the lower mantle and spread beneath the orogenic belt.

¹ For the sake of brevity, these segments will be called further merely the Alpine–Himalayan Belt.

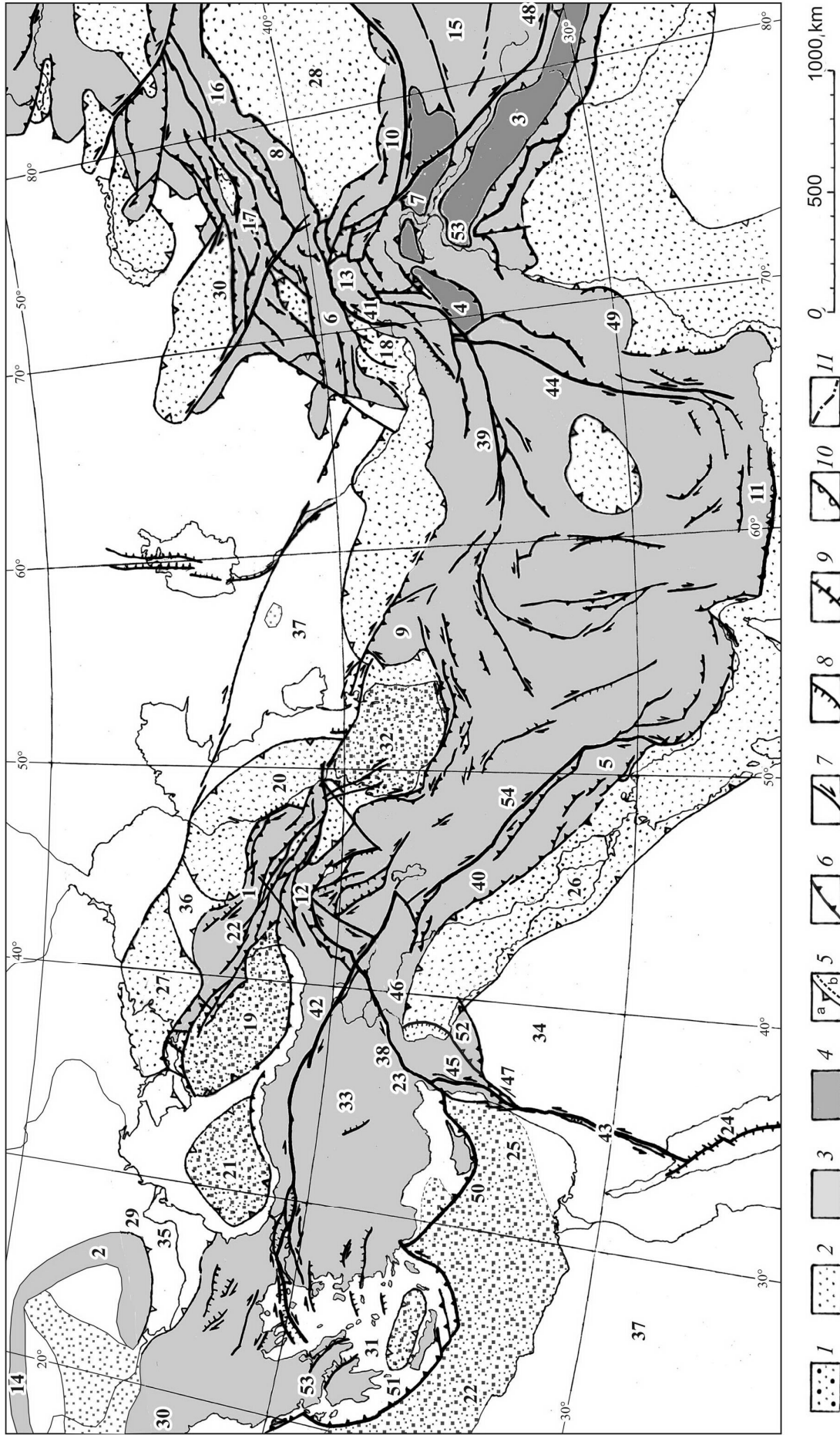


Fig. 1. Pliocene–Quaternary structure of the Alpine-Himalayan Belt from Eastern Mediterranean to Central Asia, modified after (Trifonov et al., 2012₁)
 1, basins with sub-oceanic crust; 2, major basins on continental crust; 3, mountains (in fig. 1) and uplands not higher than 1.5 km (in fig. 16,17, & 18); 4, highest mountains; 5, boundaries of mountains and basins: (a) in fig. 1 and (b) in fig. 16,17, and 18; 6–10, faults (the largest faults are shown by thickened lines in fig. 1); 6, thrust or reverse fault, 7, strike-slip fault, 8, normal fault, 9, extension fault, 10, flexure; 11, the Tesseire-Tornquist lineament (in fig. 16,17, & 18)

We suppose that the elongated Ethiopian-Afar super-plume developed as a more or less stationary structure at least from the end of the Paleozoic. The portions of moving Gondwana, which turned out to lie above the superplume, underwent rifting that developed into spreading that formed the Tethys Ocean. A flow of heated asthenosphere material from the superplume caused moving of torn-off fragments of Gondwana to the north-east toward Eurasia. The oceanic Tethyan lithosphere subducted there, and the Gondwanan fragments accreted to Eurasia. As a result, series of microplates, separated by sutures, accretionary wedges, and magmatic bodies related to different stages of the Tethyan evolution, formed on the place of the future mountain belt. Probably, the mountain segments of the belt had previously the same structure as the south-eastern Indonesian segment, where subduction has continued till now, i.e., the subducted slabs transformed there at the depths of 400–700 km into the BMW that extended beneath the future mountain belt.

Closure of the Tethys and collision of the Eurasian and Gondwanan lithosphere plates decelerated their convergence, but the hot asthenosphere flows from the Ethiopian-Afar superplume probably prolonged the former movement and gradually spread under the entire orogenic belt. On moving, the sub-lithosphere flows were enriched in aqueous fluids that could derive from the former BMW lenses related to subduction zones. The asthenosphere, activated in this manner or its fluids penetrated into the lithosphere and produced its softening and detachment that facilitated deformational thickening of the Earth's crust and, correspondingly, the tectonic uplift in areas of maximum compression. During the first stage, it was the single or, at least, main source of the rise. During the second stage (the last 5–2 Ma), the deformational effect was supplemented by two other processes that were initiated by the sub-lithosphere flows and their fluids. The first process was the partial replacing of the lithosphere mantle by the lower-dense asthenosphere material and, as a result, decrease of density of the uppermost mantle.

The second process was the retrograde metamorphism of high-metamorphosed rocks of the crustal origin within the lower crust and near the crust-mantle boundary

In Fig. 1: *Mountains*: (1) Greater Caucasus, (2) Eastern Carpathians, (3) the Himalayas, (4) Hindu Kush, (5) Zagros, (6) Western Tien Shan, (7) Karakoram, (8) Kokshaal, (9) Kopet Dagh, (10) Kunlun, (11) Makran, (12) Lesser Caucasus, (13) Pamirs, (14) Northern Carpathians, (15) Tibet, (16) Khan Tengri, (17) Central and Eastern Tien Shan, (22) Elbrus, (30) Dinarides, (45) Coastal Range (in Syria), (47) Lebanon Range; *basins*: (18) Afghan-Tadjik, (19) Eastern Black Sea, (20) Terek-Derbent, (21) Western Black Sea, (23) Misis-Andirin (paleo-basin), (24) Red Sea (rift), (25) Levantine, (26) Mesopotamian, (27) Azov-Kuban, (28) Tarim (microplate), (29) Focsani (a part of the Carpathian Foredeep), (31) Aegean, (32) South Caspian; *platforms*: (33) Anatolian, (34) Arabian, (35) Moesian, (36) Scythian, (37) African; *fault zones*: (38) East-Anatolian Zone, (39) Herat, (40) Main Recent Fault of Zagros, (41) Darvaz, (42) North-Anatolian Zone, (43) Dead Sea Transform, (44) Chaman, (46) South Taurus; *tectonic zones*: (48) Indus-Tsang Po, (49) Quetta, (50) Cyprus Arc, (51) Crete-Hellen Arc, (52) Palmyrides, (53) Hellenides, (54) Sanandaj-Sirjan

with participation of the asthenosphere fluids and, as a result, decrease of density of these rocks. The both processes produced additional rise of the land surface and caused the acceleration of total uplift of the belt during the Pliocene–Quaternary.

The determining role in this model of the Alpine-Himalayan Belt evolution belongs to the sub-lithosphere upper mantle flows that spread away from the Ethiopian-Afar superplume. We have analyzed the neotectonic and seismic tomography data on other territories and have found similar features. The other orogenic belts demonstrate acceleration of tectonic uplift in the Pliocene–Quaternary. Several super-plumes and upper mantle flows, which spread away from them, were found by the analysis of seismic tomography data. Comparison of the data gives a possibility to propose the following model of the global tectonic processes. Lithosphere plates are moved by the sub-lithosphere upper mantle flows because of viscous friction in the lithosphere-asthenosphere boundary. The flows spread away from the superplumes that represent the upwelling strands of the mantle convection. As a rule, zones of the lithosphere spreading do not correspond to the superplumes. The MORB volcanism is a result of adiabatic melting of the uppermost asthenosphere and the lithosphere due to the extension. Because majority of the subducted slabs transforms into the BMW in the depths about 400–700 km, only a part of the subducted material penetrates into the lower mantle and is not enough to compensate a grow of the lithosphere in the spreading zones. The sinking strands of the mantle convection are represented also by volumes of dense and depleted upper mantle as well as high-metamorphosed basic rocks beneath cratons and collision zones. The plate tectonic mechanism is not the only result of the upper mantle flows. It is supplemented by tectonic processes that are caused by phase mineral transformations of the mantle and lower crustal rocks, by formation of the BMW and their fluid potential. The tectonic uplift producing mountain building is one of such processes.

In this paper, we use the new stratigraphic division of the Pliocene and Quaternary, confirmed in the 33rd IGC (www.stratigraphy.org). We use the following abbreviations in some tables and figures: E₁, Paleocene; E₂, Eocene; E₃, E₃¹, E₃², & E₃³, Oligocene, correspondingly Lower, Middle, and Upper; N₁, N₁¹, N₁², & N₁³, Miocene, correspondingly Lower, Middle, and Upper; N₂, N₂¹, & N₂², Pliocene, correspondingly Lower (Zanclean) and Upper (Piacenzian); Q₁, Q₁¹, & Q₁², Lower Pleistocene, Gelasian, and Calabrian, Q₂, Q₂¹, & Q₂², Middle Pleistocene, correspondingly lower and upper; Q₃, Upper Pleistocene; Q₄ – Holocene.

Part 1. Neotectonic development of the central part of the Alpine-Himalayan belt

1.1. Pre-history

The longitudinal tectonic zoning dominating in the orogenic belt is expressed in the progressive rejuvenation of the crust to the south and southwest in compliance with the evolution of the Tethys Ocean. Over its entire history, rifting passed into spreading at the south-western (in present-day coordinates) passive continental margin of the ocean, which was underlain by Precambrian basement. The continental fragments separated from Gondwana moved to the northeast, where the Tethyan oceanic lithosphere was subducted beneath the island arcs or active south-western (in present-day coordinates) margins of the northern plates and the fragments of Gondwana accreted to Eurasia. Because of this, the subduction zone jumped back to the rear sides of the accreted fragments. The recurrence of this process during formation of the Paleo-, Meso-, and Neotethys led to the consecutive attachment of new microplates (fragments of Gondwana) to the northern plates. These fragments were separated by sutures, accretionary wedges, and zones of subduction-related and collision-related magmatism and metamorphism. The poorly reworked fragments retained the platform tectonic regime. This process has developed since the breakdown of Pangea in the Carboniferous and became especially distinct in the Mesozoic and Cenozoic, when the northern plates merged to form the Eurasian plate.

In the present-day outlines, most of the orogenic belt is made up of tectonic units of the northern active margin of the Neotethys, whereas only a few mountain systems occur at its southern passive margin; the Himalayas and Zagros are the largest. The mountains of the northern margin of the belt (the Greater Caucasus, Kopet Dagh, Tien Shan, Northern Afghanistan, Northern Pamir, Kunlun, and Northern Tibet) are superposed on the Paleozooids, the participation of which diminishes westward. For example, the northern part of the Tien Shan is Caledonian, whereas the southern part is Hercynian. To the west, only part of the Hercynides entered into the belt, while their northern extensions formed the basement of the Turanian and Scythian post-Paleozoic platforms and Hercynides of Central Europe. The sutures and other structural elements of the Mesotethys are localized further to the south, while the Neotethys is situated in the extreme south. Relics of the backarc troughs either inheriting older Tethyan basins or partly superposed on other structural elements

occur at the active margin. As a result of multiple closures of basins with oceanic and sub-oceanic crust, relics of the oceanic crust are retained in the lithosphere of the belt. They are detected as high-velocity bodies at various levels of the lithosphere and as xenoliths in igneous rocks.

From the Late Paleozoic to the Paleogene, the Tethys was a gulf of the Pacific extending to the north-west and narrowing in this direction. This is why the horizontal offsets during its closure and formation of the orogenic belt generally increased eastward. In the Late Cenozoic, this tendency was expressed in the magnitudes of lateral offsets increasing from the west-eastward both in particular structures, e.g., the greater magnitude of shear at the western flank of the Indian Plate as compared with the western flank of the Arabian Plate (Trifonov et al., 2002), and in variable dimensions of the belt's segments, which have shortened in the transverse direction to different magnitudes (Molnar, Chen, 1978; Bazhenov, Burtman, 1990).

The contemporary mountain edifices originated in different parts of the Alpine–Himalayan Belt asynchronously, but mostly in the Oligocene (Shultz, 1948; Trifonov, 1999). Therefore, the history of recent mountain building is considered below since the Oligocene; the Eocene is regarded as a preceding epoch. In the Eocene, the lithosphere of the future orogenic belt was a combination of microplates, sutures, accretionary wedges, and magmatic zones related to the earlier collision stages of the Eurasia and Gondwana plates. In the west and the center of the belt, the vast areas were territories of epicontinental and shallow-water marine sedimentation. Such seas covered the microplates and the former fold-thrust zones and spread over the neighboring Moesian, Scythian, Turanian, Arabian, and African platforms. In the east, marine sedimentation covered the Afghan–Tajik Basin and the western Tien Shan, extending up to the western parts of the Shu Basin and Tarim microplate (Dmitrieva, Nesmeyanov, 1982; Burtman, 1999).

The rest of the future High Asia (the Central and Eastern Tien Shan, Tarim, Pamir–Hindu Kush–Karakoram, Kunlun, and Tibet) was a land. The widespread granitic batholiths, the first phases of which are dated at the Cretaceous and the final ones at the Miocene, was one of a cause of relatively high standing of the Pamir–Hindu Kush–Karakoram region (Shvolman, 1977; Searle, 1991). In the Paleocene and Eocene, the territory of the Central and Eastern Tien Shan was a peneplain with relative elevations of a few hundred meters accepted as a pre-orogenic planation surface (Shultz, 1948; Trofimov, 1973; Chediya, 1986). The Paleocene and Eocene sequence is composed of mainly fine-clastic red beds (the redeposited Late Mesozoic weathering mantle) with basaltic flows in the lower part (see section 1.2). The

thickness of this sequence commonly does not exceed a few tens of meters and is greater than 100 m in some basins.

Deeper troughs with thinned (sub-oceanic) crust stand out against the background of the land and areas of epicontinental marine sedimentation (Fig. 2). These were relics of the Neotethys and backarc basins (Golonka, 2004; Kazmin et al., 2010). The Eocene relics of the Neotethys existed in the Trans-Himalayas (Indus–Zangpo Zone); to the south of Makran, where a basin was retained which would later become the periphery of the Indian Ocean; and between the Arabian Plate and the Sanandaj–Sirjan Zone of Iran, where relics of the basin comprise accreted Paleogene sedimentary rocks and Mesozoic ophiolites.

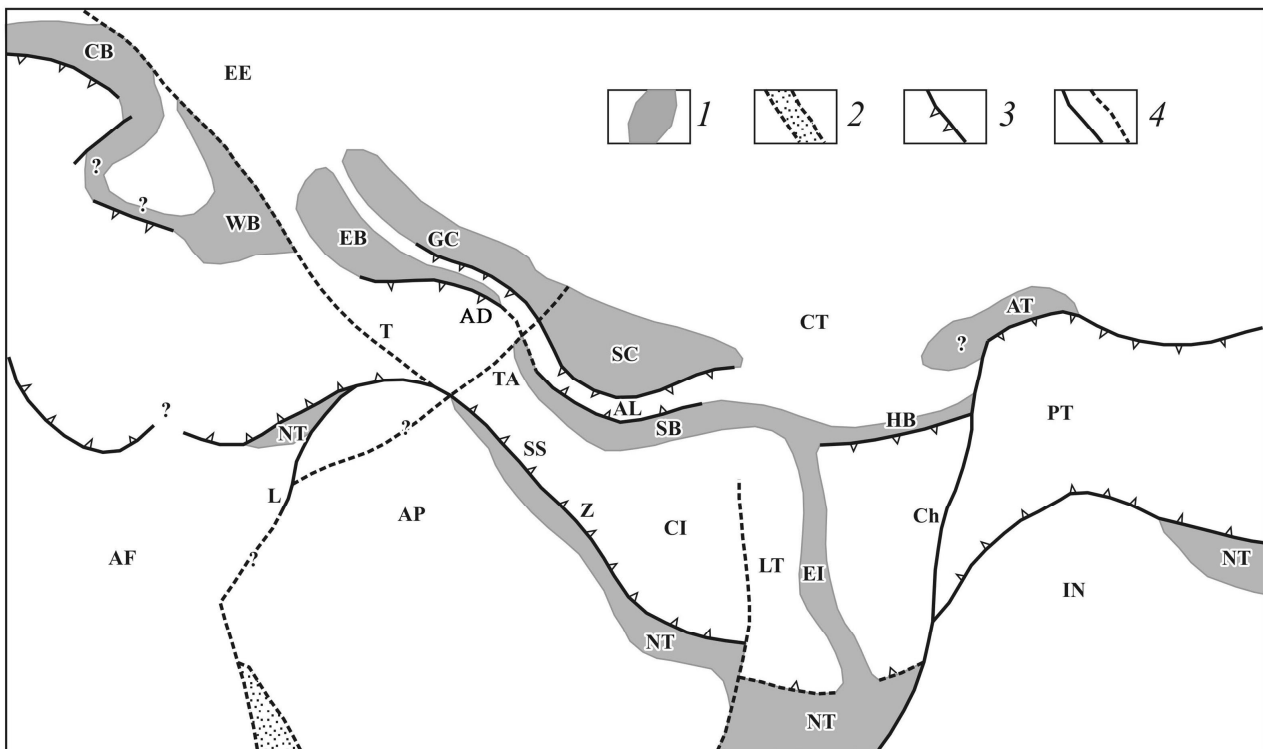


Fig. 2. Conceptual map of the basins with a thin (suboceanic?) crust in the Alpine-Himalayan Belt in the Eocene (~45 Ma ago), modified after (Golonka, 2004; Robertson et al., 2004; Alpine history..., 2007; Kaz'min et al., 2010; Trifonov et al., 2012_{1,2})

1, thin-crust basins; 2, Red Sea proto-rift basin; 3, major thrusts and subduction zones; 4, major transform and other faults and their supposed continuations. AD, Adjaro-Trialetia; AF, African Plate; AL, Alborz; AP, Arabian Plate; AT, Afghan-Tadjik Basin; CB, Carpathian Basin; Ch, proto-Chaman Transform; CI, Central Iran Microplate; EB, Eastern Black Sea Basin; EE, East European Platform; EI, East Iranian Basin; GC, Greater Caucasus Basin; HR, Hari-Rud Basin; IN, Indian Plate; L, proto-Levant Transform; LT, Lut Microplate; NT, Neo-Tethys relics; PT, Pamirs, Tibet; SB, Sabzevar Basin; SC, South Caspian Basin; SS, Sanandaj-Sirjan zone; T, proto-North Anatolian Fault, extending into the Pechenega-Kamena Fault and the Tesseire-Tornquist Line; TL, Talysh; WB, Western Black Sea Basin; Z, Main Zagros Thrust

The region between the Taurus microplate and the northwestern margin of the Arabian part of the African Plate has a complex tectonic history (Krylov et al., 2005).

Before the end of the Cenomanian, this region was a part of the Tethys subducted to the north beneath the Taurides. In the Late Cenomanian–Early Turonian, the ensimatic proto-Cyprus arc arose, having separated the backarc trough from the Tethys, and the oceanic Troodos Complex was formed there. In the Late Campanian–Early Maastrichtian, this complex was deformed and became a part of the arc as a paraautochthon. At the same time, the northeastern continuation of the arc and oceanic rocks in front of this arc were obducted on the margin of the Arabian Plate (Knipper et al., 1988). The retained Kilikia–Adana backarc basin deepened in the late Maastrichtian and continued to subduct beneath the Taurides. The pelagic cherty-clayey sedimentation therein is dated at the Paleocene–Middle Eocene in the Misis–Andirin melange complex of the South Taurus (Robertson, 2000; Robertson et al., 2004). In the south, this basin connected with the Levantine and Ionian basins of the Mediterranean Sea, which developed at the southern passive margin of the Neotethys and probably were at that time shallower than now.

The earlier closure of the Neotethys in the south of the South Taurus Zone (northern flank of the Arabian Plate) as compared with its western part (East Mediterranean margin of the African Plate), as well as the greater thickness of the Upper Mesozoic and Cenozoic sediments in the Levantine Basin than in its eastern continental framework (Garfunkel, 1998) allow us to suggest that a transform-type structural boundary existed between them, at least beginning from the Late Mesozoic. This boundary followed from the South Taurus Zone along the present-day East Anatolian Fault Zone and extended southward along the continental slope of Eastern Mediterranean, where it is expressed in seismic sections as faults (Ben-Avraham et al., 2002; Ben-Gai et al., 2004). In the south, this zone probably merged with a proto-rift developing in the Late Cretaceous–Eocene partly on the place of the future Red Sea Rift (Almeida, 2010).

Among the backarc basins, the approximately W–E-trending Carpathian–Greater Caucasus system of troughs, extending from the outer Carpathian Zone to the proto-South Caspian Basin, was the largest (Kopp, Shcherba, 1993; Shcherba, 1994; Golonka, 2004; Alpine history..., 2007). The system was en echelon arranged: the troughs extended in the NW–SE direction in such a manner that the southeastern termination of each trough was situated to the south of the northwestern end of more eastern trough. The troughs were separated by relative uplifts (partly shoals) striking in the northwestern direction. The Sabzevar Trough, situated in the south and reaching Talysh in the west, extended to the east as the Herirud Trough and

connected with the pre-Makran relic of the Neotethys via the Central Iran Basin (Kazmin et al., 2010).

The origin of the backarc troughs remains conjectural. The Cretaceous ophiolite in the relics of the Sabzevar and East Iranian Troughs indicate spreading (Kazmin et al., 2010). As concerns the Carpathians–Greater Caucasus system, arguments have been stated about Cretaceous and even locally developed Late Jurassic rifting as a mechanism of sagging (Nikishin et al., 2001; Golonka, 2004; Alpine history..., 2007). These troughs inherited from the Cretaceous, however, did not show magmatic indications of spreading or deep rifting in the Eocene. In contrast, they underwent transverse shortening with deposition of flysch and volcanic activity in the adjacent territories. Therefore, deepening of troughs in the Carpathians–Greater Caucasus system in the Paleogene (Kopp, Shcherba, 1993) and similar deepening of the relict Kilikia–Adana Basin (Robertson et al., 2004) should be related to other causes, e.g., to compaction of the lower crust mafic rocks as a result of metamorphism rather than to ongoing extension.

The Paleogene troughs are not everywhere inherited from the Cretaceous. Indications of their superposition on the Upper Cretaceous shallow-water sedimentary rocks overlapping the destroyed island arcs of the Mesotethys were found in the Adjara–Trioletia continuation of the East Black Sea Basin and in the Talysh continuation of the Sabzevar Trough (Shcherba, 1994). This gives grounds to suggest that they could have been parts of a single trough overthrust later by the Lesser Caucasus; i.e., the Sabzevar Basin continued or added to in an en echelon way the East Black Sea Basin.

At the end of the Middle Eocene and in the Late Eocene most of the belt except for its northern periphery underwent folding and thrusting (Bazhenov, Burtman, 1990). The Neotethyan backarc basins became narrower or partly closed (Khain, 2001; Golonka, 2004; Kazmin et al., 2010). In the regions where the Neotethys had been closed before the Eocene, for example in front of the Punjab indenter of the Indian Plate, a peak of high-pressure metamorphism fell on the Eocene (50–40 Ma) (Searle, 1996; Guillot et al., 2007). Intensive deformation did not lead to the formation of mountain topography. Fine clastic fractions dominated in the regions of sedimentation; large fragments and blocks occurred only in some accretionary wedges of the subduction zones.

1.2. Neotectonic evolution of the Central Tien Shan

Long-term research showed that the neotectonic (Oligocene-Quaternary) structure of Tien Shan is a result of deformation of the Cretaceous-Paleogene peneplain, which formed on the Paleozoic basement of the Turan Plate and the Kazakh Shield. The structure is a system of anticlinal and synclinal folds of the basement, expressed as ridges and molasses-filled intermontane basins, respectively. The folds are separated and complicated by large faults with reverse or thrust component of motion. It is generally recognized that starting from the Oligocene, this structure developed under transverse horizontal shortening (Shultz, 1948; Makarov, 1977; Dmitrieva, Nesmeyanov, 1982; Chediya, 1986; Nikolaev, 1988; Mikolaichuk, 2000). Its continuing development is confirmed by the inherited tectonic movements along active faults (Abdrakhmatov et al., 2001; Trifonov et al., 2002) and data of repeated geodetic observations (Nikonov, 1977; Abdrakhmatov et al., 1996; Recent geodynamics..., 2005; Zubovich et al., 2001, 2010). The average rate of tectonic uplifting in the period embracing the Oligocene to Quaternary was lower than that in the Quaternary alone and still lower than in the Late Pleistocene and Holocene. This evidences that the mountains rose with acceleration (Krestnikov et al., 1979; Chediya, 1986).

Our research was aimed at studying the change in the rate of rise of mountains in time and geodynamic processes that might have caused it. For study, we chose the Central Tien Shan (CTS), a part of the mountains between the Talas-Fergana Fault in the west and Khan-Tengri mountain plexus in the east (Fig. 3). In the north, the CTS borders the post-Paleozoic Chu and Ili basins, and in the south, the Tarim Basin, which originated on the late Proterozoic basement probably as early as in the Paleozoic.

1.2.1. Changes in the regime of vertical movements during the neotectonic evolution

The CTS Paleozoic orogen passed through a platform stage of evolution in the Mesozoic and Early Paleogene. In the Early Paleogene, the CTS area was a peneplain with uplifts reaching few hundreds of meters, which was earlier considered a preorogenic planed surface (Shultz, 1948; Trofimov, 1973; Chediya, 1986). Redeposited crust of weathering that formed on the peneplain by the late Mesozoic composes a continental red-colored, mainly fine clastic rock unit with the Middle-Late Eocene and, probably, Early Oligocene fossils (Dmitrieva, Nesmeyanov, 1982).

Its lower part includes basalt lavas, whose total thickness reaches 20 m on the north-western edge of the Issyk-Kul Basin and 80 m in the Aksai Basin (Chediya et al., 1973; Bazhenov, Mikolaichuk, 2002). The K-Ar and Ar-Ar ages of the basalts are 54–70 Ma (Krylov, 1960; Nesmeyanov et al., 1977; Simonov et al., 2005; Bachmanov et al., 2008). The unit thickness usually does not exceed few tens of meters, though locally is greater than 100 m in the Chu, Ili, Issyk-Kul, and Aksai basins, thus probably reflecting their started sinking.

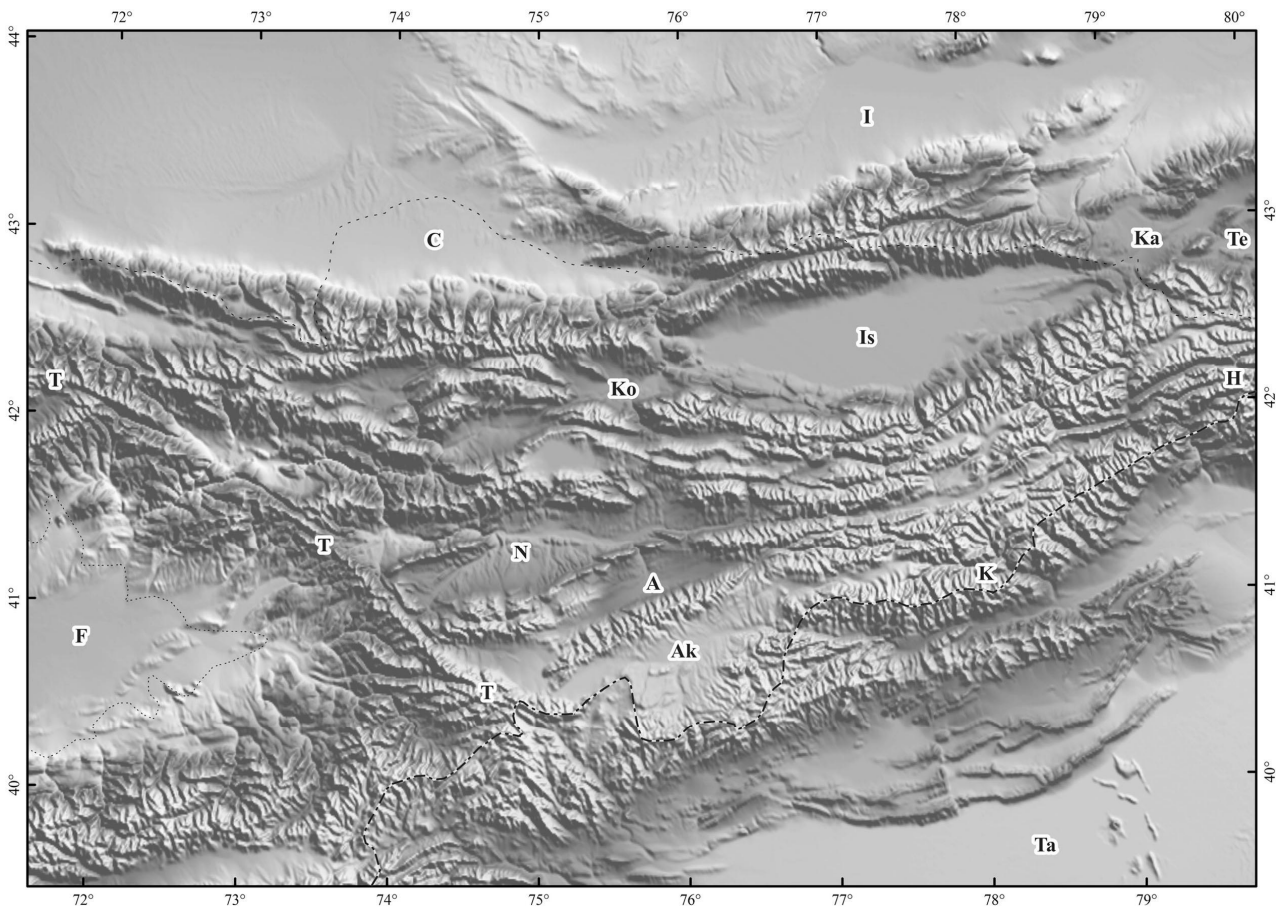


Fig. 3. The Central Tien Shan, modified after (Trifonov et al., 2008). A, Atbashi Basin; Ak, Aksai Basin; C, Chu Basin; F, Fergana Basin; H, Khan Tengri; I, Ili Basin; Is, Issyk-Köl Basin; Ka, Karkara Basin; Ko, Kochkor Basin; K, Kokshaal; N, Naryn Basin; T, Talas-Fergana Fault; Ta, Tarim Basin; Te, Tekes Basin. The China-Kyrgyzstan boundary is shown

Figure 4 shows a map of the CTS mountain peak surface combined with the position of the pre-orogenic surface in recent basins, which was determined from a complex of geological, drilling and geophysical data (Geological Map..., 1982). The central parts and slopes of ridges have preserved relics of preorogenic surface under conditions of intense linear erosion that accompanied their growth (Makarov, 1977; Chediya, 1986). Thus, besides rare cases of significant erosional decline of these relics, the map reflects recent deformation and uplift of the pre-orogenic surface. This is a generalized map of all neotectonic vertical movements. The axial parts of the

ridges rise above the bottoms of neighboring basins to ~3–5 km, and the maximum magnitude of the surface relief is 10 km.

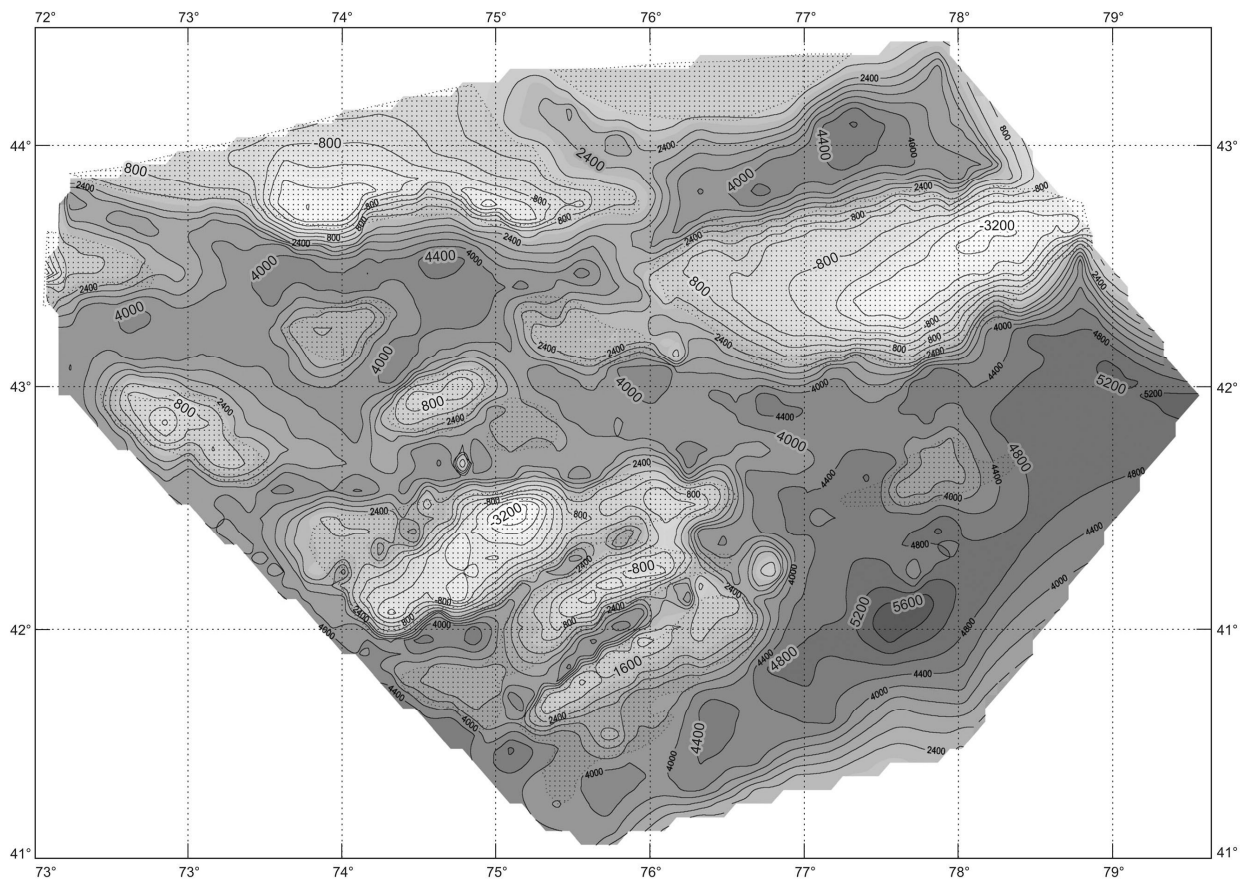


Fig. 4. Assumed position of the pre-orogenic surface drawn by peak surface isolines within the ridges and by basement surface isolines within basins (speckled sites), modified after (Trifonov et al., 2008). The position of the surface beneath recent molasses was designed from geological, drilling, and geophysical data (Geological Map of Kyrgyzstan, 1982)

The step-like structure of the ridge slopes, which is accounted for the most researchers by pulse rise, formed the basis for concepts of the step-like levels of the CTS topography (Shultz, 1948; Trofimov, 1973; Makarov, 1977; Krestnikov et al., 1979; Chediya, 1986). According to these concepts, intensification of vertical movements promotes erosion, which results in an erosional-tectonic scarp (incision) resting upon the bottom of basin or valley serving as a local basis of erosion and accumulating erosion products. The higher is the rate of rise, the coarser and thicker are accumulating deposits. The next pulse of rise leads to the uplifting of the scarp-bordering site of the depression, below which a younger incision forms. The uplifted site becomes a slope step. The steps, located at close hypsometric levels on slopes of different ridges and the incisions resting upon them form a regional topographic layer. This suggests that the incision is correlated with the lower coarse part of a corresponding molasse unit and that the steps are correlated with the upper finer part

of the unit (Makarov, 1977). Comparison of the topographic layer with related molasse unit helps to clarify the evolution of the mountain system.

Deposits of CTS basins were described elsewhere (Shultz, 1948; Nesmeyanov, Makarov, 1974; Dmitrieva, Nesmeyanov, 1982; Chediya, 1986; Dodonov, 2002; Mikolaichuk et al., 2003). Our goal was to correlate these data and supplement them with results of our research (Trifonov et al., 2008). The post-Eocene molasses are subdivided into four complexes: Kyrgyz, Tien Shan, Sharpyldak, and Middle Pleistocene–Holocene, each being divided into local units (Fig. 5 and Table 1). Their comparison and dating (still debatable) are based on the composition and color of deposits, incomplete paleomagnetic data, and scarce fauna remains.

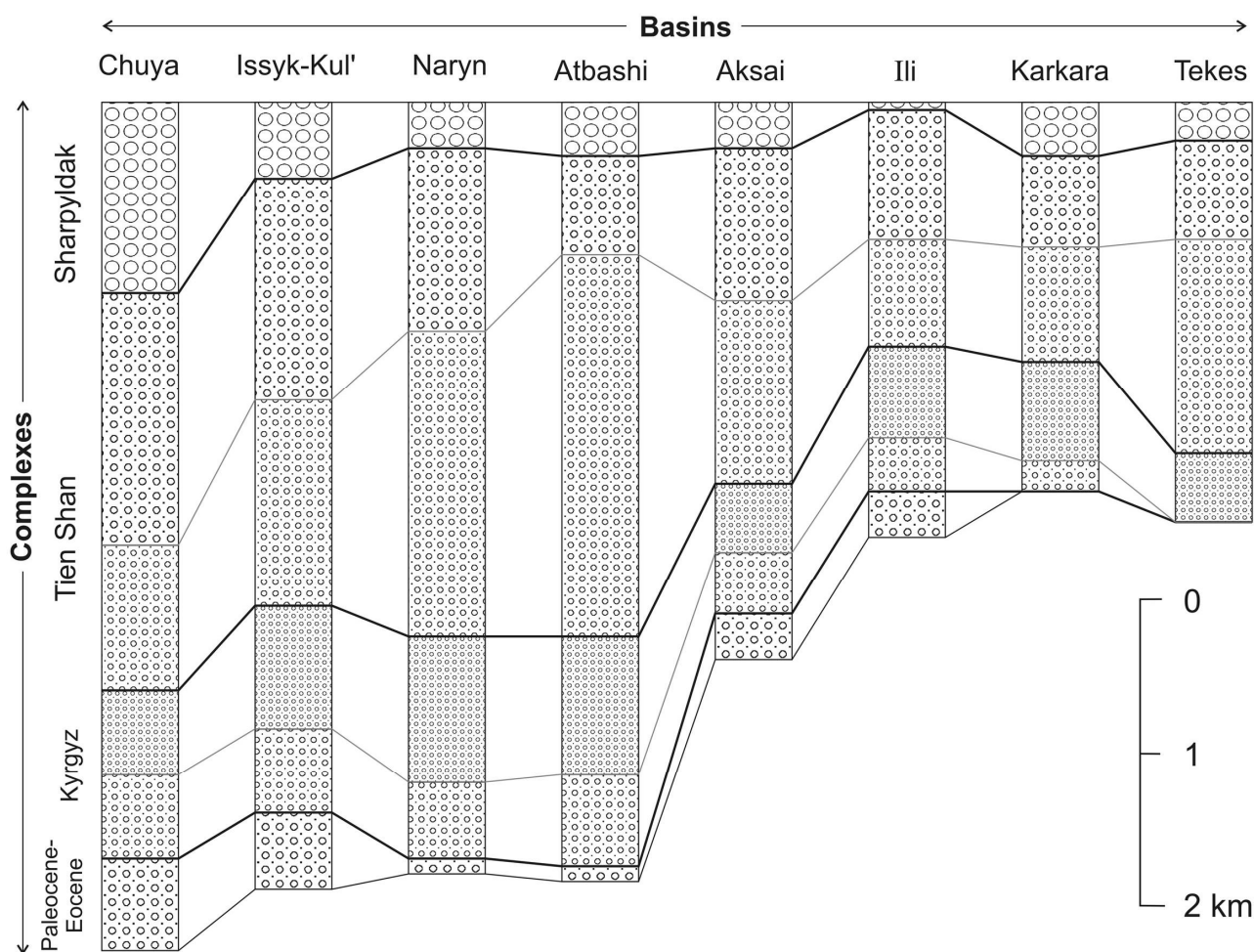


Fig. 5. Comparison of sections of the Cenozoic deposits in the Central Tien Shan basins, modified after (Trifonov et al., 2008). Different units are shown by different symbols

The lower Kyrgyz complex consists of two series, lower red and upper brown. The lower series is composed of fluvial fine- and, seldom, medium-pebble conglomerates, gravelstones, and sandstones, which give way to sand-clayey deposits with gypsum at the central parts of large basins. Based on the fossils found in the Issyk-Kul and Ili

Basin													
Complex	Age	Chu (south)		Kochkor		Issyk-Kul		Ili		Naryn		Atbashi	
sh	$N_3^2 - Q_1$	Noruz unit	N_2^3	Sharpyldak unit		Q_1	Khorog unit	Q_1	Sharpyldak unit		Kulnei unit		
Tien-Shan	$N_2^2 - N_2^3$	Chu unit	N_2^3	Upper subunit	N_2^{2-3}	Djoukin unit (Upper Issyk-Kul subunit)	Ili unit	N_2^3	Upper Naryn subunit	Aktal unit	Upper subunit	Kulnei unit	
		Saryagach unit	$N_1^3 - N_2^1$	Lower subunit	$N_2^1 - N_2^1$	Sogutin unit (Lower Issyk-Kul subunit)	Santash unit	$N_1^3 - N_2^1$	Middle Naryn subunit		Middle, Lower subunit		
	Djeldisuy unit	$N_2^1 - N_2^1$	Djanaryk unit		Issyk-Kul unit		Chuladyr unit	N_1^{1-2}	Lower Naryn subunit	Kyrgyz unit	Upper subunit	Lower subunit	
Kyrgyz	$N_1^1 - N_1^2$?	Kokomeren unit		Sharybkol unit		Upper subunit							
	$E_3(E_3^{2-3}) - N_1^1 a$			Bizhin unit		Lower subunit	Aktal unit	E_3	Upper subunit				
Paleocene	$E_{1-2} (-E_3^1?)$	Suluterek unit		Kokturpak unit		Chonkurchak unit Ar-Ar and K-Ar age of basalts 54-70 Ma	Akbulak unit	$E_3^3 - E_2^2 - E_2^2$					
						Detyoguz unit							

Table 1. Comparison and age of the Paleocene – Lower Pleistocene units in intermontane and piedmont basins of the Central Tien Shan; data from (Abdrakhmatov et al., 2001; Aleshinskaya et al., 1972; Bullen et al., 2001; Chediya et al., 1973; Dmitrieva, Nesmeyanov, 1982; Dodonov, 2002; Makarov, 1977; Mikolaichuk et al., 2003; Nesmeyanov, Makarov, 1974; Nesmeyanov et al., 1977; Shultz, 1948; Simonov et al., 2005; Trifonov et al., 2008; Trofimov, 1973; Trofimov et al., 1976)

basins, the lower beds of the series were dated to the Middle Oligocene, and the upper ones, to the Late Oligocene – Early Miocene (Dmitrieva, Nesmeyanov, 1982). The upper series differs from the lower one in finer composition and the presence of carbonate and gypsum (and, locally, mirabilite and halite) interbeds, which points to plain landscape and the existence of drying lakes at the time of their formation. The position of the series in sections evidences its Early-Middle Miocene age.

The Tien Shan complex includes two series. Based on fauna remains, the lower series was dated to the Late (Middle?) Miocene – Early Pliocene, and the upper series, to the Late Pliocene (Dmitrieva, Nesmeyanov, 1982). According to paleomagnetic data, the series boundary in the south of the Chu Basin lies within 8–5 Ma (Bullen et al., 2001). Probably, it lies in the lowermost part of the Pliocene.

The above series differ in color (the lower series are variegated, and the upper ones are straw-gray) and are composed of terrigenous, mainly clay-silt-sandy rocks with interbeds of carbonate and, in the Naryn Basin, gypsum and, seldom, halite (Fig. 6). In the east of the region (Issyk-Kul, Tekes, and Karkar basins), conglomerates are predominant. Their amount increases in the upper parts of sections in the Naryn Basin and the southern Chu Basin. Upsection coarsening of deposits is also observed in the Ili Basin.

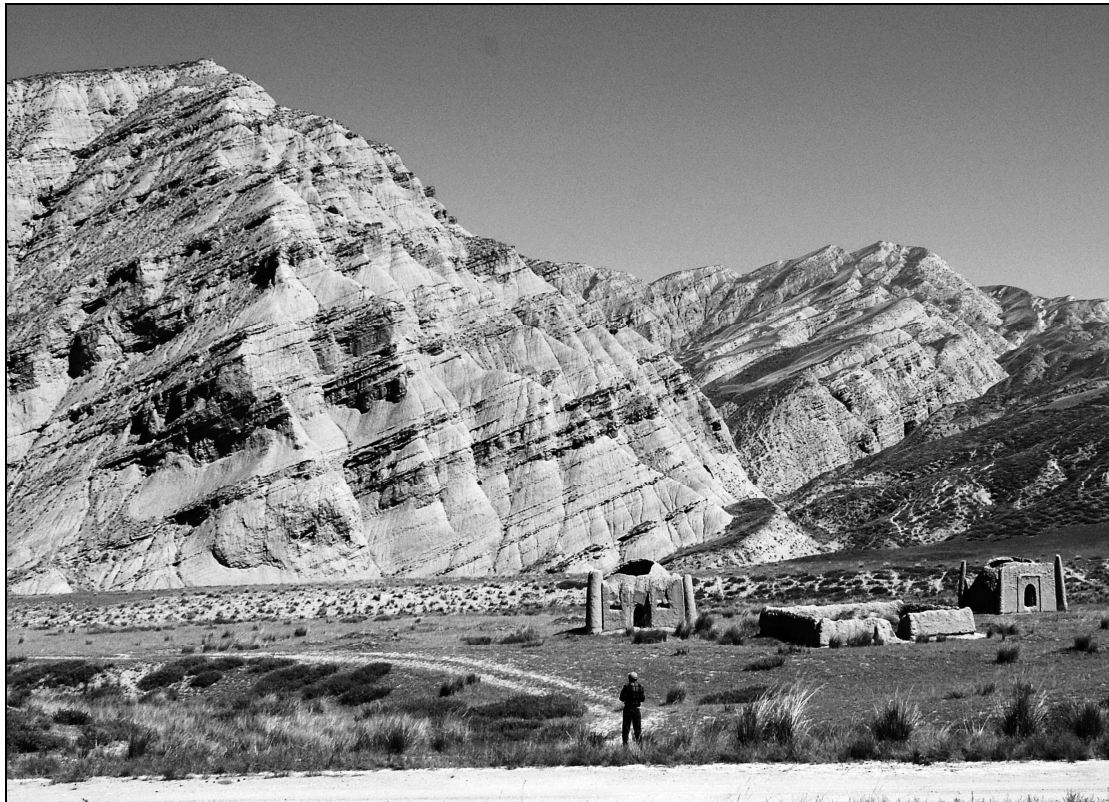


Fig. 6. The Naryn unit in the northern side of the Naryn Basin. Photo by D.M. Bachmanov

According to fauna remains and paleomagnetic data for the Issyk-Kul, Ili, and Chu basins, the Sharpyldak complex is of the Lower Pleistocene (Eopleistocene in the Russian terminology) age (~2–0.8 Ma) (Aleshinskaya et al., 1972; Trofimov et al., 1976; Dmitrieva, Nesmeyanov, 1982; Dodonov, 2002). It is composed of fluvial grey coarse conglomerates and conglomerate-breccias (up to boulder size) with gravel, sand and silt interbeds (Fig. 7).



Fig. 7. The Sharpyldak unit in the Issyk-Kul Basin. Photo by D.M. Bachmanov

The Middle Pleistocene–Holocene complex, compositionally similar to the Sharpyldak one, is formed by fluvial sediments of seven cyclic terraces (Shultz, 1948), floodplains, and recent channels as well as glacial and basin (at the centers of the Chu, Ili and Issyk-Kul basins) deposits. Three series of the complex are dated to: (1) Middle Pleistocene, (2) Late Pleistocene, and (3) Late Pleistocene–Holocene (Chediya, 1986; Dodonov, 2002).

First uplifts serving as sourcelands of debris appeared in the Oligocene (Bachmanov et al., 2009), but the predominance of small-pebble conglomerates and gravelstones in the lower series of the Kyrgyz complex indicates a minor amplitude between uplifts and basins. According to the data on magnitude of the incision, it was not more than 1 km in most of the CTS area (Makarov, 1977; Chediya, 1986). Judging from the deposit composition, the topographic contrast was reduced during

the accumulation of the upper series of the Kyrgyz complex and the lower series of the Tien Shan complex (Bachmanov et al., 2009). The sediments covered a part of the Oligocene uplifts. Lake basins formed, which were isolated from the regional basis of erosion under highly arid conditions (presence of evaporates) and thus might rise together with uplifts supplying clastic material. Lake conditions also existed locally during the accumulation of the upper series of the Tien Shan complex, but evaporates became scarcer. The coarsening of clastic material began in the south-east of the region (near the Khan Tengri) during the accumulation of the lower series of this complex and penetrated later to the north-west (Trifonov et al., 2008). It points to an increase in the amplitude between the uplifts subjected to erosion and the basin bottoms. Strong coarsening of clastics occurred in the Early Pleistocene. It evidences a considerable increase in the above-mentioned amplitude, i.e., the formation of high mountain topography.

The change in the rate of vertical movements in the basins can be judged from the average rates of accumulation of various series of molasses in them (Fig. 8 and Table 2), though these estimates are only tentative because of the complex structure of the molasses and the incomplete sections of the basins.

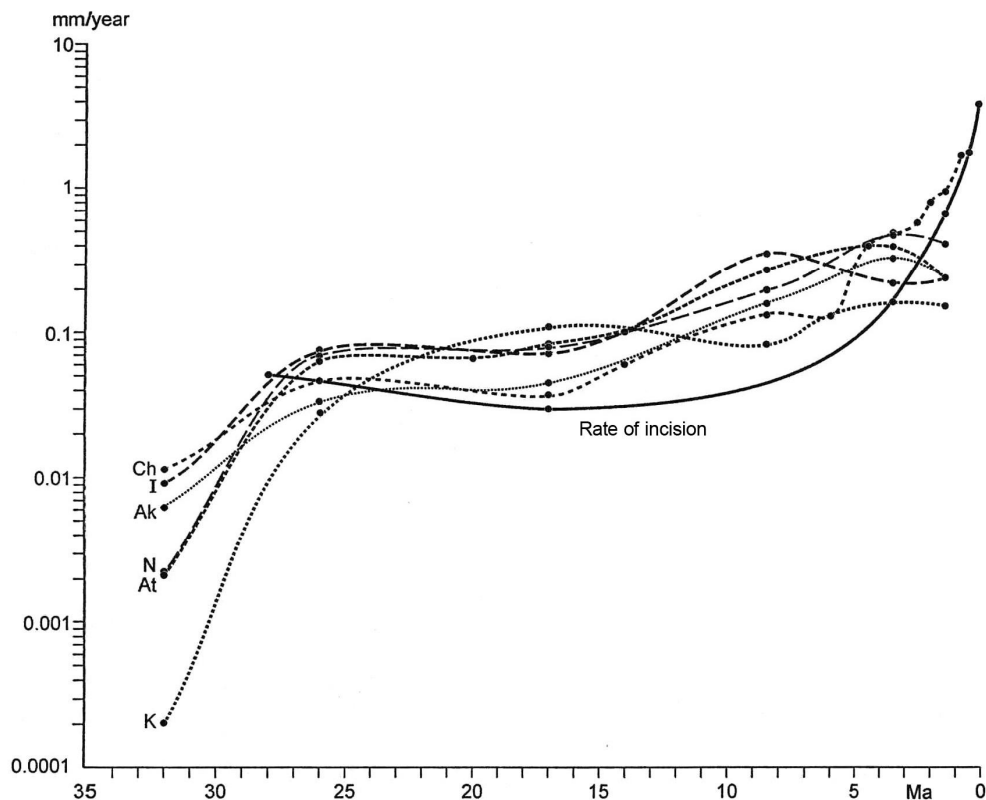


Fig. 8. Changes in the rates of sedimentation in the Cenozoic basins and in the rates of incision of drainage systems into ridges of the Central Tien Shan, modified after (Trifonov et al., 2008). Deceleration of deposit accumulation in the Aksai, Kochkor, Naryn basins in the Quaternary was caused by the transition from basin sedimentation to terrace regime. Basins: Ak, Aksai; At, Atbashi; Ch, Chu; I, Issyk-Köl; K, Kochkor; N, Naryn

Complex	Stage	Series	Duration, Myr	Boundaries, Ma	Basin									
					Chu (south)	Kochkor	Issyk-Kul'	Tekes	Karkara	Ili	Naryn	Atbashi	Aksai	
Thickness, m / Rate, mm/year														
sh	$N_3^2 - Q_E$	sh	1.2	0.8	$\frac{1000-1300}{0.8-1.08}$	$\frac{200}{0.167}$	$\frac{500}{0.417}$	$\frac{250}{0.208}$	$\frac{350}{0.28}$	$\frac{>20}{>0.017}$	$\frac{300}{0.25}$	$\frac{>300}{>0.25}$	$\frac{300}{0.25}$	
					$\frac{1250-1700}{0.4-0.57}$	$\frac{200-850}{0.067-0.283}$	$\frac{1450}{0.483}$	$\frac{650}{0.217}$	$\frac{600}{0.2}$	$\frac{380-880}{0.127-0.293}$	$\frac{1200}{0.4}$	$\frac{650}{0.217}$	$\frac{1000}{0.333}$	
					$\frac{950}{0.136}$	$\frac{150-1000}{0.0214-0.143}$	$\frac{1380}{0.197}$	$\frac{1400}{0.2}$	$\frac{230-800}{0.033-0.144}$	$\frac{125-760}{0.018-0.109}$	$\frac{2000}{0.286}$	$\frac{2500}{0.357}$	$\frac{1200}{0.171}$	
Tien Shan	$N_2^2 - N_2^3$	ts ₂	3	2	$\frac{150-600}{0.015-0.06}$	$\frac{450-1700}{0.045-0.17}$	800	$\frac{170-500}{0.017-0.05}$	$\frac{150-700}{0.015-0.07}$	$\frac{160-670}{0.016-0.067}$	$\frac{670-1000}{0.067-0.1}$	$\frac{450-1000}{0.045-0.1}$	$\frac{450}{0.045}$	
					$\frac{150-600}{0.019-0.075}$	$\frac{200-250}{0.025-0.031}$	$\frac{500-600}{0.063-0.075}$	No data	$\frac{200}{0.025}$	$\frac{390}{0.049}$	$\frac{500}{0.063}$	$\frac{600}{0.075}$	$\frac{100-450}{0.012-0.056}$	
					$\frac{150-635}{0.0041-0.0176}$	$\frac{7}{0.0002}$	$\frac{100-550}{0.0028-0.0153}$	No data	No data	$\frac{320}{0.0089}$	$\frac{100}{0.0022}$	$\frac{80}{0.0022}$	$\frac{10-350}{0.0003-0.0098}$	
Kyrgyz	$N_1^3 - N_1^2$	ts ₁	7	5	$\frac{150-600}{0.015-0.06}$	$\frac{450-1700}{0.045-0.17}$	800	$\frac{170-500}{0.017-0.05}$	$\frac{150-700}{0.015-0.07}$	$\frac{160-670}{0.016-0.067}$	$\frac{670-1000}{0.067-0.1}$	$\frac{450-1000}{0.045-0.1}$	$\frac{450}{0.045}$	
					$\frac{150-600}{0.019-0.075}$	$\frac{200-250}{0.025-0.031}$	$\frac{500-600}{0.063-0.075}$	No data	$\frac{200}{0.025}$	$\frac{390}{0.049}$	$\frac{500}{0.063}$	$\frac{600}{0.075}$	$\frac{100-450}{0.012-0.056}$	
					$\frac{150-635}{0.0041-0.0176}$	$\frac{7}{0.0002}$	$\frac{100-550}{0.0028-0.0153}$	No data	No data	$\frac{320}{0.0089}$	$\frac{100}{0.0022}$	$\frac{80}{0.0022}$	$\frac{10-350}{0.0003-0.0098}$	
Paleogene	$E_3(E_3^{2-3}) - N_1^1 a$	kz ₂	10	12	$\frac{150-600}{0.015-0.06}$	$\frac{450-1700}{0.045-0.17}$	800	$\frac{170-500}{0.017-0.05}$	$\frac{150-700}{0.015-0.07}$	$\frac{160-670}{0.016-0.067}$	$\frac{670-1000}{0.067-0.1}$	$\frac{450-1000}{0.045-0.1}$	$\frac{450}{0.045}$	
					$\frac{150-600}{0.019-0.075}$	$\frac{200-250}{0.025-0.031}$	$\frac{500-600}{0.063-0.075}$	No data	$\frac{200}{0.025}$	$\frac{390}{0.049}$	$\frac{500}{0.063}$	$\frac{600}{0.075}$	$\frac{100-450}{0.012-0.056}$	
					$\frac{150-635}{0.0041-0.0176}$	$\frac{7}{0.0002}$	$\frac{100-550}{0.0028-0.0153}$	No data	No data	$\frac{320}{0.0089}$	$\frac{100}{0.0022}$	$\frac{80}{0.0022}$	$\frac{10-350}{0.0003-0.0098}$	
Paleogene	$E_3(E_3^{2-3}) - N_1^1 a$	kz ₁	8	22	$\frac{150-600}{0.015-0.06}$	$\frac{450-1700}{0.045-0.17}$	800	$\frac{170-500}{0.017-0.05}$	$\frac{150-700}{0.015-0.07}$	$\frac{160-670}{0.016-0.067}$	$\frac{670-1000}{0.067-0.1}$	$\frac{450-1000}{0.045-0.1}$	$\frac{450}{0.045}$	
					$\frac{150-600}{0.019-0.075}$	$\frac{200-250}{0.025-0.031}$	$\frac{500-600}{0.063-0.075}$	No data	$\frac{200}{0.025}$	$\frac{390}{0.049}$	$\frac{500}{0.063}$	$\frac{600}{0.075}$	$\frac{100-450}{0.012-0.056}$	
					$\frac{150-635}{0.0041-0.0176}$	$\frac{7}{0.0002}$	$\frac{100-550}{0.0028-0.0153}$	No data	No data	$\frac{320}{0.0089}$	$\frac{100}{0.0022}$	$\frac{80}{0.0022}$	$\frac{10-350}{0.0003-0.0098}$	
Paleogene	$E_{1-2} (-E_3^1?)$	E	36	66	$\frac{150-600}{0.015-0.06}$	$\frac{450-1700}{0.045-0.17}$	800	$\frac{170-500}{0.017-0.05}$	$\frac{150-700}{0.015-0.07}$	$\frac{160-670}{0.016-0.067}$	$\frac{670-1000}{0.067-0.1}$	$\frac{450-1000}{0.045-0.1}$	$\frac{450}{0.045}$	
					$\frac{150-600}{0.019-0.075}$	$\frac{200-250}{0.025-0.031}$	$\frac{500-600}{0.063-0.075}$	No data	$\frac{200}{0.025}$	$\frac{390}{0.049}$	$\frac{500}{0.063}$	$\frac{600}{0.075}$	$\frac{100-450}{0.012-0.056}$	
					$\frac{150-635}{0.0041-0.0176}$	$\frac{7}{0.0002}$	$\frac{100-550}{0.0028-0.0153}$	No data	No data	$\frac{320}{0.0089}$	$\frac{100}{0.0022}$	$\frac{80}{0.0022}$	$\frac{10-350}{0.0003-0.0098}$	

Table 2. Thicknesses and rates of accumulation of the Paleogene – Lower Quaternary molasse complexes in the Central Tien Shan, data from (Dmitrieva and Nesmeyanov, 1982; Makarov, 1977; Shults, 1948; Simonov et al., 2005; Trifonov et al., 2008)

Calculations showed that the average rates of accumulation did not exceed thousandths of a millimeter per year and reached ~ 0.02 mm/year only at some sites of the future basins at the Paleocene-Eocene platform stage. The accumulation rates increased to hundredths of a millimeter per year during the formation of the lower series of the Kyrgyz complex and stayed the same during the sedimentation of its upper series. The Tien Shan complex accumulated with acceleration of the rates up to 0.1–0.6 mm/year.

In the Sharpyldak time, the basin sedimentation regime was changed by the terrace regime, which evidences a drastic intensification of linear erosion as a result of the acceleration of uplift. In the Middle-Late Pleistocene, this led to the formation of terraces within the more ancient deposits. Because of the change in regimes, the average rates of the Sharpyldak sedimentation in most basins became commensurate with or lower than the rates of earlier sedimentation. The rate of the accumulation increased twice only at some sites of the Chu Basin, where the basin sedimentation lasted. A single estimate for the later Pleistocene sedimentation was obtained for the Chu Basin, where up to 500 m deposits accumulated for that epoch (Abdrakhmatov, 1988). Its rate is close to the rate of the Sharpyldak sedimentation. But the thickness of the Quaternary coarse-clastic deposits is obviously smaller than the amount of removed clastic material, because the formed river runoff and aeolian processes transported fine-clastic fractions from the mountain system.

Thus, analysis of Cenozoic deposits showed a significant acceleration of rise in the Quaternary. The same is evidenced from the data of analysis of the levels of topography of the CTS ridges. Three levels were recognized in the mountain system (Shultz, 1948; Trofimov, 1973; Makarov, 1977; Krestnikov et al., 1979; Chediya, 1986). The upper level that is formed by one or two steps, incised into the preorogenic surface is correlated with the Kyrgyz complex ($E_3-N_1^2$); the middle level, formed by two steps is correlated with the Tien Shan and Sharpyldak complexes ($N_1^2-Q_1$); and the lower level is correlated with the Middle Pleistocene to Holocene basin deposits of the Chu and Ili basins. The highest of seven cyclic terraces of the lower level has been incised into the roof of the Sharpyldak complex and is dated to the earlier Middle Pleistocene (Q_2^1). Makarov (1977) established that the magnitude of the Oligocene incision into the CTS ridges were no more than 200–400 m. According to Chediya (1986), this magnitude reaches 700 m; that of the middle level reaches 1500 m (more than a half of this value falls onto the lower incisions formed in the Sharpyldak time); and the magnitude of the lower level incision reaches 1500 m. Krestnikov et al. (1979) reported similar magnitudes: ~ 1000

m for the Sharpyldak incision in the CTS ridges and >1000 m in the north and up to 1500 m in the south-east of the CTS for the Middle Quaternary–Holocene incision.

Taking into account the duration of the epochs of sedimentation of correlated molasse complexes (Table 2) and using the above estimates, we can tentatively calculate (ignoring variations of the incision during each cycle) the average rates of incision for different levels and sublevels of the topography of the CTS anticlinal ridges, which, to a first approximation, reflect the rates of their rise (Trifonov et al., 2008). The rates of incision were 0.03–0.05 mm/year during the accumulation of the Kyrgyz unit and its analogs ($E_3-N_1^1$), ~0.04 mm/year during the deposition of the Kyrgyz complex ($E_3-N_1^2$), ~0.07 mm/year during the sedimentation of the Tien Shan complex ($N_1^2-N_2$), 0.6–0.7 mm/year in the Sharpyldak time (Q_1), and 1.6–2.5 mm/year in the Middle Pleistocene to Holocene (Q_2-Q_4). Thus, the rate of incision increased ~10 times in the Early Pleistocene and 20–30 times in the Middle Pleistocene to Holocene (Fig. 8).

The CTS intermontane basins, which developed for a long time in the regime of sinking down and basin sedimentation, also began to be involved in the rise in the Sharpyldak time. In the early Middle Pleistocene, linear incision covered all intermontane basins (probably, except for the center of the Issyk-Kul Basin), thus forming the lower level of their topography. The average rates of incision in the basins were 1.5–2 times lower than those in neighboring ridges; the rates were higher in the south and south-west of the region than in the north (Krestnikov et al., 1979). In the Middle and Late Pleistocene, zones of sinking and basin sedimentation still existed in the central parts of the Chu, Ili and, probably, Issyk-Kul basins, but their areas were reduced, giving way to terraces.

Thus, since the Early Pleistocene, the CTS has undergone an intense uplifting, which was maximum in the south and south-east. The mountain building was expressed as a drastic coursing of molasses and acceleration of incision. The uplifting was not dome-like, because the intermontane basins rose less intensively than neighboring ridges. The Early Pleistocene orogenic activation was also manifested by the form of contacts between molasses series. Ancient series usually overlap each other concordantly, and their “transgressive” relationships are observed only on the basin periphery, whereas the Sharpyldak series lie with an angular unconformity (few to >10°) almost ubiquitously (Trifonov et al., 2008).

In the same epoch, the uplifts widened at the expense of the basins. In the south of the Chu Basin, the rise of the Kyrgyz Ridge involved sites that were first covered with molasses and then were uplifted to several kilometers (Chediya, 1986;

Mikolaychuk et al., 2003). These sites formed a high piedmont there and on the periphery of the Issyk-Kul, Susamyr and Atbashi basins. Within the CTS mountain system, the basins began to be separate by sownecks, which appeared first in the south and then in the north. For example, the sowneck between the Tuyun and Aksai basins appeared as early as the Pliocene and was overlapped by the Sharpyldak deposits. The Baibichetau-Narynan sowneck, which separated the Naryn and Atbashi basins and was uplifted above their bottoms to ≥ 2 km, was formed by the left en echelon row of ridges combining transverse shortening (with extension of the Baibichetau dome) and longitudinal sinistral slip (Makarov, 1977). The late age of the sowneck is proved by the fact that between the Naryntau and Karatau ridges (the eastern part of the sowneck) and in the western slope of the sowneck, the fine-grained deposits of the Naryn unit do not contain the clastic material from these uplifts. The Sharpyldak deposits are absent in the sowneck slopes and do not contain its clastic material around. Therefore, the Baibichetau-Narynan sowneck formed finally as an topographic feature as late as the Middle Pleistocene (Trifonov et al., 2008). The same relationships were observed around the 2-km high sowneck between the Dzhungol and Kyzylol basins that are composed of the Kyrgyz and Tien Shan complexes deposits.

One more Quaternary formation is the K k meren-Minkush zone (Sadybakasov, 1972; Bachmanov et al., 2008), striking approximately along the Paleozoic Nikolaev's structural line west of Lake Song-Kel. The zone forms an intensively deformed ramp, narrowed by a transverse shortening, with signs of a longitudinal sinistral slip. The Late Quaternary strike slip fault is expressed by shift of topographic features and inherits earlier displacement that is manifested by slickensides on the fault planes. Within the zone, the Lower Carboniferous red-colored deposits, Jurassic sediments, and the thin Kokturpak unit with basalts in the lowest part (68.4 \pm 2.3 Ma, dated by V.A. Lebedev in the Institute of geology of ore deposits, petrography, mineralogy and geochemistry, Moscow, Russian Academy of Sciences) underlie conglomerates of the lower series of the Kyrgyz complex; they are overlapped by deposits of the Naryn and Sharpyldak units (Bachmanov et al., 2008). All strata, from the Lower Carboniferous to Naryn unit change one another without serious angular unconformity. The latter appears only in the base of the Sharpyldak unit (locally) and the Middle Pleistocene deposits (ubiquitously). This points to the young age of the ramp and its deformation.

1.2.2. Horizontal shortening of the Earth's crust in the Oligocene-Quaternary

The CTS ridges and intermontane basins evolved in the Late Cenozoic under horizontal compression caused by the north-westward pressure of the Tarim microplate, which, in turn, was due to the movement of the more southern parts of the Alpine-Himalayan orogenic belt (Ivanova, Trifonov, 2005). Many researchers relate the mountain uplift to these lateral movements. Let us check the possibility of the relationship between the Quaternary acceleration of the uplift and the lateral movements by comparing the average rates of the CTS shortening in the Oligocene–Quaternary and the Late Pleistocene–Holocene.

The GPS measurements of lateral movements in the Kyrgyz part of the Tien Shan that had been carried out since 1992 showed that the rates of the CTS shortening reach 12–13 mm/a (mm per year), with the shift vectors in the east departing from the normal to the ridge strike, thus pointing to the presence of the longitudinal sinistral component of movements (Abdrakhmatov et al., 1996; Zubovich et al., 2001; Recent geodynamics..., 2005). Later Zubovich et al. (2010) recalculated the data, taking into account the recent underthrust of the Tarim Basin beneath the CTS with the rate of 4–7 mm/a, and estimated the total rate of the CTS shortening (convergence of the Tarim Basin and the Kazakh Shield) at 20 ± 2 mm/a. The rates of recent vertical movements in places reach 10 mm/a (Nikonov, 1977).

Since the period of the GPS observations was too short for estimating the rates of lateral movements, the data on faults that were active in the Late Pleistocene and Holocene were used. Eight large active thrusts were studied, and the rates of movements along each of them were determined at 0.1 to 4 mm/a (Abdrakhmatov et al., 2001). The quoted authors suggested that most of recent transverse shortening of the Kyrgyz CTS falls just on these faults and estimated its total rate at 10 mm/a. But this estimate cannot be accepted because the studied faults die out along the strike and there are also active faults that were ignored by the quoted authors.

We carried out an analysis of the set of known active faults in the Kyrgyz CTS (Trifonov et al., 2002) and revealed that many longitudinal faults have not only a thrust, but also a substantial sinistral component of slips. Faults of the NW trend were recognized as dextral strike-slip ones. Based on the analytical results, we calculated tensors of deformation rates in the region. The total rate of the Late Quaternary horizontal shortening of the Kyrgyz CTS was estimated at ~6 mm/year. In the calculations, we ignored folded bends and shifts along fractures, whose contribution

to the total deformation is 10–20% in other active regions of this kind (Anatolia and Middle East). Therefore, the rates of the Kyrgyz CTS lateral shortening should be increased to ~7 mm/a, with the transverse-shortening component not exceeding ~6 mm/a. The farther studies showed that we had underestimated the rates of slip on same faults, and the transverse-shortening rate has to be increased as minimum to ~7 mm/a. We do not know the rate of shortening in the Chinese part of the CTS, but can suggest (by analogy with the results of GPS measurements) that it reaches about a half of the shortening in the Kyrgyz CTS. So, the estimate of the total Late Quaternary transverse-shortening rate of the CTS at ~10 mm/a seems to be reasonable.

Calculation of the total neotectonic (Oligocene-Quaternary) deformation of the CTS transverse shortening is based on the measurement of fold bends and shifts along the faults that deform the preorogenic peneplain and the Cenozoic molasses (Chediya, Utkina, 1975; Yunga, Yakovlev, 2000). Chediya (1986) reported that reverse faults became steeper with depth and ignored their gentle dip near the land surface in the calculations. He estimated the total transverse shortening of the Kyrgyz CTS at 4–5% of its width (14–18 km at the longitude of the Naryn Basin) and considered that the shortening is smaller at the longitude of the Khan-Tengri mountain plexus, where the CTS is the most uplifted. Yunga and Yakovlev (2000) made a similar calculation, not introducing corrections to observed fold bends, dip and offsets on faults. They estimated that the total shortening varied from 9–12% at the longitudes of the Naryn Basin and the city of Bishkek to 5–6% at the longitude of Khan-Tengri, i.e., from 40 to 20 km.

The representativeness of the obtained data depends on the model of the CTS neotectonics. The quoted calculations were based on the conventional model implying that the CTS mountain system is a combination of anticlinal ridges and synclinal basins complicated by reverse faults and thrusts. In recent years, a new model has been elaborated, which relates fold bends to movements along large thrusts flattening at depth (Abdrakhmatov et al., 2001). The new model admits the total shortening of 35–80 km, i.e., 10–20% of the CTS width. The validity of both models can be tested by three methods (Trifonov et al., 2008).

Structural method. Following the new model, thrust zones must exist throughout the whole length of the mountain system irrespectively of changes of fold forms. According to the conventional model, thrusts seldom extend beyond the folds that the thrusts complicate.

Geomorphological method. Following the new model, the preorogenic peneplain is eroded near thrusts, and if it were preserved, it would be uplifted abnormally highly. According to the conventional model, the peneplain reaches its maximum height in the axial part of anticlinal ridges and lowered to their near-thrust edges.

Geological method. Following the new model, ascent metamorphosed rocks should expose in the most uplifted and eroded near-thrust part of the ridge. According to the conventional model, the distribution of rocks of different metamorphism grades is determined by their pre-Mesozoic history; near thrusts, there might occur weakly metamorphosed rocks exposed during shallow erosion.

Study of marginal thrusts at the boundary of uplifts and basins shows that in most of the region including the North and Central Tien Shan megazones, the Cenozoic thrusts and reverse faults usually do not extend beyond ridges and their magnitude vary along the strike. Locally on the northern flank of the CTS (Fig. 9, *a–c*) and within it (Fig. 9, *d*), the thrusts transform along their strike into overturned folds of the basement surface or are complicated by similar folds of the lower molasse series, with molasses being present in both fold limbs (Fig. 9, *e*). The thrust magnitude or its deformation is relatively small in all observed cases. In ridges, the peneplain surface outlines an anticlinal bend, and the Devonian-Permian weakly metamorphosed rocks are often exposed in the near-thrust marginal parts of the ridges. All this agrees with the conventional model.

A different pattern was observed in the zone of the Late Cenozoic Atbashi Fault at the boundary of the Atbashi Basin and the Atbashi Ridge that belongs to the South Tien Shan megazone (Trifonov et al., 2008). Where the Sarybulak stream flows into the Karakoyun River (western part of the structure), the fault zone is separated into two main strands. The northern strand borders the southern part of the basin. The strand runs along the Karakoyun River and is overlapped by the Late Quaternary alluvium. According to the geophysical data, the basement is subsided to 3–4 km north of the strand (Geological Map..., 1982). South of the strand, only thin Paleogene–Lower Miocene deposits are locally exposed. Near the Sarybulak stream, the Permian clay and silty slates and sandstones with cleavage cracks (dipped at 70° to the south) are stripped beneath glacial and fluvial deposits of the terrace cover. The southern strand of the fault zone dips at 60–70° to the south and forms a scarp separating the terrace from the highly uplifted ridge slope that is composed of metaterigenous quartz-sericite and, southward, quartz-mica schists tentatively dated to the Riphean (Fig. 9, *f*). Schistosity dips to the south; it dips at 70° just near the fault, and farther to the south, it is characterized by a steep dip in the upper part of the

slope, which decreases to 60° and then to 40° near the channel (Trifonov et al., 2008). Studies by apatite fission track thermochronology showed that the schists reached the subsurface as late as ~20 Ma (Sobel et al., 2000), though their presence in the upper horizons of the Earth's crust is related to the Hercynian nappe formation (Burtman, 2006). The near-fault ridge slope is strongly eroded and lacks relics of the preorogenic peneplain.

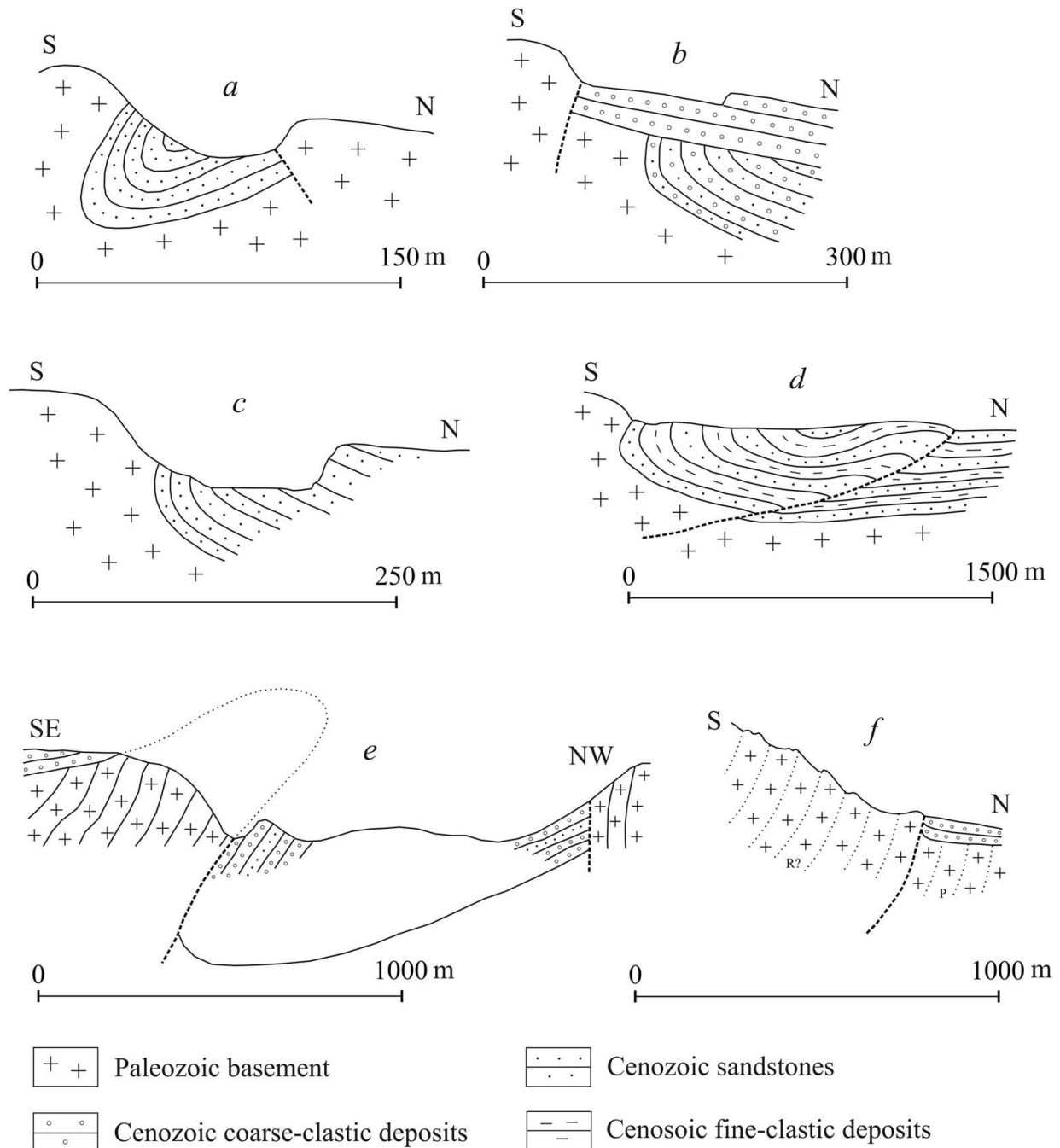


Fig. 9. Geological profiles across the boundaries of basins and uplifts in the Central Tien Shan, modified after (Trifonov et al., 2008): *a-c*, the northern flank of the Tien Shan: *a*, Chonkurchak, *b*, Dzhalamysh sai, *c*, Aksu River; *d*, southern edge of the Kochkor Basin; *e*, southern edge of the Toguz-Torou Basin (Shultz, 1948); *f*, southern edge of the Atbashi Basin along the Sarybulak Stream. The horizontal and vertical scales are equal

The reported data fit the new model better as compared with the conventional one and suggest that the Atbashi Fault is flattened at depth. Since the rocks exposed in its southern side might have been earlier situated at depths reaching 5 km (judging from the degree of their metamorphism) and the basement north of the fault zone is subsided to 3–4 km, the magnitude of the Late Cenozoic thrust is estimated at ~10 km. The thrust is listric; the increase in the uplift of its southern side toward the Khan-Tengri mountain plexus points to an increase in its magnitude and, correspondingly, shortening.

Large Late Cenozoic south-vergent thrusts were revealed in China along the southern flank of the Tien Shan (Deng Qidong, 2000; Recent geodynamics..., 2005). In the southern piedmont at the longitudes of Issyk-Kul and Khan-Tengri, the total magnitude of offsets on listric thrusts was estimated at 12–15 km (Yin et al., 1998). East of them, at the longitude of Lake Lobnor, the total shortening of the South Tien Shan is 20–40 km (Yin et al., 1998). Burtman (2012) reported similar estimates for the Eastern (Chinese) Tien Shan. With regard to the thrusts in the South Tien Shan megazone, the total Oligocene-Quaternary transverse shortening in the CTS is estimated at 50–70 km during ~30 Ma that yields the average rate of shortening of ~2 mm/a (Trifonov et al., 2008).

The obtained estimate ignores the strike slip along faults. The sinistral shift along the CTS is inferred from the en echelon mutual location of neotectonic structures (Makarov, 1990; Recent geodynamics..., 2005). We discover the Late Cenozoic longitudinal sinistral shifts in the K ok omeren-Minkush zone (Bachmanov et al., 2008) and on the northern slope of the Baibichetau Ridge (Trifonov et al., 2008). Dextral offsets and shear zones of the NW strike were revealed earlier (Bogachkin et al., 1997; Trifonov et al., 2002). Lacking detailed data on the magnitudes of slip along the faults, we admit that their contribution to the total Oligocene-Quaternary deformation is proportional to the contribution of active strike-slip faults to the total Late Quaternary deformation. With regard to the strike slip, the average rate of the Oligocene-Quaternary lateral CTS shortening might reach 2.5–3 mm/a that is 3–4 times lower than the rates of the Late Pleistocene–Holocene shortening. Thus the acceleration of horizontal movements during the Late Quaternary was lower than the acceleration of the Quaternary uplift.

Let us analyze the physical mechanisms responsible for the crustal uplift in the region.

1.2.3. Contribution of compression to crustal thickening and uplift in the Central Tien Shan

The represented data showed the following. In the Oligocene, the CTS paleotopography was at average heights of ~ 300 m. From Oligocene to the Early Pleistocene (beginning of the formation of the Sharpyldak unit), the average height of uplifts did not exceed 1.5 km, and the difference between the heights of uplifts and surfaces of adjacent basins was no more than 1 km. Based on these data and distribution of the uplifts and basins, we accepted that the average height of the CTS reached ~ 1 km by the Early Pleistocene. At present, the average height is ~ 3 km. Thus, the CTS was uplifted by on average ~ 700 m (up to ~ 1000 m in the NE of the region) from Oligocene to Early Pleistocene, i.e., for ~ 28 Myr, and by ~ 2 km for the last 2 Myr. In the SE and the east of the region, the height of the Quaternary uplift has been no less than 3 km. Based on the above data, Artyushkov estimated the role of compression of the Earth's crust in the Oligocene-Quaternary CTS uplift (Trifonov et al., 2008).

Let us denote the initial and final values of the width of compressed area and its thickness of the Earth's crust as L_0 , L_1 and h_0 , h_1 , respectively. Then, an increase in crustal thickness due to compression, Δh_{comp} , and crustal uplift $\Delta \zeta_{\text{comp}}$ under local isostasy are:

$$\Delta h_{\text{comp}} = h_1 - h_0 = [(L_0 - L_1) / L_1] h_0; \quad (1)$$

$$\Delta \zeta_{\text{comp}} = [(\rho_m - \rho_c) / \rho_m] \Delta h_{\text{comp}}, \quad (2)$$

where $\rho_m = 3330 \text{ kg/m}^3$ is the mantle density and ρ_c is the average crustal density. At present, the average width of the CTS is $L_1 \approx 400$ km. The Oligocene-Quaternary CTS shortening is $L_0 - L_1 = 50-70$ km, i.e. the initial width of the CTS was $L_0 = 450-470$ km. The average rate of the Late Quaternary shortening was ~ 10 mm/a. Taking this value for the last ~ 2 Myr, we obtain the CTS shortening $L'_1 - L_1 \approx 20$ km and the CTS width equal to $L'_1 \approx 420$ km ~ 2 Ma.

From Jurassic to Eocene, the CTS together with the southern part of Kazakhstan were a young platform. In the southern Kazakhstan, the thickness of the Earth's crust is ~ 42 km (Fig. 10). We accept that the same crustal thickness $h_0 = h_{\text{pl}} = 42$ km was also in the CTS in the Eocene. The average density of the platform crust is $\rho_c = 2830 \text{ kg/m}^3$ (Artyushkov, 1993; Christensen, Mooney, 1995). With these values of ρ_c and h_0 , we obtain that 2 Ma, when L_1 was equal to ~ 420 km, $\Delta h_{\text{comp}1}$ was 4.7–6.5 km and $\Delta \zeta_{\text{comp}1}$ was 0.7–1.0 km. The latter value is close to the above-given geological-geomorphological estimate of the CTS uplift that occurred by ~ 2 Ma (0.7–1.0 km).

Therefore, it is most likely that the CTS uplift that proceeded from Oligocene to the beginning of Pleistocene was mainly due to the compression of the Earth's crust.

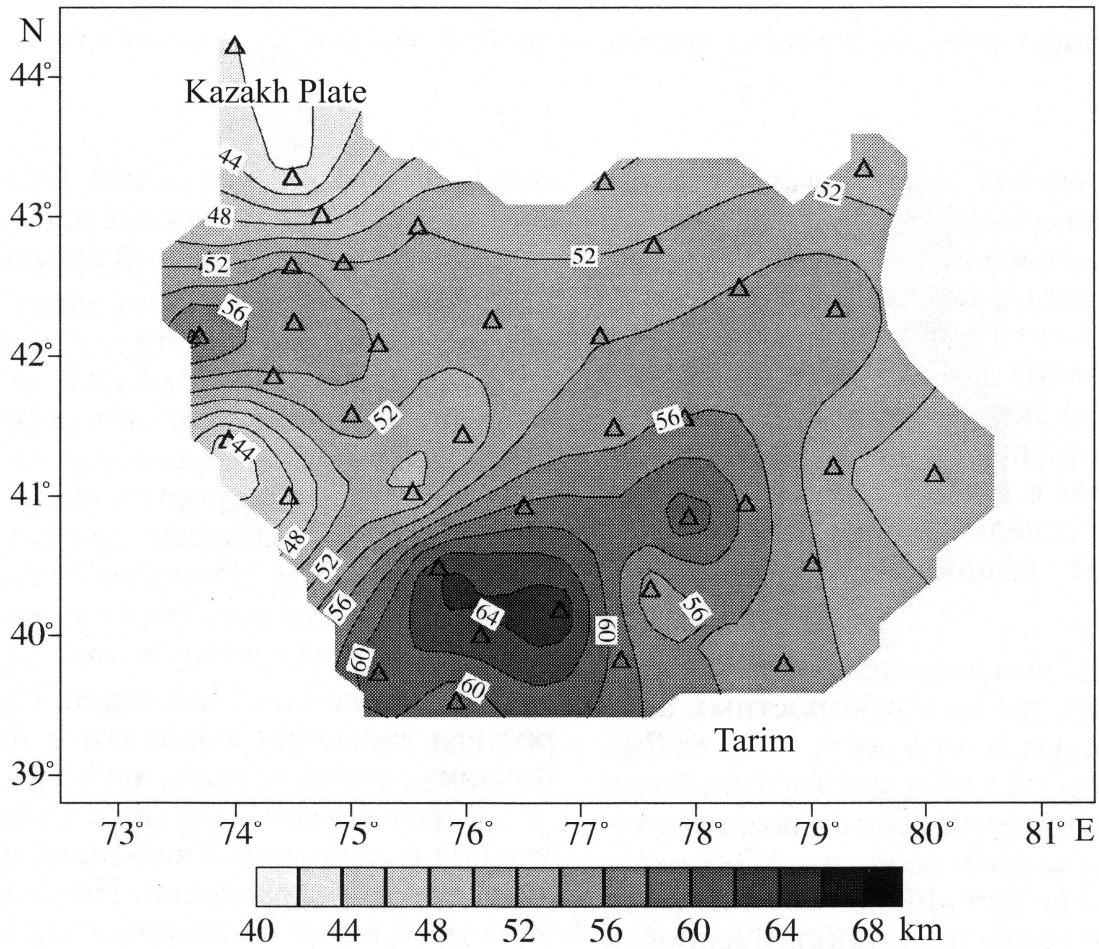


Fig. 10. The Earth's crust thickness in the Central Tien Shan, modified after (Vinnik et al., 2006). Triangles mark seismic stations

By the beginning of the accelerated uplift of the CTS ~ 2 Ma, the 4.7–6.5 km thickening of the crust must have increased its thickness to $h'_0 = 46.7\text{--}48.5$ km. Introducing this value as h_0 into (1) and assuming that $L_0 = L'_1 = 420$ km, from (1) and (2) we obtain the following values of crustal thickening and uplift for the last ~ 2 Myr: $\Delta h_{\text{comp}2} = 2.2\text{--}2.3$ km and $\Delta \zeta_{\text{comp}2} = 330\text{--}350$ m. The latter value is 6–9 times less than the actual 2–3 km uplift occurring for the last ~ 2 Ma. Even if accepting the average rate of shortening for the last ~ 2 Ma equal to the GPS rate of ~ 20 mm/a (Zubovich et al., 2010), the uplift due to the crustal compression will not exceed 650 m. This is only 22–32% of the actual uplift. The other portion requires other mechanisms for explanation.

The total Oligocene-Quaternary CTS uplift due to the crustal compression is $\Delta \zeta_{\text{comp}} = \Delta \zeta_{\text{comp}1} + \Delta \zeta_{\text{comp}2} \approx 1000\text{--}1300$ m.

1.2.4. The rise of the asthenosphere roof beneath the Central Tien Shan

Compared with the platform adjacent in the north, the velocities of transversal (V_S) and compression (V_P) waves beneath the Moho are significantly lower in the CTS mountains (Yudakhin, 1983; Lithosphere of the Tien Shan, 1986; Vinnik et al., 2004, 2006; Recent geodynamics..., 2005). This points to the ascent of the asthenosphere roof to the Earth's crust. According to the gravimetric data, deconsolidation of the mantle beneath the CTS reaches $\sim 0.1 \text{ g/cm}^3$ (Artemjev, Kaban, 1994). The rise of the asthenosphere roof is nonuniform throughout the region. Seismic data evidence that the asthenosphere roof reaches the Moho beneath high ridges and is separated from the crust by thick lenses of the lithosphere mantle beneath intermontane basins.

The replacement of the dense lithosphere mantle by the less compact asthenosphere matter (density ρ_a) must be accompanied by uplift of the crust. The uplift value is proportional to the squared thickness of the lithosphere mantle layer that has been replaced (Artyushkov, Hofmann, 1998). This value is unknown for the CTS, although negative isostatic gravity anomalies of up to -150 mGal were detected (Artemjev, Kaban, 1994). According to the Artyushkov calculation (Trifonov et al., 2008), these anomalies would correspond to anomalous masses $\Delta m \approx -3.6 \cdot 10^6 \text{ kg/m}^2$. The mantle deconsolidation leads to isostatic uplift of the crust by

$$\Delta \zeta_a = -\Delta m / \rho_a. \quad (3)$$

with $\Delta m \approx -3.6 \cdot 10^6 \text{ kg/m}^2$, $\Delta \zeta_a \approx 1.1 \text{ km}$. Since the width of areas with the above-mentioned anomaly intensity does not usually exceed 100 km , the anomalous masses in the mantle beneath them and the corresponding uplift of the crust can be greater. Assuming that $\Delta m \approx -7 \cdot 10^6 \text{ kg/m}^2$, we obtain from (3) that $\Delta \zeta_a \approx 2 \text{ km}$. In the most uplifted parts of the CTS, the deconsolidated mantle occurs in places immediately beneath the crust. This suggests that the uplift of the crust due to the asthenosphere rise might reach $\Delta \zeta_a = 1.5\text{--}2 \text{ km}$ there.

The complete or partial replacement of the mantle lithosphere by the asthenosphere takes place during a drastic softening of the former (Artyushkov, 2003). The softening is caused by the infiltration of active fluids from the underlying mantle into the lithosphere. This leads to a drastic decrease in viscosity and strength of rocks as a result of the Rebinder effect (Rebinder, Venstrem, 1937; Salnikov, Traskin, 1987).

1.2.5. Great thickness and density of the Central Tien Shan crust before its Cenozoic compression and possible transformation of the lower crust during the Quaternary uplift

As shown above, the compression of the CTS crust resulted in the increase in its thickness by $\Delta h_{\text{comp}} = \Delta h_{\text{comp1}} + \Delta h_{\text{comp2}} \approx 7\text{--}9$ km. The present-day thickness of the CTS crust varies from 40–52 km beneath a foredeep and largest intermontane basins to $h = 52\text{--}64$ km beneath ridges (Lithosphere of the Tien Shan, 1986; Recent geodynamics..., 2005; Vinnik et al., 2006) (Fig. 10). The crustal thickness beneath ridges is 10–22 km greater than that in the southern Kazakhstan ($h_0 = h_{\text{pl}} = 42$ km), which we accepted as the pre-orogenic thickness of the CTS crust by the Oligocene. The value of 10–22 km is 1.5–2.5 times greater than the calculated crustal thickening of the CTS crust due to the Cenozoic compression. Artyushkov paid attention to the following discrepancy (Trifonov et al., 2008). If the Cenozoic crustal thickening have been related to the compression only, the CTS crustal thickness by the Oligocene would have been $h_0 = h - \Delta h_{\text{comp}} \approx 45\text{--}55$ km, i.e., higher than h_{pl} by $\Delta h_0 \approx 3\text{--}13$ km. Introducing this value as Δh_{comp} into (2), we obtain that with the average crustal density $\rho_c = 2830$ kg/m³, typical of platforms, the CTS peneplain would have been localized at heights of $\sim 0.5\text{--}2$ km. In fact, its height was close to ~ 0.3 km. Artyushkov (Trifonov et al., 2008) suggested that the average crustal density was at that time higher than the usual platform density. Under isostatic equilibrium, it must have been 2900–3000 kg/m³. If this average density might have existed in the Eocene, the CTS lower crust had a layer of deeply metamorphosed basic rocks close in density to the mantle.

Heavy metabasites, garnet granulites and eclogites form in the lower crust of the fold belts as a result of phase transitions during strong compression (Artyushkov, 1993). In the CTS, they could have resulted from the Caledonian and Hercynian collision, when huge volumes of paleo-oceanic crustal matter got into the crust of the Northern and Southern Tien Shan, respectively (Kurenkov, 1983; Lomize et al., 1997; Burtman, 2006). Artyushkov (Trifonov et al., 2008) proposed a simplified model for the high-density crust that can be taken as a first approximation for the late Mesozoic and Eocene CTS. The upper layer of the crust is 42 km thick and has a density of 2830 kg/m³; beneath it, there is the 3–13 km thick layer of garnet granulites and eclogites that is close in density to the upper mantle.

The ascent of the hot lower-density asthenosphere to the uppermost mantle might have been accompanied by two processes in the lower crust (Artyushkov, 1993).

Eclogites and basic garnet granulites, denser than the asthenosphere matter, were replaced by it, being detached from the crust and submerged together with the lithosphere mantle. Under influence of the asthenosphere fluids, garnet granulites, less dense than the lithosphere mantle and asthenosphere, might have undergone the retrograde metamorphism accompanied by the serpentinization of neighboring peridotites. This led to the deconsolidation and, correspondingly, additional uplift of the land surface. Since the Oligocene, the CTS has uplifted as a result of compression to ~1–1.3 km, and the uplift due to the asthenosphere ascent and replacing of the lithosphere mantle might have reached 1.1–2 km. In total, this yields the uplift of ~2.5–3 km that is commensurate with the actual average uplift of ≥ 3 km. Therefore, the possible additional uplift due to the lower-crust deconsolidation did not probably exceed 0.5 km.

1.2.6. Relative significance of different processes producing neotectonic uplift of the Central Tien Shan

The performed analysis of the data permitted to describe the neotectonic evolution of the CTS as the following (Trifonov et al., 2008). By the Early Paleogene, the surface of the Earth's crust (Paleozoic basement) was situated at a small height above the sea level. The density of the upper layer of the crust, ~42 km thick, was close to the average density of the crust in platform regions. Beneath this layer, there was a layer of garnet granulites and eclogites with an average density close to the mantle one. The boundary between the lower crustal layer and the mantle lithosphere was probably very uneven and uncertain. The Early Cenozoic basaltic eruptions indicate a possible ascent of small volumes of deep-seated mantle matter containing active fluids, to the lithosphere. Later the infiltration of fluids increased that reduced the lithosphere strength. In the Oligocene, under the compression caused ultimately by the India-Eurasia collision, the lithosphere including the Earth's crust was subjected to folding and faulting. From the Oligocene to the Pliocene, i.e., over the period of ~28 Myr, the average rate of crustal lateral shortening was ~2 mm/year. The compression led to a slow isostatic uplift of the crust, and its average height reached 1–1.3 km by the beginning of Pleistocene.

By the Late Pliocene or Early Pleistocene, large portions of the asthenosphere matter that were enriched by fluids, penetrated beneath the CTS. Infiltration of the fluids into the lithosphere drastically reduced the viscosity of the latter. The deconsolidated lithosphere was detached into layers along the surfaces with the

highest gradient of the deformational properties. The detached lithosphere mantle began rapidly to destruct, submerge, and be convectively replaced by the matter of the hot and less dense asthenosphere that resulted in the rapid uplift of the CTS in the last ~ 2 Myr. This process was most intensive beneath ridge zones, where the asthenosphere closely approached the base of the crust (Lithosphere of the Tien Shan, 1986; Vinnik et al., 2006). Beneath the crust of large intermontane basins, lenses of the lithospheric mantle had been preserved; therefore, the basins rose to a smaller height than the ridges. Unlike the subsided heavy lithospheric mantle including the garnet granulites and eclogites of the crustal origin, the high-pressure metabasites, less consolidated than the asthenosphere, remained near the Moho. As the crust was uplifted, they transferred into the stability fields of less consolidated basites. After the supply of the cooled asthenosphere fluids, these rocks underwent the retrograde metamorphism that led to their partial deconsolidation and, as a consequence, the additional uplift of the crust during the last ~ 2 Myr.

In general, the Oligocene-Quaternary collision compression of the Earth's crust led to ~ 1 – 1.3 km uplift of the CTS; the replacement of the lithospheric mantle by the asthenosphere produced 1.1 to 2 km of the uplift in different parts of the region; and the probable metamorphic deconsolidation of metabasites near the crust-mantle boundary gave ~ 0.5 km of the uplift (Trifonov et al., 2008). These three processes gave rise to the mountain system of ≥ 3 km in average height. The proportion between influence of each of the processes is about 7/10/3.

Relative significance of three mentioned processes changed in time. During the long period from the Oligocene to the beginning of Pleistocene (~ 28 Myr), the collision compression was the only factor responsible for the slow rise of neotectonic structures. Its average magnitude reached 0.7–1 km. In the Quaternary, during the last ~ 2 Myr, the compression intensified and the average rate of the shortening increased probably 3–4 times. Nevertheless, the contribution of the compression into the total rise was limited only by 11–17%. Two other factors that had not acted before, were mainly responsible for the rapid uplift of the CTS during the last ~ 2 Myr. They were the replacement of the lithospheric mantle by the asthenosphere and the metamorphic deconsolidation of metabasites near the crust-mantle boundary. Their contribution to the total uplift in the last ~ 2 Myr is estimated approximately at 60–70% and 20–25%, respectively.

1.3. Neotectonic evolution of the Pamirs and surrounding

The mountain system of Pamirs consists of topographic features convex to the north. The eastern Pamirs is the high-elevated plateau that represents the axial part of this arc. Ridges of the western Pamirs strike to the NE–SW and ridges of its eastern (Chinese) termination strike to the NW–SE. More southern mountain systems, the Hindu Kush and Karakorum and the Kohistan and Ladakh, have the same arc-type pattern, which reflects the Mesozoic tectonic zonation of the region. All these tectonic zones and topographic features form the Pamir-Penjab syntaxis. This is an area of intense tectonic deformation related to Neotethys closure. Collision at its northern flank was accompanied by volcanic activity and large-scale granite formation that testifies to heating of the Earth's crust. This heating could promote delamination of the crust along surfaces with the highest gradient of mechanical properties. Such delamination provides differentiated displacements of crustal sheets and blocks under variously oriented horizontal compression. By the end of Miocene, this resulted in substantial disturbance of isostatic equilibrium, which was produced by compressive thickening of the Earth's crust and decrease of density of the lithospheric mantle and stimulated intense and contrasting vertical movements in the Pliocene and Quaternary.

The present-day tectonic zoning of the syntaxis [Desio, 1976; Shvolman, 1980; Shvolman, Pashkov, 1986; Geological Map of the Tajik SSR..., 1989; Ruzhentsev, 1990; Searle, 1991; Gaetani, 1997, Burtman, Samygin, 2001; Pashkov, Budanov, 2003) (Fig. 11 & 12) reflects its crustal structure, which was formed as a result of multifold deformational events during the stage-by-stage closure of the Tethys. The existing structural pattern was eventually formed at the late collision stage following the closure of the Neotethys. This span of time corresponds to the neotectonic epoch lasting from the Oligocene to the Recent (Trifonov, 1999). This period is subdivided into the early stage (Oligocene–Miocene), when heating and tectonic delamination of the crust were the most important factors of tectogenesis; the late stage commenced in the Pliocene–Quaternary, when the role of these processes decreased and intense vertical movements were occurring.

1.3.1. Mesozoic zoning and its deformation due to neotectonics

In the present-day structure of the eastern Pamirs, the consecutive series of tectonic zones exhibits the evolution of the early Mesotethys. The Hercynides of the Northern Pamirs, where the main structure-forming processes ceased by the end of the

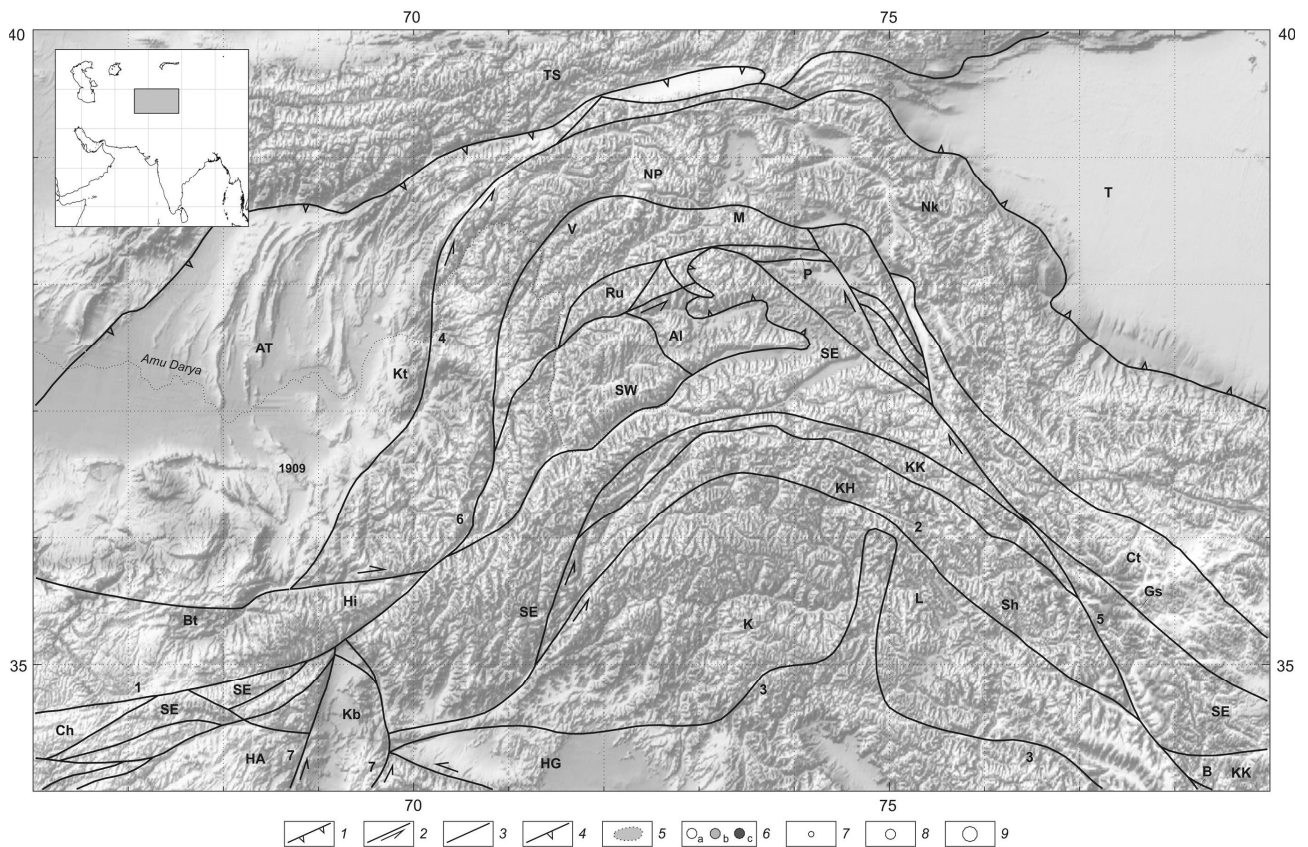


Fig. 11. The orographic map of the Pamir–Karakorum region and its surrounding with contours of tectonic zones that are shown in fig. 12, modified after (Ivanova, Trifonov, 2005). Symbols of the tectonic zones are the same as in fig 12

Paleozoic, developed in the Triassic as a volcanic arc at the active northern flank of the basin underlain by oceanic crust. The arc is marked by Triassic subduction-related granites and calc-alkaline volcanics. The nonvolcanic part of the arc that comprised continental blocks of the Central Pamirs, heterogeneous in their geological history and structure, accreted to the Hercynides during the Permian after the closure of the Paleotethys. In the considered part of the region, the Central Pamirs, represented by the Muzkol Zone (Ruzhentsev, 1990), is underlain by crust 60–65 km thick; its lower part (approximately 35 km) is seismically homogeneous (Seismic models..., 1980; Pamirs–Himalayas..., 1982). The basin itself is designated by the Pshart Suture, where the Upper Permian–Triassic sequence is largely composed of clayey and cherty slates, basalts, and basaltic andesites; volcanics prevail in its Upper Triassic portion (Pashkov, Budanov, 2003). This sequence is overlain with unconformity by Norian (?) volcanogenic and terrigenous rocks with olistoliths of Paleozoic limestone. Northward, in the western Pshart and the northern Dunkeldin blocks, the Permian–Triassic calcareous–terrigenous sequences with sporadic volcanics mark the northern periphery of the basin (Pashkov, Budanov, 2003). Its southern periphery is made up of an allochthon of the South-Eastern Pamirs, where relatively deep-water flyschoid

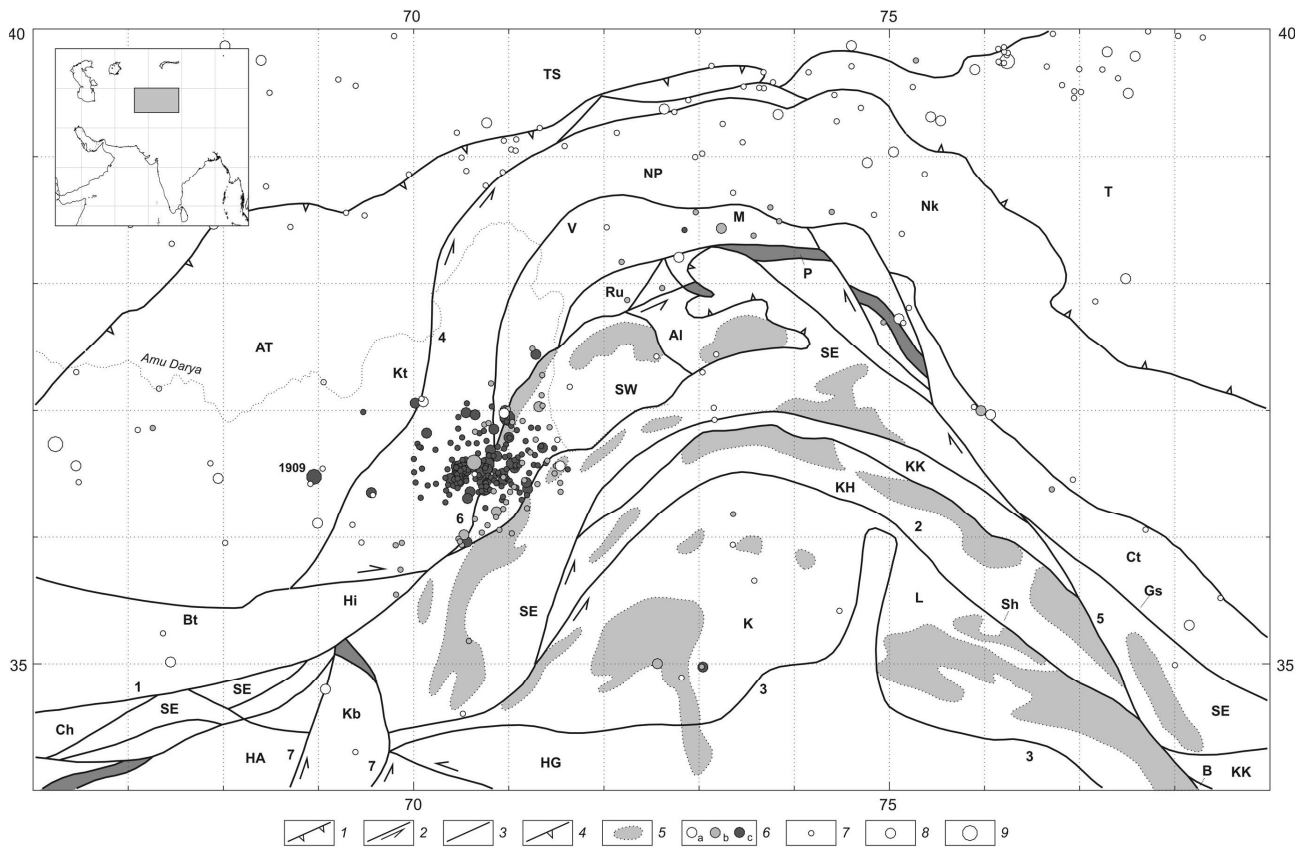


Fig. 12. The Pamir–Karakorum region, modified after (Ivanova, Trifonov, 2005): tectonic zones after (Burtman, Samygin, 2001; Desio, 1976; Gaetani, 1997; Pashkov, Budanov, 2003; Ruzhentsev, 1990; Searle, 1991; Shvolman, 1980), granitic nagmatism after (Desio, 1976; Geological Map of the Tajik S.S.R., 1989), and epicenters of strong earthquakes ($M_S \geq 5.7$)

1, nappes and thrusts; 2, strike-slip faults; 3, other major faults; 4, boundaries of basins; 5, granitic batholiths that continued to develop in the Miocene; 6, epicenters of earthquakes with different depths (h) of hypocenters: a , $h \leq 70$ km, b , $70 < h < 150$ km, c , $h \geq 150$ km; 7–9, magnitudes of earthquakes: 7, $M_S = 5.7–6.5$, 8, $M_S = 6.6–7.4$, 9, $M_S = 7.4–8.3$.

Tectonic zones: AT, Afghan-Tajik Basin with the Kulyab trough (Kt); T, Tarim Basin; NP, North Pamir zone and its continuations: Nk, NW Kunlun, Hi, Western Hindu Kush, and Bt, Bandi-Turkestan; zones of the Central Pamir type: M, Muzlol, V, Vanch, SW, South-Western Pamir and Badakhshan, AI, Alichur Block, Ru, Rushan zone, Kb, Kabul Block, Ct, continuation of the Central Pamir zone in Tibet, and Ch, fragments of the Central Pamir type in the Herat fault zone in Afghanistan; P, Pshart suture and its continuations (shown by dark-grey color): Db, Dunkeldin Block, Gs, its Tibetan continuation that continues to the SE as the Ganmatso-Shuanhu suture, Vf, Vatasaiif fragment, Ar, Altimur ophiolites, and H, Khashrud zone; SE, the South-Eastern Pamir and Nuristan zone and its continuations; KK, the North Karakorum zone and its Tibetan continuation; HA, Helmand-Argandab Block; KH, the Southern Karakorum and Eastern Hindu Kush zone; Sh, Shyok suture, and B, Bangun suture; K, Kohistan, and L, Ladakh; HG, the Khazar segment of the Himalayas. Batholiths: 1, Bagarak; 2, Karakorum; 3, Kohistan; 4, Lagman; and 5, Shugnan. Faults: 6, Alichur Thrust; 7, Andarab strike-slip fault; 8, Herat (Main Herirud) fault zone; 9, Main Karakorum Thrust; 10, Main Mantle Thrust; 11, Gunt Fault; 12, Darvaz reverse-sinistral fault; 13, Zebak Fault; 14, Kunar-Tashkupruk zone; 15, Pamir-Karakorum strike-slip fault; 16, Central Pamir Fault; 17, Chaman strike-slip fault

facies of the passive slope give way to the carbonate platform facies (Ruzhentsev, 1968, 1990). Both of these facies extends toward Nuristan (Geology and Mineral Resources..., 1980). The similarity in the early collision evolution of the Pshart and

South-Eastern Pamir–Nuristan regions is expressed in the pre-Jurassic unconformity (Pashkov, Budanov, 2003) and in the occurrence of Cretaceous orogenic complex (Shvolman, 1977).

Farther southward, there is a succession of tectonic zones related to the late Mesotethys and Neotethys:

(1) The Northern Karakorum is underlain by the Proterozoic–Cambrian continental basement overlapped by the polycyclic Ordovician–Jurassic cover, with carbonate rocks prevailing over terrigenous sediments and with signatures of the mid-Cretaceous orogeny (Gaetani, 1997);

(2) The Southern Karakorum and the Eastern Hindu Kush that reveal intense regional metamorphism, enclose an axial batholith in the north, and are bordered by the Main Karakorum Thrust Fault in the south (Gaetani, 1997); the eastern part of this fault controls the Shyok Suture, a relict of the backarc (?) basin of the late Mesotethys that closed in the mid-Cretaceous, which is represented now by ophiolite melange (Searle, 1991);

(3) The Kohistan and Ladakh volcanic arc of the Neotethys with large granitic batholiths; the base of this section (ultramafics and garnet granulites overlain by amphibolites and gabbro-norites) is exposed in the southern part of the zone, where it is bordered by the Main Mantle Thrust Fault (Khain, 2001).

This zonal pattern of the Pamir–Karakorum region likely indicates that the relative location of zones has remained principally unchanged since the late Mesozoic (the neotectonic period included). The following tectonic units among the Afghan zones serve as the most definite analogs of the Pamirs–Karakorum zones: the volcanic arc of the early Mesotethys inheriting the Hercynides in the Hindu Kush and Bandi-Turkestan and the Quetta ophiolite zone (the Neotethys suture). The latter soundly correlated with ophiolite of the Indus–Zangbo Zone as the southeastern extension of the Ladakh Zone (Gansser, 1966). The Altimur allochthonous ophiolite melange in the northern Kabul Block composed of peridotites, pillow lavas, tuffs, and cherts that are overlain by limestone with poorly preserved Jurassic (?) fauna (Tapponnier et al., 1981) is probably an analog of the Pshart Suture.

Westward, in central Afghanistan, the SW-trending ophiolitic Khashrud Zone branches out the Herat (Main Herirud) Fault. The Upper Jurassic–Hauterivian sequence of this zone is composed of basic and intermediate volcanics replaced upward by sandy–clayish sediments; ultramafics and gabbrodiorite intrusions are widespread (Geology and Mineral Resources..., 1980). It is assumed that this section

accumulated in a trough underlain by oceanic crust (Sborshchikov, 1988). The fact that, at the northwestern periphery of the trough, the Upper Jurassic volcanics are underlain by Rhaetian–Liassic sandstones and slates, as well as by Upper Permian–Norian calcareous–terrigenous rocks alternating with basic and intermediate volcanics (Geology and Mineral Resources..., 1980), points to almost coeval origination of the Khashrud and Pshart basins. It can be assumed that the Khashrud ophiolite is a fragment of the Pshart Basin extension, which continued to evolve, in contrast to the Pamirs, in the Jurassic and Early Cretaceous. Its evolution terminated by the mid-Cretaceous, as is evident from the unconformity at the base of calcareous–terrigenous partly red-colored Aptian–Upper Cretaceous sequence.

Tectonic blocks with structural features similar to those of the southeastern Pamirs and Nuristan are indicated in the zone of the Herat (Main Herirud) Fault. Gaetani (1997) notes the similarity in sedimentary covers of the northern Karakorum and the Helmand–Argandab continental massif bordered by the Khashrud ophiolite in the northwest. The Shyok Suture appears to be coeval with the Tarnak Suture at the southeastern flank of this massif (Sborshchikov, 1988).

Thus, the systems of the Mesozoic tectonic zones in the Pamirs and Afghanistan are similar, although there is no complete identity between them. However, most of the zones, which can be regarded as analogs, are tectonically separated by faults that extend along the western flank of the Pamirs and Badakhshan (Geology and Mineral Resources..., 1980; Geological Map of the Tadjik SSR..., 1989). Here, in the Vanch Zone of the central Pamirs and tectonic nappes of the Rushan Zone corresponding to the northern margin of the Pshart Basin, the Earth's crust is thinned to 50–55 km and its granitic–gneissic portion (approximately 35 km) rests upon the layer defined by seismic velocities like a mantle–crust mixture (Khamrabaev, 1980). This layer can be a relic of the early Mesotethys oceanic crust. The Vanch and Rushan zones pinch out southeastward, and the extension of the northern Pamirs borders along the steep Central Pamir Fault on the Archaean metamorphic massif of the West Pamir–Badakhshan zone. Thrusting of the Shakh dara Group over the Goran Group in the Precambrian resulted in a doubled section of the massif. Tectonic sheets at the contact are composed of the rocks pertaining to the Khorog unit and are formed in the lower crust close to the Moho discontinuity (The Earth's crust and upper mantle..., 1981; Budanova, Budanov, 1983; Ruzhentsev, 1990). Contacts of the massif with neighboring zones are either tectonic or sealed by Cenozoic granites. Its margins experienced maximum Cenozoic tectono-metamorphic reworking (Budanova, Budanov, 1983). The Kabul Block separates the northern Karakorum and the

Helmand–Argandab Massif, as well as Nuristan and its probable extension in the Herat Fault Zone. The Precambrian basement of the Kabul Block is overlain by the Upper Precambrian–Lower Paleozoic metaterrigenous complex and by the Upper Paleozoic complex, including the Upper Permian–Norian carbonate rocks. The Kabul Block is similar in this respect to the Muzkol Zone of the Central Pamirs (Geology and Mineral Resources..., 1980; Pashkov, Budanov, 2003).

The southwestern Pamir–Badakhshan Massif has been studied better as compared with the poorly explored Kabul Block. The southeastern tectonic boundary of the massif with Nuristan is marked by the Lagman Batholith that dates to the Oligocene–Miocene up to 16.5 Ma (Geology and Mineral Resources..., 1980). Northward, the Bagarak Batholith, 32–19.5 Ma in age (Geology and Mineral Resources..., 1980), extends along the boundary with the Central Pamirs. The batholith contacts, sharp intrusive in the northwest and complicated by numerous local injections in the southeast, suggest that the batholith (and, correspondingly, the boundary of the zones) plunges beneath the Archaean complexes (The Earth's crust and upper mantle..., 1981). To the east, at the boundary of Precambrian rocks with the Rushan Zone, a similar plunge of the Alichur Thrust is confirmed by geologic observations (Ruzhentsev, 1968). South of this thrust, the Precambrian–Paleozoic Alichur Group of metamorphic rocks crops out between Archean rocks and allochthon of the South-Eastern Pamirs. The Vatasaiif fragment of the Pshart Suture, where Triassic volcanogenic rocks are overlain with unconformity by Jurassic strata, is retained farther to the east (Pashkov, Budanov, 1990, 2003). Boundaries between all these complexes are either tectonic or concealed by granites. The isotopic age of the largest Shugnan Batholith is estimated as 32–21 Ma; the recurrent metamorphism of older sequences took place approximately at the same time, 32–9 Ma ago (Shvolman, 1977).

The relationships described above suggest that the South-Western Pamir Massif has occupied its present-day location only recently, and the age of the boundary batholith emplacement corresponds to tectonic convergence of the South-Western and South-Eastern Pamirs. We suggest that the Triassic–Jurassic facial zones of the South-Eastern Pamirs that initially extend parallel to the Pshart Suture were curved during this convergence and formed an arc with the western margin that trends parallel to the boundary of the South-Western Pamirs. Judging from the bend configuration, the amplitude of the eastward or northeastward offset of the South-Western Pamirs could exceed 150 km. Thereby, the sedimentary sequences of the South-Eastern Pamirs were involved in the thrusting, and later, in the Pliocene and

Quaternary, they were subjected to strike-slip movements (Ruzhentsev, 1968). The Pshart Suture was also involved in bending that is evident from the location of its Vatasaiif fragment. The area with the exposed Alichur Group, which is probably a subsided continuation of the South-Western Pamirs, also changed its location and was deformed.

According to the geophysical data, the granitic-gneissic complex of the South-Western Pamirs is 25 km thick, while the total thickness of the crust reaches approximately 60 km (The Earth's crust and upper mantle..., 1981). A part of the displaced complex likely overlapped the crystalline basement of the South-Eastern Pamirs that reaches a thickness of 30 km. To determine the initial structural setting of the complex, it is important to note that it could not be an element of the northern Pamirs, because no indications of Paleozoic and Early Mesozoic magmatism of this zone are known. Thus, it was probably an element of the Central Pamirs.

The Precambrian clastic material derived from the South-Western Pamirs is missing in the Upper Mesozoic and Lower Cenozoic sequences of adjacent zones and first appears in the immediate vicinity of the massif only in Oligocene sediments (Shvolman, 1977). This implies that the Precambrian complex was initially covered by sediments, fragments of which are represented by the Permian–Triassic sequence of the Central-Pamir type in the Zebak Fault Zone at the southern flank of the massif (Geology and Mineral Resources..., 1980). This might be responsible for the formation of the allochthonous series of the Vanch–Muzkol segment of the Central Pamirs, the nappe structure of which is a result of neotectonic movements, because it involves Upper Cretaceous and Paleogene strata (Ruzhentsev, 1990). In the opinion of Ruzhentsev (1971), the recumbent folds characteristic of the early deformation stage began to form here in the mid-Cretaceous or in the Paleogene and continued to develop until the Neogene, because they involve Paleogene sediments. Later, already in more recent times, structures of sedimentary cover of the Vanch Zone, where the root belts of nappes have been formed, were thrust over southerly and easterly areas of the Central Pamirs, the Muzkol Zone inclusive. Other authors (Leonov, Sigachev, 1984; Leonov, Nikonov, 1988; Sigachev, 1990) provided persuasive structural arguments in favor of thrusting from the south. Pashkov and Budanov (2003) assumed that the nappe rocks originated in the Kunar-Tashkupruk zone between the South-Eastern Pamirs and the Karakorum. We suppose that they originated nearer to their present-day location and are a detached cover of the displaced South-Western Pamir–Badakhshan Zone. The detachment was stimulated by heating and

delamination of the massif that is reflected in intense generation of Cenozoic granites (the Shugnan Batholith) and by the uplift that followed the crust thickening.

Thus, the most evident deformation of the Mesozoic tectonic zoning caused by neotectonic deformation and offsets is confined to the transition between the Pamirs and Afghanistan; it is manifested first of all by the displacement of the massif of the South-Western Pamirs and Badakhshan.

1.3.2. The Pamirs and Afghan–Tajik Basin

The Afghan–Tajik and Tarim basins filled with Upper Cenozoic molasses are located on both sides of the northward-convex zone of the northern Pamirs. The Tarim Basin rests largely upon the Precambrian basement. The Afghan–Tajik Depression is a sedimentary basin with a heterogeneous basement that was consolidated by the end of the Paleozoic and probably inherited an ancient crystalline massif. The basin is filled with a thick (up to 18 km) sequence of alternating shallow-water and continental deposits or only continental (since the Oligocene) sediments. Compositionally similar Cretaceous and Cenozoic sequences extend along the northern periphery of the Pamirs and form its outer zone. In the northeast, the northern Pamirs is thrust over molasses of the Tarim Basin (Ding Guoyu, 1984), and this probably resulted in crust thickening to 75–80 km (Seismic models..., 1980; Pamirs–Himalayas..., 1982). To the west, the Northern Pamirs is thrust over the outer zone that determined its present-day structure (Neotectonics and recent geodynamics..., 1988). A waveguide with V_p of 6.0–6.3 km/s (Khamrabaev, 1980; Pamirs–Himalayas..., 1982; Makarov et al., 1982) at a depth of 5–10 km under crystalline rocks of the northern Pamirs favored this process.

The thrusting was accompanied by development of the fold structure in the Afghan–Tajik Basin, the formation of which was strongly influenced by the detachment of the 5–6-km-thick Cretaceous–Miocene cover along the Malm salt-bearing sequence (Zakharov, 1958; Becker, 1996). This growth of folds fell mainly in the late neotectonic stage, and the first regional unconformity in the molasse section that reflects this event is dated as the Late Miocene. During the folding, the sedimentation basin experienced differentiation, and the Kulyab Trough located in its eastern part accumulated 11 km of Pliocene–Quaternary sediments of the 17-km total of sedimentary cover. The folding and accumulation of young molasses transformed the crust beneath the depression. Its Cretaceous and Paleogene structure can be judged from the weakly deformed section in the Kurgan-Tyube area. The crust is

approximately 35 km thick there, and the thickness of its crystalline part is less than 20 km (The Earth's crust and upper mantle..., 1981).

The magnitude of the Northern Pamirs thrusting over the neighboring depressions is critical for estimating neotectonic deformations. Based on paleomagnetic studies of Cretaceous–Paleogene sediments in the Afghan–Tajik Basin (Bazhenov, Burtman, 1990) and on facies distribution, Burtman (1999) arrived at the conclusion that the Northern Pamirs was thrust over the eastern part of the Cretaceous–Paleogene trough approximately at 300 km. The sedimentary cover was detached and folded in the retained part of the basin (Becker, 1996; Burtman, 1999). We assume that the magnitude of overthrusting could have been less, particularly in the eastern part of the Pamirs. There are two reasons for this. First, the Cretaceous–Paleogene trough might have become narrower eastward prior to the neotectonic stage due to framing of ancient massifs by the Hercynides. Second, in the western Pamirs, conditions of the Hercynian complex thrusting over the thinned crust of the central part of the basin were more favorable than in the east, where the crust was normal. As concerns the folding controlled by the general detachment and displacement of sedimentary cover, this mechanism is acceptable only for the northern part of the basin and becomes doubtful in its southern part, where the detached anticlinal zones are separated by sizeable depressions that remain almost undeformed. That is why a more complex mechanism of folding has been proposed. This mechanism takes into account the change of sedimentary rock volume in response to its chemical alteration (Zakharov, 1958).

Thus, the fact that the northern Pamirs is thrust over the Afghan–Tajik Basin and partially overlaps its eastern part is beyond doubt, although the amplitude of overthrusting remains debatable. In any event, it is at least 100 km large.

Comparative analysis of the Oligocene-Quaternary sections of the closest to the Pamirs eastern part (near the Darvaz Ridge) and the central part of the Afghan–Tajik Basin is important to understand a history of neotectonic uplift in the Pamirs. The base of these sections is represented by the lower Sumsar and upper Shurysay beds that demonstrate a change of the Eocene mainly marine sedimentation to the younger continental one. The Shurysay Beds contain the Upper Oligocene fossils. All younger deposits belong to the fluvial or subaerial continental types of sedimentation. They are divided to several units (International Symposium..., 1977).

The Baljuan unit is represented in the eastern part of the basin by red sandstones and siltstones with gravelstone and conglomerate interbeds (Fig. 13). Their thickness

is up to 1200 m. In the central part of the basin, they are replaced by sandstones, siltstones, and shales.

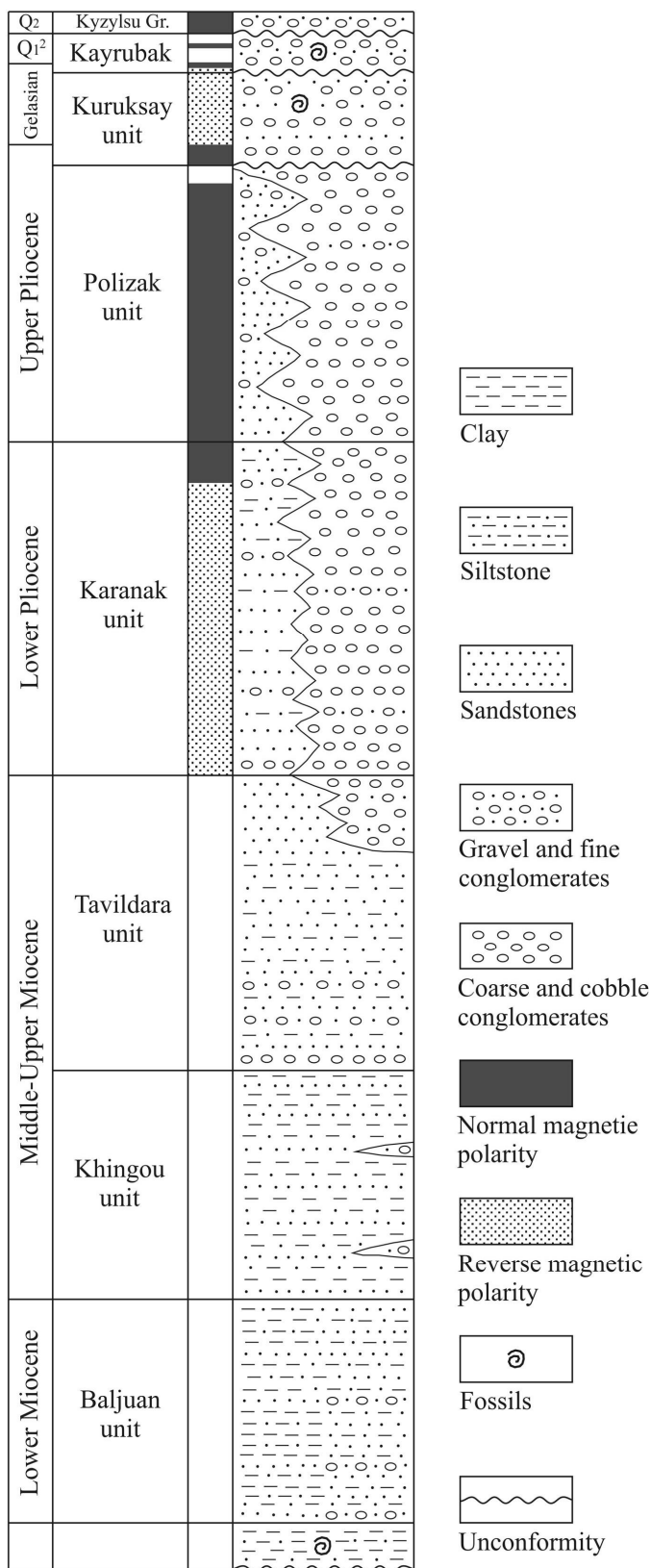


Fig. 13. Composite section of the Oligocene-Quaternary molasses in the eastern Afghan-Tajik Basin, compiled after (International Symposium..., 1977)

The alluvial sections of the Khingou unit are composed near the Darvaz Ridge of alternating variegated (mainly brown-colored, red-colored and grey) sandstones, siltstones and shales with conglomerate lenses that were sedimented by temporal streams. Thickness varies from 400 m to 1700 m. The following Tavildara unit consists of three members in the Darvaz foothills. A member of alternating layers of red-brown and brownish-grey siltstones, sandstones, and conglomerates occurs at the base of the unit. Higher up, there occur brownish-grey sandstones with siltstone interbeds. The unit is crowned with strata of grey conglomerates that disappear to the south and west of the town of Kulyab. Total thickness of the Tavildara unit is up to 1600 m. In the central basin, two mentioned units are replaced by the Kafirnigan unit that is composed of grey sandstones with interbeds of brown siltstones.

The up to 1800 m thick Karanak unit consists of coarse and cobble conglomerates near the Darvaz Ridge. They contain rare lenses of brown siltstones. In the central basin, the unit is mainly composed of fine-grained sediments. The next Polizak unit is represented in the Darvaz foothills by over 1500 m sequence of grey coarse

and cobble conglomerates. Southwestwards, conglomerates gradually change to sandstones. In the central basin, the Polizak deposits are partially denuded and cannot often be distinguished in the younger strata.

The younger units demonstrate change of the basin regime of sedimentation to the terrace one. Correspondingly, the younger units are distributed locally and have smaller thickness. These deposits were primary recognized as the Kulyab group. Later it was divided into the Kuruksay and Kayrubak units (International Symposium..., 1977). The Kuruksay unit covers the older molasses with angular unconformity. The unit is represented in the Kuruksay River by 180–200-meter thick sequence of coarse clastic material with predominance of boulder gravels. Other sections of the unit contain lenses and layers of sand and silt. The maximum registered thickness of the unit is 500 m, The Kayrubak unit covers the older deposits also with unconformity and consists of rhythmically alternating pebble and sand layers up to 200 m thick totally. This type of Kuruksay and Kayrubak deposits represents alluvial sedimentation. At the same time, alternation of loess-like silts and carbonate paleosoils were accumulated on watershed slopes. There were found signs of a synchronism between coarser members of fluvial sections and paleo-soil horizons within the Kayrubak unit (International Symposium..., 1977). The younger units form the Kyzylsu group that is represented by loess-soil and fluvial deposits. The fluvial deposits compose series of terraces set into the older molasse formations. Their total thickness is up to 120 m.

The units mentioned above are dated by combination of paleomagnetic and paleontological data together with geological correlation of the units (International Symposium..., 1977). The Baljuan unit is assigned to the Lower Miocene by its occurrence: according to paleontological data, the underlying Shurysay beds are correlated with Upper Oligocene and the overlying Kafirnigan unit corresponds to the Middle to Upper Miocene. The last estimate is based on the find of a skull of *Mastodon cf. angustidens* in the upper part of the Kafirnigan unit and gives also the age of the Khingou and Tavildara units that are correlated with the Kafirnigan one.

The lower part of the Karanak unit, as well as the upper part of the Tavildara unit are characterized by reverse magnetic polarity. The uppermost part of the Karanak unit, the Polizak unit, and the lowest part of the Kuruksay unit demonstrate normal polarity (the Gauss chron). The upper and main part of the Kuruksay unit as well as the Kayrubak unit and the upper terrace deposits of the Kyzylsu group show reverse polarity (the Matuyama chron). Two episodes of normal polarity were found within the Kayrubak unit and identified as the Jaramillo and Olduvai subchrons. All younger

deposits of the Kyzylsu group have normal polarity (the Brunhes chron). Mammal remnants from the upper Kuruksay deposits were attributed to the middle Villafrancian and the fauna from the upper Kayrubak bone beds was identified as post-Villafrancian (International Symposium..., 1977). These data give a possibility to assign the Karanak unit to the Lower Pliocene, the Polizak unit to the Upper Pliocene, the Kuruksay unit to the lower part of the Lower Pleistocene (Gelasian), and the Kayrubak unit to the upper part of the Lower Pleistocene (Calabrian, probably including the uppermost Gelasian). The Kyzylsu group is attributed to the Middle and Upper Pleistocene.

The analysis of composition and age of different molasse units show that the Pamir region did not highly rise till the Upper Miocene. Signs of local mountain uplifts arrived in the Late Miocene, but the total uplift with erosion and transportation of coarse clastic material including boulders occurred only in the Pliocene–Quaternary.

1.3.3. Recent geodynamics of the Pamir–Hindu Kush region

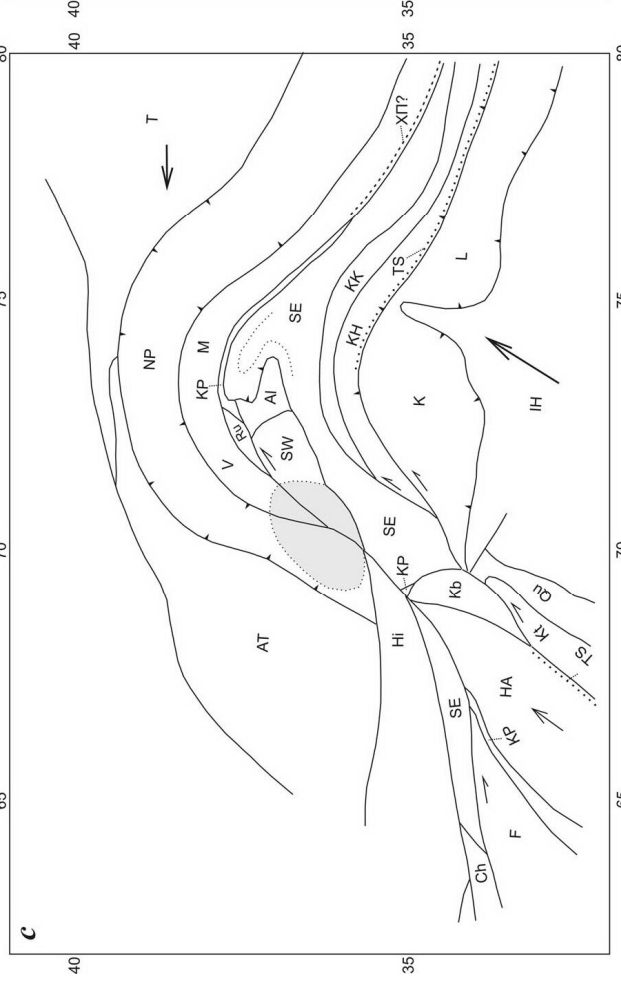
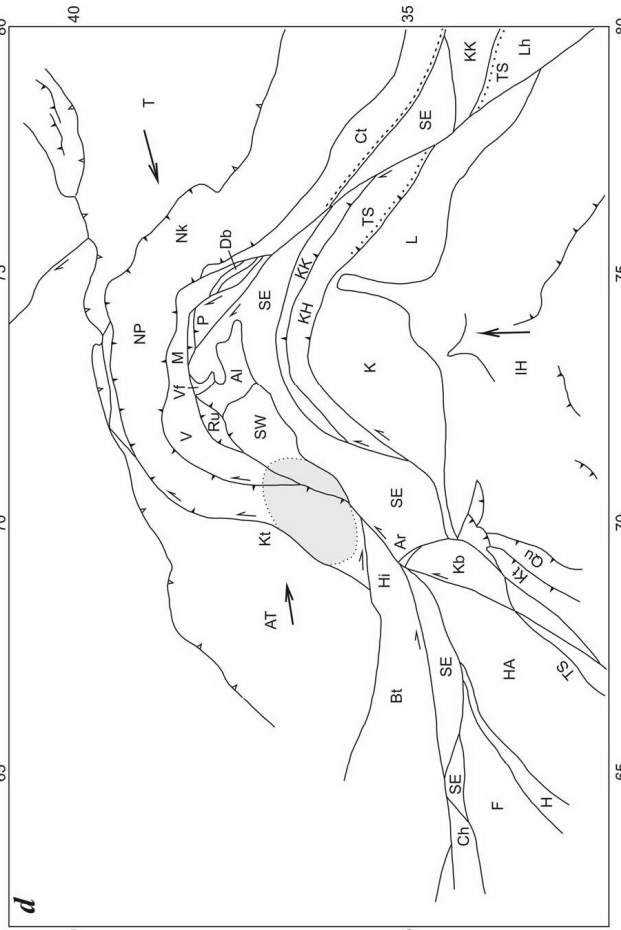
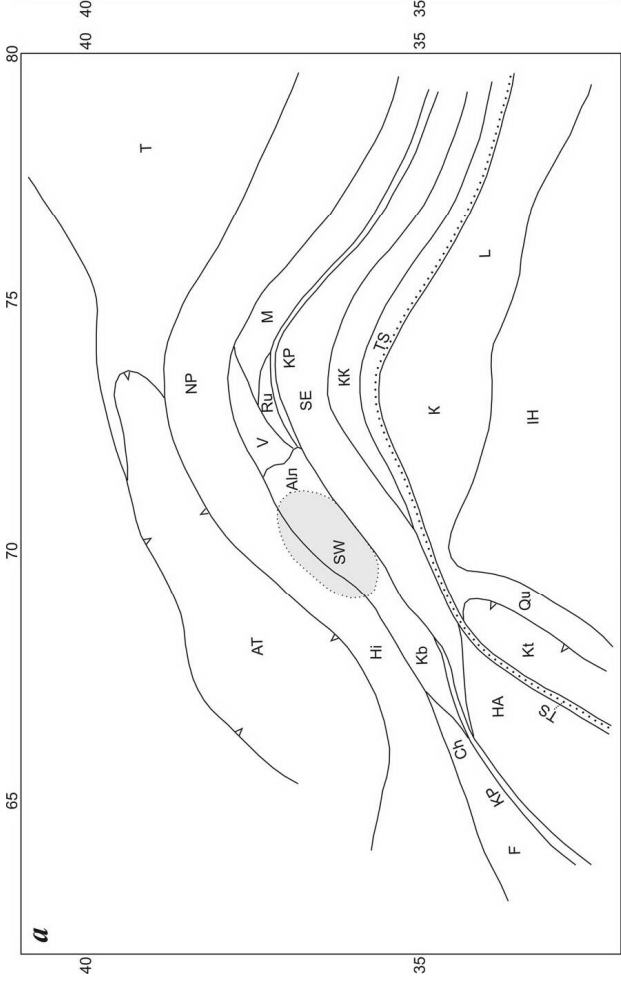
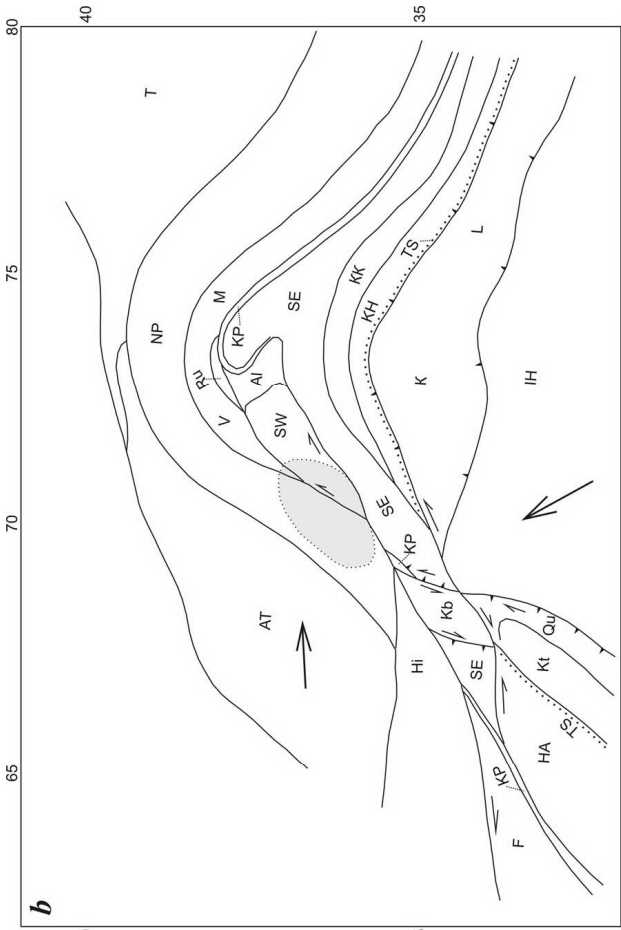
The most recent structure of the Pamirs was formed under horizontal compression commonly interpreted as a result of the pressure from the Punjab indenter of the Indian Plate. This assumption is consistent with the arcuate bend of the Pamir Zone: in particular, a bend of the northern Pamirs for 350–400 km with indications of N-trending compression and shortening in the W–E-trending thrusts and folds, the conjugated left-lateral slip along the Darvaz Fault, and right-lateral displacements in the southeastern Pamirs. However, magnitude of the arcuate bend in the southerly located Karakorum and Kohistan–Ladakh tectonic zones is only 200 km. This bend is conformable to the northern margin of the Indian Plate, and probably was formed immediately after the Neotethys closure, that is preceding, at least partly, the neotectonic epoch.

At the same time, the western and eastern flanks of the Pamirs bear indications of nearly W–E-trending recent compression and shortening. In the west, where the Hindu Kush and the North Afghan Hercynides join the Southwest Pamir–Badakhshan and Central Pamir zones, this deformation is expressed in the N–S-trending steep wedges, slices, and compressed folds with signs of transverse rock flattening, while the northwestern Kunlun demonstrates signs of the Hercynides thrusting over the Tarim Basin. Thus, the neotectonic structure of the Pamirs was formed under differently oriented compression.

Such an intricate structure of the Pamirs could result from variation of geodynamic settings during the neotectonic period. Its early stage (Late Eocene, Oligocene, and Early Miocene) was characterized by significant, although irregular, heating of the Earth's crust that gave rise to the emplacement of numerous large batholiths both along the fault-related boundaries and in axial zones of tectonic uplifts. These batholiths (Kohistan, Ladakh, Karakorum, Shugnan, and others) began forming in the Cretaceous or Paleogene at the onset of collision in the respective tectonic zones and continued to form until the Miocene. In some batholiths, the main phases of granite formation are related to the late collision (neotectonic) stage. Heating stimulated delamination of crustal rocks along the surfaces with the highest gradients of mechanical properties and differentiated lateral displacements. The heating of the thinned crust of the Afghan–Tajik Basin likely resulted in extension and volcanic activity at its southern flank, which was intensive at the early stage of the neotectonic period and lasted until the Mid-Pleistocene (Geology and Mineral Resources..., 1980). Since the Late Miocene, the heating of the Earth's crust waned, and the crust became more homogeneous in its physical properties and less favorable for tectonic delamination.

This background was complicated by changes in direction of maximal lateral compression in the orogenic belt (Fig. 14) that were similar to the changes in other regions of the Alpine-Himalayan Belt (Trifonov, 1999). Since the Late Eocene and until the Early Miocene (approximately 40–20 Myrs ago), the axis of maximal compression at the northern and western flanks of the Indian plate was probably oriented in the NW–SE direction. Intense transverse shortening was also recorded in the northern Quetta Zone, where the Eocene Katavaz Trough was deformed and the NE-trending tectonic nappes and thrust sheets were formed in the Khost, Tarnak, and Khashrud ophiolitic zones (Geology and Mineral Resources..., 1980; Tapponnier et al., 1981; Sborshchikov, 1988). They were conjugated with right-lateral movements along the nearly W–E-trending Gerat Fault Zone, along which the Khashrud Zone was displaced for 150 km relative to the Altimur ophiolite. The dextral displacement could also result from extension in the Afghan–Tajik Basin that was brought about by movement at 40 km along the W–E-trending Andarab Fault (Geology and Mineral Resources..., 1980).

Intense heating of the crust and its rheological delamination in the narrowest tract of the orogenic belt between the western Khazar Massif of the Himalayas and the salient southeastern margin of the Turan Plate could result in destruction and squeezing of crustal blocks away from this area. The South-West Pamir–Badakhshan



Block, which was formerly a part of the Central Pamir zone, moved eastward; this led to the detachment and sigmoid bend of the Pshart Suture and lithotectonic zones of the South-Eastern Pamirs, where tectonic nappes began forming. The sedimentary cover of the South-Western Pamirs became detached and formed the Vanch–Muzkol nappes of the Central Pamirs. It appears likely that the Kabul Block moved southward at that time dividing Nuristan from its western continuation and separating the Karakorum and Helmand–Argandab massifs.

Since the Early Miocene and until the Late Miocene (20–8 Ma ago), the Indian Plate moved to the northeast, and, correspondingly, the maximal compression and lateral shortening were oriented in the north-eastern direction. This was expressed in thrusting, granitization, and metamorphism in the Himalayas and the Karakorum (Gansser, 1964; Desio, 1976; Ratschbacher et al., 1993) and volcanism in Tibet. Involved in intense deformations, Tibet and Qaidam might have, in turn, exerted influence upon the Tarim Massif. The left-lateral Altyn Tagh strike-slip fault zone arose along its southeastern boundary; as a result, the Tarim drift acquired a substantial western component and compressed the Pamirs. Central Afghanistan was also involved in the northeastward drift. The sinistral slip occurred along the Herat Fault and continued with the Gunt Fault as its extension. These movements enhanced the displacement of the South-Western Pamir–Badakhshan Block and reinforced deformation of neighboring zones. In particular, the nappe structure of the South-Eastern Pamirs was eventually formed, and the northward-bent North Pamir Zone began to thrust over the Afghan–Tajik Basin.

Since the Late Miocene and at the Pliocene–Quaternary stage of the neotectonic epoch, when the Earth's crust was homogenized in its physical properties, direction of the Indian Plate pressure in the Pamir segment of the orogenic belt became close to the N–S, giving rise to the W–E-trending thrusts and folds and related strike-slip fault zones at the eastern and western flanks of the region. These zones have remained active till now (Trifonov et al., 2002). Simultaneously, W–E-trending compression of

Fig. 14. Conceptual maps of geodynamics and tectonic zonation of the Pamir-Karakorum region in the different substages of neotectonic epoch, modified after (Ivanova, Trifonov, 2005): a, the tectonic zonation at the Late Eocene; b, the geodynamics from the end of Eocene till the Early Miocene and the tectonic zonation at the late Early Moicene; c, the geodynamics from the end of Miocene till the Late Miocene and the tectonic zonation at the Late Miocene; d, the geodynamics from the end of Miocene till present time and the recent tectonic zonation

IH, Indian Platform and the Himalayas; KP, Khashrud-Pshart zone indiffereniated; Kt, the Katavaz Trench; Qu, the Quetta zone including the Host ophiolites; Lh, Lhassa Block; TS, the Tarnak-Shyok-Bangun suture; F, Farakhrud zone. Other symbols are the same as in fig. 12

the Pamirs continued. In the east, it experienced pressure from the Tarim Block, the drift of which had a western component due to the left-lateral movements along the Altyn Tagh Fault with a rate that reached 1 cm/yr in the Quaternary. The Tajik–Karakum Block of the Turan Plate could move in the opposite direction because of the right-lateral displacement along the Main Kopet Dagh Fault (>2 mm/year in the Quaternary). The countermovement of flanks shortened the Pamirs in the W–E direction and stretched it in the N–S direction, so that the North Pamir Zone was thrust over the Afghan-Tajik Basin. The convergence of the Pamirs and Tien Shan was caused by this process, and the westward removal of sedimentary sequences from the area of maximal shortening has been occurring until now, as follows from geodetic and geologic evidence (Guseva et al., 1993; Trifonov et al., 2002).

Intensive Pliocene–Quaternary vertical movements, the magnitude of which during only the Quaternary exceeded 6 km, were the most important process at the late stage of neotectonic period. Uplifting was driven by ongoing stacking of crustal blocks and by decrease of density of the upper mantle and the lower crust. The deformation was most large-scale in the western Pamirs; therefore, its uplift rate in the Pliocene–Quaternary was higher than in the eastern Pamirs (Krestnikov et al., 1979). The Quaternary rise was accompanied by gravity-driven overthrusting at the northern, western and eastern flanks of the Pamirs and by extension in its axial zone (Lake Karakul Depression).

The decrease of density of the upper mantle in the Pamir–Kindu Kush–Karakorum region was justified by the seismological data on lowered seismic wave velocities to 0.1–0.2 km/s relative to their worldwide background (Vinnik, Lukk, 1974; Lukk, Vinnik, 1975; Vostrikov, 1994) and by analysis of the gravimetrical data (Artemjev, Kaban, 1994). The decrease of density could be a result of the partial replacement of the lithospheric mantle by the asthenosphere matter. In the process of collision deformation, big volumes of the former oceanic crust within the lithosphere were pressed into the mantle to depths of 40–70 km, where they underwent the high-pressure metamorphism, being partly transformed into garnet granulites and eclogites (see section 2.2.3.1). A part of them that had the lesser density than the surrounding mantle and did not subside because of this, could undergo the retrograde metamorphism with participation of the cooled asthenosphere fluids during uplift at the Pliocene–Quaternary stage of neotectonic deformation. This decreased the density of the lower crust rocks and produced additional uplift in the region.

1.4. Neotectonic evolution of the Greater Caucasus

To understand sources of uplift of the Greater Caucasus (GC), we estimated consequently the following characteristics: (1) thickness and composition of the Earth's crust before its deformation by compression; (2) values of transverse shortening, thickening and uplift of the crust because of the compression; (3) transformation of the deformed crust into the recent mountain system. The used data on the Mesozoic-Cenozoic geology of the GC are based on the publications (Milanovsky, Khain, 1963; Panov, 1988; Shcherba, 1993; Alpine history..., 2007; Marinin, Rastsvetaev, 2008). The main part of the GC formed in the margin of the post-Paleozoic Scythian Plate. Its part, weakly deformed in Mesozoic and Cenozoic is separated from the GC by the foredeeps, Azov-Kuban in the west and Terek-Derbent in the east (Fig. 15).

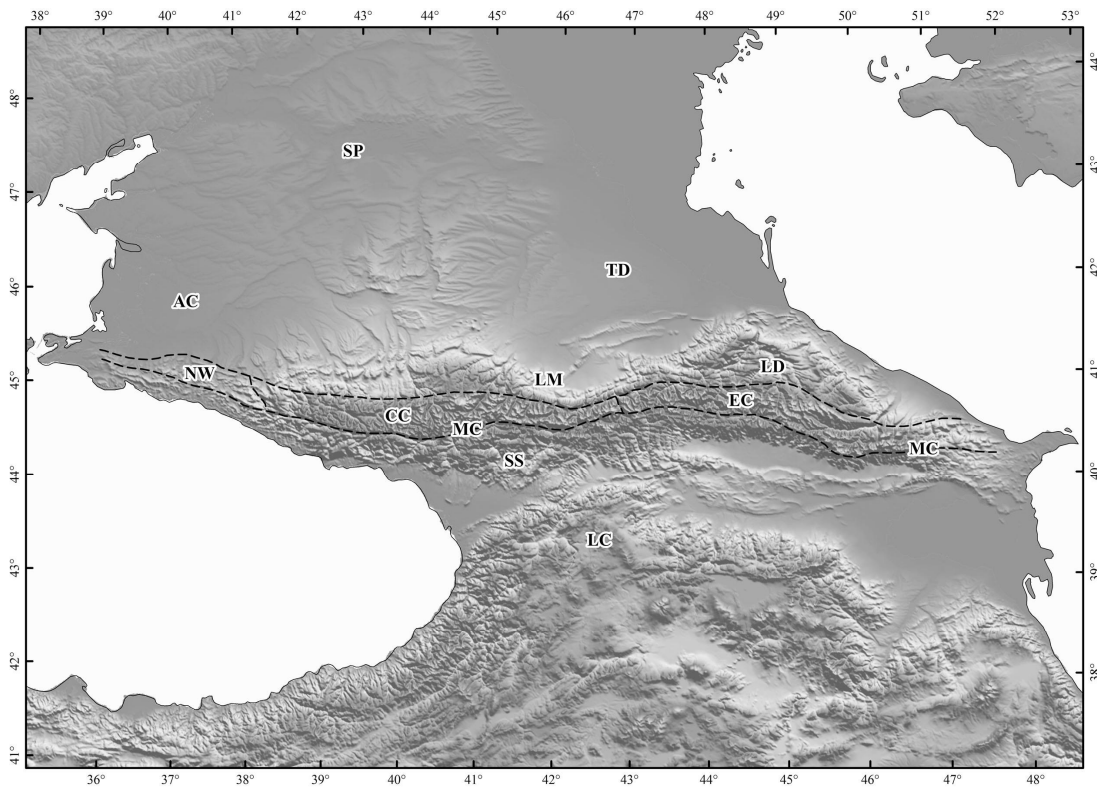


Fig. 15. The Greater Caucasus. AC, Azov-Kuban Basin; CC, Central Caucasus; EC, Eastern Caucasus; LC, Lesser Caucasus; LD, Limestone Daghestan; LM, Laba-Malka Zone; MC, Main Caucasus Fault; NW, North-western Caucasus; SP, Scythian Platform; SS, Southern Slope Zone; TD, Terek-Derbent Basin

The transitional Laba-Malka Zone (LMZ), including the East Balkar subzone and Limestone Daghestan, extends along the northern slope of the GC (Alpine history..., 2007). The thickness of the LMZ sedimentary cover varies from 5–5.5 km in the central part to 6.5–7 km in the east and ~10 km in the north-west. The GC itself consists of the northwestern, central and eastern segments. The North-Western

Caucasus is composed of the Jurassic, Cretaceous, and Paleogene (in the peripheral parts) deposits; their total thickness is up to 14 km. The same deposits were ~11 km thick in the Eastern Caucasus in the Early Miocene, although that region was subjected to the Cimmerian (pre-Bathonian and pre-Callovian) folding. In the Central Caucasus, the Lower and Middle Jurassic deposits were intensively deformed by the Cimmerian folding and preserved only in compressed synclines between the Paleozoic blocks. The Upper Jurassic to Paleogene deposits covered this uplift of the basement. We estimated their total thickness in the Early Miocene as ~2–2.5 km. The southern part of the GC (Zone of Southern Slope, ZSS) is separated from the GC itself by the Main Caucasus Reverse Fault. Near this fault, the ZSS is composed of the Lower and Middle Jurassic deposits, which are overlaid with the Upper Jurassic to Paleogene mainly flysch deposits farther to the south. Both parts of the ZSS represented a single basin with the 15–20-km total thickness of the sediments in the Early Miocene. Reconstructing the Earth's crust structure of different zones of the GC in the Early Miocene (Table 3), we considered that the crust was in isostatic balance at that time and the land surface differed from the sea level not more than to ~300 m. We estimated the average density of the sedimentary cover as 2.5 g/cm³ and considered that the density of the basement beneath thick sedimentary basins increased up to 2.9–2.93 g/cm³, by analogy with other similar structures (Artyushkov, 1993).

Tectonic zone	Thickness of J–Pg cover	Thickness of basement	Density of basement	Thickness of the crust
Zone of the Southern Slope	18±2 km	~16±1 km	2.93 g/cm ³	~34±2 km
North-Western Caucasus	~14 km	~21 km	2.9 g/cm ³	~35 km
Central Caucasus	2–2.5 km?	~40 km	2.83 g/cm ³	~42 km
Eastern Caucasus	~11 km	~25 km	2.87 g/cm ³	~36 km
LMZ, western segment	~10 km	~26 km	2.85 g/cm ³	~36 km
LMZ, central segment	~5 km	~34 km	2.84 g/cm ³	~39 km
LMZ, eastern segment	~7 km	~31 km	2.85 g/cm ³	~38 km

Table 3. Calculated characteristics of the Earth's crust of Greater Caucasus in the Early Miocene. LMZ is the Laba-Malka Zone

The Mesozoic and Cenozoic deposits of the GC are deformed by folds and faults. We analyzed deformation that was due to compression and resulted in transverse shortening of the Earth's crust. Using the published data (Gamkrelidze P.D., Gamkrelidze I.P., 1977; Panov, 2002; Alpine history..., 2007; Yakovlev, 2006, 2008,

2012; Marinin, Rastsvetaev, 2008), supplemented by our calculation of shortening in the LMZ and Limestone Daghestan, we estimated the transverse shortening and, correspondingly, the deformational uplift of the land surface in different zones by equations (1) and (2) in section 1.2.3 (Table 4).

Tectonic zone	Initial thickness of the crust, km	Shortening	Post-folding thickness of the crust, km	Thickening of the crust, km	Isostatic uplift, km
ZSS	~34±2	~50%	~68±4	~34±2	~4.8–5.4
North-western Caucasus	~35	~20%	~44	~9	~1.4
Central Caucasus, Cimmerian	~38?	20–30%?	~48–52?	~10–14?	~1.5–2.1?
Central Caucasus, Late-Alpine	~42	10–20%?	~47–52	~5–10?	~0.8–1.5?
Eastern Caucasus, Cimmerian	~38	20–30%	~48–52	~10–14	~1.5–2.1
Eastern Caucasus, Late-Alpine	~36	10–20%	~40–45	~4–9	~0.6–1.4
Limestone Daghestan	~38	10–20%	~42–48	~4–10	~0.6–1.5
LMZ, east and center	~36–39	<10%	~39–43	<3–4	<0.4–0.6

Table 4. Calculated values of the fold thickening of the Earth's crust and related isostatic uplift of the land surface in the Greater Caucasus

The age of main phase of the late Alpine deformation is under discussion. We consider it to be post-Maykopian, i.e., late Early and Middle Miocene, because the Maikopian (Oligocene – Lower Miocene) marine deposits covered the Greater Caucasus and the Maikopian Basin inherited the previous sedimentation in the region (Kopp, Shcherba, 1993; Shcherba, 1993). But the actual situation is more complicated. In the Central Caucasus, the significant deformation occurred at the pre-Bathonian and pre-Callovian time. As a result, the area became the uplifted block of the consolidated crust. Thickening and isostatic uplift of the Central Caucasus crust explain erosion of the Lower and Middle Jurassic deposits and exhumation of the Paleozoic basement. However, the Cimmerian deformation in the Eastern Caucasus did not produce significant pre-Late Jurassic uplift and erosion. The *Moho* is characterized there by the boundary velocities $V_p=8.2–8.3$ km/s. The seismic profiling found the layer with the velocities decreased up to 7.8 km/s under the *Moho* at the depths of 59–66 km and the discontinuity with boundary velocity $V_p=8.5$ km/s under it (Krasnopevtseva, 1984). Perhaps, this lower discontinuity is a relic of the former bottom of the crust. Its lower layers were subjected to metamorphism and

their density came nearer to the mantle one. The densification compensated the thickening of the crust in the Eastern Caucasus and the Cimmerian uplift was not significant. The calculated crust thickness after the late Alpine deformation differ in majority of the GC zones from the recent thickness of the Earth's crust, as it is determined by seismic profiling (Krasnopevtseva, 1984; Grekov et al., 2008). The ZSS demonstrates the highest difference. This abnormally high calculated crust thickness and uplift are not corroborated by geophysical, geomorphological and geological (composition of molasses) data. Perhaps, there, as in the Eastern Caucasus at the Cimmerian epoch, the densification of the lower crust compensated the deformational thickening of the crust.

During the main phase of the late Alpine deformation and immediately after it, i.e., in the Middle and early Late Miocene, the fine-grained material dominated in the molasses. Probably, the magnitudes of deformational uplands did not exceed mid-level mountains (up to ~1.5 km). This corresponds to calculated elevation, except the ZSS (Table 4). Essential portions of the pebbles arrived in molasses of the GC and its surrounding only at the end of Miocene and became abundant at the Pliocene (Milanovsky, Khain, 1963; Shcherba, 1993). Designing the conditional pre-orogenic surface of planation, Milanovsky (1968) estimated the magnitudes of Late Cenozoic rise in different zones of the GC (Table 5).

Zone	h_0 , km	S_0 , km	h_F , km	S_F , km	H_F , km	h_R , km	S_R , km	H_R , km
ZSS	32–36	16–20	64–72	32–40	4.8–5.4	35 (W) – 45–50 (C– E)		≤1.5 (W) – up to 2.5– 3.5 (C–E)
NW Caucasus	~35	~14	~44	~17	~1.4	~41		1–1.5
Central Caucasus	~42	~2.5 (0– 10)	~47–52		~0.8–1.5?	50–55	~2	2.5–3.5
Eastern Caucasus	~36	~11	~40–45	~13	~0.6–1.4	54–55	~10	≥3
LMZ	36–39	5–10	~39–43	~6–11	<0.4–0.6	~43		0.5–2
LD	~38	~7	~42–48		~0.6–1.5	~45		1–2

Table 5. Correlation between the calculated values of the Earth's crust thickness before and after the main phase of the Late-Alpine folding and post-folding uplift and the recent values of the crust thickness and uplift of the land surface.

h_0 is the initial (before the Late-Alpine folding) thickness of the crust; S_0 is the initial thickness of the sedimentary cover; h_F is the post-folding thickness of the Earth's crust; S_F is the post-folding thickness of the sedimentary cover; H_F is the post-folding uplift of the land surface; h_R is the recent position of the *Moho* surface (below s.l.); S_R is the recent thickness of the sedimentary cover; H_R is the recent uplift of the land surface (above s.l.); LD, Limestone Daghestan.

Everywhere, except the North-Western Caucasus and ZSS, the recent altitudes are higher than the calculated deformational uplift. This means that the GC grew more intensively from the end of Miocene (Milanovsky, 1968) or the beginning of Pliocene (Map of neotectonics of the south ..., 1971) than it was caused by the deformational thickening of the crust. The magnitudes of additional uplift reached 1.5–2 km in the Central and Eastern Caucasus. The additional uplift probably occurred also in the zones, where the difference between H_F and H_R is unessential. For example, the topographic reversal presupposes erosion of the deformational topography and, correspondingly, additional uplift in the North-Western Caucasus.

1.5. Evolution of the Alpine-Himalayan Collisional Belt in the Oligocene-Quaternary

Two main stages of deformation, metamorphism and tectonic uplift, the Oligocene–Miocene (or Oligocene–Early Pliocene) and the Pliocene–Quaternary ones, are distinguished in the Alpine-Himalayan Belt. The stage 1 is differentiated into three substages differing in direction of compression of the orogenic belt related to the motion of the Gondwana plates (Trifonov, 1999; Ivanova, Trifonov, 2005; Rukieh et al., 2005). These substages correspond to Oligocene–Early Miocene, Middle Miocene, and Late Miocene–Early Pliocene.

1.5.1. Oligocene–Early Miocene (35–17 Ma)

Compressive deformation, which started in the east of the region at the end of the Middle Eocene continued in the Oligocene and resulted in closure of the sub-oceanic Sabzevar Trough (Kazmin et al., 2010) and the Indus–Zangpo Zone (Aitchison et al., 2007) (Fig. 16). The intense compressive deformations, which took place in the Herat Zone in northern Afghanistan and in the northwestern Pamir–Hindu Kush brought about squeezing of the South-Western Pamir to the east and its thrusting over the zone of the South-Eastern Pamir (Ivanova, Trifonov, 2005; see section 1.3.1). Transverse compression in the northern part of the Quetta Zone was expressed in folding of the Eocene Katawaz Trough and formation of the NE-trending thrust faults in the Khost, Tarnaka, and Khash Rud ophiolite zones (Geology and Mineral Resources..., 1980; Tapponnier et al., 1981).

Syn- and postfolding uplifts arose in the compressed zones. The Oligocene–Miocene conglomerates overlapped the deformed rocks of the Indus–Zangpo Zone

with unconformity (Tewari, 1964; Aitchison et al., 2007) and were found in the foothills of the Pamir (Shvolman, 1977) and Kunlun (Recent geodynamics..., 2005). Differential vertical movements spread over the Tien Shan. In the Central Tien Shan, the Oligocene fine-pebble conglomerate and more fine clastic sediments are known (Shultz, 1948; Makarov, 1977; Dmitrieva, Nesmeyanov, 1982; Chediya, 1986). Local clastic material occurs and occasionally dominates in the pebbles (Bachmanov et al., 2009). This implies that the recent ridges as provenances of clastic material and the basins as depocenters originated in the Oligocene. In the Early Miocene, vertical movements became more sluggish; deluvial and lacustrine clayey sediments locally with evaporites were deposited at that time.



Fig. 16. Conceptual map of tectonic elements of the Alpine-Himalayan Belt at the end of the Oligocene (~25 Ma ago); modified after (Bachmanov et al., 2009; Bazhenov, Burtman, 1990; Dronov, 1980; Golonka, 2004; Alpine history..., 2007; Ivanova, Trifonov, 2005; Kazmin et al., 2010; Kopp, Shcherba, 1993; Robertson et al., 2004; Rukieh et al., 2005; Trifonov et al., 2012₂; Trifonov, Sokolov, 2014). See fig. 1 for legend

Judging from the relatively fine clastic material and shallow (a few hundreds of meters) incision of valleys formed at that time (Makarov, 1977; Chediya, 1986), the vertical range of the Oligocene topography in the Central Tien Shan did not exceed a kilometer. The anomalously coarse conglomerates of the Minkush–Kökömeren ramp are a product of destruction of reactivated Late Paleozoic nappes and unrelated to significant hypsometric contrast (Bachmanov et al., 2008). The fine clastic molasses

in the foothills of the Pamir and Hindu Kush (Afghan–Tajik Basin) and Kunlun (south of the Tarim Basin) indicate that no high mountains existed at that time. Nevertheless, the isotopic data on the paleosol in Central Tibet show that high mountains existed there ~26 Ma ago (De Celles et al., 2007). A high isostatic uplift at that time is also suggested in the South-Western Pamir, the upper crustal sheet of which, reaching 25 km in thickness, is thrust over the continental crust of the South-Eastern Pamir (The Earth's crust and upper mantle..., 1981; see also section 1.3.1). These high mountains were not widespread and were later subjected to erosion.

In the Arabian–Caucasus segment of the orogenic belt, the subduction in front of the South Taurus led to the formation of the accretionary wedge on the northern slope of the Kilikia–Adana Trough in Late Eocene–Early Oligocene. This wedge is composed of fragments of the Mesozoic oceanic crust and its Lower Paleogene cover. The blocks of carbonate cover of the Taurides slid over them. The process completed with the collision of the Taurides with the Arabian Plate in the northeast of this region and overlapping of the accretionary wedge by Lower Miocene sediments (Robertson, 2000; Robertson et al., 2004). A relic of the southern margin of this basin was retained in the southwest. In the Early Miocene (~17 Ma ago), it was isolated by the renewed Cyprus arc, and the Levantine Basin at the southern margin of Tethys began to subduct beneath this arc. Deformation reached a culmination at that time. The sharp angular unconformity between the Eocene and Helvetian is documented in the northwest of Syria (Rukieh et al., 2005).

Deformation developed in other zones of the Arabian–Caucasus Orogenic Belt up to the southern flank of the Caucasus part of the Carpathian–Caucasus system of troughs. Their underthrusting beneath the Lesser Caucasus was accompanied by formation of flysch along with tectonic and gravity mixtures (Leonov M.G., 1975; Shcherba, 1994; Alpine history..., 2007). The troughs themselves did not undergo deformation. In the Oligocene, they even locally deepened despite a global regression, especially intense in the early Late Oligocene (Vail, Mitchum, 1980), whereas an epicontinental sea spread over the entire Greater Caucasus and the adjacent Scythian Plate adjacent to the Caucasus and the Carpathians (Kopp, Shcherba, 1993). The supply of clastic material into the sedimentary basin was reduced in the Early Miocene.

The origination of a graben on the spot of the future Aden–Red Sea Rift was the most important event in the Oligocene, which initiated moving of Arabia apart from the African Plate. In this connection, the Dead Sea Transform arose in the Early Miocene (~20 Ma ago) (Garfunkel, Ben-Avraham, 2001). Its northern segment

extended along the continental slope of the Levantine Basin (Rukieh et al., 2005), inheriting an earlier transform zone.

In the Balkan Mountains, the Late Eocene phase of thrusting was followed by development of a foredeep, where flysch sedimentation gave way to deposition of molasses (Golonka, 2004). The displacement of the Carpathian inner zones gave birth to the Carpathian arc, which completed by thrusting of the detached nappes of the Northern Carpathians over the foredeep at the end of the Early Miocene.

The Oligocene uplifts (mainly low-mountain as judged from the composition of the piedmont molasses) were confined to compression zones in the west of the belt. Except for the Caucasus troughs of the Paratethys, the uplifts grew in area, while the sediments in the epicontinental basins, e.g., in northern Arabia, were related to the regressive phase of the Paleogene sedimentation cycle. This was probably caused by increase in collisional compression, though it can be partially explained by the global drop of ocean level.

All structural units of the orogenic belt, which underwent compressive deformation in the Oligocene and Early Miocene extend W–E or in north-eastern directions. This implies that the principal compression axis was oriented in the north-northwestern direction, which coincides with the directions of movement of the Gondwanan plates.

1.5.2. Middle Miocene (16–11 Ma)

During the second substage (end of the Early Miocene and the Middle Miocene), the most intensive lateral displacement and deformation of crustal blocks took place in the east of the belt corresponding to the region of the Indian–Eurasian collision. The Himalayas, Karakoram, and NW-trending Pamir zones were involved in deformation and thrusting accompanied by a peak of metamorphism and granite formation (Searle, 1991, 1996; Ivanova, Trifonov, 2005) (Fig. 17). At the same time, the intensity of tectonic movements decreased in the Central Tien Shan, where Oligocene uplifts extended in the ENE direction. The average rate of erosion became lower than in the Oligocene (Chediya, 1986). The Miocene lacustrine fine clastic sand-shale sediments are predominant, whereas alluvial sediments are second in abundance (see section 1.2.1). The areas of sedimentation expanded having overlapped some Oligocene uplifts (Bachmanov et al., 2009). Each sedimentary basin was a chain of lakes connected by permanent or intermittent channels. The basins were separated by flat uplifts, which act as additional provenances. To the south and the east, approaching the present-day Kakshaal-Too Range and the Khan Tengri

Massif, the clastic material becomes coarser, indicating higher elevations and more intensive erosion. They were the main sources of removed clastic material. Carbonate interlayers were replaced with evaporites moving away from the uplifts.

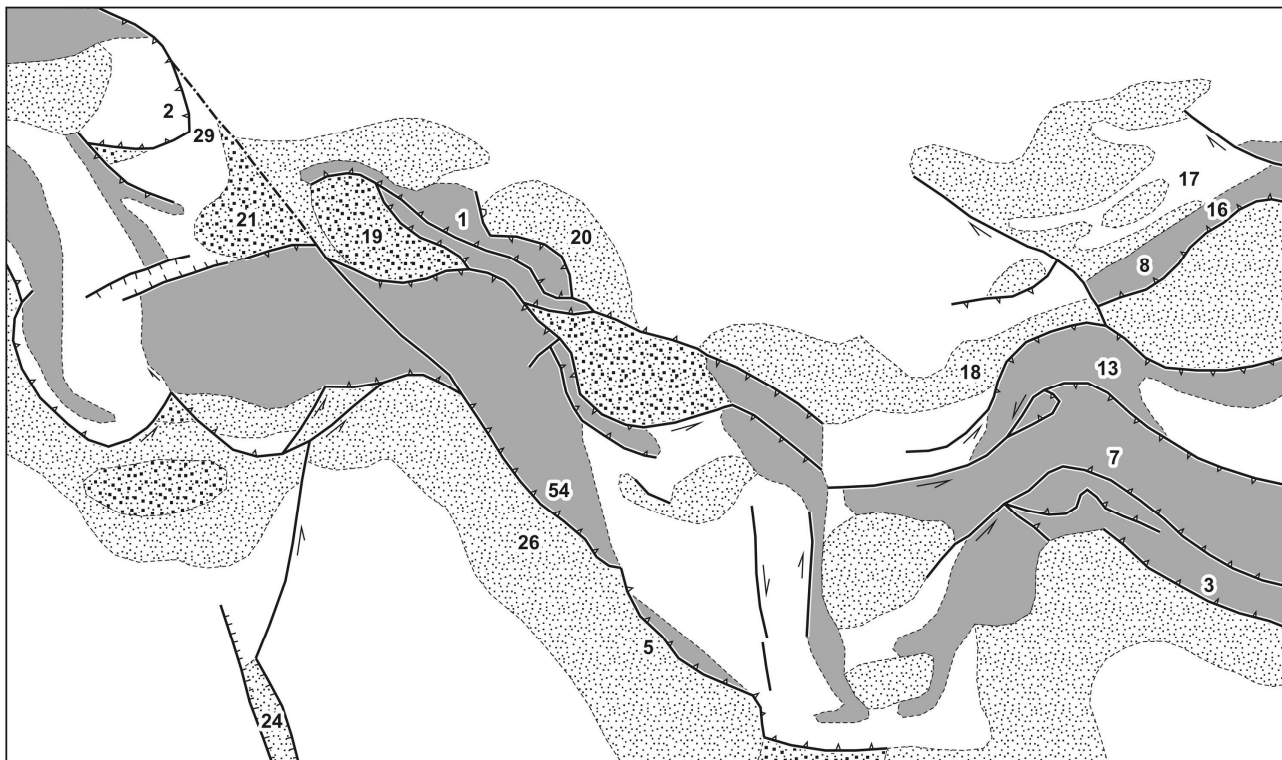


Fig. 17. Conceptual map of tectonic elements of the Alpine-Himalayan Belt at the Middle Miocene (~18 Ma ago); modified after (Artyushkov et al., 1996; Bachmanov et al., 2009; Golonka, 2004; *Alpine history...*, 2007; Ivanova, Trifonov, 2005; Kazmin et al., 2010; Kopp, Shcherba, 1993; Rukieh et al., 2005; Searle, 1991, 1996; Tapponier et al., 1981; Trifonov et al., 2012₂; Trifonov, Sokolov, 2014). See fig. 1 for legend.

Evidence for rearrangement of the principal compression direction with its shift to the northeast in the late Early and Middle Miocene was also documented in the western segments of the belt. A tectonic quiescence in the northwest of the Arabian Plate came with development of the Helvetian–Tortonian sedimentation cycle. The intensive movements along the Main Thrust of Zagros led to the closure of the Neotethys relic basin between the Arabian Plate and the Sanandaj-Sirjan Zone (Golonka, 2004). This event initiated onset of the development of the Mesopotamian Foredeep, which inherited the formerly sagging northeastern part of the plate. Folding started to develop at the northeastern flank of the trough in the late Middle–early Late Miocene.

The Caucasus troughs of the Paratethys were shoaled and then closed; at the end of the second stage, their sedimentary fill underwent folding (Kopp, Shcherba, 1993; *Alpine history...*, 2007). Thrusting of the Outer zone of the Eastern Carpathians over the Focsani Basin of the Carpathian Foredeep in the late Middle–early Late Miocene

was probably also related to the rearrangement of compressive stresses (Artyushkov et al., 1996). The thickness of the sedimentary cover in the Eastern Carpathians is now estimated at 8–12 km and initially could have been 10–14 km. Such an increase in the thickness of the sedimentary cover did not bring about a rise of the surface to the calculated value of 1.5–2.4 km, and the surface remained at a height of ~0.5 km. Thus, the uplift to 1–2 km was compensated by compaction of matter at a deeper level of the lithosphere. A similar phenomenon probably took place at the southern slope of the Greater Caucasus, where intensive folding and stacking of sedimentary sequences also did not lead to the formation of high mountains. Judging from the composition of the clastic complexes, highlands were not formed in other regions of the belt either. Moreover, the Pannonian Basin was formed on the place of the deformed inner zones of the Carpathians.

1.5.3. Late Miocene–Early Pliocene (10.0–3.6 Ma)

During the third, Late Miocene–Early Pliocene substage, the prevalent orientation of compression again became north-northwestern or nearly N-trending. The peak of diastrophism fell on the Messinian. A system of south-vergent thrusts developed on the southern slope of the Greater Caucasus (Fig. 18). At the southern flank of the region of interaction of the Arabian and Eurasian plates, the main phase of folding and thrusting took place in the Palmyrides. Folding in the Hellenides and thrusting in the Pamir were resumed. The fold–thrust zones expressed in the topography shifted to the south from the Main Thrust of Zagros and the Taurus (Bitlis) Thrust. In the Himalayas, such a propagation was marked by shift of the maximum displacements and deformation to the zone of the Frontal Fault.

In some intermontane basins of the Central Tien Shan, the Upper Miocene sequences were enriched in coarse clastic rocks, which gave way to fine clastic rocks upsection, in the Lower Pliocene. These coarse clastic rocks were products of destruction of the Late Paleozoic tectonic nappes; i.e, of activation of horizontal rather than vertical movements (Bachmanov et al., 2009). In some places, for example, in the Greater Caucasus (Kopp, Shcherba, 1993), the Late Miocene displacements and folding resulted in formation of dissected topography; however, the composition of clastic material in the intermontane basins and foredeeps indicates that the uplifts were characterized here, as in other segments of the belt, by moderate height of mountains.

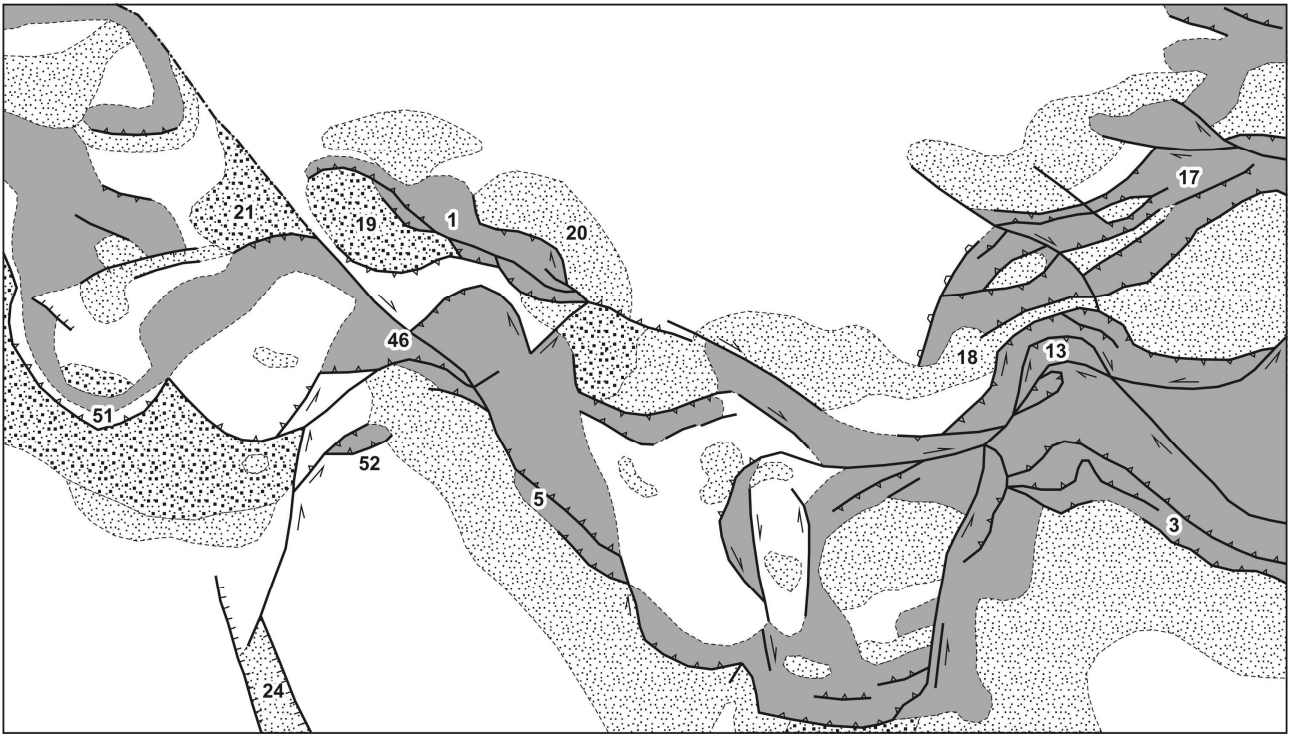


Fig. 18. Conceptual map of tectonic elements of the Alpine-Himalayan Belt at the Messinian (~6 Ma ago); modified after (Artyushkov et al., 1996; Bachmanov et al., 2009; Golonka, 2004; Alpine history..., 2007; Ivanova, Trifonov, 2005; Kazmin et al., 2010; Kopp, Shcherba, 1993; Rukieh et al., 2005; Searle, 1996; Tapponier et al., 1981; Trifonov et al., 2012₂; Trifonov, Sokolov, 2014). See fig. 1 for legend

1.5.4. Late Pliocene–Quaternary (the last ~3.6 Ma)

The contemporary network of large active faults of the belt was formed by the Late Pliocene. The displacements along these faults (mainly strike-slip) indicate approximately N-trending orientation of the principal compression axis. In the northwest of Arabia, the onset of the fourth stage (4.0–3.5 Ma) was accompanied by rearrangement of the northern segment of the Dead Sea Transform. While in the Miocene, its main branch extended along the continental slope, now the main displacements concentrate along the Yammunneh and El Gharb segments (Rukieh et al., 2005) (Fig. 1). Approximately at the same time, the East Anatolian and North Anatolian Fault Zone, as well as the Main Recent Fault of Zagros demarcating the present-day plate boundaries (Saroglu, 1988; Trifonov, 1999; Westaway, 2004; Westaway et al., 2006), eventually formed.

The rates of vertical tectonic movements sharply increased over the last 5–2 Ma. The height of mountains at least doubled or tripled. The contemporary mountain systems and high plateaus were formed during this time, when coarse molasses were deposited in the foredeeps and intermontane basins. The most significant increase in uplifting is established in Central Asia (Fig. 19). The onset of acceleration of vertical

movements was not synchronous. The average height of the Himalayas has increased by over 3 km (Mörner, 1991) and the Central Tien Shan by ~2 km (Krestnikov et al., 1979; Chediya, 1986; Trifonov et al., 2008) since the Early Pleistocene (~2 Ma). The rapid rise of Tibet started 2.8–2.4 Ma ago and reached 2500–3600 m; the Kunlun and Tarim have grown simultaneously for 2600–3100 and ~1200 m, respectively (Mörner, 1991; Li Jijun, 1995; Recent geodynamics..., 2005). This yields an average rate of growth of Tibet and the Kunlun as 1.0–1.5 and 1.0–1.2 mm/yr, respectively. The particular substages of rapid uplift are outlined; thus, the rate of uplifting increased with time. The last substage began at the end of the Middle Pleistocene and the velocity of uplifting during this substage locally reached 10 mm/yr. According to the data of recurrent leveling, the velocity of contemporary uplift of Tibet is 6.8 mm/yr, on average, and increases from the Kunlun and northeastern Tibet to the Himalayas (Zhang Qingsong, 1991). Over the last 5 Ma, the Pamirs has grown ~2 km on average.

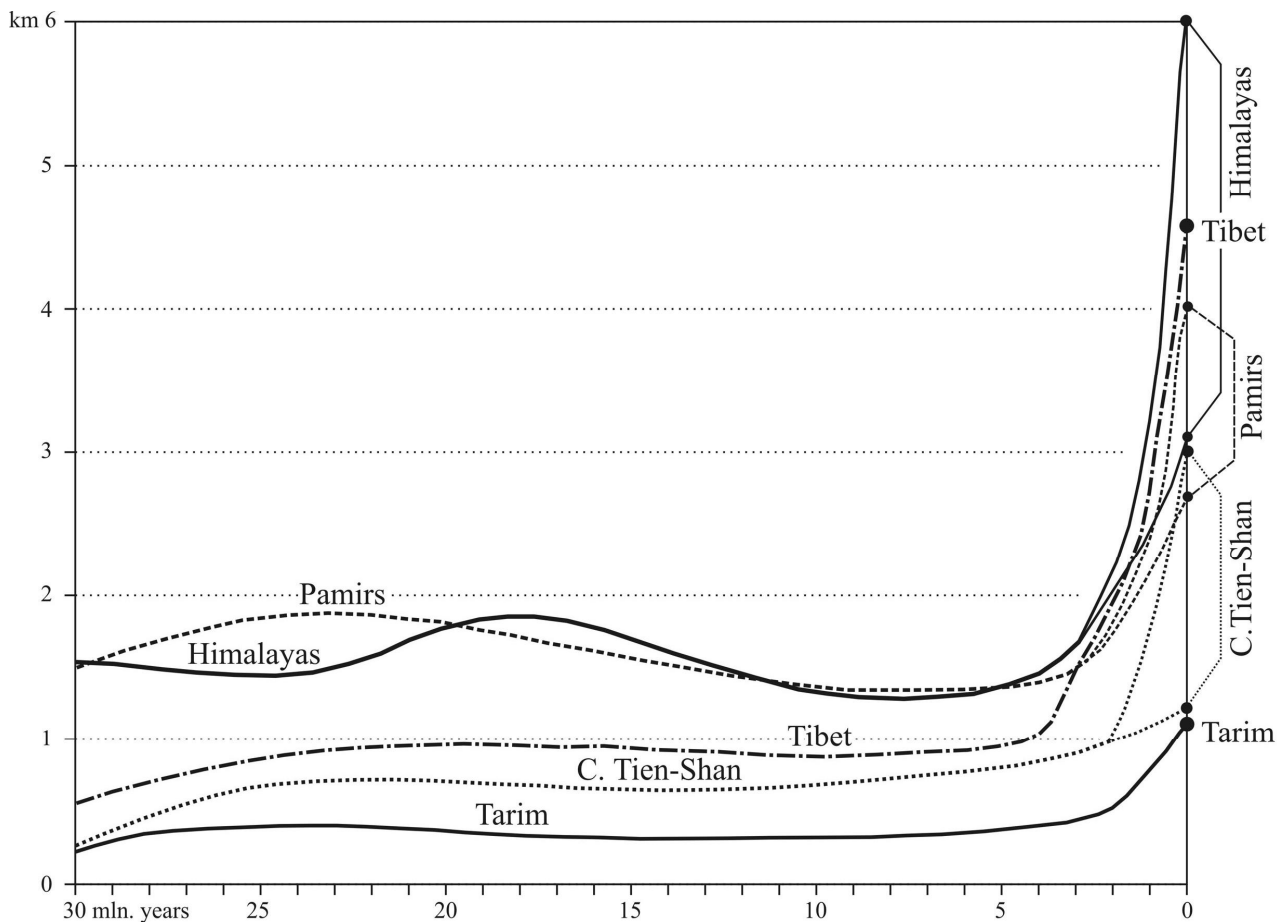


Fig. 19. Acceleration of mountain rise in High Asia in the Pliocene-Quaternary, modified after (Trifonov et al., 2012₁). At the right, the lower calculated curves showing what heights would be reached by the Pliocene-Quaternary uplift only as a result of increased compression, are compared with the upper curves showing the actual heights of the Himalayas, Pamirs, and Central Tien Shan

The intense mountain growth in the Pliocene and Quaternary has been established in the Greater Caucasus (Milanovsky, 1968; see also section 1.4), the Carpathians (Artyushkov et al., 1996), the Alps (Artyushkov, 1993), and other mountains of Southern Europe (Ollier, 2006). To estimate the Quaternary uplift in the Lesser Caucasus, we studied stratigraphy and tectonics of the Upper Pliocene–Quaternary deposits in NW Armenia (Trifonov et al., 2014, 2015). This territory is formed by the southern Javakheti volcanic ridge and adjacent basins, the Upper Akhurian in the west and the Lori in the east (Fig. 20). The Bazum Ridge with the Mesotethys suture borders the area to the south. Basalts, basaltic andesites, andesites, and dacites that cover the Pliocene volcanic formation and compose the southern Javakheti Ridge and bottoms of the adjacent basins are dated by the K-Ar technique in the time interval between ~2.5 and ~1.85 Ma. In the basins, these volcanic rocks underlie tuffaceous-clastic deposits. We divided them to the Karakhach and Kurtan units. By a combination of paleomagnetic, SIMS ^{238}U - ^{206}Pb , $^{40}\text{Ar}/^{39}\text{Ar}$, K-Ar and paleontological including pollen methods, the lower Karakhach unit was dated at 1.85–1.75 Ma and the age of the upper Kurtan unit was estimated as the Upper Calabrian (including the Jaramillo subchron) and the lowest Middle Pleistocene, i.e. ~1.2–0.5 Ma. The episodes of eruptions of andesites (~1.7 Ma) and dacite pumices and ashes (1.4 – 1.5 Ma) occurred between accumulation of these two units.

For estimation of magnitudes of the following rise of the area, it is important that the Kurtan unit covers volcanic rocks as a vast mantle. This means that topography was relatively flat. After accumulation of the Kurtan unit, the area was undergone to flexure-fault deformation and was uplifted. We can estimate the magnitude of uplift by intensity of incision of recent channels to the volcanic surface covered by the Kurtan unit. The incision reaches 370 m in the most upstream Debed River. Excluding the 20-meter effect of the Baku transgression of the Caspian Sea that was a final basis of erosion for the drainage system of the area, we conclude that the incision, approximately corresponding to the magnitude of uplift of the eastern Lori Basin, reached 350 m (Fig. 21). The rise reached as minimum 500 m in the Upper Akhurian Basin. The Karakhach Pass and, correspondingly, the Javakheti Ridge that is the northern continuation of the pass rose to ~500 m relative to the Lori Basin. The flexural bend of the basalts in the southern side of the Lori Basin expresses the minimum several hundred meters uplift of the Bazum Ridge relative to the basin. These values correspond to the average rates of uplift at 0.7–1 mm/yr for the basins and 1.2–1.6 mm/yr for the ridges during the last ~0.5 Myrs.

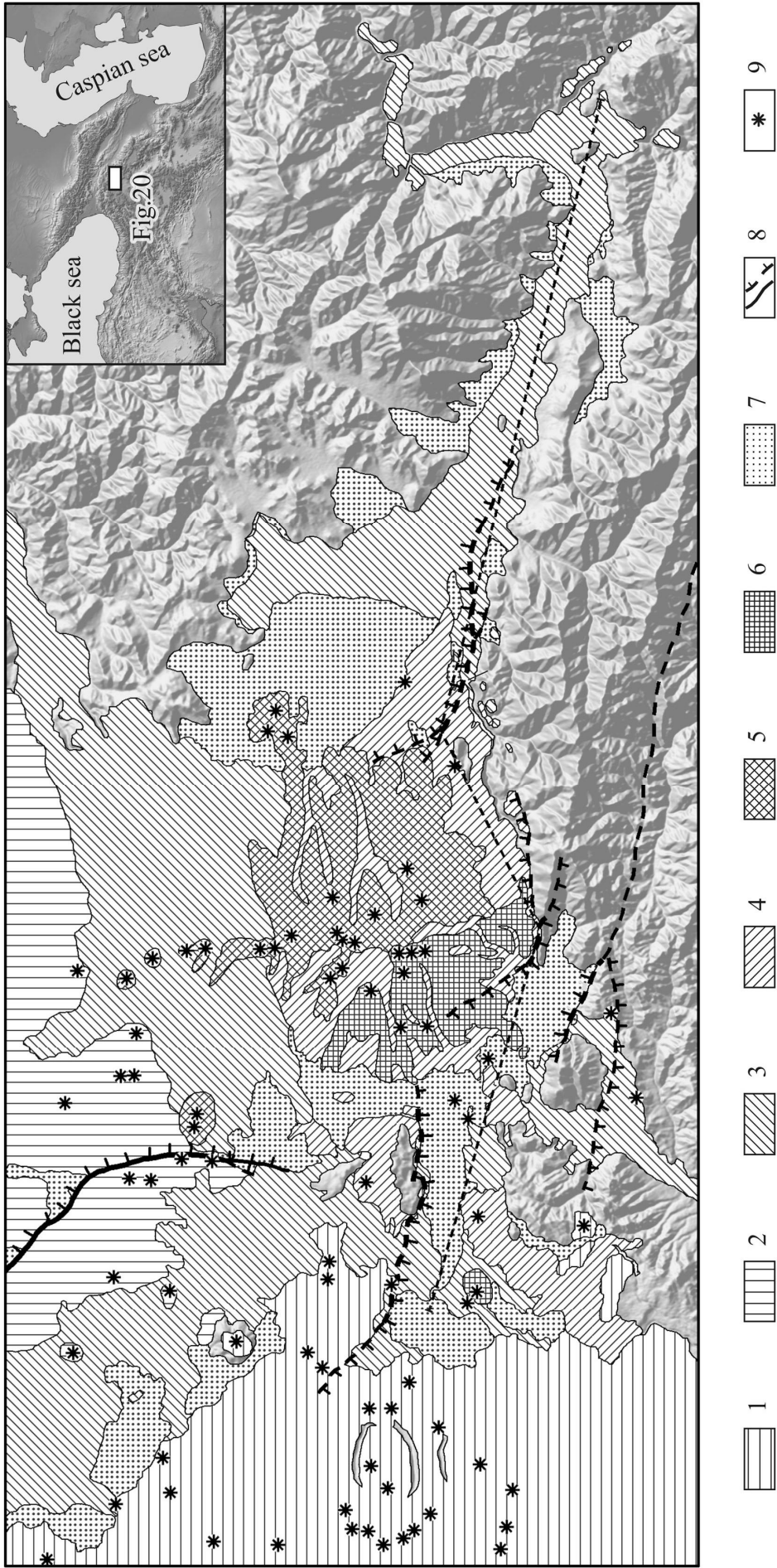


Fig. 20. Upper Pliocene and Pleistocene volcanic units in the southern Javakheti Ridge, Upper Akhurian and Lori basins; the dotted line shows position of the Fig. 21 profile; compiled by V.A. Lebedev with additions and corrections of V.G. Trifonov and D.M. Bachmanov.

1, unit I, Pliocene (mainly Upper Pliocene), basalts, andesites and more acid rocks including obsidians; 2, Upper Pliocene, basalts and andesites that are present in the Georgian part of the region and corresponds to the third phase of the Georgian volcanism, 2.7–2.4 Ma (Lebedev et al., 2008); 3, unit II, Gelasian basalts and basaltic trachyandesites; 4, unit III, upper Gelasian basaltic trachyandesites, trachyandesites and andesites; 5, unit IV, upper Gelasian dacites; 6, unit V, lower Calabrian basaltic trachyandesites, trachyandesites and andesites; 7, Quaternary sediments; 8, Middle-Late Quaternary flexure-fault zones; 9, volcanos and extrusive domes. Geological sections: Ag, Agvorik; Ar, Ardenis; Dm, Dmanisi; Ka, Karakhach; Ko, Koghes; Kr, Krasar; KuI, Kurtan I; KuII, Kurtan II; Mu, Muradovo; Va, Vardaghybur; Ya, Yaghdan. 1–10, sites of K–Ar sampling. 12–15, other sites of observation

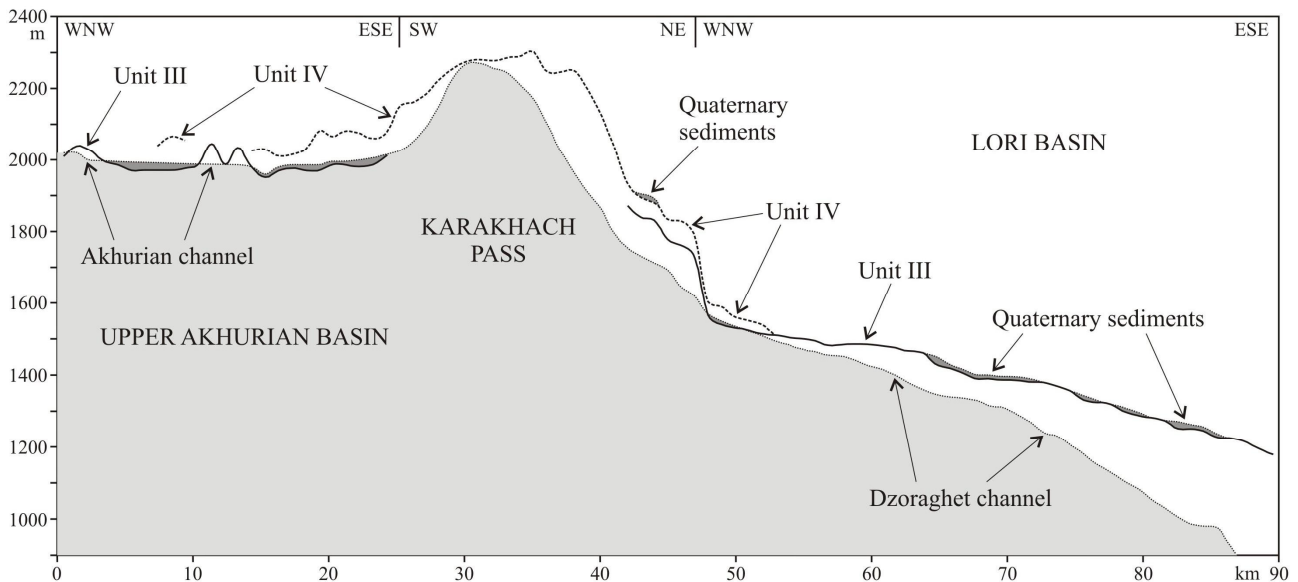


Fig. 21. W–E-trending geological-geomorphological profile along the Upper Akhurian Basin, Karakhach Pass and southern Lori Basin; compiled by D.M. Bachmanov and V.G. Trifonov

At the northwestern end of the Mesopotamian Trough (middle reaches of the Euphrates River), the lagoon and lacustrine sedimentation continued into the Early Pliocene, but then it gave way to coarse clastic alluvium fed by anticline uplifts propagating to the south. At the Syrian shore of the Mediterranean Sea (Fig. 22), a rapid growth of the Coastal Anticline has been established. The anticline began to evolve in the Miocene, when its axial part was eroded 500 m deeper than the eastern limb. The eroded surface was covered by basalts, the K–Ar age of which was estimated at 6.3 ± 0.3 to 4.3 ± 0.2 Ma (Trifonov et al., 2011). The basaltic hyaloclastites formed 5.4 ± 0.2 Ma ago under the effect of seawater are now located 260–300 m above sea level (Outline of Geology of Syria, 2000). In the axial part of the anticline, the basalts dated at 5.4–4.8 Ma have been raised to a height of 800 m. At the eastern limb of the fold, basalts are located 400 m lower. The coastal Lebanon Anticline underwent intense Pliocene–Quaternary uplift, as well (Gomez et al., 2006).

The comparative analysis of height, composition and age of the terraces of largest rivers of Syria gives more detailed estimates of the Quaternary uplift of different tectonic provinces of the region (Fig. 23). The accurate definition of ages of different stages of terrace formation gave a possibility to define average rates of incision in the river valleys using relative height of the terraces that correspond approximately to the rates of the Quaternary rise in different tectonic provinces of Syria during the Middle and Late Pleistocene. The rates are: ~ 0.22 – 0.28 mm/a in the El-Kabir River valley (the Coastal Range), ~ 0.08 – 0.13 mm/a in the Orontes valley and the Euphrates valley

upstream the Assad Reservoir (the mobile platform Aleppo Block) and $\sim 0.025\text{--}0.03$ mm/a in the Euphrates valley downstream the Assad Reservoir (the south-western side of the Mesopotamian Foredeep) (Neotectonics, recent geodynamics and seismic hazard assessment of Syria, 2012; Trifonov, Bachmanov et al., 2012, 2014).

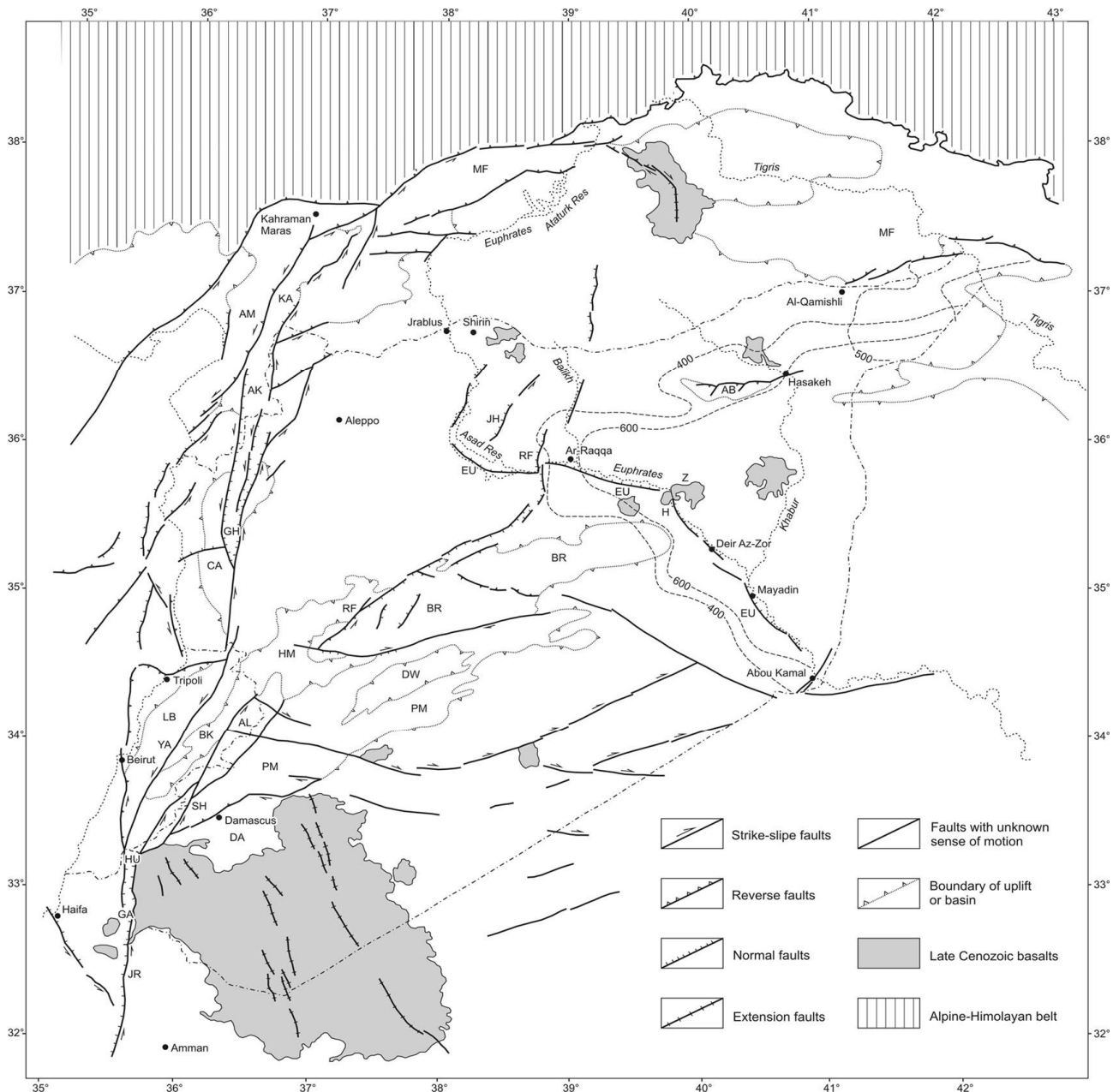


Fig. 22. Late Pliocene–Quaternary (the last ~ 3.5 Ma) tectonic features of the northern part of the Arabian plate, modified after (Trifonov, Bachmanov et al., 2012). The 400-metre and 600-metre Miocene isopachs and the 500-metre Pliocene isopach demonstrate the structure of the Mesopotamian Foredeep. *Uplifted anticline zones*: AB, Abdel Aziz; AL, Antilebanon; BR, Bishri, the Northern Palmyrides; CA, Coastal of Syria; LB, Lebanon; MF, Marginal Folds of Turkey; PM, Southern Palmyrides. *Faults and fault zones*: AM, Amanos, a segment of the EAFZ; EAFZ, East Anatolian fault zone; EU, Euphrates; JH, Beer Jabel – Heimer Kabir; JR, Jordanian, a segment of the Dead Sea Transform (DST); RF, Rasafeh–Faid and its continuation (RF2, RF3 and RF4); SH, Serghaya; YA, Yammuneh, a segment of the DST. *Basins*: AK, Amik; BK, Bekkaa syncline; DA, Damascus; DW, Ad Daw; GA, Galilee Sea pull-apart basin of the DST; GH, El Ghab pull-apart basin of the DST; HM, Homs; HU, Hula pull-apart basin of the DST; KA, Karasu graben. Basaltic fields: H, Halabieh; Z, Zalabieh

Although the uplift of the mountain systems in the Pliocene and Quaternary involved most conjugate intermontane basins and foredeeps, some large negative structural elements in the western part of the belt underwent intense subsidence. Signs of this were found in the Mediterranean, Black Sea, South Caspian Basin, and in the southeastern part of the Terek Foredeep continuing into the Central Caspian as the Derbent Trough. The maximal thickness of the sedimentary cover exceeds 14 km in the Derbent Trough and the 5 km fall on the Pliocene–Quaternary deposits. The most intense sagging began at the end of the Pliocene and continues at present, providing uncompensated sedimentation (Leonov et al., 1998). The western part of the South Caspian is a starved basin down to 1 km deep with thinned (8–10 km) consolidated crust. Up to 20 km of sediments have been deposited here, no less than half of them being Pliocene–Quaternary sediments. The thickness of the Upper Pliocene–Quaternary deposits locally exceeds 6 km (Artyushkov, 1993; Leonov et al., 1998).

The subsidence of the Aegean Sea started in the Late Miocene and became more intense in the Pliocene and Quaternary (Golonka, 2004). At the same time, from the Tortonian and especially in the Pliocene–Quaternary, the Ionian and Levantine basins of the Mediterranean Sea also deepened. Increase of sagging of the latter from the Tortonian to Pliocene–Quaternary is confirmed by the growth of the sedimentation rate by 2–6 times in various parts of the basin (Kazakov, Vasilyeva, 1992). The Levantine Basin, uncompensated by sediments, is up to 2500 m deep (3200 m at the Herodotus abyssal plain). In the north of the basin, a trough in front of the Cyprus arc is expressed in the west as a deep bathymetric depression between the Cyprus and the submarine Eratosthenes Mount and in the east as a submarine extension of the Nahr el Kabir Trough, where the thickness of the Pliocene–Quaternary sediments is greater than 1800 m.

The Levantine Basin is a relic of the southern margin of the Tethys, which now has suboceanic crust with thick (up to 10–14 km) sedimentary cover and the Moho surface at a depth of 20–25 km (Ben-Avraham et al., 2002). The lower and the upper parts of the Neogene–Quaternary section are separated by the Messinian evaporites, which are replaced in the south by alluvial and deltaic sediments of the pra-Nile. The level of the hypersaline Messinian Basin was lower than the present-day level of the Mediterranean. This is proved by the overdeepening of the Messinian channels of the pra-Nile and the other rivers influent into the sea at that time. Currently evaporites occur at a depth of 2 km and deeper.

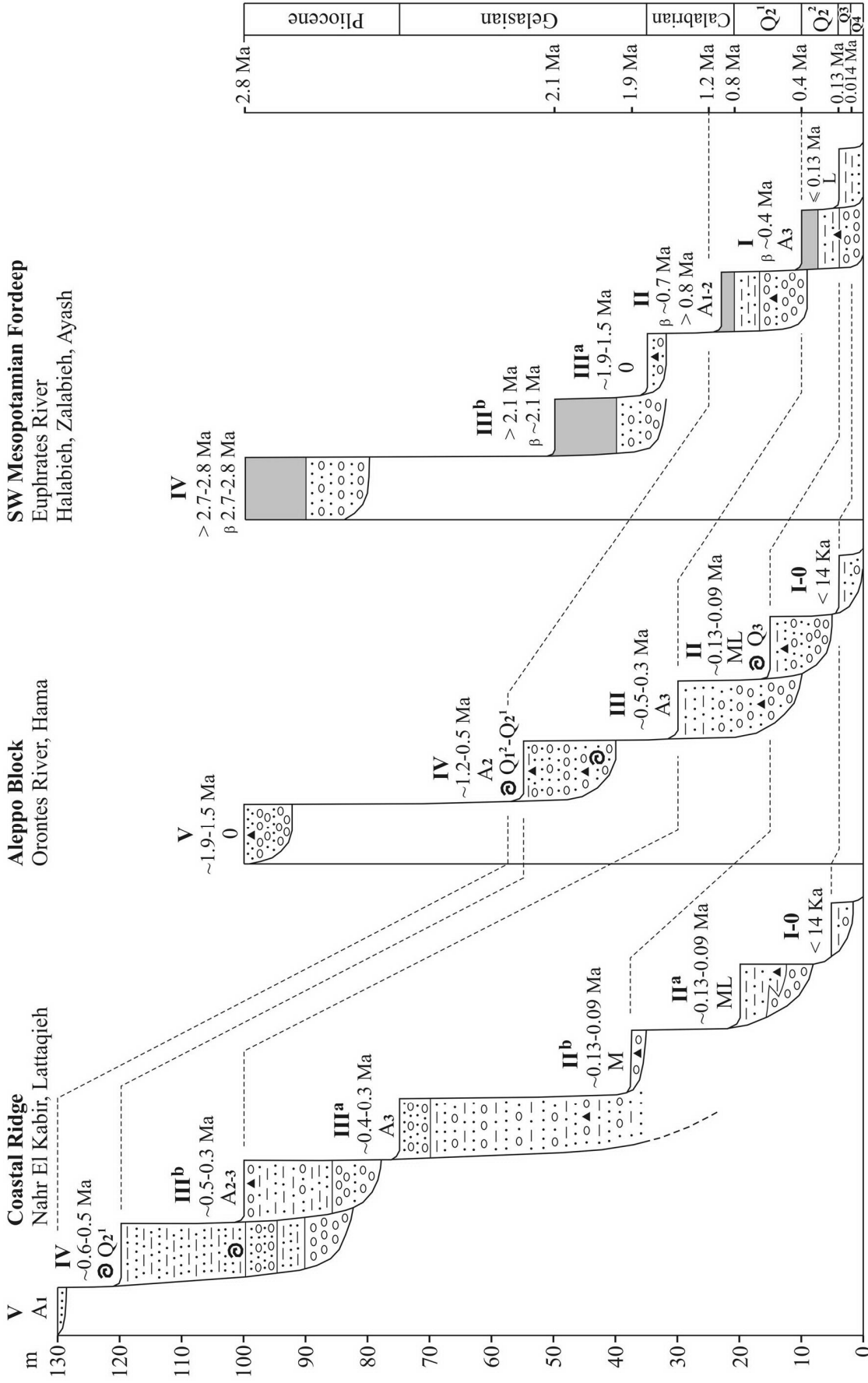


Fig. 23. Correlation of terraces of major rivers in Syria demonstrating relative Quaternary uplift in different neotectonic provinces, after Demir et al. (2007) and Trifonov, Bachmanov et al. (2012, 2014) with additions. Covering basalts (β) are shown by black color. Solid triangles (▲) are sites of archaeological finds: O, Hattabian correlated with Oldovan; A1, early Acheulian; A2, middle Acheulian; A3, late and final Acheulian; M, Middle Paleolithic; L, Late Paleolithic. See fig. 13 for other symbols

In the Early Pliocene, the breaching waters of the Black Sea and Atlantic flooded the Mediterranean, including the Levantine Basin. The depth of its bottom decreases toward its eastern shore and especially southward, where a vast shoal is occupied by the Nile delta, in the underwater part of which the thickness of the Pliocene–Quaternary sequence reaches 3.0–3.5 km (Ross, Uchupi, 1977). At the boundary of the continental slope and the basin bottom between Tel-Aviv and Beirut, their thickness is 1.3 km (Ben-Gai et al., 2004) and the bottom of the Pliocene sediments is subsided to 2.2–2.4 km (Kazakov, Vasilyeva, 1992).

At the same time, in the west of Syria, in the subaerial part of the Nahr el Kabir Trough, the 30-m section of the Messinian gypsum is exposed at a height of ~50 m a.s.l. The Pliocene marine clay overlaps it with scouring and basal breccia containing fragments of gypsum and pre-Messinian carbonates and covers the slopes of the adjacent uplifts at a height up to 250 m. No indications of ingressive attitude of the Pliocene were revealed. The submarine part of the Nahr el Kabir Trough and the neighboring part of the continental slope are disturbed by faults, along which the trough stepwise plunges to the west (Klaeschen et al., 2005). The seismic profiles across the slopes of the Levantine Basin between Tel-Aviv and Beirut demonstrate that horizontally lying Pliocene–Quaternary sediments are thinned landward, forming a flexure on the continental slope with dip angles up to 10° and complicated by faults (Ben-Gai et al., 2004). The vertical offset of the Pliocene bottom reaches 1.5–1.7 km. The steepness of the beds decreases from the Pliocene to the Quaternary, however, even the Late Pleistocene (Tyrrhenian) terraces are locally tilted seaward at an angle of 3° (Dodonov et al., 2008).

The relationships described above show that the sea level in the Messinian was lower than the contemporary sea level by several hundred meters. The Tortonian carbonate rocks deposited in the very shallow-water sea occur now in the Nahr el Kabir River valley at a height no more than a few hundred meters. Thus, the Pliocene–Quaternary uplift of the shore was not great and became significant only in the coastal anticlinal ridges (Gomez et al., 2006). Thus, increase in the vertical contrast between the Early Pliocene surface on the present-day land and in the sea is determined largely by deepening of the Levantine Basin, which underwent tectonic subsidence with a magnitude no less than 1.5 km in the post-Messinian time. An additional isostatic subsidence related to load of thick sediments took place in the Nile delta.

Thus, the Pliocene–Quaternary was the time of activation of not only rising, but also subsiding tectonic movements, that is, the time of general increase in their contrast.

1.5.5. Relationships between collision and tectonic uplift producing mountain building

The signs of the first orogeny in the Alpine–Himalayan belt are referred to the Oligocene. The mountain system became widespread in the Pliocene and Quaternary. The neotectonic epoch immediately followed, partly coinciding in time with the epoch of collision closure of the Neotethys and its backarc basins, which began at the end of the Cretaceous and completed in the time interval from the Late Eocene to Middle Miocene. The region of mountain building is juxtaposed, to a great extent, with the domain of collision, though it expands beyond the limits of collision in the east. This provides grounds to regard recent mountain building as a result of collision compression, and this view is generally accepted now. Let us consider to what extent this opinion is valid.

1.5.5.1. Methodical Approach

The occurrence and height of the uplifts, which towered above the sea level or the surface of the subaerial peneplain that existed earlier and is retained nearby, can be judged from the composition of clastic material removed from the eroded uplift and from the depth of the related incision onto the peneplain. When analyzing clastic material, it should be kept in mind that coarse facies could have been accumulated as a result of destruction of the overthrusting allochthonous sheets, which did not undergo substantial uplifting (Leonov M.G., 1975; Bachmanov et al., 2008). In some basins, clastic material was deposited as a product of remote transportation by water and does not characterize the height of the adjacent rises. All this requires ascertainment of the paleotectonic setting of sedimentation.

As concerns the depth of incision, in the case of intense linear erosion accompanying growth of mountain ranges, the remnants of the pre-orogenic surface can be retained on their summits and slopes, allowing judgment about the magnitude of uplift. The stepwise slopes of mountain ranges are commonly interpreted as evidence for pulsatory uplift and serve as the basis of the concept of step-like topography. Acceleration of vertical movements reactivates erosion so that an erosion–tectonic scarp (incision) is formed on the slope of the uplift, leaning on the bottom of the basin or valley, which serves as a local base level regulating deposition of erosion products. The higher the rate of uplifting, the coarser and thicker the accumulation of sedimentary material. The next pulse of rising leads to the uplift of an adjacent site of the basin and the formation of a younger incision below it. The uplifted site becomes a step on the slope. The steps located at similar hypsometric

levels on the slopes of different ranges make up, together with the incision leaning on them, a regional level of topography formed at the same time. This suggests that the incision is correlated with the coarse lower part of the molasse unit, whereas the steps at the base of incision are correlated with the fine clastic upper part of the molasse unit (Makarov, 1977). Such correlation gives a possibility to use molasse units as indicators of development of a mountain system and magnitudes of its uplift during different time intervals. In the course of intensive rise, the early landforms can be destroyed and the retained landforms will not reflect its true vertical uplift that can be controlled by analysis of the recent structure of a mountain range.

Thus, origination and growth of the mountain system is recorded in a complex of sedimentary, geomorphological and structural–geological attributes. The set of such attributes, while not allowing the identification of all features of regional mountain building, nevertheless gives an idea of the general tendencies of uplifting.

1.5.5.2. Mountain building as a result of collision compression

As was shown above (Fig. 1 and 16–18), the Alpine-Himalayan Belt underwent Cenozoic transverse shortening under the effect of collision compression. The process was accompanied by rotation of separate microplates (Kopp, 1997). The orientation of the compression axis changed with time. At the first substage of the stage 1 (Oligocene–Early Miocene), the NNW orientation was predominant; during the second substage (late Early–Middle Miocene) it was oriented in the NE direction; at the third substage (Late Miocene–Early Pliocene), the orientation again was NNE or N–S. The N–S-trending compression dominated during the stage 2 (Late Pliocene–Quaternary).

The geodynamic correlation is outlined between the tectonic events at the northern flanks of the Arabian Plate and the evolution of the Aden–Red Sea Rift System (Kazmin, 1974; Rukieh et al., 2005; Trifonov et al., 2011; Neotectonics, recent geodynamics and seismic hazard assessment of Syria, 2012). At the first substage, the rift system propagated westward and the Aden Rift pulled apart more intensively than the Red Sea Rift. The Arabian Plate correspondingly moved to the north-northwest. At the second substage, the Red Sea Rift extended more intensively than the Aden Rift and the Arabian Plate moved to the northeast. During the third substage, the intensity of extension increased because of the breakup of the continental crust and the onset of spreading (Kazmin, 1974; Izzeldin, 1987). Inasmuch as the breakup of the crust and spreading developed in the Aden Rift earlier than in the Red Sea Rift, the plate

moved to the north-northwest. Finally, at the stage 2, the Red Sea Rift was involved in spreading as well, and the plate began to move northward.

As was shown above, similar variations of orientation of the compression axis also took place in other segments of the orogenic belt, which were not related to the drift of the Arabian Plate. It is obvious that they were controlled by more general geodynamic factors that caused the drift of Arabia among other phenomena.

In contrast to the above variations of the stress-and-strain state, the propagation of the Zagros Fold Belt to the SW was characterized by the stress state that remained unchanged over all stages of its evolution. This is indicated by the parallel orientation of folds differing in age and the conjugated NW-trending thrusts. In contrast to the folds, the structural framework of the Zagros as the right lateral Main Recent Fault is inscribed into the setting of near N-trending compression established in the Pliocene–Quaternary. At that time, the Main Fault was separated from the zone of active folding by previously formed fold zones, where folding ceased. The stress fields different in rank are probably combined here. The transregional field controlled by common movement and interaction of lithosphere plates and microplates caused dextral movements on the Main Fault. The regional field involving only the Zagros caused deformation on the fold-thrust Zagros Belt. Appearance of this regional field may be due to the wedge shape of the Arabian Plate, which creates compression of its northeastern margin in the process of the northward drift. A similar propagation with the same geodynamic consequences took place in the Himalayas, where the front of the maximal displacement and deformation migrated in the post-Middle Miocene time from the Central Thrust Fault to the Boundary and then Frontal faults and now is shifting to the Sub-Himalayas.

From the Late Eocene to the Early Pliocene, the uplifts expressed in the topography arose and developed in the same tectonic zones of the belt, which underwent the strongest compression and shortening. Such uplifts can be regarded as a result of isostatic compensation of thickening of the crust due to its compression. Differentiation of the peneplain with the formation of uplifts and intermontane basins took place also beyond the regions of collision diastrophism expressed in folding and thrusting, e.g., in the Central and Eastern Tien Shan. Its compression could have been induced by the movements of microplates in the course of collision. In the Tien Shan, this was the pressure of the Tarim microplate. Because the direction of principal compression varied during the Oligocene–Quaternary epoch, the uplifts differing in strike originated at different times. The growth of mountains could last after the onset of diastrophism, probably, owing to inertia of isostatic compensation.

The height of the mountain ranges was estimated in two ways: first, using the geologic–geomorphic method discussed above, and second, by calculation based on correlation between rise of the crust and its deformational shortening with using equations (1) and (2) (see section 1.2.3). The value and rate of shortening and corresponding initial width of the region were estimated from structural–geological data, whereas the initial thickness of the crust was estimated from its thickness in the adjacent undeformed regions with similar initial characteristics of the crust that is possible to do for the Tien Shan and Himalayas, or on the basis of geological features, if the region under consideration initially differed from the adjacent territories (the Greater Caucasus, Pamirs, Zagros).

Calculation of isostatic uplift since the Oligocene as a result of thickening of the crust by compression made by Artyushkov for the Central Tien Shan has shown that by the end of the Pliocene (onset of intense rising), the uplift reached 0.6–0.9 km (Trifonov et al., 2008; see section 1.2.3). This estimate is consistent with geologic–geomorphic estimates, according to which the height of the uplift by the end of the Pliocene did not exceed 1.5 km; the difference in the heights of the uplifts and the surface of the basins was 1 km and the average height of the Central Tien Shan was close to 1 km, i.e., ~0.7 km higher than the height of the initial pre-orogenic peneplain (see section 1.2.1). In other words, before intensification of mountain building, the growth of uplifts could be entirely determined by regional compression.

The characteristics of the molasse formations and rare estimates of correlative incisions into the planation surfaces and pediplanes in other mountain systems of the belt lead to similar conclusions. The uplifts, which arose from the Oligocene up to the Pliocene or Early Pliocene, aside from occasional local deviations, also towered above the pre-orogenic peneplain by not more than ~1.5 km, i.e., they were not higher than middle-level mountains. It is quite possible that they were created by thickening of the crust owing to compression. In the Eastern Carpathians and the Southern Slope Zone of the Greater Caucasus, the deformational thickening of the crust in the Middle–Late Miocene did not result in the corresponding rise of the territory. In the Carpathians, the cause could have been related to compaction of the lower crust (Artyushkov et al., 1996). A similar situation probably took place in the Greater Caucasus. The formation of the Pannonian Basin also could be caused by an increase in the lower crust density.

The transverse segmentation of the belt is clearly expressed in its contemporary structure. The eastern Pamir-Himalayan segment separated from the central Caucasus-Arabian-Iranian segment by the Darwaz–Chaman Fault System is

characterized by a maximum of rising that involves not only mountain systems, but also most conjugated basins and plains (microplates). This feature of the eastern segment was retained through the entire neotectonic epoch, increasing with time. Cenozoic granitic magmatism is widespread here, whereas in other segments granites are not so abundant in contrast to the intense recent volcanic activity. The central segment, separated from the western one by the Dead Sea Transform and East Anatolian Fault Zone, is characterized by more differentiated topography. The mountain systems here are lower than in the east, and the Caspian Basin and Persian Bay are situated at the periphery of the belt. The area of intensive recent volcanism extends along the western margin of the segment. In the western segment, mountainous domains are combined with basins. Both rising of mountains (the Alps, the Carpathians, Anatolia) and subsiding of basins were intensified here.

It would be suggested that the topographic features of the segments are related to different rates of their compression, or transverse shortening. It actually reaches a maximum in the eastern segment owing to substantial displacement of the Indian Plate; however, in the same segment, the highest tectonic uplift took place in the Himalayas rather than in the Punjab–Pamir arc, where shortening was highest. It is evident that differences in the intensity of vertical movements were related not only to intensity of compression, but also to the features of the lithosphere determined by the tectonic history and deep geodynamics.

1.5.5.3. Pliocene–Quaternary acceleration of tectonic uplift producing mountain building

The Pliocene–Quaternary mountain building fundamentally differs from the preceding stages of the evolution of the orogenic belt not only in the higher intensity of uplifting, but also in the extensiveness of the involved territories irrespective of their tectonic history. The uplifts embraced the whole of Central Asia and developed in other regions of the belt.

The intensification of Pliocene–Quaternary rising is only partly related to acceleration of plate movements and increase in collision compression. On the contrary, the intensity of compression locally decreased. For example, in the Alps and the Western Carpathians, collision was completed as early as the Middle Miocene, whereas the mountains began to grow in the Pliocene against the background of diminished compression. In the Greater Caucasus, the growth of uplifts accelerated in the Pliocene–Quaternary against the background of decreasing compression rate

recorded in the GPS data (Shevchenko et al., 1999) and total displacement along active faults (Trifonov et al., 2002). Even in the regions, where compression increased (Himalayas, Pamir, Central Tien Shan), the magnitudes of uplifting related to the thickening of the crust by compression are only a part of the total magnitude of the uplift over this time (Fig. 6). If the compression rate in the Central Tien Shan estimated from the data on Late Quaternary displacements along faults and the results of GPS measurements (10–20 mm/yr) is extrapolated over the entire phase of intense mountain building (Late Pliocene–Quaternary), then it will be higher than the average compression rate in the preceding epochs (2.5–3.0 mm/yr). The isostatic uplift at this rate of crust compression estimated from formula (1) is 330–660 m, i.e., 20–35% of the increment of average height of mountain edifice of ~2–2.5 km (Trifonov et al., 2008; see section 1.2.3). A similar calculation of the height increment of the Himalayas and Pamir in the Pliocene and Quaternary yielded no more than 40–50%. Most intermontane basins rose also, though not so intensely, and this hardly can be a manifestation of compression. Thus, regardless of either increase or decrease of regional compression in the Pliocene and Quaternary, this factor may explain only a part of the rate of uplifting, and not everywhere. The remainder must be explained by the contribution of other factors.

The tectonically delaminated lithospheric mantle including the high-metamorphosed fragments of the lower crust was partly replaced by the lower-dense asthenosphere (Artyushkov, 1993, 2003; Trifonov et al., 2008), and this abruptly intensified the growth of mountain ranges. This is indicated by the lowered seismic wave velocities beneath the highest mountain systems of Central Asia (Himalayas, Tibet, Kunlun, Pamir–Hindu Kush–Karakoram region, Central and Eastern Tien Shan) (Lukk, Vinnik, 1975; Lithosphere of the Tien Shan, 1986; Recent geodynamics..., 2005; Vinnik et al., 2006; Li Zhiwei et al., 2009), as direct evidence for the low-density upper mantle suggested from gravity measurements (Artemjev, Kaban, 1994; Jimnez-Munt et al., 2008). Kaban (2000) noted the same features in the gravity field of the Lesser Caucasus. The lowered seismic wave velocity related to the ascent of the asthenosphere was revealed beneath the Eastern Carpathians (Artyushkov et al., 1996). The decrease of density of the lower crust masses as a result of retrograde metamorphism under the effect of cooled Pliocene asthenosphere fluids may be the second factor of intensification of mountain growth. This factor probably became dominant in the uplift of the Western Tien Shan and the Greater Caucasus, where low-density mantle domains have not been detected except for the Elbrus magma source.

1.5.6. Sources of neotectonic uplift in the Alpine-Himalayan Belt

In the Cenozoic, especially since the Late Eocene, different zones of the Alpine–Himalayan Belt have undergone collision compression caused by convergence of the Gondwanan plates with the Eurasian Plate. This compression was expressed in folding, thrusting of the sheets of continental crust over one another, and closure of the Neotethyan basins and related backarc seas and eventually led to the local thickening of the crust and its isostatic uplifting. The uplifts that grew in such a way, as a rule, did not exceed the hypsometric level of low and moderately high mountains. The process continued like this up to the Early Pliocene and the areas occupied by uplifts became more extensive with each new tectonic phase. In other words, before the Early Pliocene, the growth of mountain systems was almost completely caused by collision compression of the belt, although local deviations from the isostatic compensation of compression arose, being directed toward the greater magnitudes of uplift, e.g., in the eastern segment where low-density granites were formed, and to the lower magnitudes in the Eastern Carpathians and the Greater Caucasus, probably due to metamorphic compaction of the lower crust.

The isostatic uplifting of the crust thickened by compression developed further in the Pliocene–Quaternary, locally even more intensively than before, but general rising of most part of the orogenic belt was added to this process. The general rise was greater in magnitude than the contribution of the uplift caused by local thickening of the crust by compression; it did not depend on the Cenozoic history of either territory, involved not only mountain ridges, but also the majority of adjacent basins, and eventually led to the formation of the contemporary mountain topography of the belt. This additional rise was caused by decrease of density of the uppermost mantle and the lower crust. The isostatic reaction to the decrease of density of the upper mantle was a result of partial replacement of the lithospheric mantle with the asthenosphere material, whereas the decrease of density of the lower crust was due to retrograde metamorphism under the effect of cooled asthenosphere fluids. The deep transformations also caused deepening of some basins and increased contrast of transverse segmentation of the belt.

Part 2. Result of seismic tomography analysis of the mantle and deep sources of the Pliocene-Quaternary uplift

2.1. Seismic tomography profiling of the Alpine-Himalayan Belt

Consideration of the seismic tomography data on northeastern Asia (Zhao et al., 2010) has shown that the processed data from the global network of stations, though worse in resolution compared to the data of the regional seismological network, nevertheless give a generally similar pattern. Therefore, the seismic tomography data obtained on the basis of the global network were used for the study of the Ethiopian–Afar superplume and the Alpine–Himalayan Belt (Grand et al., 1997; Van der Hilst et al., 1997; Becker, Boschi, 2002). When these data are interpreted, their lower spatial resolution in comparison with the regional models should be kept in mind. In particular, this resolution does not allow discrimination of the lithosphere and asthenosphere. Other geophysical evidence is needed for this purpose. For example, the lower average seismic wave velocities beneath continents at a depth down to 100 km are interpreted as evidence for emergence of the asthenosphere.

The lines of the seismic tomography sections are shown in maps of V_p and V_s variations in the surface layer 100 km in thickness (Fig. 24 & 25). The sections themselves (Fig. 26–29) are based on these data (Grand et al., 1997; Van der Hilst et al., 1997; Becker, Boschi, 2002). The anomalous V_p and V_s values are expressed in percent as deviations from the average value for the given layer. The $dV_p = 0.25\text{--}0.8\%$ and $dV_s = 0.5\text{--}2.0\%$ are accepted as increased and $dV_p > 0.8\%$ and $dV_s > 2\%$ as highly increased. By the same way, the $dV_p = -0.25\text{--}0.8\%$ and $dV_s = -0.5\text{--}2.0\%$ are accepted as lowered and $dV_p < -0.8\%$ and $dV_s < -2\%$ as highly lowered. Systems of mid-ocean ridges are distinctly seen in the V_s field with two exceptions. They are the Knipovich Ridge and a segment of the African–Antarctic Ridge near the Kerguelen Plateau. At the same time, systems of mid-ocean ridges are not expressed almost at all in the V_p field. In contrast, the collision zones of the Earth, in particular, the Alpine–Himalayan Belt, are clearly seen in the V_p field.

Sections 1–1' across the Tonga–Kermadec arc show that the zone of increased and highly increased dV_s corresponding to the seismic focal zone transforms at a depth of 400–800 km into the horizontal high-velocity lens beneath the sub-continental Tonga

Plain (Fig. 26). A similar passage is revealed beneath the Andaman–Indonesian arc (Fig. 26, sections 2–2'). Similar flattening of subduction zones has been found at the depths of 400–700 km along the north-western margin of the Pacific by the more detailed data of local seismic networks. Fukao et al. termed this layer a stagnant slab and Huang and Zhao (2006), Zhao (2009) and Zhao et al. (2010) termed it a big mantle wedge (BMW) (Fig. 26, sections 20 and 24).

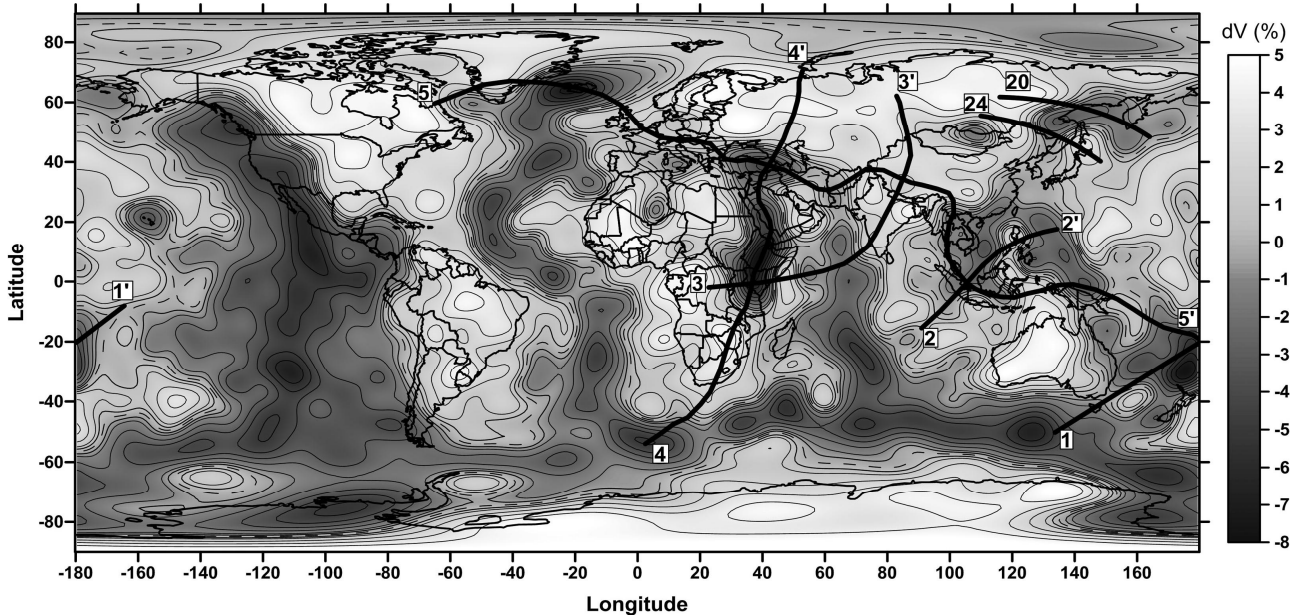


Fig. 24. Distribution of dV_s at the depth up to 100 km and lines of sections (Fig. 26–29), lines 20 and 24 after (Zhao et al., 2010). Compiled after the data in (Becker, Boschi, 2002; Grand et al., 1997; Van der Hilst et al., 1997). Contour lines are spaced at 1%; the dashed line corresponds to zero value

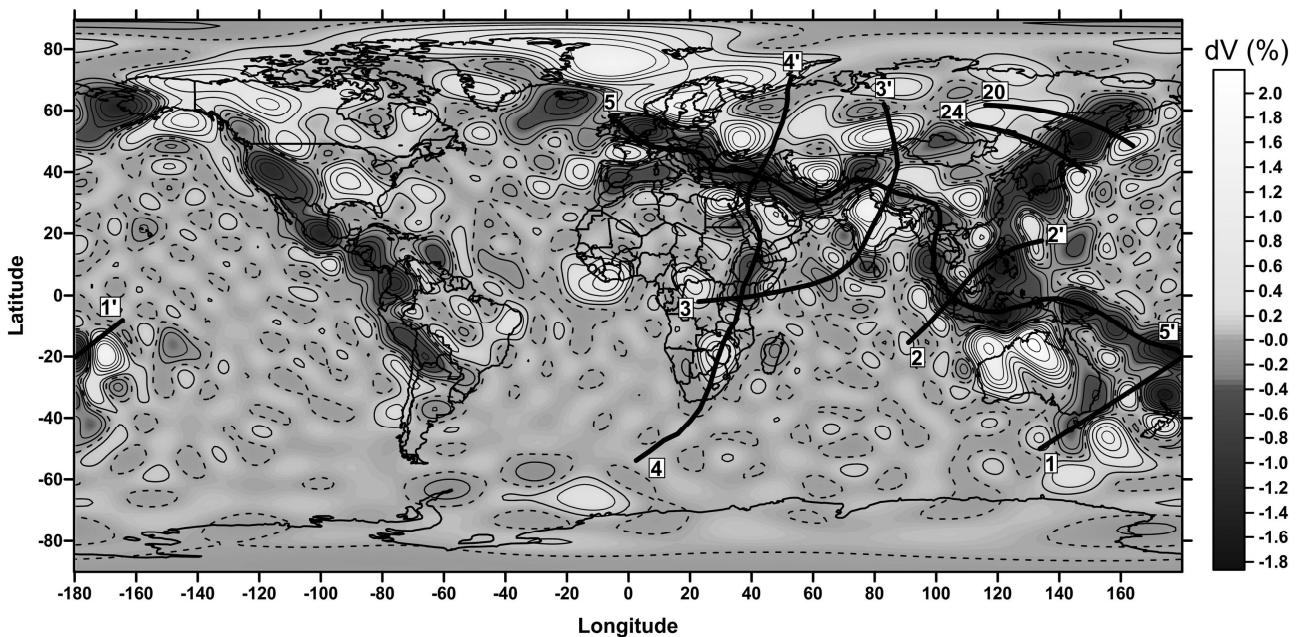


Fig. 25. Distribution of dV_p at the depth up to 100 km and lines of sections (Fig. 26–29), lines 20 and 24 after (Zhao et al., 2010). Compiled after the data in (Becker, Boschi, 2002; Grand et al., 1997; Van der Hilst et al., 1997). Contour lines are spaced at 0.2%; the dashed line corresponds to zero value

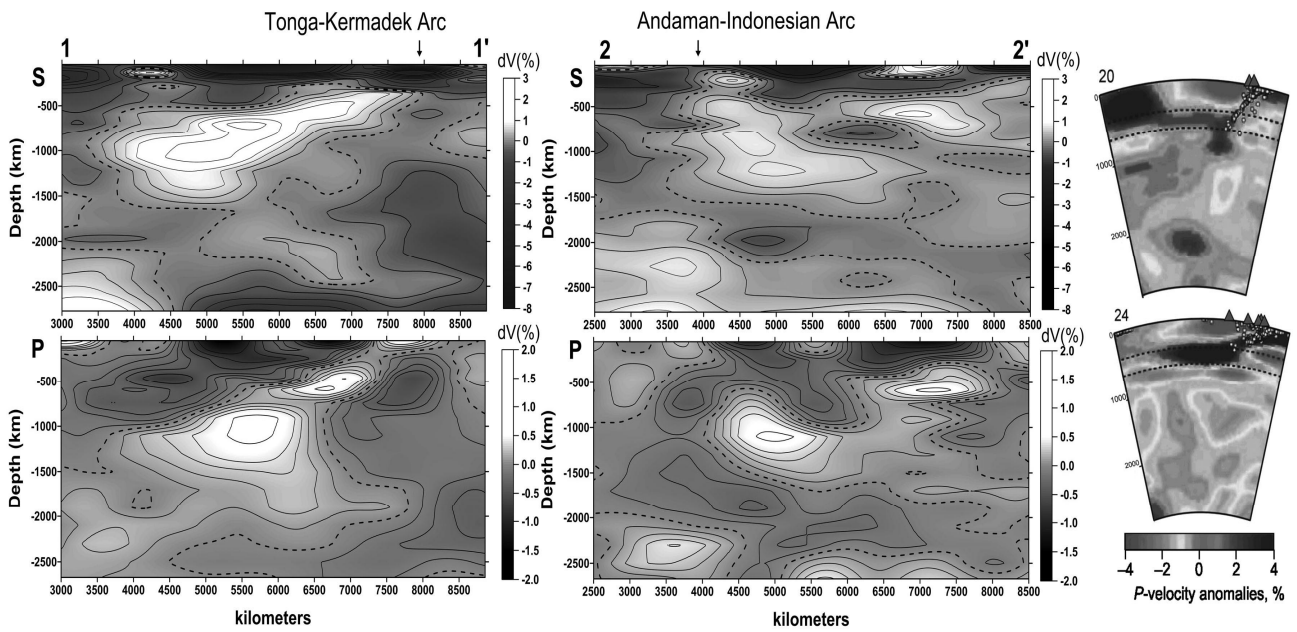


Fig. 26. Seismic tomography dV_P and dV_S sections along lines: 1–1' across the Tonga-Kermadec Arc; 2–2' across Philippines and the Andaman-Indonesian Arc. Compiled after the data in (Becker, Boschi, 2002; Grand et al., 1997; Van der Hilst et al., 1997). Contour lines are spaced at 0.25% for P -waves and 0.5% for S -waves; the dashed lines correspond to zero value. The dV_P profiles across Kamchatka (20) and Hokkaido (24) after (Huang, Zhao, 2006; Zhao, 2009; Zhao et al., 2010) are given for comparison. Small white circles are hypocenters of earthquakes and dark triangles are volcanoes in the profiles 20 and 24. See fig. 24 and 25 for position and legend

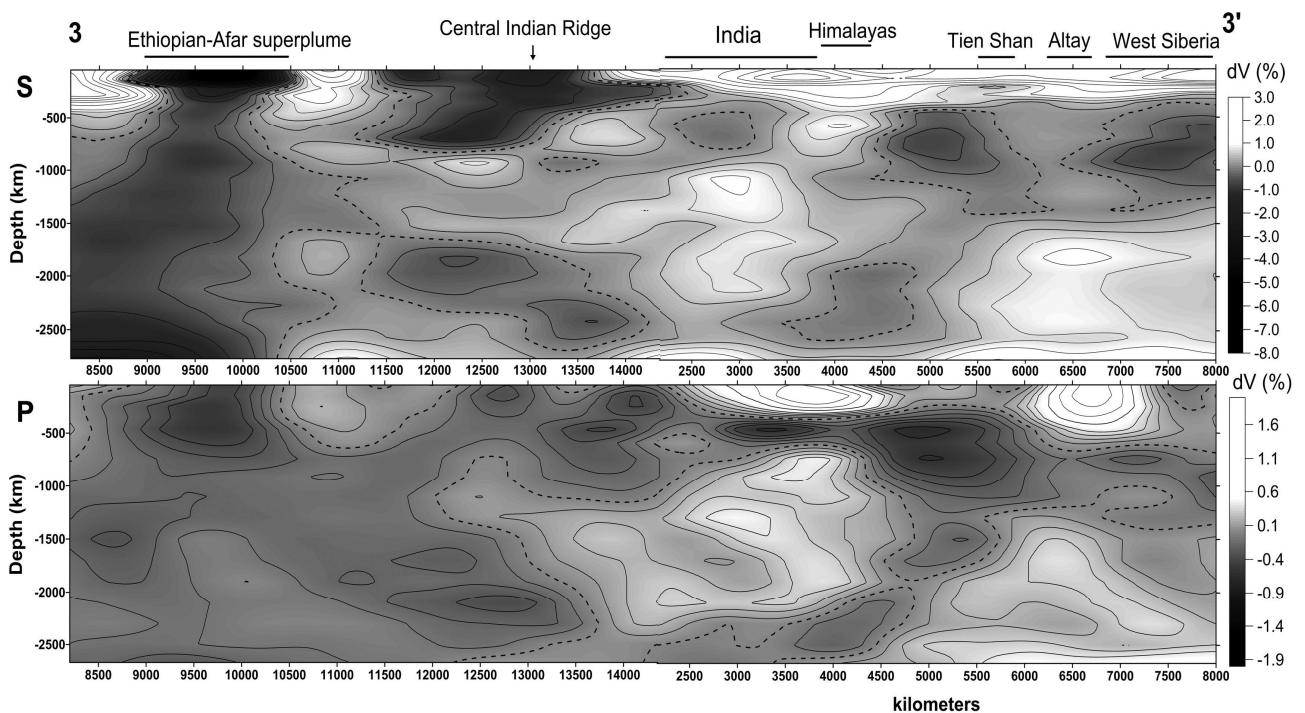


Fig. 27. Seismic tomography dV_P and dV_S sections along line 3–3' from Kenya via the Mid-Indian Ridge, Indian Platform, and High Asia to the post-Paleozoic West Siberian Platform. Compiled after the data in (Becker, Boschi, 2002; Grand et al., 1997; Van der Hilst et al., 1997). Contour lines are spaced at 0.25% for P -waves and 0.5% for S -waves; the dashed lines correspond to zero value. See fig. 24 and 25 for position and legend

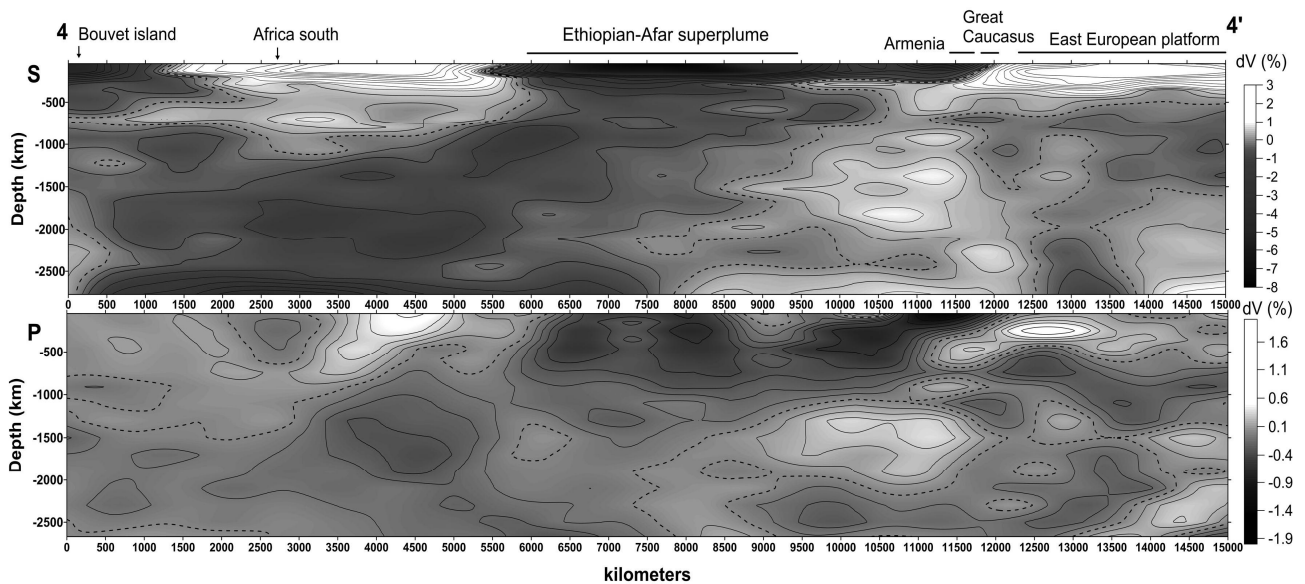


Fig. 28. Seismic tomography dV_P and dV_S sections along line 4–4' from South Africa via the Ethiopian-Afar super-plume, Arabian Platform and the Caucasus to the East European Platform. Compiled after the data in (Becker, Boschi, 2002; Grand et al., 1997; Van der Hilst et al., 1997). Contour lines are spaced at 0.25% for P -waves and 0.5% for S -waves; the dashed lines correspond to zero value. See fig. 24 and 25 for position and legend

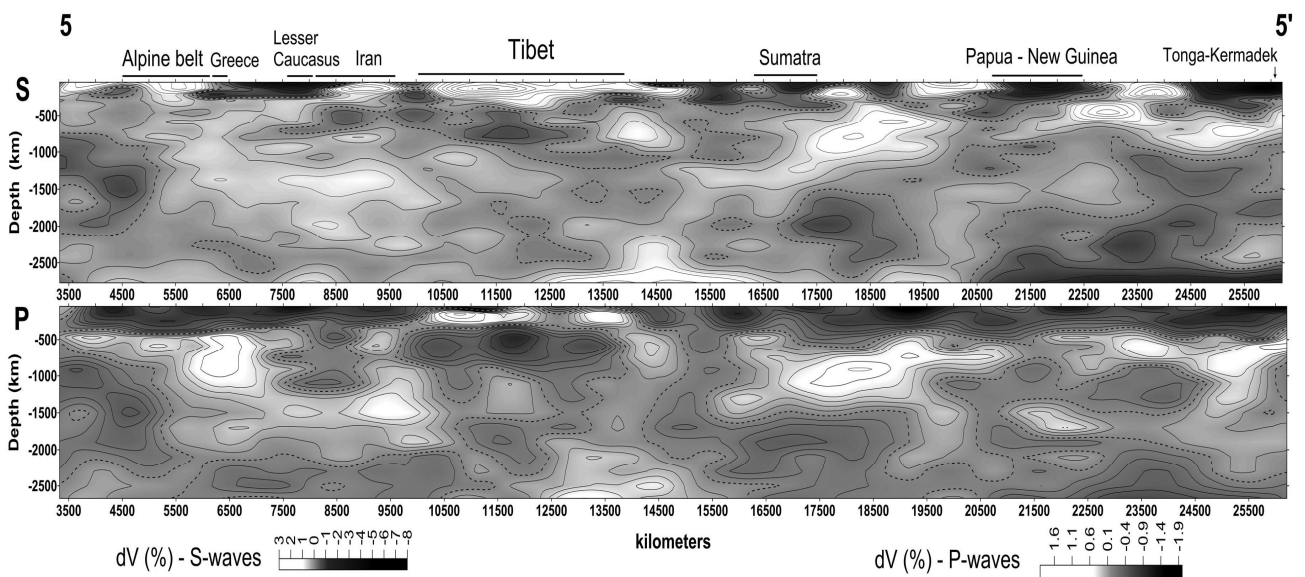


Fig. 29. Seismic tomography dV_P and dV_S sections along line 5–5' along the Alpine-Himalayan Belt from Tonga-Kermadec Arc via the Indonesian back-arc basin, Tibet, Pamirs, the Lesser Caucasus, Anatolian Plate, and the Carpathians to the West European Hercynides. Compiled after the data in (Becker, Boschi, 2002; Grand et al., 1997; Van der Hilst et al., 1997). Contour lines are spaced at 0.25% for P -waves and 0.5% for S -waves; the dashed lines correspond to zero value. See fig. 24 and 25 for position and legend

Another situation is characteristic of the Tibetan–Himalayan segment of the belt (Fig. 27, section 3–3'). The layer of highly increased dV_s down to the depth of 100–300 km extends here from the Himalayas to the northern margin of the Tien Shan and continues as a high-velocity layer beneath the Indian Platform and the Kazakhstan–

West Siberian segment of the Eurasian Plate. The high-velocity layer thickens to 400 km beneath Southern Tibet near the Neotethian Suture (Indus–Zangpo Zone). One more nearly horizontal high-velocity lens is detected there at a depth of 600–700 km.

It cannot be ruled out that a part of the upper high-velocity layer and this lens are transformed relics of the Neotethyan slab flattened at a depth. In the dVp section, a similar high-velocity lens is traced from the southern margin of the Indian Platform to the northern margin of Tibet at a depth of 100–300 km. The greatest thickness of this layer and the highest dVp values are established beneath Southern Tibet. To the north, the averaged dVp values in the upper mantle decline to a moderate level and one more high-velocity lens appears in the south of Western Siberia. A domain of lowered dVp occurs below the high-velocity layer as a narrow (400–500 km) lens beneath the Indian Platform. This domain is reduced beneath Southern Tibet and swells to a depth of 300–800 km beneath High Asia from Tibet to the Tien Shan, where locally reaches very low dVp values. In the lower mantle, a poorly delineated and fragmented zone of slightly lowered dVp values tilted to the southwest occurs beneath this thickened lens. In the dVs section, the above-mentioned features are less distinct. A domain of slightly lowered dVs values is situated beneath High Asia, and the tilted zone in the lower mantle is noted by moderate dVs against the background of slightly increased values beneath the adjacent territories.

Of principal importance are the seismic tomography sections across Africa, Arabia and the Arabian–Iranian segment of the Alpine–Himalayan Belt (Fig. 28, sections 4–4'). Relatively thin upper mantle lenses with highly lowered dVs values are seen in the section no deeper than 200 km. These are a short lens near Bouvet Island and a long lens, which extends beneath the East African Rift System and the Red Sea Rift to southern Arabia. The northern lens extends northward to the Greater Caucasus, where it is characterized by lowered dVs values. A wide domain of lowered and slightly lowered dVs values is traced below down to the bottom of the mantle. The upper part of this domain corresponds to the territory from Malawi to the Red Sea, and, being tilted to the south, is located beneath South Africa at the lower-mantle level. This domain is regarded as the Ethiopian–Afar superplume. The upper mantle of the African and Eurasian plates is distinguished by increased dVs values. A high-velocity wedge plunges from the Scythian Platform beneath the Greater Caucasus, where it flattens and is traced to the Lesser Caucasus, gradually losing its specificity. In the dVp section, the Ethiopian–Afar superplume is also expressed as a wide domain of lowered dVp values tilted to the south. In the upper mantle, this domain is traced to a depth of 600–800 km from Malawi to the Lesser Caucasus. Its segments

beneath the Kenyan Rift, Afar, and the Armenian Highland are distinguished by highly lowered dVp . Beneath the Greater Caucasus the thickness of this domain is abruptly reduced and limited from below by the high-velocity wedge plunging from the Scythian Platform. The upper mantle of South Africa and the East European Platform is characterized by slightly increased and medium dVp values.

The transverse sections are supplemented by longitudinal sections 5–5' oriented along the axis of the Alpine–Himalayan Belt and extending from the Tonga–Kermadec arc via the backarc basins of the Andaman–Indonesian arc, Tibet, the Pamirs, Afghanistan, Iran, and the Lesser Caucasus to Anatolia and via the Carpathians to the West European Hercynides (Fig. 29). These sections are important for understanding of the deep structure of the belt for two reasons.

First, they make it possible to look at the structures delineated in the transverse sections in another perspective. For example, the longitudinal sections confirm passing of the slab beneath the Tonga–Kermadec arc in a nearly horizontal zone of increased Vp and Vs values at a depth of 600–800 km. In the dVs section, this zone is supplemented by nearly horizontal high-velocity lenses at depths of 100–200 and 350–500 km at the western Pacific margin and at a depth of ~200 km between the Papua New Guinea arc and the eastern flank of the Andaman–Indonesian arc. The two-floor structure of the upper mantle beneath Tibet (increased Vp above and lowered Vp below) revealed in transverse section 3–3' is confirmed by the longitudinal section, where such a structure is detected over the entire territory from the eastern margin of Tibet to the Pamir–Hindu Kush. In the west, from Afghanistan to the Carpathians, a layer of lowered and highly lowered dVp values is depicted at a depth down to 200–300 km and extends beneath the West European Hercynides. The fact that the same structures are detected in both longitudinal and transverse sections indicates that the revealed variations are related to real mantle inhomogeneities rather than to the effect of anisotropic propagation of seismic waves.

Second, sections 5–5' demonstrate segmentation of the belt known from the relationships between the Late Cenozoic crustal structural elements (Trifonov et al., 2002). This segmentation is expressed better in the dVp section, where the difference of the segments is traced throughout the upper mantle. The boundary between the southeastern island-arc and the Tibetan section types approximately coincides with the fault zone of 105°E between the corresponding segments of the belt, whereas the boundary between the Tibetan and the Iran–Caucasus section types fits the Darwaz–Chaman Fault Zone between the Pamir–Himalayan and the Arabian–Iranian segments.

2.2. A model of structural evolution of the mantle beneath the Tethys and Alpine-Himalayan Collision Belt in Mesozoic and Cenozoic and its geological consequences

2.2.1. Ethiopian-Afar superplume and upper-mantle flows spreading away from it

Two structural features are the most important in the described above results of the seismic tomography profiling. First, the subduction zones flatten in the level of the transitional layer of the mantle (approximately 400–700 km) and form the BMW zones in the Indonesian segment of the Alpine-Himalayan Belt, where the subduction continues till now. Second, in the more northwestern Himalayan-Tibetan and Arabian-Caucasus segments of the belt, where the subduction finished in the time interval between the late Middle Eocene and Middle Miocene with a closure of the last relics of the Neothetys, the thick layer of the sub-lithosphere mantle with lowered seismic wave velocities extends uninterruptedly from the Ethiopian-Afar superplume (Sokolov, Trifonov, 2012).

Studying the Aleutian, Kurile–Kamchatka and Japanese island arcs, Huang and Zhao (2006) and Zhao et al. (2010) has shown that only in 5 of 22 transverse sections do slabs extend below 670 km. In other sections, slabs pass into a sub-horizontal layers at a depth of 410 to 670 km. In the cases when slabs go deeper, this layer is also detected in the section and is expressed in the V_p field better than the downward continuation of the slab (Fig. 26, sections 20 and 26).

Formation of the BMW structures had important geological consequences. Anomalies of seismic wave velocities (deviations from average statistical values characteristic of certain depths) corresponding to ascending hot and descending cold mantle flows reach a few percent only in the asthenosphere and local segments of subducted slabs. Elsewhere in the mantle, they are lower, deviations of 0.25% for V_p and 0.5% for V_s , i.e., 0.02–0.06 km/s, deemed to be significant. At the same time, V_p in the mantle increases with depth from ~8 to ~13 km/s and V_s from 4.3 to 7.0 km/s. At certain levels, the velocities change by fractions of km/s. Such jumps are referred to variations in rock density, which cannot be caused only by increase or decrease of density of rocks under the load of overlying rocks, but suggest a change in the crystal structure of minerals.

These transformations, confirmed by laboratory experiments at super-high pressure and temperature, have been described in the literature and recently summarized in (Pushcharovsky Yu., Pushcharovsky D., 2010). These publications rid us from the necessity of detailed discussion in this book. Note only that at a depth of 50–100 km pyroxenes of mafic and ultramafic rocks are transformed into garnets with a higher density. Several other seismic discontinuities are detected below in the upper mantle. The most distinct and extensive boundaries occur at depths of ~410 and ~670 km. The ~410-km discontinuity corresponds to the transition of orthorhombic olivine to the variety with spinel structure (wadsleyite transformed at a depth of ~520 km into ringwoodite), the density of which increases by 8%. Clinopyroxene is transformed into wadsleyite and stishovite at approximately the same depth. Within a depth interval of 410 to 500 km, pyroxenes acquire a more compact ilmenite-type structure. Thus, garnet, spinel, and silicates with ilmenite structure dominate at a depth of 410–670 km. At a greater depth, these minerals are replaced by denser perovskite-like phases occupying ~80% of the volume of the lower mantle (Pushcharovsky Yu., Pushcharovsky D., 2010).

The aforesaid shows that the jumps at seismic discontinuities and partly the general increase in the seismic wave velocity with depth are caused by modification of the crystal structure of mantle minerals, while the bulk chemical composition remains rather uniform. The variation in velocity probably reflects variation in the mantle density with depth. The descending and ascending flows of the mantle material are traced through the aforementioned seismic boundaries, and this implies that the flows undergo the same change in mineral composition as the surrounding mantle, retaining a difference in temperature. Because of the temperature difference, the transition of olivine into a spinel phase, as well as of pyroxene with segregation of stishovite, proceeds in a cold slab at a lower pressure at a depth of 300–380 km. In hot superplumes, the depth of transition probably increases. It should also be kept in mind that phase transitions may be exothermic, e.g., transformation of olivine into spinel or pyroxene into the phase with ilmenite structure, or endothermic, for example, transition to perovskite-type structure (Sorokhtin, 2007), with additional complication of the seismic tomography patterns.

The water content in the asthenosphere is a principal parameter determining its geodynamic role. Ringwood (1975) estimated the water content at 0.1%. According to the data published by Pugin and Khitarov (1978), the water content in the mantle is measured by 0.1%. Green et al. (2010) showed that the water content decreases 2–3 times from subduction zones to spreading zones. At the same time, Letnikov (1988,

2003_{1,2}) supposes that deep fluids play an important role in the formation of lithospheric (including crustal) magma sources and in metamorphism of the lithosphere. He suggests that the asthenosphere is the main source of fluids and also assumes that they may be supplied from a greater depth (Letnikov, 2001, 2006).

According to petrological and geochemical data, most minerals in the sublithosphere mantle are anhydrous (Ryabchikov, 2005). Only the rocks within the depth interval 410–670 km (a transitional layer of the mantle) may be an exception. The crystal structure of wadsleyite and ringwoodite allows replacement of a part of the oxygen anions in these anhydrous minerals with a hydroxyl group (Smyth, 1994; Jacobsen et al., 2005). The subducted slabs, which contain incompletely dehydrated amphibolites and metasedimentary rocks, can be a source of hydroxyl. As was shown above, such slabs are transformed into almost horizontal high-velocity lenses at a depth of 410–670 km (Otani, Zhao, 2009). The appreciable attenuation of shear waves along with insignificant change of their velocities (Lawrence, Wysession, 2006) and increased electric conductivity (Kelbert et al., 2009) indicate that fluids occur at those depths. As concerns deeper sources of aqueous fluids, recent data on the density of the Earth's core allows the occurrence of hydrogen therein. Iron hydride is stable at the temperature and pressure characteristic of the lower mantle (Pushcharovsky Yu., Pushcharovsky D., 2010), but the minerals of the lower mantle contain a minimal amount of oxygen, and this rules out its coupling with hydrogen. Such a possibility appears only at the depth interval 410–670 km. Thus, the transitional layer is the main potential source of water fluids in the mantle.

The Ethiopian-Afar superplume is a vast N-trending zone corresponding in the lithosphere level to the entire East African Rift System and continuing southward of the latitudes of Madagascar in the south (Fig. 30). The flows of the upper mantle material spread from the superplume up to the northern margins of the Alpine-Himalayan Belt. The trails of sublithosphere flows are marked in the seismic tomography sections across the Arabian-Iranian segment of the belt by the decreased seismic wave velocities throughout the entire upper mantle, the flow being seen better in the dV_P section (Fig. 28 & 29). The flow trails are also seen in the dV_P section 3–3' (Fig. 27), where the flow layer underlies the thin lithosphere of the Indian Ocean and is covered farther to the north by the high dV_P lens corresponding to the thickened lithosphere of the Indian Platform and High Asia. Beneath the flow layer, within the lower mantle, the zone of weakly lowered dV_P values is found. Like the Ethiopian-Afar superplume, this zone dips to the south-west. Perhaps, it is a relic of a previously existing plume.

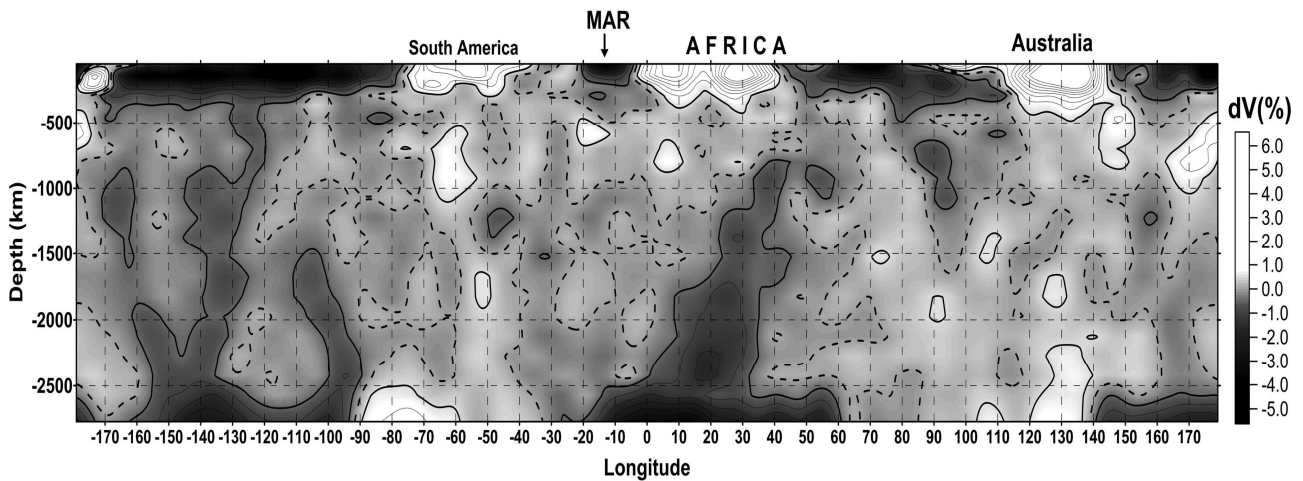


Fig. 30. Seismic tomography dV_S section along $S22^\circ$ latitude. The "branches" of Pacific superplume are at the left part of section, the Ethiopian-Afar superplume is at the center of section. The both superplumes have continuation as lateral flows in upper mantle. Compiled after the data in (Becker, Boschi, 2002; Grand et al., 1997). Contour lines are spaced at 0.5%; the dashed line corresponds to zero value

We suppose that the elongated Ethiopian-Afar superplume developed as a more or less stationary structure at least from the end of the Paleozoic. The portions of moving Gondwana, which turned out to lie above the super-plume, underwent rifting that developed into spreading forming the Tethys Ocean. A flow of heated asthenosphere material from the superplume caused asymmetry of the spreading and moving of torn-off fragments of Gondwana to the north-east toward Eurasia. The oceanic Tethyan lithosphere subducted there and the Gondwanan fragments accreted to Eurasia. Because of this, the subduction zone jumped back to their rear (relative to Eurasia) parts. As a result, series of microplates, separated by sutures, accretionary wedges, and magmatic bodies related to different stages of the Tethys evolution, formed on the place of the future mountain belt. The recent structure of the mantle under the Indonesian segment, where the described process is lasting till now, give a possibility to suppose that the more north-western segments of the belt had previously the same structure, i.e., the subducted slabs transformed there at the depths of 400–700 km into the BMW that extended beneath the entire future mountain belt. The bulge of the upper high-velocity layer beneath the Southern Tibet (down to 400 km in the dV_S section) and the lower (~ 600 km) lens with slightly increased V_S may be the BMW relics. In the dV_P section, these lenses are separated by the low-velocity layer, which continues the sub-lithosphere flow related to the Ethiopian-Afar superplume.

The difference between the segments of the Alpine-Himalayan Belt is caused by their different Cenozoic history. The island-arc structure of the Indonesian segment has remained until now, whereas the last relics of the Neo-Tethys in the Pamir-

Himalayan segment were closed in the Oligocene. The relics of the Neo-Tethys and the related back-arc basins in the Arabian-Iranian segment were closed at the time from the Late Eocene to the Middle Miocene. In line with this, the subduction and the BMW formation gave way in the Pamir-Himalayan and Arabian-Iranian segments to the collision of the Eurasian and Gondwanan lithosphere plates. This process decelerated their convergence, but the hot asthenosphere flows from the Ethiopian-Afar super-plume probably prolonged the former movement and gradually spread under the entire orogenic belt. The propagation developed successively. For example, the sub-lithosphere low-velocity layer thinned sharply beneath the Greater Caucasus. The thinning could have been caused by subduction of the Para-Tethyan Caucasus basins under the Lesser Caucasus before the Middle Miocene (Leonov M.G., 1975; Alpine history..., 2007). The subduction hindered the northward propagation of the sub-lithosphere flow till the subduction had finished.

The hot sublithosphere flows reworked the upper mantle of the Alpine-Himalayan Belt. This is expressed in reduced average V_p values in the most upper mantle beneath all mountain systems of the belt, except a part of the Himalayan-Tibetan region (Fig. 25 & 29). The decrease of the velocities can be interpreted as a thinning of the lithosphere at the expense of the asthenosphere and/or decrease of density in the lithosphere mantle and the lower crust under the effect of the asthenosphere (Artyushkov, 1993; Ranalli et al., 2007; Trifonov et al., 2008; Trifonov, Sokolov, 2014; see sections 1.2.6 and 1.5.6). Beneath High Asia, where the lithosphere was essentially thickened by Cenozoic deformation, the high-velocity layer up to 300-km thick remained above the low- V_p layer.

On moving, the sublithosphere flows were enriched in aqueous fluids that could derive from the former BMW lenses related to subduction zones. The asthenosphere, activated in this manner or its fluids penetrated into the lithosphere and gave rise to the important Cenozoic geological processes. The effect of the active asthenosphere and related fluids induced softening of the lithosphere (Artyushkov, 2003) that promoted intensive deformation, detachment, and large lateral displacement resulted in the formation of local uplands in the stage 1 of mountain building. Local uplands formed in the areas of concentrated deformation. Their position depended on orientation of maximum compression that was different in different substages of the stage 1. Formation of the local uplifts occurred against the background of neotectonic evolution of the lithosphere that developed according to two scenarios, the Central Asian and the Mediterranean.

In Central Asia, the lithosphere was thickened by previous significant deformation and contained a lot of metabasic relics of the former oceanic crust. The effect of the active asthenosphere and related fluids caused the metamorphic reworking of metabasic relics and the formation of intra-lithosphere magmatic sources, including crustal ones that were expressed by gigantic granitic batholiths (Letnikov, 2003₁). These processes resulted in predominating rise of the territory that combined with the local deformational uplifts.

In the Mediterranean, the deformational uplift in the areas of maximum compression developed parallel to subsidence of secondary basins that formed after the closure of Neotethys and majority of its back-arc basins. Some secondary basins were deep enough for pelagic sedimentation. Such basins developed around the northern flank of the Arabian Plate in the Eocene and were deformed and closed in the Miocene (Robertson et al., 2004). In Western Mediterranean, similar structures (the Ligurian, Tyrrhenian, and possibly Alboran basins) have formed after the folding of late Middle Eocene and develop till now. Their origin can be related to the upper mantle diapirs that rise from the active asthenosphere through the relatively thin lithosphere of the region.

Large-scale deformation of the stage 1, accompanied by metamorphism and crustal magmatism caused a consolidation of the Earth's crust to the Early Pliocene. The consolidation was expressed by cessation of the large-scale granite formation in the Pliocene–Quaternary and localization of volcanic activity within strike-slip zones (Koronovsky, Demina, 1999; Karakhanian et al., 2002; Wang et al., 2007; Trifonov et al., 2011). The latter became the leading form of transverse shortening of the belt at the stage 2, whereas the fold-thrust deformation concentrated within the basins with thick sedimentary cover, such as the Sub-Himalayas, Afghan-Tajik Basin, foothills of the Taurus, the Lower Zagros, and periclinal folds of the Greater Caucasus.

Huge strike-slip fault system formed in the Alpine-Himalayan Belt during the stage 2 (Fig. 31). Some segments of these systems developed as strike-slip faults earlier, another ones appeared only in the Pliocene–Quaternary. The largest dextral system striking in the NW–SE to the W–E direction begins in the NW by the Talas-Fergana Fault. It continues to the SE en echelon by the Karakorum Fault Zone and the W–E-trending en echelon row of the South Tibetan strike-slip faults. Farther to the SE the system bifurcates to two strands. One of them is the Red River Fault that extends into Vietnam. The second strand extends to the south by the dextral strike-slip faults of the southern Yunnan and the northern Burma that continue en echelon by the dextral Sagaing Fault and probably by the faults of the off-shore East Indian

Ridge. The similar large system includes several right lateral fault zones: the North Aegean, North Anatolian, Main Recent Fault of Zagros, and its continuations in the Fars tectonic province of Iran. One more such system is represented by the reverse-dextral Main Copet Dagh Fault that continues en echelon to the west by the Isak-Cheleken, Apsheron Threshold and Main Great Caucasus fault zones.

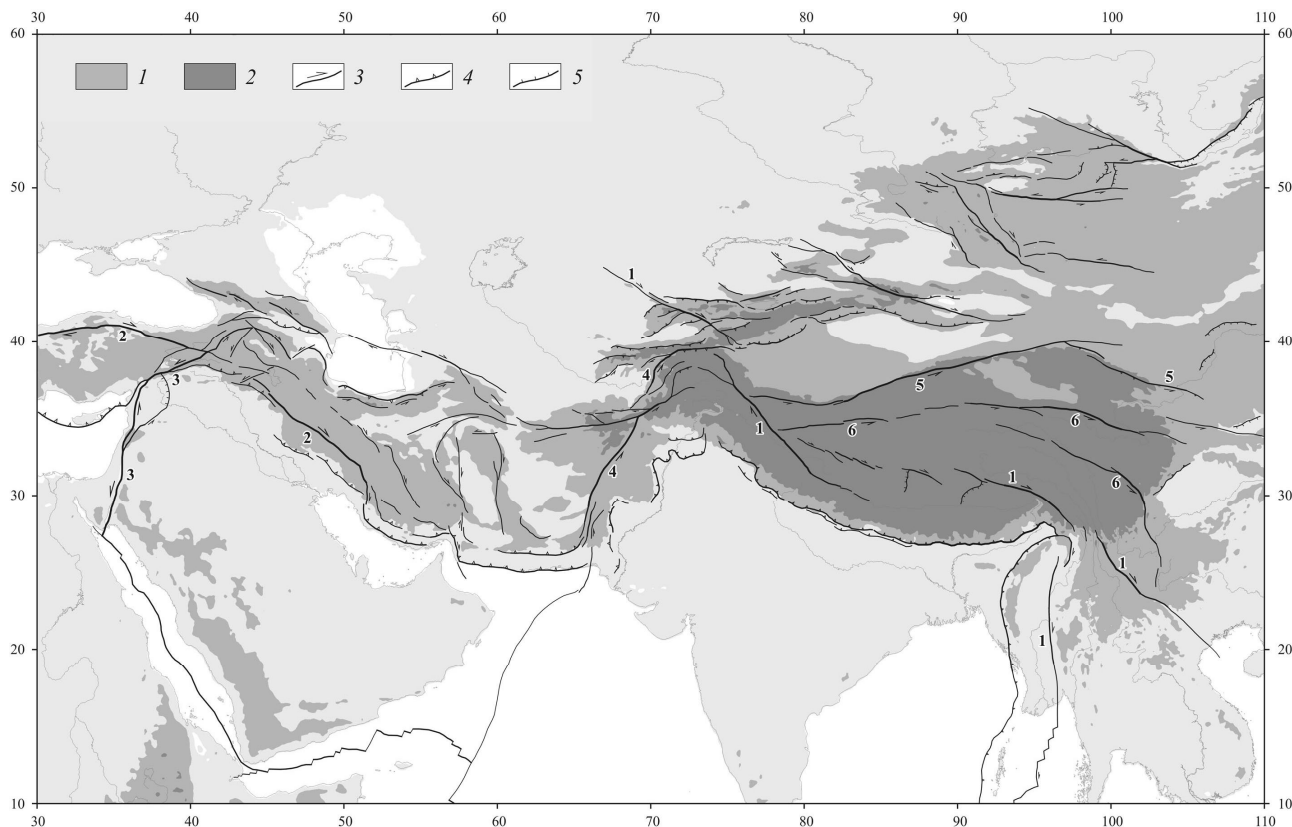


Fig. 31. The Pliocene-Quaternary strike-slip systems in the Alpine-Himalayan Belt

1, highlands 1000–3000 m; 2, ridges and plateau higher than 3000 m; 3–5, major active faults: 3, strike-slip faults, 4, thrusts and reverse faults, 5, normal faults. The largest dextral strike-slip systems: 1, the system from the Talas-Fergana Fault up to the Red River and Sagaing faults; 2, The North Anatolian fault zone and Main Recent Fault of Zagros with its continuation. The largest sinistral strike-slip systems: 3, Levant–East Anatolian; 4, Darvaz–Chaman with its southern off-shore continuation; 5, Altyn Tagh; and 6, Kunlun–Yunnan

There are also several large N–S-trending and SW–NE-trending sinistral fault systems. One of them is formed by the Dead Sea Transform (the Levant fault zone) and the East Anatolian fault zone that bifurcates in the NE to the North-East Anatolian and East Anatolian strands. They continue to the NE by the Kazbek-Tskhinval fault, possibly extending to Daghestan. Another dextral system includes the Darvaz and Chaman sinistral faults and the southern en echelon continuation of the latter that extends possibly to the south by the Owen fault zone in the off-shore Merrey Ridge of the western Indian Ocean. Two more sinistral systems are the ENE-trending Altyn Tagh and Kunlun–Yunnan fault zone in Central Asia.

Under the consolidated crust, the influence of the asthenosphere onto the lithosphere increased at the stage 2 of mountain building. According to the seismological and gravimetric data, a density of the uppermost mantle is decreased under the highest mountain systems of Central Asia (the Himalayas, the Tibet, the Kunlun, the Pamir–Hindu Hush–Karakoram region, and the Central and Eastern Tien Shan) as well as under the Lesser Caucasus and the Eastern Carpathians (see the section 1.5.5.3). The most probable mechanism of the decrease of density is partial replacing of the lithosphere mantle by the lower-dense asthenosphere (Artyushkov, 1993, 2003; Trifonov et al., 2008, 2012₁). The decrease of density of the uppermost mantle leads to the uplift of the Earth's crust.

The decrease of density of the lower crustal masses as a result of retrograde metamorphism under the effect of cooled Pliocene asthenosphere fluids may be the second source of intensification of mountain growth. Influence of this factor seems to be dominant on the additional uplift of the Greater Caucasus above that due to the compression deformation. The decrease of density of the uppermost mantle is found only under the Elbrus volcanic region (Milanovsky et al., 1989). At the same time, volumes of rocks with the lowered density and increased electric conductivity were found under the Central and Eastern Caucasus in the lower crust and near the crust-mantle boundary (Grekov et al., 2008). Such volume under Elbrus at the depths of 35–50 km is characterized by the lower seismic wave velocities and is identified as a magmatic source (Modern and recent volcanism..., 2005). However, this interpretation cannot be applied to the other similar volumes. Decrease of their density is probably due to the retrograde metamorphism of rocks near the crust-mantle boundary with participation of the cooled asthenosphere fluids (Trifonov, Sokolov, 2014). Their main source was the asthenosphere flow from the Ethiopian-Afar superplume that reached the Greater Caucasus only in the Late Miocene (Ershov, Nikishin, 2004). Small thickness of the flow explains its weak expression in the field of seismic wave velocities. However, this thin flow and its fluid influence were able to facilitate the metamorphic decrease of density of the high-grade metamorphic rocks of the crustal origin that resulted in the uplift of mountain system. We suppose the same development of the Late Cenozoic tectonic processes in the Western Tien Shan (Trifonov et al., 2012₂).

The both above-mentioned processes produced additional rise of the land surface and caused the acceleration of total uplift of the belt during the Pliocene-Quaternary.

2.2.2. Cenozoic volcanism in the Arabian Plate and Arabian-Caucasus Segment of the Alpine-Himalayan Belt

An analysis of dates of the Cenozoic volcanic rocks in the East African rift system and the Arabian-Caucasus segment of the Alpine-Himalayan Belt give a possibility to estimate spread of the sublithosphere upper mantle flow away from the Ethiopian-Afar superplume (Fig. 32).

2.2.2.1. Basaltic volcanism in the Arabian Plate

The East African rift volcanism began in the Eocene 45–37 Ma (Ebinger, Sleep, 1998). In the Oligocene, the Aden–Red Sea rift system was originated, and the belt of basaltic parallel dykes, small volcanoes and extrusions formed in the northeastern side of the Red Sea rift. According to the data on Saudi Arabia, volcanism started in the belt 32–30 Ma and continued till ~20 Ma with maximum 21–24 Ma (Camp, Roobol, 1992). In the Sinai part of the belt, dykes, sills and extrusions have the K-Ar ages from $24,8 \pm 1,5$ Ma till $20,3 \pm 0,7$ Ma [Segev, 2005]. During the Late Oligocene–Early Miocene, the basaltic volcanism occupied large areas in the central and northern parts of the Arabian Plate (Camp, Roobol, 1989). The basalts are in Syria (Geological Map of Syria, 1964; Ponikarov et al., 1967; Mouty et al., 1992; Chorowicz et al., 2004) and in adjacent territories of Turkey up to the Taurus suture (Çapan et al., 1987; Yilmaz et al., 1998) and in Jordan up to Saudi Arabia (Barberi et al., 1979; Ilani et al., 2001). Similar, but less extensive volcanism occurs in the Dead Sea Transform (DST) zone (Garfunkel, 1989; Sharkov et al., 1994; Polat et al., 1997; Yürür, Chorowicz, 1998; Abdel-Rahman, Nassar, 2004; Segev, 2005).

All researchers agree that the basalts were generated in the mantle, but attribute their origin to different processes. In the opinion of Garfunkel (1989), the basalts were related to “several short-lived upwellings, which formed intermittently beneath a wide region”. Stein and Hofmann (1992) came to the conclusion that relative homogeneity of the basalts in terms of the Sr–Nd isotopic ratios was due to their common source represented by a plume at the base of the Arabian lithosphere. Sobolev et al. (2005) agreed with the “plume” origin of the Arabian basalts, but argued they are related to the Ethiopian-Afar deep mantle superplume. Ershov and Nikishin (2004) shared this opinion. They reasoned that the superplume penetrated to the upper mantle from the lower mantle 45–37 Ma (Ebinger, Sleep, 1998) and formed two lateral sub-lithosphere flows: to the south (Kenya) and to the north.

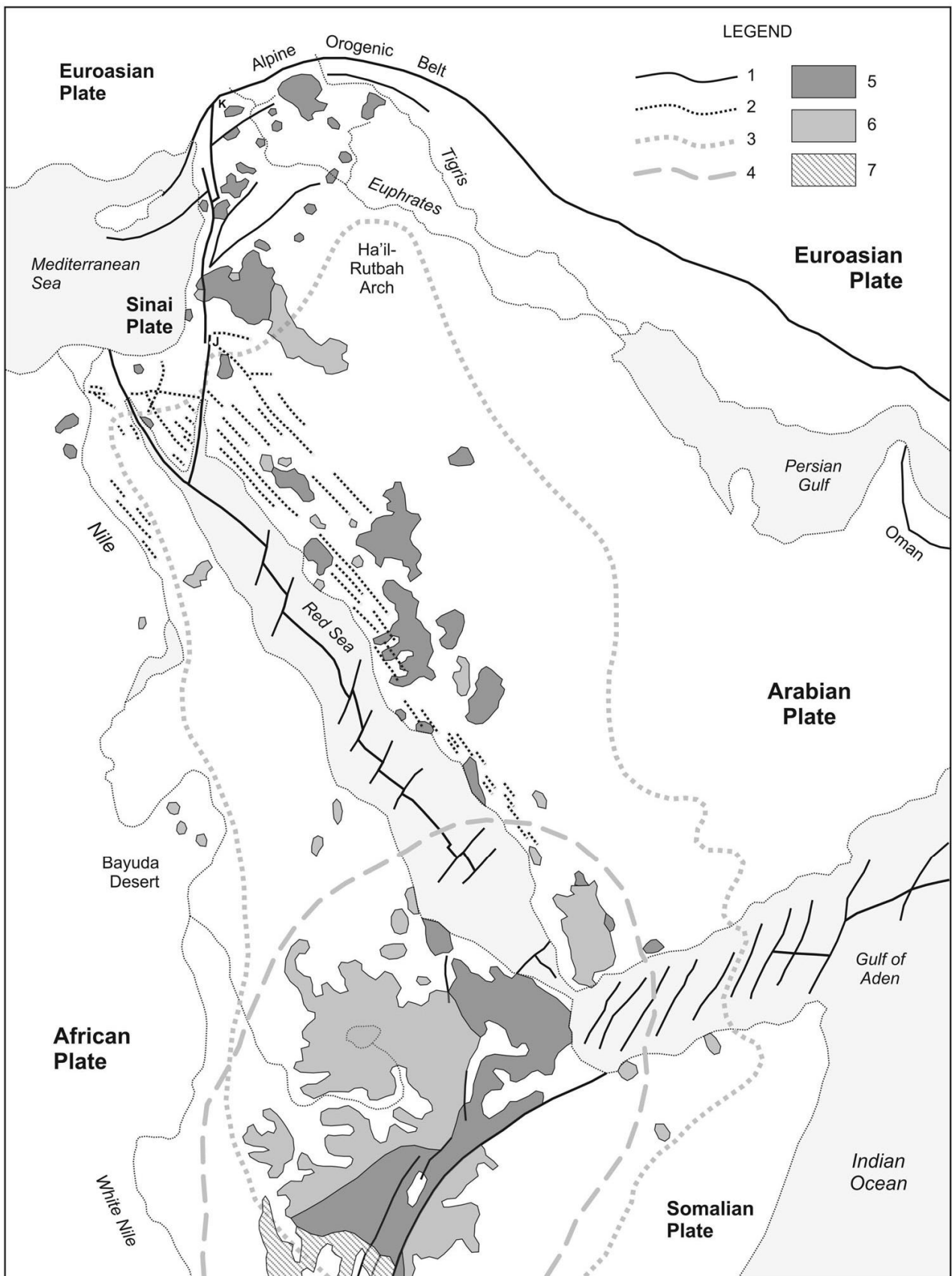


Fig. 32. The Ethiopia–Arabian plate volcanism, modified after (Segev, 2005). 1, main faults; 2, Middle Cenozoic dykes; 3, boundaries of the Afro-Arabian dome; 4, boundaries of the Ethiopia–Afar mantle plume; 5, Late Cenozoic volcanics; 6, Middle Cenozoic volcanics; 7, Early Cenozoic volcanics

The second flow propagated in succession beneath the southern Arabia and Red Sea region (~28–27 Ma), beneath central and northern Arabia (13–9 Ma), the Armenian Highland (~11 Ma) and the Greater Caucasus (9–7 Ma). Ershov and Nikishin referred to the seismic tomography data on existence of the “hot” (low-velocity) sublithosphere volumes beneath these regions (Debayle et al., 2001; Ershov et al., 2001) as an evidence of the flow.

However, Lustrino and Sharkov (2006) raised objections against links between the basalts and sublithosphere plumes: (1) “the spinel/garnet-bearing lherzolitic sources evidenced by semi-quantitative geochemical modeling can be related only to relatively shallow sources (generally <90 km deep)” (p. 136), i.e., in the lower lithosphere; (2) the absence of one-way progression of the magmatic activity age and the long time span of eruptions in the same areas do not correspond to the deep mantle plume volcanism; (3) the differences in Sr and Pb isotopic ratio exclude any participation of the Afar plume in generation of the central-northern Arabia basalts. Lustrino and Sharkov (2006) “propose that lithospheric extension is the main cause of igneous activity” and emphasize its “structural control by lithospheric discontinuities representing preferential pathways for uprising magmas” (p. 135). According to Weinstein’s data, quoted by Segev (2005), the Galilee–Dead Sea region basalts were lithosphere-derived and could have “two principal sources: amphibole-rich peridotite”, related to the Late Proterozoic slab and “amphibole-garnet-rich pyroxenitic veins within the peridotite source, produced by the Paleozoic within-lithosphere partial melting event”. Weinstein et al. (2006) linked the basalts with heat “from thermally anomalous zone within the sublithospheric mantle”.

Contradiction of views on the basalt origin is caused by the lack of the data on or attention to geological history of the volcanism and relationships between it and neotectonic evolution of the Arabian Plate. This impelled us to carry out the studies of geology and additional K-Ar dating of the Late Cenozoic basalts in Syria. We corrected distribution of Holocene basalts, carried out the K-Ar dating (21 new dates) and paleomagnetic studies of some lava flows, studied relationships of the flows with bedrock and capping layers (Trifonov et al., 2011; Neotectonics, recent geodynamics and seismic hazard assessment of Syria, 2012). The new ages of the basalts together with 71 earlier K-Ar and ^{40}Ar - ^{39}Ar age determinations (Giannérini et al., 1988; Sharkov et al., 1994, 1998; Sharkov, 2000; Demir et al., 2007) give a possibility to correct the map of basalts (Fig. 33), to outline the history of the Late Cenozoic Syrian volcanism and to correlate it with tectonic structure and evolution. This gives a new view on origin of the basalts.

One of the lesser fields is the Shin Plateau on the eastern side of the DST to the west of the city of Homs. Analogous basalts are known there on the western side of the young strand of the DST, some of them form a continuation of the Shin basalts, offset sinistrally to 16–20 km on that strand (Chorowicz et al., 2004). Until the beginning of the Pliocene, the most active strand of the DST was the Roum Fault and its continuation on the continental slope (Trifonov et al., 1991; Barazangi et al., 1993; Rukieh et al., 2005; Neotectonics, recent geodynamics and seismic hazard assessment of Syria, 2012). So, the basalts on both sides of the young DST strand were erupted on the Arabian Plate. Relatively small basaltic flows are known in the Palmyrides and in the northern part of the Syrian Desert. The basalts are more widely spread on the Aleppo Plateau near the cities of Hama and Aleppo and continue from there northwards up to the Turkish town of Kahraman-Maraş (Çapan et al., 1987). Lava fields formed by one or several flows are known in the Euphrates valley and in the northwestern part of the Mesopotamian Foredeep. Basalts of the northern margin of the Foredeep are continued with larger basaltic fields in the southeastern Turkey.

In the DST zone, the Late Cenozoic basalts are exposed in the northern part of the El Ghab pull-apart basin and in the Karasu graben between the northern termination of the DST and the Amanos Fault of the East Anatolian fault zone (EAFZ). Farther south, the basalts are exposed on the surface or are penetrated by bore holes in the Hula pull-apart basin and the Jordan valley; they cover vast areas in the Yizre'el depression near the Galilee Sea (Garfunkel, 1989; Hirsch, 2005; Segev, 2005). The latter areas represent the western termination of the Jebel Arab lava field, offset sinistrally on the DST (Segev, 2005). Near the Dead Sea, the basalts are exposed on the eastern side of the DST and appear along its western side only near the Red Sea as a part of the Dyke Belt.

The Late Cenozoic basalts were erupted by small volcanoes, ruins of which are found on the basaltic fields. Some eruption centers are so morphologically inexpressive that their location was identified only by relative elevation of different parts of the lava surface and by traces of lava flow, if the surface was preserved sufficiently well. In the Jebel Arab Highland, fissure eruptions predominate. Centers of eruption form the NW-trending and NNW-trending linear chains, which represent extensional faults. Some chains are formed by volcanoes of different age, for example, the Late Miocene and Pliocene or Pliocene and Pleistocene. That indicates a long duration and inheritance of the volcanic process, in contrast to basaltic volcanism in rift zones of Iceland as a part of the Mid-Atlantic Ridge. The Icelandic linear volcanic chains have been active for a short time (Trifonov, 1978). Linear

location (the NW–SE trend) is characteristic also of volcanoes in the Shin Plateau (Chorowicz et al., 2004). The N–S-trending groups of volcanoes are situated on the normal-sinistral faults or form short parallel chains in the northern part of the DST. Besides the fissure eruption zones, there are single small volcanoes and their nonlinear groups as well as rare shield volcanoes (such as the Safa Holocene center) in the Jebel Arab Highland.

Composition of the Late Cenozoic Syrian basalts is generally similar to that of basalts in the adjacent parts of the Arabian Plate (Alici et al., 2001; Shaw et al., 2003; Segev, 2005). The Syrian basalts are mostly alkaline mafic rocks with high (1.8–3.7 %) content of TiO_2 (basanites, hawaiites and alkali basalts) and more rarely transition/tholeiitic basalts with 44.3 to 52.5 % of SiO_2 . The $\text{Na}_2\text{O}/\text{K}_2\text{O}$ ratios vary from ~1.5 to 5.6 and show positive correlation with the SiO_2 content (Sharkov et al., 1994; Sharkov, 2000; Lustrino, Sharkov, 2006). The $^{87}\text{Sr}/^{86}\text{Sr}$ ratios (0.70321 to 0.70485) show negative correlation with the $^{143}\text{Nd}/^{144}\text{Nd}$ ratios (0.512938 to 0.512842) (Lustrino, Sharkov, 2006). There are some peculiarities of basalt composition in different volcanic areas. The relatively high alkalinity is characteristic of basalts in the Shin Plateau and its coastal continuation; low alkalinity basalts predominate in the Jebel Arab Highland, while tholeiites are typical of the southern Aleppo area (Sharkov, 2000).

Lustrino and Sharkov (2006) divided the Syrian basalts into two groups: (1) with ages between ~25 and ~5 Ma and (2) younger than ~5 Ma. In each group, content of the incompatible trace elements increases with decrease of the age as a result of fractional crystallization in magmatic sources. An abrupt change in basalt composition occurred ~5 Ma ago. That was decrease in TiO_2 , Na_2O , K_2O , P_2O_5 and incompatible trace elements, while neither MgO proportion decreased, nor that of SiO_2 increased. The authors above explain these phenomena by “increasing degree of partial melting and/or shallower depths of partial melting (i.e., increasing percentage of spinel in lherzolitic mantle)”. By Lustrino and Sharkov (2006), the ~5 Ma adiabatic melting could follow the upper mantle decompression caused in turn by some re-organization in plate motions (Barazangi et al., 1993; Zanchi et al., 2002; Rukieh et al., 2005). It is worth noting, however, that the conclusion of Lustrino and Sharkov (2006) about the ~5 Ma event is based only on the data from the Shin Plateau and its coastal continuation, so that the event could have rather local than regional geodynamic cause.

The Late Cenozoic pyroclasts and some basalts include mantle xenoliths mainly of the spinel lherzolites and the spinel and garnet-spinel websterites, and rare xenoliths

of pyroxene granulites, probably representing the old oceanic crust (Sharkov et al., 1996; Sharkov, 2000). The absence of xenoliths of the lower crust garnet granulites and of the upper crust material suggests that the intermediate magmatic sources were not characteristic of the Late Cenozoic volcanism.

There is some correlation between periodicity in volcanism activity and structural evolution of the plate boundaries. Four phases of neotectonic evolution in active zones surrounding the Arabian Plate, corresponding to the same phases in other parts of the Alpine-Himalayan Belt (see chapter 1.5) were identified. During the first, Late Oligocene–Early Miocene, substage, the Aden–Red Sea rift system was originated, and the belt of parallel dykes, small volcanoes and extrusions formed in the northeastern side of the Red Sea rift. The Arabian Plate moved to the NNW and produced sinistral slip on the DST and shortening in the northwestern margin of the plate. The NNW–SSE compression was accompanied by the ENE–WSW extension. That favored opening of extensional faults and volcanic activity, as most of magmatic channels marked by volcanic chains and interpreted as extensional faults strike NNW–SSE here. Two Late Oligocene dates (26.2 ± 2.1 and 24.7 ± 1.4 Ma) were obtained in the western part of the Ed Dau Basin in the Palmyrides, where the basalts occur near the bottom of the Upper Cenozoic fine-grained continental deposits. The Early Miocene basalts dated from 21.1 ± 0.9 Ma to 17.3 ± 0.8 Ma are more widespread (Fig. 33). In general, the Late Oligocene and Early Miocene sub-aerial volcanic area forms a relatively narrow N-trending band in the western part of the Arabian Plate approximately parallel to the DST (Trifonov et al., 2011). The band extends from the northern slope of the Jebel Arab Highland up to the Aleppo Plateau and the Kurd Dagh foothills and continues beyond the Syrian boundaries to the north and to the south. In the north, in Turkey, the K-Ar dates 18.6 ± 0.8 , 17.1 ± 0.8 and 16.5 ± 0.6 Ma (Arger et al., 2000), and 19.1 ± 1.3 and 17.0 ± 0.7 Ma (Tatar et al., 2004) were obtained in the large lava field to the SE of the town of Kahmaran-Maraş. In the south, in Jordan, the oldest basalts with the K-Ar ages of 26–22 Ma were found at the eastern margin of the Harrat Ash Shaam and in its central part, where the basalts compose ruins of older volcanoes (Ilani et al., 2001).

After the short episode of the rifting abatement, during the second, Middle Miocene, phase, the Arabian Plate moved to the NE. The NE–SW compression and the NW–SE extension did not favor volcanic activity in the N-trending band. Volcanism waned in Syria and ceased in the Jordanian part of Harrat Ash Shaam. The Middle Miocene basalts (17–13 Ma) were found only in the north of the Jebel Arab Highland and near the city of Homs. Decrease of volcanic activity was reported also

in Saudi Arabia, in the north-eastern side of the Red Sea rift (Camp, Roobol, 1992). This phase of the tectonic and volcanic quiescence began in the north later (~17 Ma) than in the south (~20 Ma), as seen in the distribution of dated basaltic flows (Fig. 34).

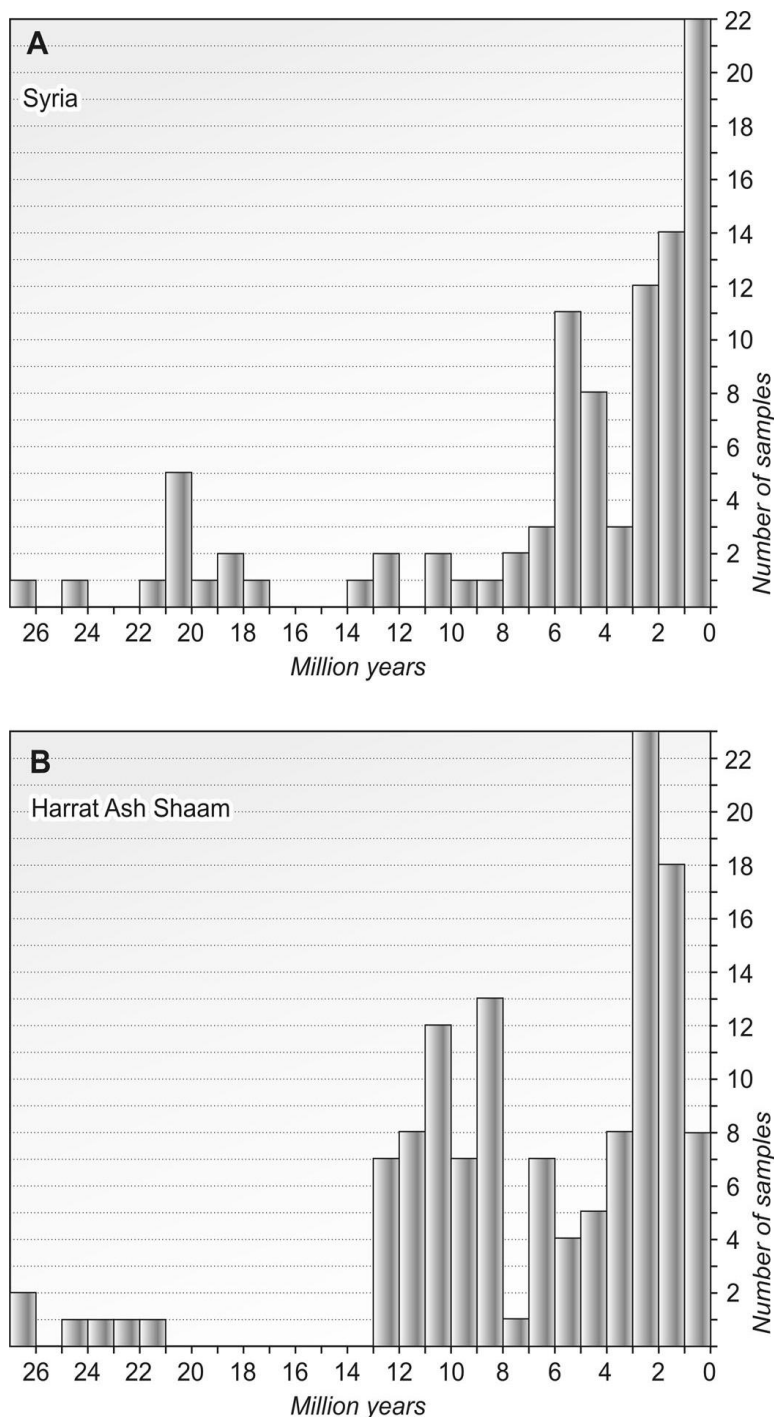


Fig. 34. Histogram of age distribution of the available K–Ar and Ar–Ar dates of the Syrian basalts, by the data in (Giannérini et al., 1988; Sharkov et al., 1994, 1998; Demir et al., 2007; Trifonov et al., 2011), in comparison with analogous histogram for the Jordanian part of the Harrat Ash Shaam (Ilani et al., 2001). N is number of the dates

At the third phase, in the Late Miocene and particularly in Messinian, the compression and shortening was directed again to the NNW that favored volcanism. Renewal of eruptions began ~12 Ma, though the volcanism was weak till the end of the Tortonian. The lava flows, dated at 12–7 Ma are confined to the same N-trending band, the latter in its northern segment expanded eastwards to the Euphrates and westwards onto the north-eastern part of the Shin Plateau. The date 9.7 ± 0.6 Ma from the Shin Plateau marks beginning of its activity, which propagated later to the west.

The tectonic movements intensified in the Messinian. That caused folding and thrusting in the Palmyrides. At the same time, ~6.3 Ma, volcanism sharply intensified and continued in the Early Pliocene till ~4 Ma. It occupied not only the Jebel Arab Highland, but large areas in the Shin Plateau and its western continuation up to the

Mediterranean coast near the towns of Tartous and Banias. The geochemical features of the Shin basalts described above suggest either a higher degree of partial melting or its shallower depth, i.e. decompression in the mantle source (Lustrino, Sharkov, 2006). It is not inconceivable that the formation of the source of the Shin lavas was somehow related to shortening in the Palmyrides. A probable scenario implies that, together with sinistral motion on the DST, the shortening caused the NE-directed movement of the Aleppo Block and subsequent decompression in the southwestern part of the block, which resulted in the Shin volcanism. Changes in the lithosphere, associated with the magmatism caused drastic changes in the northern part of the DST. New strand of the DST formed in the Shin area. It became the main strand and propagated to the south (Yammuneh segment) and to the north (El Ghab segment) up to junction with the newly formed EAFZ (Zanchi et al., 2002; Rukieh et al., 2005). The moment of restructuring of the DST system was manifested by brief wane of volcanism ~4–3.5 Ma.

The Late Miocene – Early Pliocene phase of volcanism was somewhat different in the Jordanian part of the Harrat Ash Shaam. Volcanism was resumed ~13 Ma there and continued (with brief hiatus at ~7 Ma) until 3 Ma, when the next reactivation of volcanism took place (Ilani et al., 2001). We estimate these changes by number of the basaltic dates of different ages (Fig. 34). Of course, they show only distribution of dated basaltic flows over the land surface and can not correspond exactly to epochs of rise and fall of volcanic activity, but general tendency is probably indicated by number of the dates.

The Yizre'el depression between the Galilee Sea – Lower Jordan valley and the Haifa fault zone occupies a particular position among volcanic areas of the region (Garfunkel, 1989). Five basaltic flows alternate with clastic deposits of the Herod Formation on the southwestern coast of the Galilee Sea near the village of Poriya (southwards of the town of Tiberias). Three lower flows are characterized by the ^{40}Ar - ^{39}Ar dates from 16.05 ± 0.07 to 15.34 ± 0.05 Ma, and the upper flow is dated as 13.31 ± 0.06 Ma (Segev, 2005). These flows are covered by several flows with the K-Ar dates 12.5–10 Ma. In addition, ^{40}Ar - ^{39}Ar dates have been obtained eastwards of the village of Afula: 14.9 ± 0.1 and 13.9 ± 0.1 Ma [Segev, 2005]. The described rocks are united into the Lower Basalt Group with thickness up to 630–650 m to the southwest of the Galilee Sea and near the village of Afula (Segev, 2005). The dates of the Lower Group show that the volcanic activity continued through the Middle Miocene without any signs of attenuation typical of Syria and Jordan. The Late Miocene basalts with ages ~9 to 6–5.7 Ma form flows of small thickness in the Lower Galilee

and on the Golan Hills and represent an epoch of relative wane of volcanic activity. The next burst of eruptive activity produced the Cover Basalt (Bashan Group) 55–175 m thick dated by the ^{40}Ar - ^{39}Ar from 5.1 ± 1 to 3.5 ± 0.1 Ma (Segev, 2005). So, a sequence of the Miocene–Early Pliocene volcanic events near the Galilee Sea and in the Yizre’el depression repeated the Syrian “scenario” with some delay. Voluminous eruptions occurred there ~ 16 – 10 Ma and in the interval between 5.1 ± 0.1 and 3.5 ± 0.1 Ma, with an epoch of low volcanic activity in-between (Segev, 2005). Perhaps, that depended on location of the depression in the area of the two major faults junction (Garfunkel, 1989), where the geodynamic changes were manifested somewhat differently from the Arabian Plate.

During the Pliocene–Quaternary stage, the Arabian Plate moved to the north and underwent shortening in its northern boundary. The N–S-trending compression and the W–E-trending extension favored eruptions on the NNW-trending and N-trending extensional faults in Central and Northern Arabia. After the brief wane of volcanism ~ 4 – 3.5 Ma corresponding to the moment of the DST system restructuring, the volcanic activity resumed, became more intensive in the Late Pliocene and continued through the Pleistocene and locally Holocene. This volcanism was well pronounced on the Jebel Arab Highland and its Jordanian continuation, and showed itself farther to the east, in the northern part of the Syrian Desert, the Euphrates valley and the northern margin of the Mesopotamian Foredeep near the Turkish-Syrian boundary. There is no evidence of one-way rejuvenation of eruptions. For example, the Late Pliocene and Early Pleistocene lavas erupted nearly at the same location in the northern margin of the Mesopotamian Foredeep between the upper reaches of the Nahr El Khabour and the Tigris valley. A lava flow near the town of Hassake was dated even to the Middle Pleistocene (0.24 ± 0.06 Ma) and eruptions could continue there in the Late Pleistocene. The same situation is characteristic for the Euphrates valley. In the DST, the eruptions began in the Early Pleistocene. Volcanoes were located on the N-trending boundary and inner faults of the Karasu valley (~ 2 – 0.4 Ma) (Yürür, Chorowitz, 1998), in the El Ghab pull-apart basin (from 1.9 ± 0.1 until 1.1 ± 0.2 Ma) (Sharkov et al., 1994; Sharkov, 2000), the Hula pull-apart basin and the Jordan valley (from 2.16 ± 0.28 until 0.95 ± 0.03 Ma, according to the ^{40}Ar - ^{39}Ar dating) (Segev, 2005).

The correlation between the main phases of evolution of the basaltic volcanism and neotectonics demonstrates genetic links between these processes in the Arabian Plate and its boundary zones and has to be taken into account for better understanding of the volcanism origin.

2.2.2.2. Correlation of the Cenozoic volcanism in the Arabian Plate and in the Arabian-Caucasus segment of the Alpine-Himalayan Belt

A model of origin of the Late Cenozoic basaltic volcanism in Syria and the adjacent parts of the Arabian Plate must account for the following specific features of that volcanism.

1. Principal geochemical similarity of the basalts suggestive of mantle sources for the basalts (Stein, Hofmann, 1992).

2. Volcanic areas are characterized by inherited development. The largest of them evolved for a long time, 26 million years in Jebel Arab – Harrat Ash Shaam and more than 15 million years in the Aleppo Plateau. Moreover, even some of individual volcanic chains (e.g., in Jebel Arab) developed as inherited structures for several million years. There are no signs of one-way migration of the volcanism. Such a persistence of the volcanic areas means that the magmatic sources moved together with the Arabian Plate, i.e., magmatic sources were situated within the lithosphere mantle. This geological conclusion complies well with the results of geochemical studies of Weinstein (Segev, 2005) and Lustrino and Sharkov (2006).

3. Although only a part of volcanoes and basaltic fields demonstrate direct links with individual crustal structures of the Arabian Plate and its surroundings, there is a chronological coincidence between variations of volcanism intensity and its spatial distribution on one hand and geodynamic changes and tectonic events along the Arabian Plate boundaries on the other (Trifonov et al., 2011). In the favorable geodynamic situation the volcanism was renewed in the former zones or expanded into new areas. In the Shin area, geodynamically-controlled decompression of the lithosphere caused changes in chemical composition of basalts and essential changes in structure of the northern DST zone.

We propose the following explanation of origin of the Syrian Cenozoic basalts that may account for all the distinctive features mentioned above. A portion of the northern drift of the Arabian lithosphere plate is caused by motion of the plate on the asthenosphere flow. The flow moved away from the Ethiopia–Afar superplume, which rose from the lower mantle (Ebinger, Sleep, 1998; Ershov, Nikishin, 2004). The flow eroded the Arabian Plate deep interface, and magmatic sources were formed within decompressed sites of the lower lithosphere. As the potential of the sources was supported by the sublithosphere lateral flow, the sources could produce basaltic eruptions at the same areas for a long time. At the same time, eruptions were only possible, when the geodynamic setting favored initiation and activity of channels for

magma passage. Dependence of volcanism on the geodynamic situation explains synchronism in the occurrence of volcanic activity and tectonic events within and near the Arabian Plate. The local geodynamic changes in the Shin area led not only to the structural changes in the northern DST zone, but even caused temporal geochemical changes in the composition of the erupted basalts.

The composition of material involved in the sub-lithosphere flow changed in process of northward movement due to partial crystallization and inclusions of the asthenosphere material. The magma chambers in the lower lithosphere also included some local melted material. That is why geochemical traces of the Ethiopia–Afar superplume have been reliably established only in volcanic rocks in the southern part of the Arabian Plate (Altherr et al., 1990; Baker et al., 1997; Bertrand et al., 2003). Farther north, as in Syria, basalts lack the superplume characteristics (Lustrino, Sharkov, 2006).

The Arabian–Caucasus segment of the Alpine-Himalayan belt latter bears numerous manifestations of the Early Cenozoic volcanism. They are situated mainly near the former back-arc basins of the Neotethys and are probably related to their closing. The Oligocene was noted for attenuation of volcanism and formation of small granitic and granodioritic intrusions. Manifestations of the Early and Middle Miocene volcanism are very rare (Milanovsky, Koronovsky, 1973). Intensive volcanism began in the Late Miocene and continued until the Early Pleistocene and its weaker manifestations continued through the Middle and Late Pleistocene and locally occurred even in the Holocene. The volcanism occupied the inner zones of the orogenic belt from Central Anatolia up to Alborz and was most intensive on the Armenian Highland (Fig. 35). It spread to the central part of the Greater Caucasus as early as the Late Miocene and formed the subvolcanic extrusions in the area of Caucasus Mineral Waters. But maximum activity in the Elbrus and Kazbek volcanic areas is dated to the Late Pliocene – Early Pleistocene (2.8–1.5 Ma) (Koronovsky, Demina, 2007). Evidence of the historical eruptions was found in the Armenian Highland (the Syinik and Porak groups of volcanoes near the Khanarassar strike-slip fault in the Gegharnik–Vardenis Upland, Ararat, and Tendurek and Nemrout volcanoes in the Van region) as well as in Central Anatolia (Ergiyas Dag and Hasan Dag), the northern Iran (Demaverd) and the Greater Caucasus (Elbrus) (Milanovsky, Koronovsky, 1973; Karakhanian et al., 1997, 2002; Bogatkov et al., 1998; Modern and recent volcanism..., 2005; Trifonov, Karakhanian, 2008).

Thus, the sublithosphere flow penetrated northward into the Arabian–Iranian segment of the Alpine-Himalayan belt only as early as the subduction of Tethys relics

at the southern margin of the belt completed in the Early Miocene (Robertson, 2000; Ershov, Nikishin, 2004; Robertson et al., 2004). The intensive volcanism, which rapidly spread from the Armenian Highland and Central Anatolia to Mount Elbrus, started in the Late Miocene. These volcanic manifestations are represented by wide spectrum of rocks from basalts up to ultra acid rocks. As a whole, the total composition evolved from andesite-dacites to andesites and basalts. They belong to the calc-alkaline series, although an increased alkalinity is reported in periphery of the volcanic areal (the Caucasus Mineral Waters, Kazbek, the north-east of the Armenian Highland, and the Demaverd volcano) (Koronovsky, Demina, 1999, 2007; Imamverdiev, 2000).

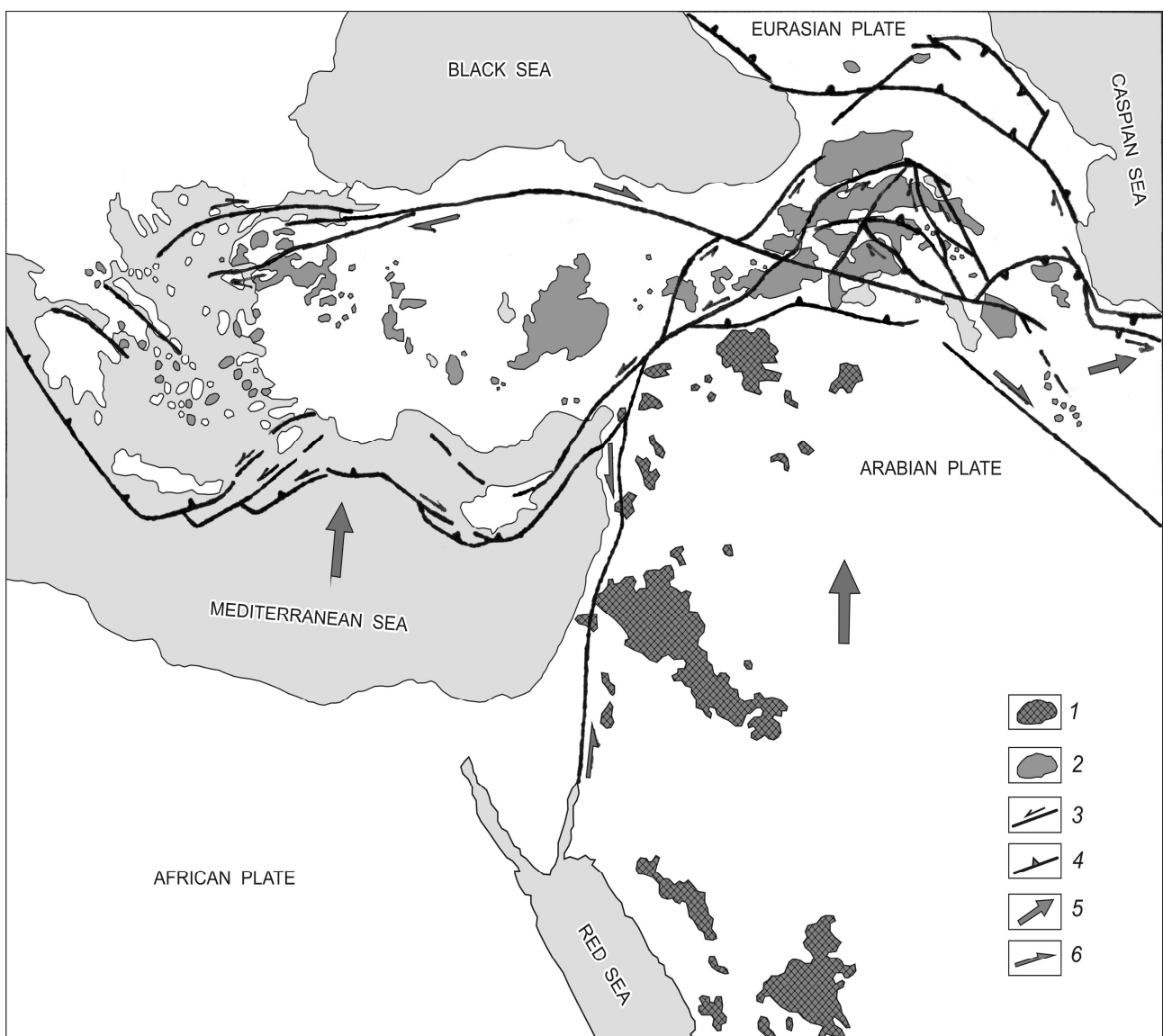


Fig. 35. The Oligocene-Quaternary volcanic formations and main faults of the Arabian-Caucasus region, modified after (Trifonov, Karakhanian, 2008)

1, Oligocene-Quaternary basalts of the Arabian Plate; 2, Neogene-Quaternary volcanic rocks of the Alpine-Himalayan Belt; 3, strike-slip faults; 4, thrusts and subduction zones; 5, direction of motion of plates and blocks; 6, direction of strike slip

Thermo-dynamic calculations based on the results of geochemical and petrological studies showed that magmas in the south of the Armenian Highland were generated under the pressure $P=1.1-1.2$ Gpa characteristic for the upper mantle, while in the north of the Highland and in the Greater Caucasus, the level of the magma generation is characterized by $P=0.95-1.05$ Gpa and $T=850-1100^{\circ}$ that corresponds to the depths of 35–40 km, i.e. the bottom of the Earth's crust in the Highland and the lower crust in the Greater Caucasus (Koronovsky, Demina, 1999, 2007). In the Elbrus area, a depth of the acid magma generation is characterized by $P=0.5-0.7$ Gpa, corresponding to the depths of 17–25 km. At a depth of 35 to 50 km beneath Elbrus there have been found a rock body with decreased velocities of seismic waves and increased electrical conductivity that may be identified with the magmatic source (Modern and Recent Volcanism..., 2005). So, the sources of the Late Cenozoic volcanism of the region were situated mainly in the lower crust and near the crust–mantle boundary.

Data of the Sr–Nd–O isotopic analysis of the volcanic rocks in the region, as well as high $^3\text{He}/^4\text{He}$ ratios in water springs of Elbrus and Kazbek strongly suggest the mantle material to have penetrated to the magmatic sources (Ivanov et al., 1993; Bubnov et al., 1995; Polyak et al., 1998). Karyakin (1989) noted a similarity between the Armenian Highland basalts and basalts from ensialic island arcs and active continental margins. The decrease of the seismic wave velocities by 1.5% was found in the uppermost mantle beneath the Elbrus area (Milanovsky et al., 1989). Based on these data, Koronovsky and Demina (1996, 2004, 2007) proposed a model of the Late Cenozoic magma generation in the region. According to the model, the magma sources in the lower crust and the uppermost mantle formed under influence of heat and oxidation of fluids, transported from the deeper levels in the mantle. One of sources of the fluids could be deformational heating of the Mesotethys suboceanic slabs persisting within the lithosphere. At the same time, we agree with the idea of Ershov and Nikishin (2004) that the sublithosphere flow from the Ethiopia–Afar superplume could be another, and essential, source of the magma generation. The flow penetrated beneath the inner zones of the Alpine–Himalayan collision belt in the Miocene and reached the Greater Caucasus to the Upper Miocene. The Armenian Highland was subjected to both sources of the magma generation, which may account for the most intensive volcanism in the region (Trifonov et al., 2011).

2.2.3. Intracontinental mantle seismic-focal zones in the Alpine-Himalayan Belt

To contradict the study, we summarized catalog data (Kárník, 1968; Kondorskaya, Shebalin, 1982; Kondorskaya, Ulomov, 1995; Moinfar et al., 1994; National..., 2007; Papazachos, Papazachou, 1997; Trifonov, Karakhanian, 2004) on the earthquakes, which took place in 1850–2007 and had $M_S \geq 5$ and hypocenters at depths of ≥ 40 km (≥ 50 km in thick-crust areas). Almost all such earthquakes are concentrated in the Hellenic and Cyprus arcs, Aegean region, Zagros Mountains, Vrancea megafocus, Middle Caspian, and Pamir–Hindu Kush zone with the Hindu Kush megafocus. The earthquakes in the Hellenic and Cyprus arcs are related to recent subduction zones. The other areas do not show such a relationship. The most active ones are Hindu Kush and Vrancea.

2.2.3.1. The Pamir–Hindu Kush mantle seismic zone

Analyzing the catalog of strong ($M_S \geq 5.7$) earthquakes in the central Alpine–Himalayan belt (Trifonov, Karakhanian, 2004), one may point out a small (100 x 150 km) area in northeastern Afghanistan with coordinates of 36–37°N and 69–71.5°E that is characterized by an anomalously great amount of released seismic energy (Fig. 12). About 20% of the energy released in the 20th century from all the earthquakes in the Alpine–Himalayan belt extending from the Dinarides to the Himalayas and Central Asia fell on this area. The overwhelming majority of earthquake hypocenters in this Hindu Kush seismic megacluster are concentrated in the upper mantle at depths of 110 ± 20 and 190–240 (down to 270–300) km. East of the N-S-trending bend of the Pyandzh River (Fig. 11), the epicenters of strong mantle earthquakes are shifted farther to the north (up to 38°N) and are traceable as isolated clusters up to the southeastern termination of the Afghan-Tajik Basin. There, together with the Hindu Kush megacluster, they form the Pamir–Hindu Kush seismic focal zone. In the Pamirs, strong earthquakes are rare, their released energy is hundreds of times less than in the Hindu Kush, and their sources are concentrated at a depth of 110 ± 20 km.

Geophysical characteristic of the zone. According to the seismological data, including low-magnitude events, the Pamir–Hindu Kush focal zone of intermediate earthquakes is a steep lens with variable thickness and changing density of hypocenters (Lukk, Nersesov, 1970). In both the Hindu Kush and Pamir segments of the zone, strong earthquakes occur at depths of 110 ± 20 km (Fig. 36). Deeper, at

depths of 130–170 km, the thickness of the focal lens decreases. Strong earthquakes are not recorded in the Pamirs and are extremely rare in the Hindu Kush. Deeper, at 190–240 km, the thickness of the lens beneath the Hindu Kush abruptly increases, the number of hypocenters also increases, and the amount of released energy becomes greater than in the upper part of the lens. Seismic activity attenuates with depth, although it remains traceable to depths of 270–300 km. In the Pamir segment of the zone at a depth of approximately 200 km, the thickness of the lens is also noted, but strong earthquakes did not occur here, and the amount of released seismic energy is less than in the upper part of the lens.

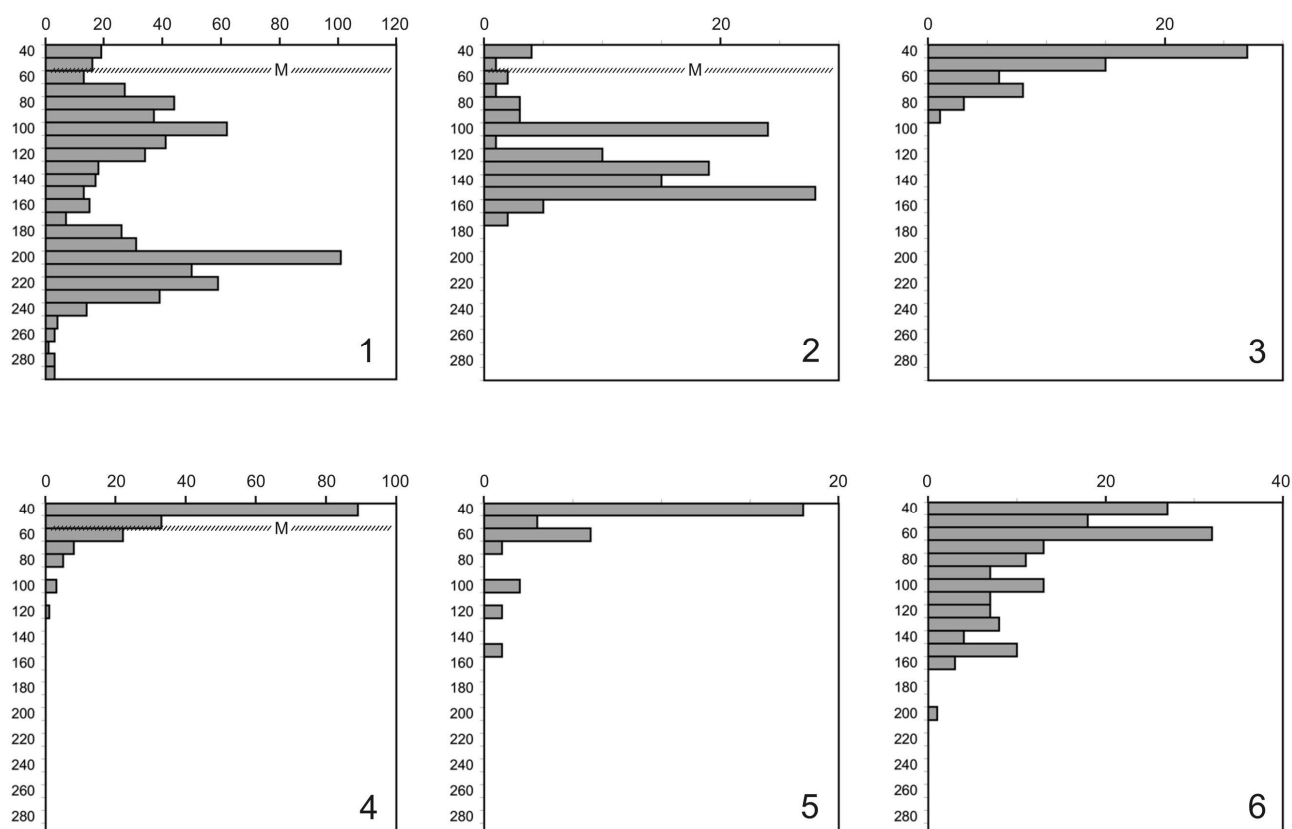


Fig. 36. Histograms showing the distribution of $M_S \geq 5$ earthquakes (N) over depth (h) in mantle seismic focal zones, modified after (Trifonov et al., 2012₁): 1, Pamir – Hindu Kush; 2, Vrancea; 3, Middle Caspian; 4, Zagros; 5, Aegean region; 6, Hellenic arc. Cross ruling shows the approximate position of the crustal bottom (Moho discontinuity) if it is localized at a depth lower than 40 km

The Hindu Kush segment of the focal zone is very compact. If the extremely strong earthquake of July 7, 1909 ($M_S = 8$; 36.5°N , 69°E), is ruled out because of inaccurately determined coordinates, almost 95% of strong earthquake epicenters fall within an isometric area $1.5 \times 1.5^\circ$ with the maximum concentration located near 36.5°N and 70.8°E . Over 90% of strong earthquakes in the Pamir–Hindu Kush zone and over 95% of the released seismic energy are concentrated in this area. In the east, near the N-trending bend of the Pyandzh River (71.5°E), the mantle seismicity

abruptly drops, earthquakes with $M_s \geq 5.7$ are absent, and the maximal depth of hypocenters is reduced to 150 km (Lukk, Vinnik, 1975). Thereby, the area with maximal seismic activity shifts northward up to $37\text{--}38^\circ$ N. To the east, in the Pamirs, mantle seismicity rises, although it remains substantially lower in comparison with the Hindu Kush. Earthquakes are scattered irregularly, particularly as it concerns strong events that are clustered into four compact groups. The depth of hypocenters reaches 240–250 km, but the amount of released seismic energy is at least three orders of magnitude lower than in the Hindu Kush region (Vostrikov, 1994).

Lukk and Vinnik (1975) have analyzed all the available data set on mantle earthquakes in the Hindu Kush and Pamir segments of the zone and showed that their hypocenters steeply dip northwestward and southward, respectively. The distribution of only strong earthquake hypocenters reveals an almost vertical orientation of the Hindu Kush segment (Fig. 37); data on the Pamirs turned out to be insufficient for such a suggestion.

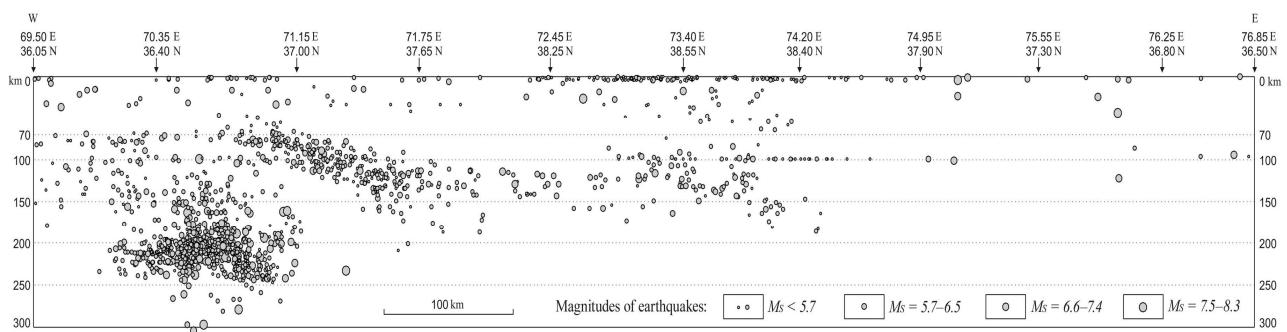


Fig. 37. Location of hypocenters of earthquakes along the Pamir – Hindu Kush seismic focal zone; compiled by D.M. Bachmanov with using the catalog (Kondorskaya, Ulomov, 1999)

The velocity section of the upper mantle in the Pamir–Hindu Kush region is known from deep-sounding data (Khamrabaev, 1980; Seismic models..., 1980; Pamirs–Himalayas..., 1982) and from the processed kinematic parameters of intermediate earthquake records (Vinnik, Lukk, 1974). Both of these sources point to increased P-wave interval velocities and V_p/V_s ratios at depths of 90–120 km and to the drop of these parameters at depths of 120–150 km, which are consistent with the seismicity distribution at these levels of the focal zone. Values of V_p/V_s increase within a depth interval of 150–200 km, and P-wave interval velocities also rise at these depths and reach higher values at deeper levels.

Lateral heterogeneities of the upper mantle in the region are of particular importance for understanding the structure of the focal zone, which has been studied with various modifications of two methods. The first method is based on

measurements of spectral characteristics of waves recorded at different distances and in different directions from sources of local intermediate earthquakes. This method helped to determine a large domain of the upper mantle, including the Pamir–Hindu Kush zone, which is distinguished by the anomalously high mechanical Q-factor (Molnar et al., 1976).

The second method of seismic tomography based on the measurement of P-wave travel times from remote earthquakes to the network of local stations allows this domain to be specified. This method makes it possible to define a smaller mantle domain comprising the entire Hindu Kush part and to a great extent the Pamir part of the focal zone, where P-wave velocities down to a depth of 300 km are 0.3–0.4 km/s higher than in comparison with their average worldwide values (Vinnik, Lukk, 1974; Lukk, Vinnik, 1975). According to the calculations by Vostrikov (1994) and based on his method of interpretation of earthquake-recurrence plots and his investigation of spatial variations in the seismic flow, the high-velocity domain is characterized by the increased effective viscosity of rocks. This domain is restrained by the upper mantle masses with an average P-wave velocity 0.1–0.2 km/s lower than against their average worldwide background.

Using seismic tomography, Nikolaev and Sanina (1982) constructed a three-dimensional velocity model of the focal zone and its vicinity that demonstrates the distribution of mantle domains with P-wave velocities distinguished from, to a variable extent, the average worldwide values at the same depth. Subsequently, these anomalies were recalculated into absolute velocity values (Nikolaev et al., 1985). The obtained velocity field within the focal zone and south of it is characterized by complexly alternating high- and low-velocity domains. This contrast is the most significant (up to 11–12%) in the Hindu Kush segment of the zone. North of the seismic focal zone, no similar anomalies are observable.

The seismic focal zone as a result of neotectonic evolution. It is evident that the horizontal shortening of the upper crust, which has been convincingly deduced for neotectonic regional evolution both from the relationships between geologic zones and bodies and from recent geodynamics, must be accompanied by a similar or greater shortening of the lithospheric mantle. The origin of the Pamir–Hindu Kush focal zone is commonly interpreted exactly in this way.

The geophysical and, first and foremost, seismological study of the zone revealed an increased strength of rocks from this zone relative to the surrounding mantle. In combination with recent high-rate strain, this gives rise to the rock failure accompanied by earthquakes (Vinnik, Lukk, 1974; Vostrikov, 1994). Assuming a

similar rate of transverse shortening of the orogenic belt at the crustal and mantle levels, the increased rate of mantle strain calculated from seismological parameters was ascribed to their concentration in a smaller rock body in comparison with the Earth's crust as follows from the spatial distribution of crustal and mantle earthquakes (Neotectonics and recent geodynamics of mobile belts, 1988). The increased strength of rocks in the seismic focal zone was attributed to subduction of lithospheric masses deep into the mantle; this was argued on the basis of the northwestward dip of the Hindu Kush focal zone and the southward dip of the Pamir focal zone (Lukk, Vinnik, 1975; Tapponnier et al., 1981; Burtman, Molnar, 1990). It was also assumed that the oceanic lithosphere of the Hindu Kush segment is compositionally similar to rocks of the Indus–Zangbo Suture subducted beneath the Hindu Kush, whereas the lithosphere of the extending Afghan–Tajik Basin enriched in mafic components is subducted beneath the Pamirs and Karakorum in the Pamir segment (Tapponnier et al., 1981).

However, a subduction-related model of the focal zone provokes some objections. First, the distribution of strong earthquake hypocenters indicates a vertical rather than a tilted Hindu Kush focal zone (Fig. 37). Second, the assumed localization of subduction zones nowise follows from structural relationships between tectonic zones and neotectonic displacements. It is unclear, why the seismic focal zone is situated in its present-day position and is not traceable at the extension of the same structures. For instance, assuming the recent lithosphere subduction of the Indus–Zangbo type, there are no geologic reasons to constrain it by the Hindu Kush area and not extend it farther eastward, where geologic conditions are more favorable, but the focal zone is missing. Similarly, a question arises as to why underthrusting of the Afghan–Tajik Basin beneath the Pamirs is expressed only in the east and not observable in the Hindu Kush, where it is geologically more suitable. Additionally, the question arises as to why the rate of recent strain in the focal zone is higher than in other active structures of the region.

At the same time, the above hypotheses contain a sound point concerning the relationship between mantle earthquakes and mafic elements of the lithosphere. We also impart the decisive role to this aspect, although from a distinct standpoint.

With maximal clustering of mantle earthquakes, the highest release of seismic energy, and a depth of hypocenters as low as 270 km, the Hindu Kush zone corresponds on the Earth's surface to the adjacent areas of the Hindu Kush Hercynides with prevalent exposures of the Proterozoic basement and, to a lesser extent, the Archaean massif of the South-Western Pamir–Badakhshan Zone (Fig. 12).

If we assume that prior to the neotectonic period this massif was located at least 150 km to the west and was a crustal element of the Central Pamirs between the volcanic arc and the oceanic trough of the early Mesotethys, then in the depths of the area of its initial location there might have been preserved deep-seated relics of the overridden oceanic crust; these relics are presented in the seismic velocity section of the neighboring Vanch–Yazgulem part of the Central Pamirs by the approximately 15-km-thick crustal–mantle mixture. The deep extensions of the Hercynian sutures overridden by nappes of the continental crust might have occurred immediately near these areas.

Deep-seated analogs of the Khorog Formation exposed now in the zone of the tectonic contact between the Archaean Shakhdara and Goran groups of the South-Western Pamirs could be also a source of mafic material. The Khorog Formation is 0.5–2.0 km thick and mainly composed of amphibole gneisses and garnet amphibolites with boudines of eclogites and eclogitized rocks. Ruzhentsev (1990) considered the Khorog Formation to be the basement of the continental crust of the overthrust Shakhdara Group. Budanova and Budanov (1983) view it as a relic of the mafic riftogenic formation crushed between the converged Goran and Shakhdara continental massifs. In the last case, volumes of metabasic rocks beneath the initial location of this complex may be especially great.

The Hindu Kush field of mantle earthquake epicenters fits the area of initial location of the above-mentioned metabasic complexes (Fig. 14). The area stands out as a depression of the Earth's surface occupied by valleys of the left tributaries of the Pyandzh River filled with Quaternary sediments. In the course of neotectonic deformation, the metabasic rocks were overthrust by thick sheets of the continental crust and pressed into the mantle to a depth of 40–70 km, where a moderately elevated temperature and a high pressure induced by intensive lateral compression and the load of the overlying continental masses were favorable for eclogitization. It is indicated by petrologic studies and deep-sourced xenoliths (The Earth's crust and upper mantle of Tadjikistan, 1981). The crust that got heavier by eclogitization submerged into a relatively low-velocity and hotter mantle (Fig. 12, profile) that retained its high viscosity and strength, that is, the ability to accumulate the elastic strain that gives rise to the brittle failure producing mantle earthquakes.

In the easterly areas of the Pamir–Hindu Kush zone, epicenters of mantle earthquakes are confined to the Central Pamirs and to its boundaries with neighboring zones. If detachment and northward displacement of the upper-crustal tectonic zones during the neotectonic epoch are taken into consideration, the roots of Hercynian

sutures, as well as Mesotethyan relics buried beneath the continental crust of the Central Pamirs, might have become sources of deep-seated metabasic rocks. Inasmuch as neotectonic lateral compression in this area was weaker than in the Hindu Kush, large sialic massifs are not typical. Thus, the lithostatic load of the overlying continental masses was lower, and eclogitization was less intensive and occurred here only locally. Therefore, mantle earthquakes are much weaker in this area and strong events are recorded only at a depth of about 110 km being irregularly distributed.

Tectonic zones located on either side of the Pamir arc (to the east in Tibet and to the west in Afghanistan) widen, indicating a decreased intensity of their recent stacking and the above-mentioned consequences of this process. This is probably why mantle seismicity is almost completely lacking west of the Hindu Kush and east of the town of Tashkurgan.

This model of the Pamir–Hindu Kush focal zone is internally consistent, and its most important statements are based on reliable facts. For instance, the suggestion of significant heating of the Earth's crust and its role in tectonic delamination at the early stage is substantiated by isotopic ages available for many granitic batholiths. Paths of crustal slices and blocks detached along delamination surfaces are reconstructed by analyzing alpine structures. Occurrence of eclogites at the base of the crust is deduced from petrologic data. At the same time, the model remains hypothetical in many respects because of insufficient geologic and geophysical data, particularly those for Afghanistan. Only further research can eliminate these uncertainties.

2.2.3.2. The Vrancea mantle seismic megafocus

Since 1862, 113 earthquakes have been recorded in the Vrancea area at depths of 60–170 km (Fig. 38). Except two early events whose coordinates might be imprecise, all the earthquakes occurred at N45.2–45.9° and E26.2–27.3°. In the first approximation, the seismic focal zone is a near-vertical column ~80 km in diameter and up to 170 km deep.

Mantle earthquakes are confined to the bend between the Eastern and Southern Carpathians and their hypocenters are located under the Outer Carpathians and the Focsani Foredeep (Fig. 39). The Outer zone is the accretionary wedge of the Mesozoic-Paleogene flysch detached and overthrust in the Late Miocene upon the Middle Miocene sediments of the Focsani Basin, in which up to 3 km sediments had

accumulated by the time of the overthrusting (Artyushkov et al., 1996). The thickness of the nappe complex was 8–12 km (with regard to erosion, it might have reached 10–14 km). However, the thickening of the cover did not cause an isostatic crustal uplift to the calculated value of 1.5–2.4 km. According to the authors cited, the land surface remained at a height of ~0.5 km, i.e., an uplift of 1–2 km was compensated for by bedrock compaction. The Neogene-Quaternary sediments up to 9 km thick accumulated in the Focsani Basin southeast of the nappes; near their front, the sediments are folded and thrust (Sandulescu, 1984; Artyushkov et al., 1996). The Focsani Basin is superimposed on the Precambrian Moesian Plate (Sandulescu, 1984). The north-eastern edge of the basin is lined by the Pechenyaga-Kamena Thrust, which is inclined beneath the basin and the Outer Carpathians and separates the Moesian Plate from the post-Paleozoic Scythian Plate. The north-eastern side of the fault is composed of the Cymmerian Northern Dobruja – a nappe system overthrust upon the Scythian Plate. Two nappes are separated by the Triassic mafic volcanics (Khain, 2001). Now they belong to the Pechenyaga-Kamena thrust zone and might extend along it at depth towards the Carpathians.

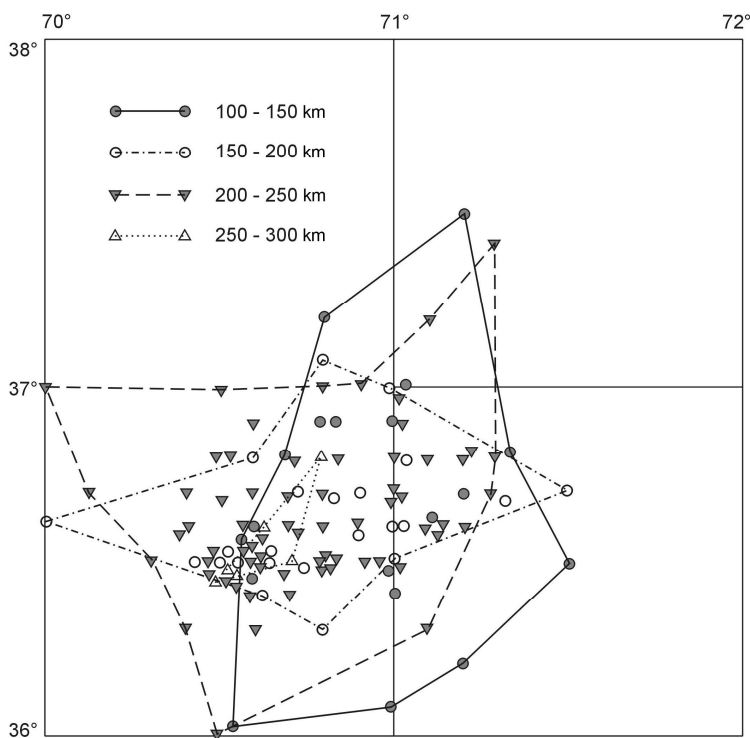


Fig. 38. Comparison of location of hypocenters and contours of their distribution in different depths of the Hindu Kush seismic mega-source (Ivanova, Trifonov, 2005)

On seismic profile O–Z, the Moho is located at depths of 35–40 km under the Inner Carpathians, at depths of 45–47 km under the Outer Carpathians and the Focsani Basin, and at a depth of ~44 km under the Moesian Plate (Hauser et al., 2007). Similar changes were observed on a more northern seismic profile crossing the Ukrainian Carpathians. The crust is ~60 km thick here beneath the Outer Carpathians and the foredeep; in the lower crust, a layer was detected with V_p velocities of 7.4–7.6 km/s, with a thickness increasing to ~20 km from the Inner to the Outer Carpathians and the foredeep (Chekunov, 1993). On the profile O–Z, the V_p velocities are 7.0–7.1 km/s in the lowest part of the crust.

The high-velocity lower-crust layer of the Ukrainian section might be indistinguishable there from the uppermost mantle. Artyushkov (1993; Artyushkov et al., 1996) considers that the high-velocity layer in the lower crust indicates metamorphic compaction of mafic rocks, which kept the Focsani Basin, filled with the nappes of the Outer Carpathians and the Neogene-Quaternary sediments, at a low height. The mafic rocks might have originated from the Inner Carpathians, where ophiolite outcrops, for example, in the Mureş zone. Their underthrusting resulted from the detachment of the lower crust and was simultaneous with the thrusting of the Outer Carpathians.

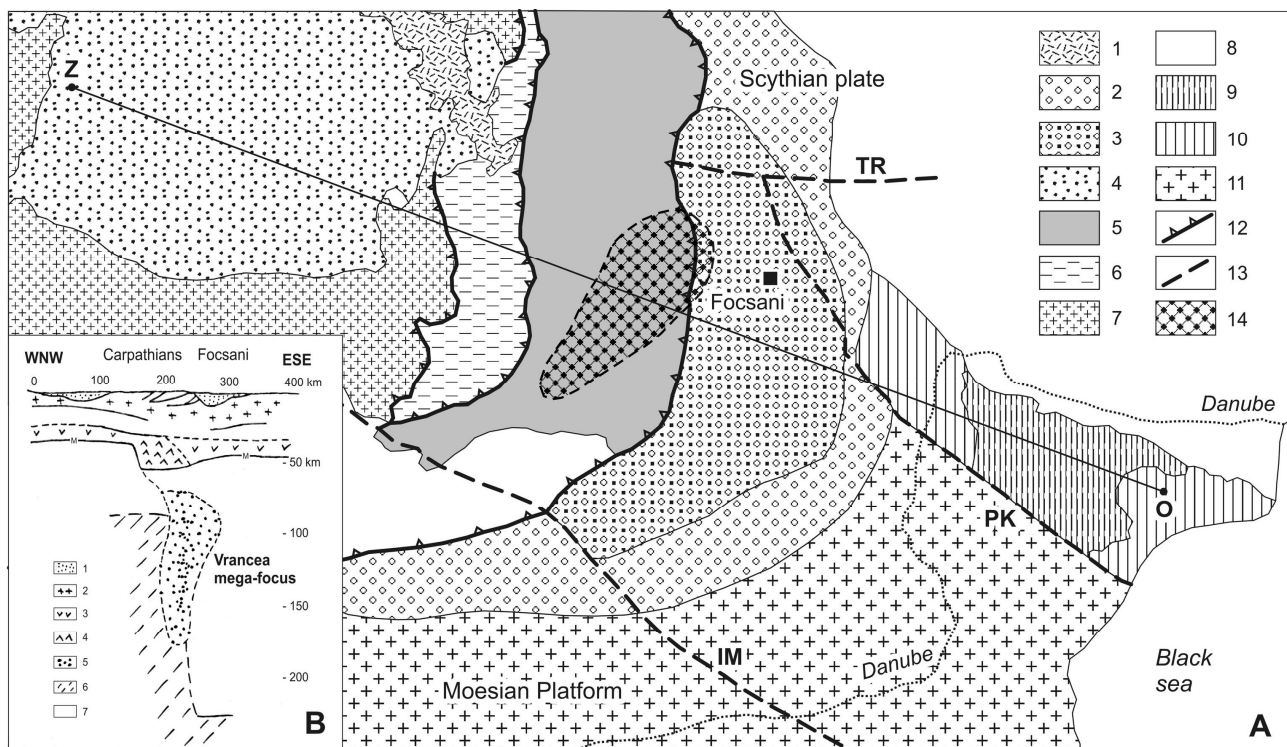


Fig. 39. Tectonic sketch map of the Carpathians around the Vrancea seismic region (A) and a sketch profile of the formation of the Vrancea mega-source of mantle earthquakes, modified and supplemented after (Artyushkov et al., 1996; Hauser et al., 2007; Trifonov et al., 2010, 2012₁).

A: 1, Neogene-Quaternary volcanics; 2, Neogene-Quaternary sediments of the Carpathian Foredeep; 3, Focsani Basin; 4, Neogene sediments of the Transylvanian Basin; 5, nappe complex of the Outer Carpathians (Moldavides); 6, External Dacides with the Cretaceous parautochthon; 7, Median Dacides and Transylvanides with the Cretaceous parautochthon; 8, Carpathian tectonic zones under the Pliocene-Quaternary cover; 9, 10, Cymmerian orogen of Northern Dobruja: exposed or overlain by thin sediments (9), under a sedimentary cover (10); 11, Moesian Platform cover; 12, major thrusts; 13, faults: IM, Intramoesian, PK, Pechenyaga-Kamena, TR, Trotus River; 14, Vrancea epicentral area; ZO, seismic-profile line. *B:* 1, sedimentary cover; 2, upper crust; 3, lower crust; 4, lower crust saturated with dense metamafic rocks; 5, dense metamafic slab (zone of mantle earthquakes); 6, asthenosphere; 7, lithospheric mantle

We think that the metamafic rocks extended as a slab into the lithospheric mantle and their additional source might have been the mafic rocks of Northern Dobrudja, which underthrust beneath the Focsani Basin along the Pechenyaga-Kamena Thrust

(Fig. 39). In the upper mantle, the mafic rocks underwent additional metamorphism with the formation of garnet granulites and eclogites, close in density to the lithospheric mantle. During the rise of the asthenosphere beneath the Carpathians to a level of about –80 km (Artyushkov et al., 1996), the slab found itself between the lower-density mantle of the Carpathians and the dense lithosphere of the Moesian Plate. This led to its subsidence, accompanied by earthquakes.

2.2.3.3. Origin of mantle seismicity

In the both examples, the mantle earthquakes are related to the paleo-oceanic metabasic rocks. The upper-mantle decrease of density in the Pliocene–Quaternary led to the breakoff and subsidence of dense cold metamafic slabs. Along with the subsidence, the earthquakes were powered by the phase transformations of the slab rocks: deserpentinization and, at greater depths, the eclogitization of the remnants of less metamorphosed mafic rocks and the transformation of quartz into coesite. The seismic shifts might have resulted not so much from high deviator stress as from rock weakening in mylonitized zones, intensified by fluids (Rodkin et al., 2009). The latter originated from the products of dehydration of serpentine and amphibole as well as from the asthenosphere.

Thus, the subsidence of the earthquake-inducing slabs and the intense uplift of the mountains were simultaneous and both resulted from the upper-mantle decrease of density under the effect of the asthenosphere. However, the tectonic uplift took place in a larger territory of the Alpine-Himalayan Belt. Evidently, the local geodynamic factors of seismicity played a role. First, this might have been the large initial size of the slab, which permitted its long-lasting isolation. Second, this might have been the presence of a large trans-lithospheric fault zone related to within-slab slip zones. These are the Pamir-Afghan (Chaman-Darvaz) zone of sinistral strike-slip faults in Hindu Kush (Ivanova, Trifonov, 2005) and the Carpathians–Moesian Plate boundary in the Eastern Carpathians (Sandulescu, 1984).

Three other regions of mantle earthquakes within the orogenic belt (Aegean, Zagros, and Middle Caspian) show the same, but weaker, factors of seismicity, and the number of hypocenters decreases quickly with depth (Fig. 38). This might be because the slab subsidence is only incipient or is slow owing to the slight density difference between the slab and neighboring mantle.

2.3. Plate tectonics and tectonics of mantle flows

The principles of the tectonics of lithosphere plates, or plate tectonics, were formulated first about a half of century ago. Since that time the theory has been essentially complicated. At the same time, it has been found that some tectonic processes can not be satisfactory explained by the plate-tectonic theory. This is related to some sources of vertical movements and first of all neotectonic uplifts producing formation of recent mountain systems. Comparison of the geological data, which can and cannot be explained by the plate-tectonic theory, with the results of seismic tomography of the mantle give a possibility to propose the new tectonic model. According to it, the sources of tectonic processes are the upper mantle lateral flows spreading away from the superplumes that are the flows of matter and energy rising from the lower mantle. These lateral flows not only move the lithosphere plates with all consequences of the movement, but also cause structural and mineral transformations in the lithosphere and sublithosphere upper mantle, which lead to additional vertical movements and mountain building.

2.3.1. Development of plate tectonic theory

Plate tectonics was created as a kinematic model. According to it, the ~50-km thick under oceans and ~100-km thick under continents lithosphere plates occupying the Earth's crust and the uppermost part of the mantle move from spreading zones along transform faults to zones of subduction and collision. The deep mantle material builds up the lithosphere in the spreading zones. In the zones of subduction and collision, the accretion of the lithosphere is compensated by its sinking into the lower mantle. The plate movement is described by their rotation around the Euler's poles (Vine, Matthews, 1963; Wilson, 1965; Dickinson, Hatherton, 1967; Isacks et al., 1968).

The researchers tried to find the sources of plate motion in the plate-tectonic mechanism itself, for instance, in moving apart effect of magmatic intrusion into the spreading zones or sucking in by the subducted parts of the plates. However, Sorokhtin (1974, 2007) showed that these processes influence locally and can not produce the plate motion as a whole. Forsyth and Uyeda (1975) proposed the mantle thermal convection as the general mechanism of the plate motion, but Artyushkov (1968) and Sorokhtin (1974) argued the higher efficiency of the convection caused by the transformations of chemistry and density of rocks and related to the mantle differentiation and enriching of the outer core of its ferriferous components.

The main achievement of the plate tectonics was that it consolidated affords of geologists, geophysicists and geochemists for solution of common tasks. This essentially improved their mutual understanding and cognition of tectonic processes. At the same time, accumulation of new knowledge required complication of the initial plate-tectonic model. The important subjects of discussion were parameters of the mantle convection as a source of the plate motion. The transition layer between the upper and lower mantle was distinguished by the seismological data. The jumps of seismic wave velocities in its upper (~410 km) and lower (~670–680 km) boundaries are so high that they can occur only with mineral transformations of the mantle matter. With some parameters of the system, these exothermic and endothermic transformations make the all-mantle convection impossible. The reasons for absence of essential exchange of the matter between the lower and upper mantle (Hamilton, 2003; Ivanov, 2011) conform to this idea. However Sorokhtin (2007) produced convincing reasons for the chemical-thermal density all-mantle convection. Proceeding from the assumption of full circulation of the mantle matter during the tectonic cycle, he came to the conclusion on sufficiently high rates of the mantle flows, with which the mineral transformations do not interrupt the flow and manifest themselves only in rise or subsidence of the transitional layer at a magnitude up to ~20 km. The reasons for combined influence of the all-mantle and upper mantle convection onto the lithosphere seem now to be the most ponderable (Dobretsov et al., 2001; Kovalenko et al., 2009).

The initial variant of the plate-tectonic theory assumed that the spreading zones represent the rising strands of the mantle convection and the subduction zones correspond to its sinking strands that are expressed at the depths up to ~650 km by the mantle seismic focal zones. Tracing of the subducted slabs down to ~900 km (Creager, Jordan, 1984) strengthened this view. The seismic tomography studies corroborate that some slabs continue to the lower mantle, but show that this is not universal rule (Grand et al., 1997; Van der Hilst et al., 1997). At the same time, it has become evident that the spreading zones can not directly correspond to the rising strands of the mantle convection. The surrounding of the African Plate clearly demonstrates this. Some segments of the spreading zones bounding the plate by the west and east are parallel to each other. Because the plate widens in time, a distance between the spreading zones increases. This means that one or both the spreading zones change their position relative to the upwelling strands of the convection. As a result, it was admitted that the zones of spreading and subduction correspond to the rising and sinking strands of the convection only in general.

Two other discrepancies with the initial plate-tectonic model were grounded by new geological data. They are the tectonic layering of the lithosphere and the diffuse plate boundaries. The Russian term of tectonic layering approximately corresponds to the English-language term of detachment tectonics, but includes also some tectonophysical effects of this phenomenon. The tectonic layering is the difference of stress and/or strain conditions in different layers of the lithosphere that leads to their detachment and movement relative to each other. Peive (1967) was the first who stated this idea. Developing it, he wrote: “The matter in different layers of the lithosphere moves laterally with different rates. If we consider that the asthenosphere is the main zone of tectonic flow, we can consider also the important role of relative lateral movements on the bottom of the crust and within it” (Peive, 1977, p. 7). Later the Russian scientists grounded this idea in detailed studies of paleotectonics and neotectonics in different regions (Tectonic layering..., 1990). Trifonov (1987) showed that the lower crust plays the same role for the upper crust in some regions that the asthenosphere plays for the lithosphere as a whole. Lobkovsky (1988) proposed the model of the two-level plate tectonics. According to it, the plate-tectonic mechanism works in the mobile belts more or less independently in the crustal and mantle levels.

The diffuse plate boundary within more or less wide belt is characteristic of the zones of subduction and collision (Gordon, 1998). The arc-type structural belt around the northern Pacific is shown in fig. 40. The northern and northwestern parts of this belt are characterized by subduction of the Pacific plate beneath the North-American and Eurasian plates (the Aleutian, Kurile-Kamchatka and Japanese arcs). The system of oceanic trenches in front of the island arcs is considered to be the boundary of the Pacific. However, there is uncertainty in location of the Eurasian–North American plate boundary within the backarc basin and the island arc. Some researchers outline the Okhotsk Sea lesser plate here. Other researchers include the Okhotsk Sea into the North American plate. Kozhurin (2004) showed that both these solutions contradict geological data. He argued that all the belt of deformation including the trench, island arc and backarc basin with surrounding structures is the diffuse plate boundary.

The diffuse character of plate boundaries is more evident in the regions of collision interaction of the plates, where structural records of the collision diffuse within the belts up to several hundreds of kilometers wide (Fig. 41). The belt consists of series of weakly deformed blocks (microplates) that are separated and bounded by zones of concentration of deformation. In the recent structure of the Himalayan-Tibetan segment of the Alpine-Himalayan Belt, such zones were identified in the

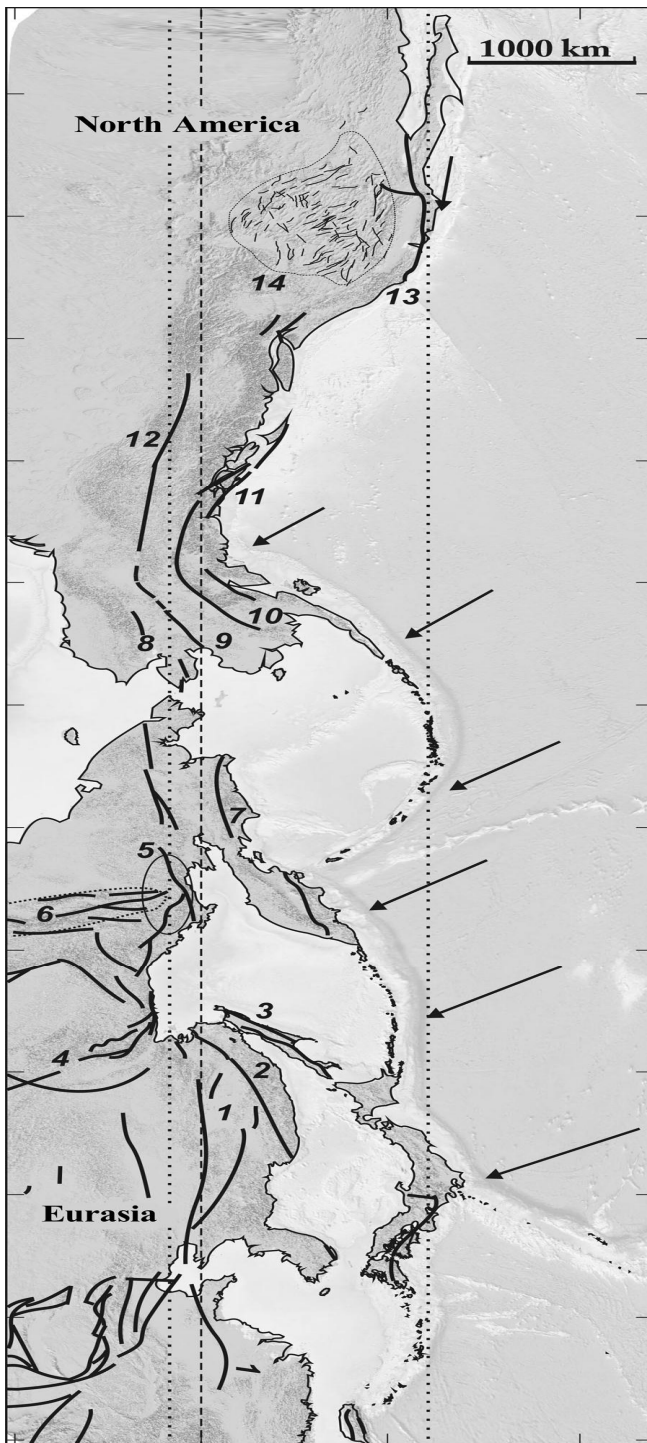


Fig. 40. The mobil belt of the northern surrounding of the Pacific, modified after (Kozhurin, 2004)

Points draw the belt boundaries. Dotted line corresponds to the major circle arc. Active mainly strike-slip faults are shown by solid lines. The main fault zones and systems: 1, Tanlu; 2, Central Sikhote-Alin; 3, East Sakhalin; 4, of the Stanovoy Highland; 5, Lankovo-Omolon; 6, Moma-Chersky; 7, Khatyrka-Vyven; 8, Kobuk; 9, Kaltag, 10, Totchunda; 11, Fairweather and Queen Charlotte Islands; 12, Denali; 13, San Andreas; 14, Basin and Range Province

southern flank of the Himalayas, in the boundary of the Southern and Central Tibet, the northern flank of Tibet and Qaidam (the Altyn Tagh Fault) and the southern flank of the Tien Shan (Fig. 1 & 31). The rate of the Late Quaternary movements on each of the zones mentioned above reaches $\sim 1-1.5$ cm/a (Trifonov et al., 2002), and it is impossible to give a preference to any of them as the boundary of Indian and Eurasian plates. The all belt became deformed as the diffuse boundary of these plates.

The aforecited geological peculiarities complicate the plate-tectonic theory and induce to refuse some postulates of its initial version, but do not change the sense of the theory. The main its principle that the structural manifestations of tectonic processes are the results of plate interaction remains immutable.

2.3.2. Tectonics of mantle flows

The data represented in this book give a possibility to propose the following model in the tectonic development of the Tethys Ocean and the Alpine-Himalayan Belt in the Mesozoic and Cenozoic. The main sources of tectonic processes were the sublithosphere upper mantle lateral flows that spread away from the Ethiopian-Afar superplume. In the

Mesozoic and Paleogene, the flows moved the oceanic lithosphere formed above the superplume, together with the torn off Gondwanan fragments towards the Eurasian Plate. The oceanic lithosphere subducted there and the Gondwanan fragments joined the Eurasia. A closure of the Tethys decelerated the convergence of the southern plates and Eurasia, but the upper mantle flows continued the former motion and spread beneath the all future orogenic belt. On moving, the flows were enriched in aqueous fluids that could derive from the former BMW lenses related to subduction zones. The asthenosphere activated by this way produced structural and mineral transformations in the uppermost mantle and the lower crust that resulted in decrease of their density and correspondingly intensive tectonic uplift and mountain building in the Pliocene–Quaternary.

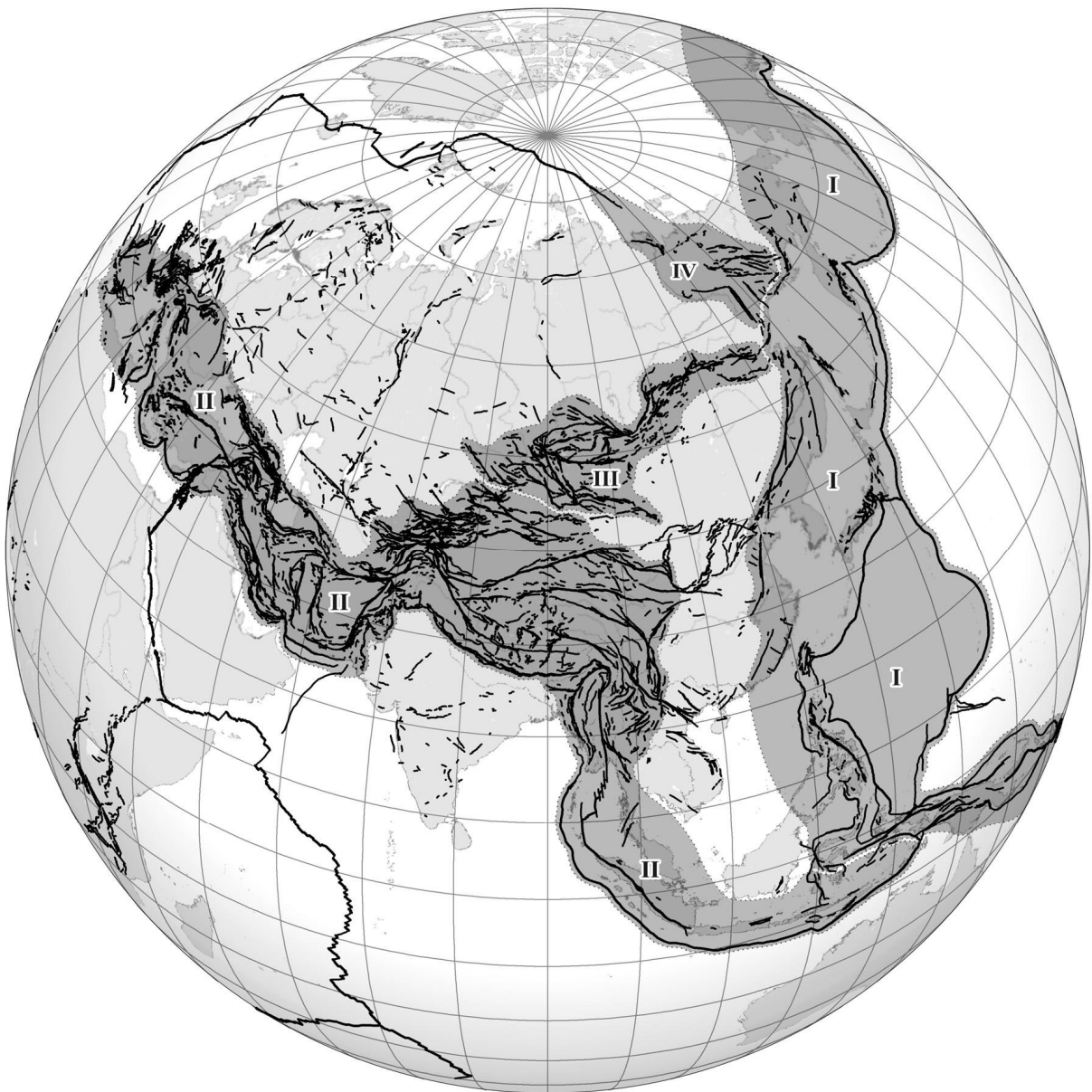


Fig. 41. Mobil belts in Eurasia with diffuse plate boundaries (grey color): I, around the Pacific; II, Alpine-Himalayan; III, Altai-Stanovoy; IV, Moma-Chersky. The largest active faults are shown

Records of intensive Pliocene–Quaternary tectonic uplifts were found in other mountain belts of the World. The neotectonic development of the Gorny Altai forming the western part of the Altai–Stanovoy Belt (Fig. 41) demonstrates some features similar to the Tien Shan development. In the Chuya Basin of the Gorny Altai, the Lower Paleogene continental silty–clayey sequence up to 30 m thick is known (Zykin, Kazansky, 1995). The Oligocene and early Miocene are composed of lacustrine and swamp sand–shale sediments with interbeds of brown coal. The alluvial sandy–gravely–pebble sediments in the marginal parts of the basin provide evidence for origination of neighboring uplifts (Devyatkin, 1965; Zykin, Kazansky, 1995, 1996). From the Middle Miocene to the Early Pliocene, the lacustrine fine clastic sand–shale sediments were deposited in the center of the basin and they were replaced with coarser clastic alluvial–deltaic deposits varying from fine-grained sand to pebbles at the basin margins (Bogachkin, 1981). In the Upper Miocene, the content of coarse clastic deposits increases in the fill of the basin (Zykin, Kazansky, 1995, 1996). The accelerated uplift of Altai over the last ~3.5 Ma has been revealed from the fission track dating (De Grave et al., 2007). At the same time, the topography of the East Baikal region became more contrasting. The molasses in the Tunka, South Baikal, and other basins became coarser, owing not only to activation of rifting, but also to growth of high mountain ridges on the place of former low mountains.

The significant rise of mountain systems in the NE Asia occurred during the last several million years (Map of neotectonics of the USSR..., 1977). Ollier (2006) summarized the data on recent tectonic uplift in different mountain system of the World and reported the Pliocene–Quaternary and rarely the Upper Miocene–Quaternary age of the dominant uplift in the western North America (the Rocky Mountains, Coast Ranges, Cascades, and adjacent areas like Basins and Ranges and Colorado Plateau), the Andes, and the western surrounding of the South Pacific. The Pliocene–Quaternary tectonic rise, sometimes reaching and even exceeding 1 km occurred in the surrounding of the East African Rift System and in some territories of the African, Arabian and Siberian platforms (Artyushkov, 1993, 2003; Partridge, 1997; Artyushkov, Hofmann, 1998). These data show that the regularities, found in the Alpine–Himalayan Belt can be global. To estimate a possibility to apply the Alpine–Himalayan model to other regions of the World, let us discuss the data on the rising, lateral and sinking strands of the global mantle convection.

Morgan (1971) introduced the term of mantle plumes. He understood them as the streams of matter and heat upwelling from the lower mantle, burning through the lithosphere and manifesting in the land surface by volcanism (hot spots). This idea

was criticized (Hamilton, 2003; Sorokhtin, 2007). Sorokhtin (2007) considered that it is incompatible with the concept of mantle convection as the source of plate motion. Nevertheless, the idea of plumes as the sources of intraplate volcanism was recognized by geologists (Kovalenko et al., 2009).

The existing geochemical data do not contain records of magma formation deeper 700 km (Ivanov, 2011). This does not prove that the material can not come to the upper mantle and the Earth's crust from the larger depths and means only that, if it comes, it loses marks of the former depth because of rebuilding. Thus, the only source of information about the lower mantle flows is the data on seismic tomography. They have helped to find not only the Ethiopian-Afar, but several other superplumes rising from the lower mantle. The largest of them is the N-trending Pacific superplume dividing in the upper part into several strands (Fig. 30). It does not reach the lithosphere, being transformed to the upper mantle lateral flows. The eastern flow extends up to the East Pacific spreading zone. The smaller superplume is identified under the Islands of Green Cape westwards of Africa (Fig. 42). It is also transformed in the upper mantle to the lateral flow that extended to the west and reaches the Mid-Atlantic spreading zone.

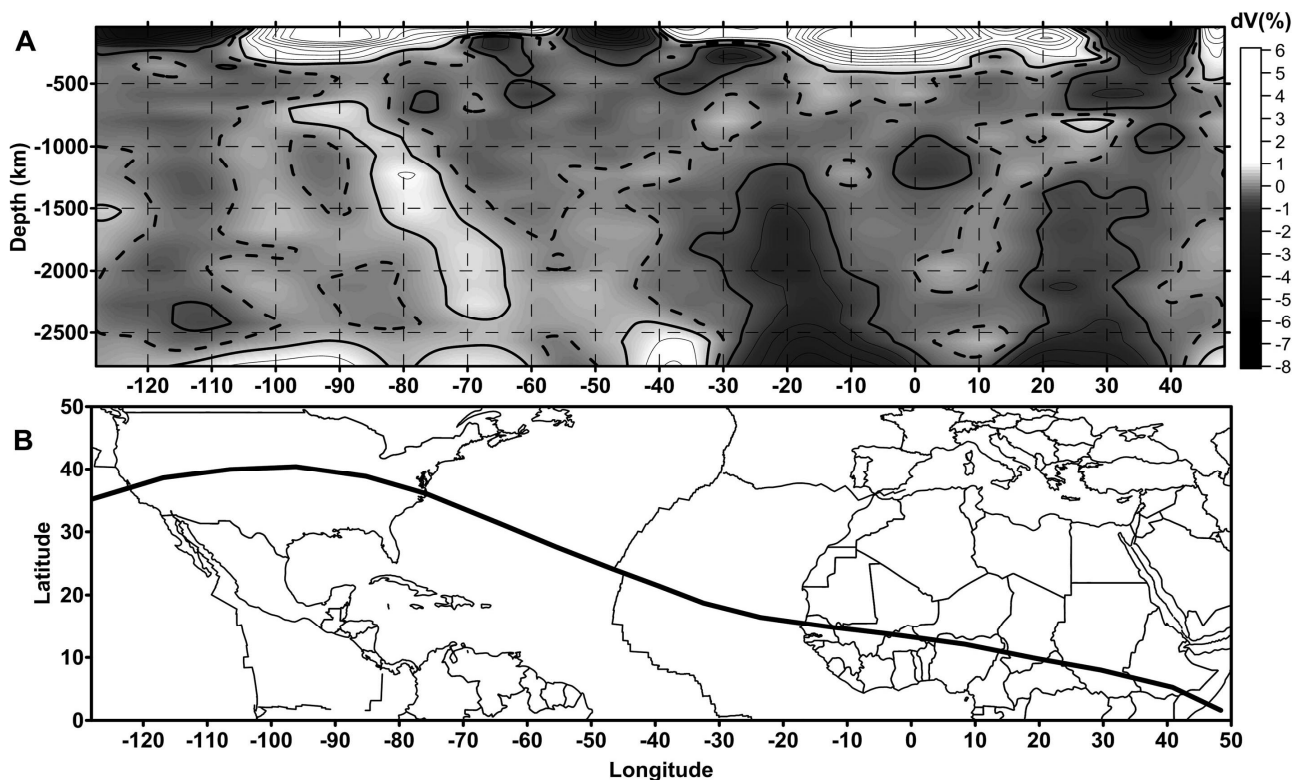


Fig. 42. Seismic tomography section (A) of dV_S through Central Africa, Atlantic Ocean and North America. The Ethiopian-Afar superplume is at the right part of the section. The plume under Cape Verde Islands is at the center; the sub-lateral flow in upper mantle propagates into Atlantic from it. The upper mantle flow beneath western part of North America propagating from Pacific superplume is at the left part of the section. The profile position is shown in (B). Compiled after the data in (Becker, Boschi, 2002; Grand et al., 1997). Contour lines are spaced at 0.5%; the dashed line corresponds to zero value

In Northern Atlantic, the similar superplume is dipped to the east and reaches the Earth's crust in the Icelandic region (Fig. 43). There have not been found some records of the through-mantle upwelling structures, except the superplumes mentioned above and several other that are expressed not so clearly in the lowered velocities of seismic waves. We consider that just the found superplumes correspond to the upwelling strands of the all-mantle convection.

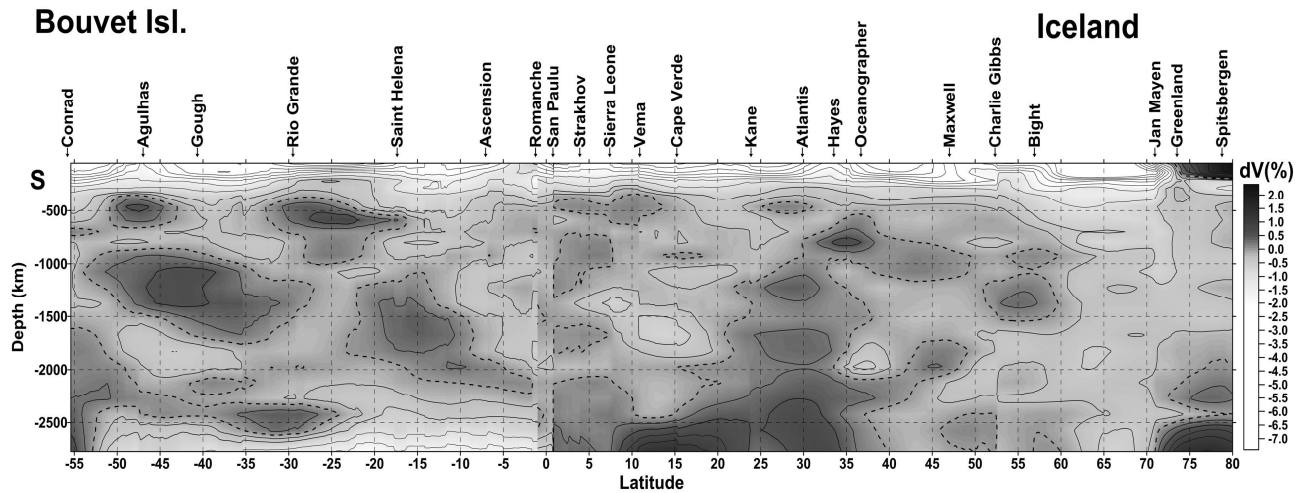


Fig. 43. Seismic tomography section of dV_S along Mid Atlantic Ridge (MAR). The Icelandic superplume is at the right part of the section. Other parts of MAR are featured by low-velocity lenses in the lower parts of lithosphere and the upper mantle. This low-velocity zone of MAR decays to the depths of 200–300 km. Compiled after the data in (Becker, Boschi, 2002; Grand et al., 1997). Contour lines are spaced at 0.5% (0.25% at values lower 1%); the dashed line corresponds to zero value

According to the seismic tomography data, the lateral upper mantle flows spread away from the superplumes. Because of viscous friction between the asthenosphere and the lithosphere, the flows move the lithosphere plates. A location of the spreading zone just above the superplume is rather an exception than a rule. Only the Icelandic superplume is identified in the profile along the Mid-Atlantic Ridge, while the “hot” areas under the other parts of the spreading system that are evident in the levels of the lithosphere and the uppermost asthenosphere, disappear at the depths lower than 200–300 km (Fig. 43). So, the spreading zones are not related exactly to the superplumes and their origin is due to the weakened zones in the heterogeneous lithosphere and to the extension of the lithosphere because of interactions of the sublithosphere flows. Formation of magmatic sources erupting the MORB in the spreading zones is the forced reaction to the uneven plate divergence and is caused by the adiabatic melting of the lithosphere and the uppermost sublithosphere mantle in the zones of the divergence concentration. So, these magmatic sources are not deep.

The majority of the studied subduction zones are completely or partly transformed into the sub-horizontal BMW. Their influence on tectonic processes can be different. The studies of BMW in the NE Asia led to the conclusion about the related upper mantle convection resulting in the mantle diapirism and intraplate volcanism (Dobretsov et al., 2001; Zhao et al., 2010; Ivanov, 2011). The convective movements of the upper mantle could produce the deformational thickening of the Earth's crust, which combined with decrease of its density by fluids from the BMW and resulted in recent uplift of mountains (Artyushkov, 2012). In the Alpine-Himalayan Belt, as it was shown in the chapter 2.2, the reworking of the fluid-enriched BMW by the upper mantle flows from the Ethiopian-Afar superplume activated the flows. Their influence decreased the density of the uppermost mantle and the lower crust that resulted in the acceleration of tectonic uplift and formation of high mountain systems. This process was the most effective in the Central Asian segment of the belt, where the lithosphere was significantly thickened by the collision deformation and enriched by relics of the former Tethyan oceanic lithosphere. In the Mediterranean part of the belt, the rise of mountain ridges combined with the subsidence of basins under influence of the mantle diapirism due to the activated upper-mantle flows. Some details in tectonics of the Alpine-Himalayan Belt can be also caused by the sublithosphere upper-mantle flows. They are the abnormal motion of the Anatolian Plate and the high volcanism in the Armenian Highland (see section 2.2.2) as well as the intracontinental mantle seismic focal zones like the Hindu Kush and Vrancea megafoci (see section 2.2.3).

Because the majority of subduction zones are transformed into the BMW, the sinking of the rest of subducted slabs into the lower mantle can hardly compensate the lithosphere accretion in the spreading zones. Probably, the sinking strands of the mantle convection are formed not only by the subducted slabs, but also by the delaminated and condensed by high metamorphism lithosphere fragments under the collision zones and old cratons. Volumes of rocks with weakly increased velocities of seismic waves under the collision zones and cratons below the transitional layer of the mantle justify a possibility of such deep subsidence (Fig. 27, 28, & 30).

Thus, we propose the global model of tectonics of mantle flows that includes completely the plate-tectonic theory and, at the same time, explains some geological phenomena that can not be satisfactory explained by the plate tectonics. According to this model, the plate moved by the upper mantle flows because of the viscous friction between them and the lithosphere. These lateral flows are parts of the all-mantle convection. Its upwelling strands correspond to the superplumes and the sinking

strands are formed not only by a part of subducted slabs, but also by some delaminated dense fragments of the lithosphere under the collision zones and old cratons. The plate tectonics are the main, but not single results of the upper mantle flows. They produce also tectonic processes that are caused by phase and mineral transformations of the crustal and mantle rocks, by formation of the BMW and related potential enrichment of the transitional layer of the mantle in aqueous fluids. The Pliocene–Quaternary intensification of tectonic uplift producing the recent mountain building is one of these processes.

The global intensive tectonic uplifts and mountain building in the Late Cenozoic might be partly due to the closure of the Tethys Ocean. At all the stages of its development, its northern (in present-day coordinates) flank had subduction zones, which compensated for spreading. The Indian Ocean, which partly took up the role of the Tethys Ocean, had no such zones all the way from Cyprus to the Andaman arc. This changed the kinematics of sublithosphere flows and the global plate balance, thus causing large-scale tectonic uplifting.

Shultz (1948, 1979) distinguished the neotectonic epoch as the specific orogenic period (period of mountain building) in the Earth's tectonic evolution. Such periods that lasted 20–40 Myrs repeated several times during the Phanerozoic (Leonov, 1976, 1980; Shultz, 1979). They took place in the Late Vendian, Early Devonian and Early Permian and occupied the regions with different previous tectonic history, overlaying the regional expressions of plate interaction.

Conclusions

The neotectonic epoch, which is characterized by tectonic uplift producing mountain building in the Alpine-Himalayan Belt, has lasted from the Oligocene to Quaternary. Detailed studies in the Central Tien Shan, the Pamirs and the Greater Caucasus and their comparison with other mountain systems of the belt show that this epoch includes two main stages. During the first stage that lasted from Oligocene till the end of Miocene and even Pliocene in some regions, local uplifts formed. They were usually not higher than the middle-level mountains (< 1500 m) and formed under collision compression as a result of isostatic compensation of thickening of the Earth's crust in zones of concentrated deformation. Because of changes in direction of maximum compression at different sub-stages of the first stage, the local uplifts formed in different tectonic zones and, as a result, occupied large territories. During the second Pliocene–Quaternary stage, the height of the mountains increased 2–3 times. This intensification of tectonic uplift producing mountain building can not be explained by effects of the collision compression. The rates of transverse shortening decrease in some regions. Even in the regions, where they increase (the Himalayas, Pamirs, Tien Shan, and some others), the increased rates could yield 20–50% of the real uplift. The remainder was provided by isostatic compensation of the decrease in the density of the lower crust and the upper mantle under two effect of the asthenosphere, which was activated by fluids. First, the tectonically delaminated lithospheric mantle including the high-metamorphosed fragments of the lower crust was partly replaced by the lower-dense asthenosphere. Second, a part of the high-metamorphosed rocks in the lower crust and near the crust-mantle boundary underwent the retrograde metamorphism under the effect of cooled asthenosphere fluids.

The analyzed seismic tomography data demonstrated two important features of the mantle under the Alpine-Himalayan Belt. First, in the eastern (Indonesian) segment of the belt, where subduction has continued till now, the higher-velocity subducted slabs become approximately horizontal at the depths of about 400–700 km and these sub-horizontal lenses spread beneath the adjacent continental upper mantle. The same continuations of the subducted slabs (stagnant slabs, or big mantle wedges, BMW) are known in the North-Western Pacific. Second, in the more western mountain part of the Alpine-Himalayan Belt, sublithosphere low-velocity (hot and lower-dense) mantle flows are identified. They begin in the Ethiopian–Afar superplume rising from the lower mantle and spread beneath the orogenic belt.

We suppose that the elongated Ethiopian-Afar superplume developed as a more or less stationary structure at least from the end of the Paleozoic. The portions of moving Gondwana, which turned out to lie above the superplume, underwent rifting that developed into spreading that formed the Tethys Ocean. Flows of heated asthenosphere material from the superplume caused the moving of torn-off fragments of Gondwana to the north-east toward Eurasia. The oceanic Tethyan lithosphere subducted there, and the Gondwanan fragments accreted to Eurasia. As a result, series of microplates, separated by sutures, accretionary wedges, and magmatic bodies related to different stages of the Tethyan evolution, formed on the place of the future mountain belt. Probably, the mountain segments of the belt had previously the same structure as the south-eastern Indonesian segment, i.e., the subducted slabs transformed there at the depths of 400–700 km into the BMW that extended beneath the future mountain belt.

Closure of the Tethys and collision of the Eurasian and Gondwanan lithosphere plates decelerated their convergence, but the hot asthenosphere flows from the Ethiopian-Afar superplume probably prolonged the former movement and gradually spread under the entire orogenic belt. On moving, the sublithosphere flows were enriched in aqueous fluids that could derive from the former BMW lenses related to subduction zones. The asthenosphere, activated in this manner or its fluids penetrated into the lithosphere and produced its softening and detachment that facilitated deformational thickening of the Earth's crust and, correspondingly, the tectonic uplift in areas of maximum compression. During the first stage, it was the single or, at least, main source of the rise. During the second stage (the last 5–2 Ma), the deformational effect was supplemented by two other processes that were initiated by the sublithosphere flows and their fluids. The first process was the partial replacing of the lithosphere mantle by the lower-dense asthenosphere material and, as a result, decrease of density of the uppermost mantle. The second process was the retrograde metamorphism and, correspondingly, decrease of density of metamorphosed rocks of the crustal origin within the lower crust and near the crust-mantle boundary with participation of the asthenosphere fluids. The both processes produced additional rise of the land surface and caused the acceleration of total uplift of the belt during the Pliocene–Quaternary.

The determining role in this model of the Alpine-Himalayan Belt evolution belongs to the sublithosphere upper mantle flows that spread away from the Ethiopian-Afar superplume. We have analyzed the neotectonic and seismic tomography data on other territories and have found similar features. Some other

orogenic belts, as the Altai-Stanovoy Belt, North-East Asia, the western North America and the western South America demonstrate acceleration of tectonic uplift in the Pliocene–Quaternary. Several superplumes and upper mantle flows, which spread away from them, were found by the analysis of seismic tomography data.

Basing on the data represented above, we propose the global model of tectonics of mantle flows. Lithosphere plates move by the sublithosphere upper mantle flows because of viscous friction in the lithosphere-asthenosphere boundary. The flows spread away from the superplumes that represent the upwelling strands of the mantle convection. As a rule, zones of the lithosphere spreading do not correspond to the superplumes. The MORB volcanism does not related to the superplumes and is a result of adiabatic melting of the uppermost asthenosphere and the lithosphere due to the extension. Because majority of the subducted slabs transforms into the BMW in the depths about 400–700 km, only a part of the subducted material penetrates into the lower mantle and is not enough to compensate a grow of the lithosphere in the spreading zones. The sinking strands of the mantle convection are represented not only by such material, but also by volumes of dense and depleted upper mantle as well as high-metamorphosed basic rocks beneath cratons and collision zones. The plate tectonic mechanism is not the only result of the upper mantle flows. It is supplemented by tectonic processes that are caused by phase and mineral transformations of the mantle and lower crustal rocks, by formation of the BMW and their fluid potential. The tectonic uplift producing mountain building is one of such processes.

Acknowledgements

T.P. Ivanova participated in preparation this book, except the authors announced in the title. Her participation is shown in the Content. The studies resulted in the book were supported by the Division of Earth Sciences of the Russian Academy of Sciences (program no. 6), the Presidium of the Russian Academy of Sciences (program no. 4), and the Russian Foundation for Basic Research (projects no. 11-05-00628-a and 14-05-00122).

References

Abdel-Rahman A.-F.-M., Nassar Ph.E., 2004. Cenozoic volcanism in the Middle East: petrogenesis of alkali basalts from northern Lebanon. *Geol. Mag.* 141, 545–563.

Abdrakhmatov K.Ye., 1988. The Quaternary tectonics of the Chu Basin. *Ilim, Frunze*, 120 p. (in Russian).

Abdrakhmatov K.Ye., Aldazhanov S.A., Hager B.H., Hamburger M.W., Herring T.A., Kalabaev K.B., Makarov V.I., Molnar P., Panasyuk S.V., Prilepin M.T., Reilinger R.E., Sadybakasov I.S., Souter B.I., Trapeznikov Yu.A., Tsurkov V.Ye., Zubovich A.V., 1996. Relatively recent construction of the Tien Shan inferred from GPS measurements of present-day crustal deformation rates. *Nature* 384, 450–453.

Abdrakhmatov K.E., Weldon R., Thompson S., Burbank D., Rubin Ch., Miller M., Molnar P., 2001. Onset, style, and current rate of shortening in the central Tien Shan (Kyrgyzstan). *Russian Geology and Geophysics* 42 (10), 1502–1526.

Aitchison J.C., Ali J.R., Davis A.M., 2007. When and where did India and Asia collide? *J. Geophys. Res.* 112 (B05423), 1–19.

Aleshinskaya Z.V., Voskresenskaya T.N., Kulikov O.A., Faustov S.S., 1972. Stratigraphic position of the Sharpyldak Formation (from paleomagnetic data). *Vestnik of Moscow State University, ser. 5, Geophysics*, 106–107 (in Russian).

Alici P., Temel A., Gourgaud A., Vidal Ph., Nyazi Gundoglu M., 2001. Quaternary tholeiitic to alkaline volcanism in the Karasu valley, Dead Sea rift zone, southeast Turkey: Sr-Nd-Pb-O isotopic and trace-element approaches to crust-mantle interaction. *Intern. Geol. Rev.* 43, 120–138.

Almeida G.A.F., 2010. Structural history of the Red Sea Rift. *Geotectonics* 44 (3), 271–282.

Alpine history of the Great Caucasus / Leonov Yu.G. (Ed.), 2007. *GEOS, Moscow*, 368 p. (in Russian).

Altherr R., Henjes-Kunst F., Baumann A., 1990. Asthenosphere versus lithosphere as possible sources for basaltic magmas erupted during formation of the Red Sea: constraints from Sr, Pb and Nd isotopes. *Earth Planet. Sci. Lett.* 96, 269–286.

Arger J., Mitchell J., Westaway R., 2000. Neogene and Quaternary volcanism of southeastern Turkey. In: Bozkurt E., Winchester J.A., Piper J.D.A. (Eds.) *Tectonics and magmatism in Turkey and the surrounding area. Geol. Soc. London Spec. Publ.* 173, pp. 459–487.

Artemjev M.E., 1975. Isostasy of the USSR territory. Nauka, Moscow, 215 p. (in Russian).

Artemjev M.E., Kaban M.K., 1994. Density inhomogeneities, isostasy and flexural rigidity of the lithosphere in the Transcaspian region. *Tectonophysics* 240, 281–297.

Artyushkov E.V., 1968. Gravitational convection within the Earth's interior. *Izvestiya of Academy of Sciences of the USSR. Physics of the Earth*, No. 9, 3–18 (In Russian).

Artyushkov E.V., 1993. *Physical tectonics*. Nauka, Moscow, 456 p. (in Russian).

Artyushkov E.V., 2003. Abrupt continental lithosphere weakening as a precondition for fast and large-scale tectonic movements. *Geotectonics* 37 (2), 107–123.

Artyushkov E.V., 2012. Neotectonic crustal uplifts as a consequence of mantle fluid infiltration into the lithosphere. *Russian Geology and Geophysics* 53 (6), 738–760.

Artyushkov E.V., Baer M.A., Mörner N.-A., 1996. The East Carpathians: Indications of phase transitions, lithospheric failure and decoupled evolution of thrust belt and its foreland. *Tectonophysics* 262, 101–132.

Artyushkov E.V., Hofmann A., 1998. The Neotectonic crustal uplift on the continents and its possible mechanisms. The case of Southern Africa. *Surv. Geophys.* 15, 515–544.

Bachmanov D.M., 2001. Age zoning of coarse molasses in the Outer Zagros and migration of the recent orogeny. *Geotectonics* 35 (6), 505–509.

Bachmanov D.M., Trifonov V.G., Mikolaychuk, A.V., Vishnyakov, F.A., Zarshchikov, A.A., 2008. Minkush-Kökömeren zone of recent transpression in the Middle Tien Shan. *Geotectonics* 42 (3), 186–205.

Bachmanov D.M., Trifonov V.G., Mikolaychuk, A.V., Dodonov, A.E., Zarshchikov, A.A., Vishnyakov, F.A., 2009. Neotectonic evolution of the Central Tien Shan by the data on structure of Late Cenozoic basins. In: *Geodynamics of intra-continental orogens and geo-ecological problems*. Scientific Station of the RAS, Bishkek, pp. 12–19 (in Russian).

Baker J.A., Mensies M.A., Thirlwall M.F., MacPherson C.G., 1997. Petrogenesis of Quaternary intraplate volcanism, Sana'a, Yemen: implications for plume-lithosphere interaction and polybaric melt hybridization. *J. Petrol.* 36, 1359–1390.

Barazangi M., Seber D., Chaimov T., Best J., Litak R.D., Sawaf T., 1993. Tectonic evolution of the northern Arabian plate in western Syria. In: Boschi, E., Mantovani, E., Morelli, A. (Eds.) Recent evolution and seismicity of the Mediterranean region. Kluwer Acad. Publ., Dordrecht, pp. 117–140.

Barberi F., Capaldi G., Gasperini P., Marinelli G., Santacroce R., Scandone R., Treuil M., Valet J., 1979. Recent basaltic volcanism of Jordan and its implications on the geodynamic history of the Dead Sea shear zone. *Acc. Naz. Lincei. Atti dei Convegni* 47, 667–683.

Bazhenov M.L., Burtman V.S., 1990. Structural arcs of the Alpine belt: Carpathians – Caucasus – Pamirs. Nauka, Moscow, 167 p. (in Russian).

Bazhenov M.L., Mikolaichuk A.V., 2002. Paleomagnetism of Paleogene basalts from the Tien Shan, Kyrgyzstan: rigid Eurasia and dipole geomagnetic field. *Earth Planet. Sci. Lett.* 195, 155–166.

Becker Ya.A., 1996. Tectonics of the Afgan-Tajik Basin. *Geotectonics* 30 (1), 64–70.

Becker T.W., Boschi L. A comparison of tomographic and geodynamic mantle models // *Geochemistry Geophysics Geosystems* G^3 , 2002, v. 3 (January 10), Paper number 2001GC000168, <http://www.geophysics.harvard.edu/geodyn/tomography/>.

Ben-Avraham Z., Ginzburg A., Markis J., Eppelbaum L., 2002. Crustal structure of the Levant Basin, eastern Mediterranean. *Tectonophysics* 346, 23–43.

Ben-Gai Y., Ben-Avraham Z., Buchbinder B., Kendall C.G.St.C., 2004. Post-Messinian evolution of the Southeastern Levant margin based on stratigraphic modelling. *Proc. of the 5th Intern. Sympos. on Eastern Mediterranean Geology. Thessaloniki*, pp. 32–34.

Bertrand H., Chazot G., Blichert-Toft J., Thorat S., 2003. Implications of widespread high- μ volcanism on the Arabian Plate for Afar mantle plume and lithosphere composition. *Chem. Geol.* 198, 47–61.

Bogachkin B.M., 1981. History of Tectonic Evolution of the Gorni Altai in Cenozoic. Nauka, Moscow, 131 p. (in Russian).

Bogachkin B.M., Korzhenkov A.M., Mamyrov E., Nechaev Yu.V., Omuraliev M., Petrosyan A.E., Pletnev K.G., Rogozhin E.A., Charimov T.A., 1997. The structure of the focus of the 1992 Susamur earthquake (from analysis of its geological and seismological manifestations). *Physics of the Solid Earth*, No. 11, 3–18 (in Russian).

Bogatikov O.A., Gurbanov A.G., Melekestsev I.V., Sulerzhitsky L.D., Sobisevich L.E., Katov D.M., Kopaev A.V., Lyashenko O.V., Puriga A.I., 1998. Problems of the Elbrus Volcano activity. In: Global changes of environment and climate. Siberian Branch of the RAS, Sci. Centre of the Joint Inst. of Geology, Geophysics and Mineralogy, Novosibirsk, pp.153–164 (in Russian).

Briem E., 1989. Die morphologische und tectonische Entwicklung des Rotem Meer Grabens. *Z. Geomorph. N.F.* 33, 458–498.

Bubnov S.N., Goltsman Yu.V., Pokrovsky B.G., 1995. The Sr, Nd and O isotope systems as indicators of origin and evolution of primary melts of the recent lavas of the Elbrus volcanic area in the Greater Caucasus. XIV Sympos. on geochemistry of isotopes. Institute of Geochemistry of the RAS, Moscow, pp. 28–29.

Budanova K.T., Budanov V.I., 1983. Metamagmatic formations of the South-Western Pamirs. Donish, Dushanbe, 276 p. (in Russian).

Bullen M.E., Burbank D.W., Garver J.I., Abdrakhmatov K.Ye., 2001. Late Cenozoic tectonic evolution of the northwestern Tien Shan: new age estimates for the initiation of mountain building. *Bull. Geol. Soc. Amer.* 113 (12), 1544.

Burtman V.S., 1999. Relationships between the Pamirs and the Tien Shan in Cretaceous and Cenozoic. In: *Geodynamics of the Lithosphere*. Nauka, Moscow, pp. 144–178 (in Russian).

Burtman V.S., 2006. Tien Shan and High Asia. Tectonics and geodynamics in the Paleozoic. GEOS, Moscow, 216 p. (in Russian).

Burtman V.S., 2012. Geodynamics of Tibet, Tarim, and the Tien Shan in the Late Cenozoic. *Geotectonics* 46 (3), 185–211.

Burtman V.S., Molnar P., 1990. Geological and geophysical evidence for deep subduction of continental crust beneath the Pamir. *Geol. Soc. Amer. Special paper* 281, Boulder, 76 p.

Burtman V.S., Samygin S.G., 2001. Tectonic evolution of High Asia in the Paleozoic and Mesozoic. *Geotectonics* 35 (4), 276–294.

Camp V.E., Roobol M.J., 1989. The Arabian continental alkali basalt province. *Geol. Soc. Amer. Bull.* 101, 71–95.

Camp V.E., Roobol M.J., 1992. Upwelling asthenosphere beneath western Arabia and its regional implication. *J. Geophys. Res.* 97, 15255–15271.

Çapan U.Z., Vidal Ph., Cantagrel J.M., 1987. K-Ar, Nd, Sr and Pb isotopic study of Quaternary volcanism in Karasu Valley (Hatav), N-end of Dead-Sea Rift zone in SE Turkey. *Verbilimleri* 14, 165–178.

Chediya O.K., 1986. Morphostructures and recent tectogenesis of the Tien Shan. *Ilim, Frunze*, 315 p. (in Russian).

Chediya O.K., Utkina N.G., 1975. The principle of determination of regional lateral compression in epiplatformal orogens. In: *Structural geomorphology of highlands*. Nauka, Moscow, pp. 73–83 (in Russian).

Chediya O.K., Yazovsky V.M., Fortuna A.B., 1973. Stratigraphic subdivision of the Kyrgyz red-colored complex in the Chu Basin and its mountain framing. In: *Regularities of geological evolution of the Tien Shan in the Cenozoic*. Ilim, Frunze, pp. 26–52.

Chekunov A.V. (Ed.), 1993. *Geophysical studies of the lithosphere*. Naukova Dumka, Kiev (in Russian).

Chorowicz J., Dhont D., Ammar O., Rukieh M., Bilal A., 2004. Tectonics of the Pliocene Homs basalts (Syria) and implications for the Dead Sea Fault Zone activity. *J. Geol. Soc. London* 161, 1–13.

Christiansen N.I., Mooney W.D., 1995. Seismic velocity structure of the continental crust: a global view. *J. Geophys. Res.* 100, 9761–9788.

Creager K.C., Jordan T.H., 1984. Slab penetration into the lower mantle. *J. Geophys. Res.* 89 (B5), 3031–3049.

Debaille E., Leveque J.-J., Cara M., 2001. Seismic evidence for a deeply rooted low-velocity anomaly in the upper mantle beneath the northeastern Afro/Arabian continent. *Earth Planet. Sci. Lett.* 193, 423–436.

DeCelles P.G., Quade J., Kapp P., Fan M., Dettman D.L., Ding L., 2007. High and dry in central Tibet during the Late Oligocene. *Earth Planet Sci. Lett.* 253, 389–401.

De Grave J., Buslov M.M., Van der Haute H., 2007. Distant effects of India–Eurasia convergence and Mesozoic intracontinental deformation in Central Asia: Constraints from apatite fission-track thermochronology. *J. Asian Earth Sci.* 29, 188–204.

Demir T., Westaway R., Bridgland D., Pringle M., Yurtmen S., Beck A., Rowbotham G., 2007. Ar-Ar dating of Late Cenozoic basaltic volcanism in northern

Syria: Implications for the history of incision by the River Euphrates and uplift of the northern Arabian Platform. *Tectonics* 26. TC 3012, doi:10.1029/2006TC001959.

Deng Qidong, 2000. *Seismotectonics of Tien Shan*, 400 p. (in Chinese).

Desio A., 1976. Some geotectonic problems of the Kashmir Himalaya–Karakorum–Hindu Kush–Pamir area. In: *Geotectonica delle zone orogeniche del Kashmir Himalaya–Karakorum–Hindu Kush–Pamir*. Accademia Nazionale del Lincei, Roma, pp. 115–129.

Devyatkin E.V., 1965. *Cenozoic Sedimentary Rocks and Neotectonics of the Southeastern Altai*. Nauka, Moscow, 242 p. (in Russian)

Dickinson W.R., Hatherton T., 1967. Andesitic volcanism and seismicity around the Pacific. *Science* 157, 801–803.

Ding Guoyu, 1984. Active faults in China. In: *A collection of papers of Intern. Sympos. on continental seismicity and earthquake prediction*. Seismol. Press, Beijing, pp. 225–242.

Dmitriyeva E.L., Nesmeyanov S.A., 1982. *Mammals and stratigraphy of Tertiary continental deposits in south-eastern Middle Asia*. Nauka, Moscow, 140 p. (in Russian).

Dobretsov N.L., Kirdyashkin A.G., Kirdyashkin A.A., 2001. *Deep geodynamics*. Publ. of Siberian Branch of Russian Academy of Sciences, GEO Branch, Novosibirsk, 408 p. (in Russian).

Dodonov A.E., 2002. *Quaternary of Middle Asia. Stratigraphy, correlation, paleogeography*. GEOS, Moscow, 250 p. (in Russian).

Dodonov A.E., Trifonov V.G., Ivanova T.P., Kuznetsov V.Yu., Maksimov F.E., Bachmanov D.M., Sadchikova T.A., Simakova A.N., Minini H., Al-Kafri A.-M., Ali O, 2008. Late Quaternary marine terraces in the Mediterranean coastal area of Syria: Geochronology and neotectonics. *Quaternary Intern.* 190, 158–170.

Ebinger C.J., Sleep N.S., 1998. Cenozoic magmatism throughout east Africa resulting from impact of a single plume. *Nature* 395 (22), 788–791.

Ershov A.V., Nikishin A.M., 2004. Recent Geodynamics of the Caucasus–Arabia–East Africa Region. *Geotectonics* 38 (2), 123–136.

Forsyth D., Uyeda S., 1975. On the relative importance of the driving forces of plate tectonics. *Geophys J. Roy. Astron. Soc.* 43, 163–200.

Fukao Y., Widiyantoro S., Obayashi M., 2001. Stagnant slabs in the upper and lower mantle transition region. *Rev. Geophys.* 39, 291–323.

Gaetani M., 1997. The Karakorum Block in Central Asia, from Ordovician to Cretaceous. *Sedimentary Geology* 109, 339–359.

Gamkrelidze P.D., Gamkrelidze I.P., 1977. Tectonic nappes in the southern slope of the Greater Caucasus. *Proc. of the Geological Inst. of Acad. of Sci. of Georgia, new ser.* 57. Metsniereba, Tbilisi, 181 p. (in Russian).

Gansser A., 1964. *Geology of the Himalayas*. Interscience, London.

Gansser A., 1966. The Indian Ocean and Himalayas: a geological interpretation. *Eclogae geol. helv.* 59 (2), 831–848.

Garfunkel Z., 1989. Tectonic setting of Phanerozoic magmatism in Israel. *Isr. J. Earth Sci.* 38, 51–74.

Garfunkel Z., 1998. Constrains on the origin and history of the Eastern Mediterranean basin // *Tectonophysics* 298, 5–35.

Garfunkel Z., Ben-Avraham Z., 2001. Basins along the Dead Sea Transform // P.A. Ziegler, W. Cavazza, A.H.F. Robertson and S. Crasquin-Soleau (eds.) *Peri-Tethys Memoir 6: Peri-Tethyan Rift/Wrench Basins and Passive Margins*. *Memoires du Museum national d'Histoire naturelle* 186, pp. 607–627.

Geological Map of Kyrgyzstan, scale 1:500000, 1982. Ministry of geology of the USSR, Moscow.

Geological Map of Syria. Scales 1:200 000 and 1:500 000, 1964 / V. Poncarov (Ed.) Damascus: Technoexport, Moscow; Ministry of Industry of the S.A.R.

Geological Map of Tadjik S.S.R. and surrounding territories. Scale 1:500000, 1989. VSEGEI, Leningrad.

Geology and Mineral Resources of Afghanistan. Book 1: Geology / Dronov V.I. (Ed.), 1980. Nedra, Moscow, 535 p. (in Russian).

Giannérini G., Campredon R., Feraud G., Abou Zakhem B., 1988. Deformations intraplaques et volcanisme associe: Exemple de la bordure NW da plaque Arabique au Cenozoique // *Bull. Soc. géol France*. No. 6. P. 938–947.

Golonka J., 2004. Plate tectonic evolution of the southern margin of Eurasia in the Mesozoic and Cenozoic. *Tectonophysics* 381, 235–273.

Gomez F., Khawlie M., Tabet C., Darkal A.N., Khair K., Barazangi M., 2006. Late Cenozoic uplift along the northern Dead Sea transform in Lebanon and Syria. *Earth Planet. Sci. Lett.* 241, 913–931.

Gordon R.G., 1998. The plate tectonic approximation: Plate nonrigidity, diffuse plate boundaries, and global plate reconstructions. *Annu. Rev. Earth Planet. Sci.* 26, 615–642.

Grand S.P., van der Hilst R.D., Widiyantoro S., 1997. Global seismic tomography: A snapshot of convection in the Earth. *GSA Today* 7, 1–7.

Green D.H., Hibberson W.O., Kovács I., Rosenthal A., 2010. Water and its influence on the lithosphere-asthenosphere boundary. *Nature* 467. DOI: 10.1038/nature09369.

Grekov I.I., Korsakov S.G., Kompaniets M.A., Lavrishchev V.A., Pis'mennyi A.N., Semenukha I.N., 2008. Geoelectric model of the Earth's crust of the Russian sector of the Greater Caucasus. In: *General and regional problems of tectonics and geodynamics 1*. GEOS, Moscow, pp. 239–244 (in Russian).

Guillot S., Replumaz A., Hattori K.H., Strzeczynski P., 2007. Initial geometry of western Himalaya and ultrahigh-pressure metamorphic evolution. *J. Asian Earth Sci.* 30, 557–564.

Guseva T.V., Lukk A.A., Trapeznikov Yu.A., Shevchenko V.I., 1993. Light range finder measurements in the Harm geodynamic test site. *Doklady of the Academy of Sciences* 330 (4), 476–479.

Hamilton W.B., 2003. An alternative Earth. *GSA Today* 13 (11), 4–12.

Hauser F., Raileanu V., Fielitz W., Dinu C., Landes M., Bala A., Prodehl C., 2007. Seismic crustal structure between the Transylvanian Basin and the Black Sea, Romania. *Tectonophysics* 430 (1-4), 1–25.

He M., He K., 1987. The planation surface of the Yunnan Plateau and its neotectonic significance. *J. Geomorph. N. F., Suppl. Bd.* 63, 51–56.

Hirsch F., 2005. The Oligocene–Pliocene. The Late Pliocene to Quaternary. In: Krashennnikov V.A., Hall J.K., Hirsch F., Benjamini Ch., Flexer A. (Eds.) *Geological framework of the Levant, vol. II, part 4*. Historical Production-Hall, Jerusalem, pp. 459–514.

Huang J., Zhao D., 2006. High-resolution mantle tomography of China and surrounding regions. *J. Geophys. Res.* 111. B09305.

Ilani S., Harlavan Y., Taravneh K., Rabba I., Weinberger R., Ibrahim K., Peltz S., Steinitz G., 2001. New K-Ar ages of basalts from the Harrat Ash Shaam volcanic field in Jordan: implications for the span and duration of the upper-mantle upwelling beneath the western Arabian plate. *Geology* 29, 171–174.

Imamverdiev N.A., 2000. Geochemistry of the Late Cenozoic volcanic formations of the Lesser Caucasus. Nafta-Press, Baku, 192 p. (in Russian).

International Symposium on the Neogene–Quaternary boundary. Excursion Guide-Book, 1977. Nauka, Moscow, 184 p.

Isacks B.L., Oliver J., Sykes L.R., 1968. Seismology and the new global tectonics. *J. Geophys. Res.* 73, 5855–5899.

Ivanov A.V., 2011. Intracontinental basaltic volcanism (Siberian Mesozoic and Cenozoic). Abstract of Dr.Sci. Thesis. Institute of the Earth's Crust of the Siberian Branch of Russian Academy of Sciences, Irkutsk, 31 p. (in Russian).

Ivanov D.A., Bubnov S.N., Volkova V.M. et al., 1993. The Sr and Nd isotope composition of the Greater Caucasus Quaternary lavas, related to the problem of their petrogenesis. *Geochemistry*, No. 3, 343–353 (in Russian).

Ivanova T.P., Trifonov V.G., 2005. Neotectonics and mantle earthquakes in the Pamir–Hindu Kush region. *Geotectonics* 39 (1), 56–68.

Izzeldin A.Y., 1987. Seismic, gravity and magnetic surveys in the central part of the Red Sea: their interpretation and implications for the structure and evolution of the Red Sea. *Tectonophysics* 143, 269–306.

Jacobsen S.D., Demouchy S., Frost J.D., Ballaran T.B., Kung J., 2005. A systematic study of OH in hydrous wadsleite from polarized FTIR spectroscopy and single-crystal X-ray diffraction: Oxygen sites for hydrogen storage in Earth's interior. *Amer. Mineral.* 90 (1), 67–70.

Jiménez-Munt I., Fernández M., Vergés J., Platt J.P., 2008. Lithosphere structure underneath the Tibetan Plateau inferred from elevation, gravity and geoid anomalies. *Earth Planet. Sci. Lett.* 267, 276–289.

Kaban M.K., 2000. Gravitational model of the lithosphere and geodynamics. In: Neotectonics, geodynamics and seismicity of the Northern Eurasia. Inst. Physics of the Earth of the RAS and GEON, Moscow, pp. 267–290 (in Russian).

Karakhanian A., Djrbashian R., Trifonov V., Philip H., Arakelian S., Avagyan A., 2002. Holocene-historical volcanism and active faults as natural risk factor for Armenia and adjacent countries. *J. Volcanol. Geotherm. Res.* 113 (1-2), 319–344.

Karakhanian A.S., Trifonov V.G., Azizbekian O.G., Hondkarian D.G., 1997. Relationship of late Quaternary tectonics and volcanism in the Khanarassar active fault zone, the Armenian Upland. *Terra Nova* 9, 131–134.

Karnik V., 1968. Seismicity of the European area. Acad. publ. house of the Czechosl. Acad. of Sci., Prague, Pt I. 364 p.; Pt II. 218 p.

Karyakin Yu.V., 1989. Geodynamics of formation of volcanic complexes in the Lesser Caucasus. Nauka, Moscow, 152 p. (in Russian).

Kazakov O.V., Vasilyeva E.V., 1992. Geological structure of deep basins of the Mediterranean. Nedra, Moscow, 188 p. (in Russian).

Kazmin V.G., 1974. On certain specific features of riftogenesis (as exemplified by the evolution of the Red Sea, Aden and Ethiopian rifts). *Geotectonics*, 8(6), 3–14 (in Russian).

Kazmin V.G., Lobkovsky L.I., Tikhonova N.F., 2010. Late Cretaceous–Paleogene deepwater basin of North Afganistan and the Central Pamirs: Issue of Hindu Kush earthquakes. *Geotectonics* 44 (2), 127–138.

Kelbert, A., Schultz, A., Egbert, G., 2009. Global electromagnetic induction constraints on transition-zone water content variations. *Nature* 469, 1003–1006.

Khain V.E., 2001. Tectonics of continents and oceans. Nauchnyi Mir, Moscow, 606 p. (in Russian).

Khamrabaev I.Kh., 1980. Structure of the Earth's crust in the Western Pamirs according to the complex geological-geophysical data along the Harm–Kalaikhumb–Khorog–Ishkashim profile. *Uzbek Geological Journal*, No. 5, 47–51 (in Russian).

Klaeschen D., Vidal N., Kopf A.J., von Huene R., Krashenninnikov V.A., 2005. Reflection seismic processing and images of the Eastern Mediterranean from cruise 5 of the research vessel “Akademik Nikolaj Strakhov”. In: Hall J.K., Krashenninnikov V.A., Hirsch F., Benjamini Ch., Flexer A. (Eds.) *Geological Framework of the Levant. Vol. II: the Levantine Basin and Israel. Part III: The Levantine Basin. Historical Production-Hall*, Jerusalem, pp. 21–40.

Knipper A.L., Savelyev A.A., Rukieh M., 1988. Ophiolite association of Northwestern Syria. *Geotectonics* 22 (1), 73–82.

Kondorskaya N.V., Shebalin N.V. (Eds.), 1982. New catalog of strong earthquakes in the USSR from ancient times through 1977. Boulder, CO: World Data Center A for Solid Earth Geophysics, NOAA.

Kondorskaya N.V., Ulomov V.I. (Eds.), 1999. Special catalogue of earthquakes of the Northern Eurasia (SECNE). Zurich, Switzerland: Global Seismic Hazard Assessment Program, <http://www.seismo.ethz.ch/gshap/neurasia/nordasiacat.txt>

Kopp M.L., 1997. Lateral escape structures in the Alpine-Himalayan collision belt. Nauchnyi Mir, Moscow, 314 p. (in Russian).

Kopp M.L., Scherba I.G., 1993. Relationships of tectonic and eustatic factors in development of the Cenozoic basins of the northern Mediterranean belt. Bull. of the Moscow society of researchers of the nature. Geol. series 68 (6), 15–31 (in Russian).

Koronovsky N.V., Demina L.I., 1996. Model of collision volcanism in the Caucasus segment of the Alpine belt. Doklady of the RAS 350 (4), 519–522 (in Russian).

Koronovsky N.V., Demina L.I., 1999. Collision stage of the evolution of the Caucasian sector of the Alpine Foldbelt: Geodynamics and magmatism. Geotectonics 33 (2), 102–118.

Koronovsky N.V., Demina L.I., 2007. Late Cenozoic volcanism of the Greater Caucasus. In: Alpine history of the Great Caucasus. GEOS, Moscow, pp. 251–284 (in Russian).

Kovács I., Szabo Cs., 2008. Middle Miocene volcanism in the vicinity of the Middle Hungarian zone: Evidence for an inherited enriched mantle source. J. Geodynamics 45, 1–17.

Kovalenko V.I., Yarmolyuk V.V., Bogatikov O.A., 2009. Geodynamic setting of recent volcanism in North Eurasia. Geotectonics 43 (5), 337–357.

Kozhurin A.I., 2004. Active faulting at the Eurasian, North American and Pacific plates junction. Tectonophysics 380, 273–285.

Krasnopevtseva G.V., 1984. Deep structure of the Caucasus seismically active region. Nauka, Moscow, 109 p. (in Russian).

Krestnikov V.N., Belousov T.P., Ermilin V.I., Chigarev N.V., Shtange D.V., 1979. The Quaternary tectonics of the Pamirs and Tien Shan. Nauka, Moscow, 116 p. (in Russian).

Krylov A.Yu., 1960. The absolute age of rocks of the Central Tien Shan and application of the Ar method to metamorphic and sedimentary rocks / Proceedings of the 21st IGC. Rubl. of Academy of Sciences of the USSR, Moscow, 222–244 (in Russian).

Krylov K.A., Silantyev S.A., Krashennnikov V.A., 2005. The tectonic structure and evolution of South-Western and Central Cyprus. In: Krashennnikov V.A., Hall J.K., Hirsch F., Benjamini Ch., Flexer A. (Eds.) Geological framework of the Levant. Vol. I: Cyprus and Syria. Part I: South-Western Cyprus. Historical Production-Hall, Jerusalem, pp. 135–164.

Kurenkov S.A., 1983. Tectonics of ophiolite complexes of the Southern Tien Shan (Alai and Atbashi Ridges). Nauka, Moscow, 96 p. (in Russian).

Lawrence J.F., Wysession M.E., 2006. Seismic evidence for subduction transported water in the Lower Mantle / S.V. Jacobsen, S. van der Lee (eds.) Earth deep water cycle. Geophys. Monograph Series 168, pp. 251–261.

Leonov M.G., 1975. Wild flysch of the Alpine region. Nauka, Moscow, 149 p. (in Russian).

Leonov Yu.G., 1976. Tectonic nature of the Devonian orogenesis. Nedra, Moscow, 192 p. (in Russian).

Leonov Yu.G., 1980. Global orogenic events: orogenic periods and tectogenesis epochs. In: Problems of global correlation of geological events. Nauka, Moscow, pp. 33–71 (in Russian).

Leonov Yu.G., Antipov M.P., Volozh Yu. A., Zverev V.P., Kopp M.L., Kostikova I.A., Lavrushin Yu.A., 1998. Geological aspects of the problem of fluctuations of the Caspian Sea level. In: Global changes of natural environment / Dobretsov N.L., Kovalenko B.I. (Eds.). Siberian Branch of the RAS, Novosibirsk, pp. 30–57 (in Russian).

Leonov Yu.G., Nikonov A.A., 1988. Problems of neotectonic development of the Pamir–Tien Shan mountain system. *Geotectonics* 22 (2), 108–119.

Leonov Yu.G., Sigachev S.P., 1984. Tectonic layering of the Bartang paraautochthon (Central Pamirs). *Geotectonics* 18 (2), 68–75 (in Russian).

Letnikov F.A., 1986. Maturity of lithospheric blocks and endogenic mineralization. In: Deep conditions of endogenic ore formation. Nauka, Moscow, pp. 16–24 (in Russian).

Letnikov F.A., 1988. Petrology and fluid regime of the continental lithosphere. *Nauka, Novosibirsk*, pp. 165–171 (in Russian).

Letnikov F.A., 2001. Ultradeep fluid Systems of the Earth and Problems of Ore Formation. *Geology of ore deposits* 43 (4), 259–273.

Letnikov F.A., 2003₁. Magma-forming fluid systems of continental lithosphere. *Russian Geology and Geophysics* 44 (12), 1219–1225.

Letnikov F.A., 2003₂. The nature of deep-seated granite-forming fluid systems. *Doklady of Russian Academy of Sciences, Earth Sci.* 391 (2), 760–762.

Letnikov F.A., 2006. Fluid regime of endogenic processes and ore formation. *Russian Geology and Geophysics* 47 (12), 1296–1307.

Li Jijun, Shi Yafeng, Li Bungyuan, 1995. Uplift of the Qinghai-Xizang (Tibet) Plateau and global change. *Univ. Press, Lanzhou*, 168 p.

Li Zhiwei, Roeker S., Li Zhihai, Wei Bin, Wang Haitao, Schelochkov G., Bragin V., 2009. Tomographic image of the crust and upper mantle beneath the western Tien Shan from the MANAS broadband deployment: Possible evidence for lithospheric delamination. *Tectonophysics* 477, issues 1–2 (1 November 2009), 1–102.

Lithosphere of the Tien Shan / Gubin, I.E. (Ed.), 1986. *Nauka, Moscow*, 158 p. (in Russian).

Lobkovsky L.I., 1988. Geodynamics of spreading and subduction zones and two-level plate tectonics. *Nauka, Moscow*, 250 p. (in Russian).

Lobkovsky L.I., Kotelkin V.D., 2010. Oceanic history and asymmetry of the Earth from viewpoint of thermal-chemical mantle convection. In: *Tectonics and geodynamics of Phanerozoic foldbelts and platforms*, v. 1. *GEOS, Moscow*, pp. 423–427 (in Russian).

Lomize M.G., Demina L.I., Zarshchikov A.A., 1997. The Kyrgyz-Terskei oceanic basin (Tien Shan). *Geotectonics* 31 (6).

Lukk A.A., Nersesov I.L., 1970. Deep Pamir–Hindu Kush earthquakes. In: *Earthquakes in the USSR in 1966*. *Nauka, Moscow*, pp. 118–136 (in Russian).

Lukk A.A., Vinnik L.P., 1975. Deep structure of the Pamirs: tectonic interpretation. *Geotectonics* 9 (5), 73–80 (in Russian).

Lustrino M., Sharkov E., 2006. Neogene volcanic activity of western Syria and its relationship with Arabian plate kinematics. *J. Geodyn.* 42, 115–139.

Makarov V.I., 1977. Recent tectonic structure of the Central Tien Shan. Nauka, Moscow, 172 p. (in Russian).

Makarov V.I., 1990. Recent orogens: structure and geodynamics. Abstr. of ScD Thesis. GIN of Academy of Sciences of the USSR, Moscow, 57 p. (in Russian).

Makarov V.I., Alekseev D.V., Batalev V.Yu., Bataleva E.A., Belyaev I.V., Bragin V.D., Dergunov N.T., Efimova N.N., Leonov M.G., Munirova L.M., Pavlenkin A.D., Roeker S.V., Roslov Yu.V., Pybin A.K., Schelochkov G.G., 2010. Underthrust of Tarim under the Tien Shan and deep structure of their junction zone: Main results of seismic studies on the MANAS profile (Kashgar–Sonköl). *Geotectonics* 44 (2), 102–126.

Makarov V.I., Trifonov V.G., Shchukin Yu.K., Kuchay V.K., Kulagin V.N., 1982. Tectonic layering of the lithosphere in recent mobil belts. Nauka, Moscow, 116 p. (in Russian).

Map of neotectonics of the south of the USSR, scale 1:1000000 / Polkanova L.P. (Ed.), 1971. VNIGNI, Leningrad.

Map of neotectonics of the USSR and adjacent areas. Scale 1:5000000, 1977. Ministry of geology of the USSR; Ministry of high and special secondary education of the USSR, Moscow.

Marinin A.V., Rastsvetaev L.M., 2008. Structural parageneses of North-Western Caucasus. In: Problems of tectonophysics. Inst. of Physics of the Earth, Moscow, pp. 191–224 (in Russian).

McClusky S.C., Balassanian S., Barka A.A., Ergintav S., Georgie I., Gurkan O., Hamburger M., Hurst K., Kahle H., Kastens K., Kekelidse G., King R., Kotzev V., Lenk O., Mahmout S., Mishin A., Nadaria M., Ouzounis A., Paradisissis D., Peter Y., Prilepin M., Reilinger R.E., Sanli I., Seeger H., Tealeb A., Toksöz N., Veis V., 2000. Global Positioning System constraints on plate kinematics and dynamics in the Eastern Mediterranean and Caucasus. *Jour. Geophys. Res.* 105 (B3), 5695–5719.

Mikolaichuk A.V., 2000. Structural position of thrusts in the recent orogen of the Central Tien Shan. *Russian Geology and Geophysics* 41 (7), 929–939.

Mikolaichuk A.V., Sobel E., Gubrenko M.V., Lobachenko A.N., 2003. Structural evolution of the northern margin of the Tien Shan orogen. *Izvestiya of the National Academy of Sciences of Kyrgyzstan*, No. 4, 50–58 (in Russian).

Milanovsky E.E., 1968. Neotectonics of Caucasus. Nedra, Moscow, 483 p. (in Russian).

Milanovsky E.E., Khain V.E., 1963. Geological structure of the Caucasus. Lomonosov's Univ. Press, Moscow, 358 p. (in Russian).

Milanovsky E.E., Koronovsky N.V., 1973. Orogenic Volcanism and Tectonics of the Alpine Belt of Eurasia. Nedra, Moscow, 280 p. (in Russian).

Milanovsky E.E., Rastsvetaev L.M., Kuhmazov S.U., 1989. Modern geodynamics of the Elbrus – Caucasus Mineral Waters region of the North Caucasus. In: Geodynamics of Caucasus. Nauka, Moscow, pp. 99–105 (in Russian).

Modern and Holocene volcanism in Russia / Laverov N.P. (Ed.), 2005. Nauka, Moscow, 604 p. (in Russian).

Moinfar A., Mahdavian A., Maleki E., 1994. Historical and instrumental earthquakes data collection of Iran. Iran Cultural Exhibitions Institute, Tehran, 450 p.

Molnar P., Chen W.P., 1978. Evidence for large Cenozoic crustal shortening of Asia. *Nature* 273, 218–220.

Molnar P., Dayem K.E., 2010. Major intracontinental strike-slip faults and contrasts in lithospheric strength. *Geosphere* 6 (4), 444–467; doi: 10.1130/GES00519.1.

Molnar P., Ghose S., 2000. Seismic moment of major earthquakes and the rate of shortening across the Tien Shan. *Geophys. Res. Lett.* 27, 2377–2380.

Molnar P., Rautian T.G., Khalturin V.I., 1976. Spectral composition of the Pamir–Hindu Kush earthquakes: evidence of the high mechanical Q-factor zone in the upper mantle. In: Soviet-American studies of earthquake prediction, v. 1, book I. Donish, Dushanbe-Moscow, pp. 140–158 (In Russian).

Morgan W.J., 1971. Convection plumes in the lower mantle. *Nature* 230, 42–43.

Mörner N.-A., 1991. Uplift of the Tibetan Plateau: a short review. Intern. Union for Quaternary Res. 13th Intern. Congr. Special Proc. Review reports. Beijing, pp.78–80.

Mouty M., Delaloye M., Fontignie D., Piskin O., Wagner J.J., 1992. The volcanic activity in Syria and Lebanon between Jurassic and actual. *Schweiz. Miner. Petr. Mitt.* 72, 91–105.

National Earthquake Information Center, 2010. Earthquake data base (NEIC, NOAA, PRE, PRE-Q, NEIS, Advanced national seismic system ANSS). Golden, CO: National Earthquake Information Center, U.S. Geological Survey; <http://neic.usgs.gov/>

Neotectonics and recent geodynamics of mobile belts, 1988. Nauka, Moscow, 366 p. (in Russian).

Neotectonics, recent geodynamics and seismic hazard of Syria / Trifonov V.G. (Ed.), 2012. GEOS, Moscow, 204 p.

Nesmeyanov S.A., Makarov V.I., 1974. Correlation of modern deposits of the Tien Shan. Bull. of Commission for Quaternary Studies 41, 82–98 (in Russian).

Nesmeyanov S.A., Reshetov V.Yu., Schmidt G.A., 1977. Fauna and age of the Toruaygyr mammal occurrence in Kyrgyzstan. Bull. of the Moscow society of researchers of the nature. Geol. series 52 (2), 83–86 (in Russian).

Nikishin A.M., Ziegler P.A., Panov D.I., Nazarevich B.P., Brunet M.-F., Stephenson R.A., Bolotov S.N., Korotaev M.V., Tikhomirov P.L., 2001. Mesozoic and Cenozoic evolution of the Scythian Platform–Black Sea–Caucasus domain. In: Ziegler P.A., Cavazza W., Robertson A.H.F., Crasquin-Soleau S. (Eds.) Peri-Tethys Memoir 6: Peri-Tethyan Rift/Wrench Basins and Passive Margins. Mémoires du Muséum national d'Histoire Naturelle, Paris, vol. 186, pp. 295–346.

Nikolaev N.I., 1988. Recent tectonics and geodynamics of the lithosphere. Nedra, Moscow, 491 p. (in Russian).

Nikolaev A.V., Sanina I.A., 1982. Method and results of seismic sounding of the lithosphere in Tien Shan and Pamirs. Doklady of the Academy of Sciences of the USSR 264 (1), 69–72 (in Russian).

Nikolaev A.V., Sanina I.A., Trifonov V.G., Vostrikov G.A., 1985. Structure and evolution of the Pamir–Hindu Kush region lithosphere. Physics of the Earth and planetary interior 41, 199–203.

Nikonov A.A., 1977. Recent crustal movements: geological-geomorphological and seismotectonic aspects. Nauka, Moscow, 240 p. (in Russian).

Obruchev V.A., 1948. Main features of kinematics and plasticity of neotectonics. Izvestiya of Academy of Sciences of the USSR, Geol. Series, No. 5, 13–24 (in Russian).

Ollier C.D., 2006. Mountain uplift and the Neotectonic period. Annales of Geophysics, Supplement to vol. 49 (1), 437–450.

Otani E., Zhao D., 2009. Role of water in deep processes in the upper mantle and transitional layer: dehydration of stagnant subducted plates and its implication for the great mantle wedge. Russian Geology and Geophysics 50 (12), 1375–1392.

Outline of Geology of Syria, 2000 / Leonov Yu.G. (Ed.). Nauka, Moscow, 200 p. (in Russian).

Pamirs – Himalayas: Deep-seated structure of the Earth' crust, 1982. Nauka, Moscow, 176 p. (in Russian).

Panov D.I., 1988. Structural-facial zoning of the Greater Caucasus at the Early-Alpine stage of evolution (Early and Middle Jurassic). Bull. of the Moscow society of researchers of the nature. Geol. series. 63 (1), 13–24 (in Russian).

Panov D.I., 2002. Tectonic structure of the Jurassic terrigenous complex of the Greater Caucasus: Mechanism and age of formation. In: Proc. of the North-Caucasus Technical Univ., Ser. Tectonics & Geodynamics, no. 1. Stavropol, pp. 60–70 (in Russian).

Papazachos B., Papazachou C., 1997. The earthquakes of Greece. Editions Ziti, Thessaloniki.

Partridge T.C., 1997. Late Neogene uplift in Eastern and Southern Africa. In: Tectonic uplift and climate change / Ruddiman W.F. (Ed.). Plenum Press, N.-Y., pp. 63–86.

Pashkov B.P., Budanov V.I., 1990. Tectonics of the boundary zone between South-Eastern and South-Western Pamirs. Geotectonics 24 (3).

Pashkov B.P., Budanov V.I., 2003. Tectonics of the Earlier Kimmerides of Southern Pamirs. Geotectonics 37 (1), 19–35.

Peive A.V., 1967. Faults and tectonic movements. Geotectonics, No. 5, 8–24 (in Russian).

Peive A.V., 1977. Geology today and tomorrow. Priroda, No. 6, 3–7 (in Russian).

Polat A., Kerrich R., Casey J.F., 1997. Geochemistry of Quaternary basalts erupted along the East Anatolian and Dead Sea fault zones of southern Turkey: implications for mantle sources. Lithos 40, 55–68.

Polyak B.G., Kamensky I.L., Prasolov E.M. et al., 1998. Isotopes of helium in gases of the North Caucasus: records of heat-matter flow from the mantle. Geochemistry, No. 4, 383–397 (in Russian).

Ponikarov V.P., Kazmin V.G., Mikhailov I.A., Razvalyaev A.V., Krashenninnikov V.A., Kozlov V.V., Souliidi-Kondratyev E.D., Mikhailov K.Ya., Kulakov V.V., Faradjev V.A., Mirzayev K.M., 1967. Geological Map of Syria, scale 1:500,000. Explanatory Notes. Part I. Ministry of Industry, Damascus, 230 p.

Pugin V.A., Khitarov N. I., 1978. Experimental Petrology and Deep Magmatism. Nauka, Moscow, 175 p. (in Russian).

Pushcharovsky Yu.M., Pushcharovsky D.Yu., 2010. Geology of the Earth's mantle. GEOS, Moscow, 140 p. (in Russian).

Ranalli G., Piccardo G.B., Corona-Chávez P., 2007. Softening of the subcontinental lithospheric mantle by asthenosphere melts and the continental extension/oceanic spreading transition. *Journal of Geodynamics* 43 (4-5), 450–464.

Ratschbacher L., Frisch W., Liu Guanghua, 1993. Distributed deformation in Southern and Western Tibet during and after the India–Asia collision. &th EUG Meeting Abstr. *Terra Nova* 5, Supplement to No 1, 267.

Rebinder P.A., Venstrem E.K., 1937. Effect of the medium and adsorption layers on plastic metal flow. *Izvestiya of OMEN, Phys. ser.* 4/5, 531–550 (in Russian).

Recent geodynamics of intracontinental areas of collision orogeny (Central Asia) / Laverov N.P. & Makarov V.I. (Eds.), 2005. Nauchnyi Mir, Moscow, 400 p. (in Russian).

Ringwood A.E., 1975. Composition and Petrology of the Earth's Mantle. McGraw-Hill, London, N.-Y. and Sydney, 618 p.

Robertson A.H.F., 2000. Mesozoic-Tertiary tectonic-sedimentary evolution of south Tethyan oceanic basin and its margins in southern Turkey. In: *Tectonics and magmatism in Turkey and the surrounding area*, Geol. Soc. London Spec. Publ. 173, pp. 97–138.

Robertson A., Unlüğenç Ü.C., Inan N., Taşlı K., 2004. The Misis-Andirin Complex: a Mid-Tertiary melange related to late-stage subduction of the Southern Neotethys in S. Turkey. *J. Asian Earth Sci.* 22 (5), 413–453.

Rodkin M.V., Nikitin A.N., Vasin R.N., 2009. Seismotectonic effects of solid-state transformations in geomaterials. GEOS, Moscow, 198 p. (in Russian).

Ross D.A., Uchupi E., 1977. The structure and sedimentary history of the southeastern Mediterranean Sea. *Amer. Assoc. Petrol. Geol. Bull.* 61, 872–902.

Rukieh M., Trifonov V.G., Dodonov A.E., Minini H., Ammar O., Ivanova T.P., Zaza T., Yusef A., Al-Shara M., Jobaili Y., 2005. Neotectonic Map of Syria and some aspects of Late Cenozoic evolution of the north-western boundary zone of the Arabian plate. *J. Geodyn* 40, 235–256.

Ruzhentsev S.V., 1968. Tectonic development of the Southern Pamirs and a role of horizontal movements in formation of its Alpine structure. Nauka, Moscow, 202 p. (in Russian).

Ruzhentsev S.V., 1971. Structural peculiarities and mechanism of formation of detached nappes. Nauka, Moscow, 168 p. (in Russian).

Ruzhentsev S.V., 1990. Pamirs. In: Pushcharovsky Yu.M., Trifonov V.G. (Eds.). Tectonic layering of the lithosphere and regional geological studies. Nauka, Moscow, pp. 214–225 (in Russian).

Ryabchikov I.D., 2005. Mantle magmas as a sensor of the composition of deep geospheres. *Geology of ore deposits* 47 (6), 455–468.

Sadybakasov I.S., 1972. Neotectonics of the Central Tien Shan. Ilim, Frunze, 116 p. (in Russian).

Salnikov D.I., Traskin V.Yu., 1987. The fundamentals of physical-chemical geomechanisms. In: Research into tectonic deformation. Nauka, Moscow, pp. 33–83 (in Russian).

Sandulescu M., 1984. Geotectonics of Romania. Editura Tehnica, Bucharest, 336 p.

Saroglu F., 1988. Age and offset of the North Anatolian fault. *METU Journal of pure and applied sciences* 21 (1-3), 65–79.

Sborshchikov I.M., 1988. Closure of Tethys and the tectonics of the eastern part of the Alpine Belt. *Geotectonics* 22 (3), 195–203.

Searle M.P., 1991. *Geology and tectonics of the Karakorum Mountains*. Wiley and Sons, Chichester, 358 p.

Searle M.P., 1996. Cooling history, exhumation and kinematics of the Himalaya–Karakorum–Tibet orogenic belt. In: Yin A., Harrison T.M. (Eds.) *The tectonic evolution of Asia*. Cambridge Univ. Press, Cambridge, pp. 110–137.

Segev A., 2005. Magmatic rocks. In: Krasheninnikov V.A., Hall J.K., Hirsch F., Benjamini Ch., Flexer A. (Eds.) *Geological framework of the Levant*, vol. II, part 4. Historical Production-Hall, Jerusalem, pp. 553–576.

Seismic models of the lithosphere in main geological structures of the USSR territory, 1980. Nauka, Moscow, 184 p. (in Russian).

Sharkov E.V., 2000. Mesozoic and Cenozoic volcanism. In: Leonov Yu.G. (Ed.). *Outline of Geology of Syria*. Nauka, Moscow, pp. 177–200 (in Russian).

Sharkov E.V., Chernyshev I.V., Devyatkin E.V., Dodonov A.E., Ivanenko V.V., Karpenko M.I., Leonov Yu.G., Novikov V.M., Hanna S., Khatib K., 1994. Geochronology of Late Cenozoic basalts in Western Syria. *Petrology* 2 (4), 385–394.

Sharkov E.V., Chernyshev I.V., Devyatkin E.V., Dodonov A.E., Ivanenko V.V., Karpenko M.I., Lebedev V.A., Novikov V.M., Hanna S., Khatib K., 1998. New data on the geochronology of Upper Cenozoic plateau basalts from northeastern periphery of the Red Sea rift area (Northern Syria). *Doklady (Reports) of Russian Academy of Sciences, Earth Sect.* 358 (1), 19–22.

Sharkov E.V., Snyder G.A., Taylor L.A., Laz'ko E.E., Jerde E., Hanna S., 1996. Geochemical peculiarities of the asthenosphere beneath the Arabian plate: evidence from mantle xenoliths of the Quaternary Tell-Danun volcano (Syrian-Jordan plateau, southern Syria). *Geochem. Int.* 34, 737–752.

Shaw J.E., Baker J.A., Menzies M.A., Thirlwall M.F., Ibrahim K.M., 2003. Petrogenesis of the largest intraplate volcanic field on the Arabian Plate (Jordan): a mixed lithosphere–asthenosphere source activated by lithospheric extension. *J. Petrol.* 44, 1657–1679.

Shcherba, I.G., 1993. Stages and phases of Cenozoic development of Alpine fold belt. Nauka, Moscow. 231 p. (in Russian).

Shcherba I.G., 1994. Paleogene Basin of the Caucasus. *Bull. of the Moscow society of researchers of the nature. Geol. series* 69, 71–80 (in Russian).

Shevchenko V.I., Guseva T.V., Lukk A.A., Mishin A.V., Prilepin M.T., Reilinger R.E., Hamburger M.W., Shempelev A.G., Yunga S.L., 1999. Recent geodynamics of Caucasus by the results of the GPS measurements and seismological data. *Physics of Solid Earth* 35 (9), 691–704.

Shultz S.S., 1948. Analysis of neotectonics and relief of Tien Shan. Geographgiz, Moscow, 224 p. (in Russian).

Shultz S.S., 1979. Tectonics of the Earth's crust. Nedra, Leningrad, 272 p. (in Russian).

Shvolman V.A., 1977. Tectonic Evolution of the Pamirs in the Late Cretaceous and Paleogene. Nauka, Moscow, 160 p. (in Russian).

Shvolman V.A., 1980. Mesozoic ophiolite complex in the Pamirs. *Geotectonics* 14 (6), 72–81 (in Russian).

Shvolman V.A., Pashkov B.P., 1986. The Earlier Mesozoic tectonic zonation in Central Asia. Doklady of the Academy of Sciences of the USSR 286, 951–954 (in Russian).

Sigachev S.P., 1990. Structures of tectonic “pile” in the Central Pamir and mechanism of their formation (in example of the Alpine nappe-folded ensemble of the Yasgulem Ridge). In: Tectonics of orogeny structures in Caucasus and Middle Asia. Nauka, Moscow, pp. 123–215 (in Russian).

Simonov V.A., Mikolaichuk A.V., Kovyazin S.V., Travin A.V., Buslov M.M., Sobel E.R., 2005. Meso-Cenozoic plume magmatism in the Central Tien Shan: age and physicochemical characteristics / Geodynamics and Geoecology of the Highland regions in the 21st Century. The 3rd Intern. Sympos. Scientific station of the Russian Academy of Sciences, Bishkek, 182–186 (in Russian).

Smyth J.R., 1994. A crystallographic model for hydrous wadsleyite: An ocean in the Earth’s interior? Amer. Mineral. 79, 1021–1025.

Sobel E., Mikolaichuk A.V., Jie C., Burbank D., 2000. Development of the Late Cenozoic Central Tien Shan in Kyrgyzstan and China recorded by apatite fission track thermochronology. Tectonophysics (T71D-03), AGU Fall Meeting, 15–19 Dec. 2000, F1156.

Sobolev S.V., Petrunin A., Garfunkel Z., Babeyko A.Y., 2005. Thermo-mechanical model of the Dead Sea Transform. Earth Planet. Sci. Lett. 238, 78–95.

Sokolov S.Yu., Trifonov V.G., 2012. Role of the asthenosphere in transfer and deformation of the lithosphere: The Ethiopian-Afar Superplume and the Alpine-Himalayan Belt. Geotectonics 46 (3), 171–184.

Sorokhtin O.G., 1974. Global evolution of the Earth. Nauka, Moscow, 184 p. (in Russian).

Sorokhtin O.G., 2007. Life of the Earth. Sci. Center of regular and chaotic dynamics; Inst. of computer studies, Moscow-Izhevsk, 452 p. (in Russian).

Sorokhtin O.G., Ushakov S.A., 2002. Evolution of the Earth. Moscow State Univ., Moscow, 560 p. (in Russian).

Stein M., Hofmann A.W., 1992. Fossil plume head beneath the Arabian lithosphere. Earth Planet. Sci. Lett. 114, 193–209.

Tapponnier, P., Mattauer, M., Proust, F., Cassaigneau, C., 1981. Mesozoic ophiolites, sutures, and large-scale tectonic movements in Afghanistan. *Earth Planet. Sci. Lett.* 52, 355–371.

Tatar O., Piper J.D.A., Gürsoy H., Heimann A., Koşbulut F., 2004. Neotectonic deformation in the transition zone between the Dead Sea Transform and the East Anatolian Fault Zone, southern Turkey: A paleomagnetic study of the Karasu Rift volcanism. *Tectonophysics* 385, 17–43.

Tectonic layering of the lithosphere and regional geological studies / Pushcharovsky Yu.M., Trifonov V.G. (Eds.), 1990. Nauka, Moscow, 294 p. (in Russian).

Tewari A.P., 1964. On the Upper Tertiary deposits of Ladakh Hymalayas and correlation of various geotectonic units of Ladakh with those of the Kumion-Tibet region. 22th IGC Rep., 2. New Delhi, pp. 37–58.

The Earth's crust and upper mantle of Tajikistan (from petrological evidence) / Kukhtikov M.M. (Ed.), 1981. Donish, Dushanbe, 284 p. (in Russian).

Trifonov V.G., 1978. Problems of and mechanism for the tectonic spreading of Iceland. *Modern Geology* 6 (3), 123–137.

Trifonov V.G., 1983. Late Quaternary tectonics. Nauka, Moscow, 224 p. (in Russian).

Trifonov V.G., 1987. Neotectonics and recent tectonic concepts. *Geotectonics* 21 (1), 24–37.

Trifonov V.G. 1999. Neotectonics of Eurasia. Moscow: Nauchnyi Mir. 254 p. (in Russian).

Trifonov V.G., 2012. Problems of mountain building: Alpine-Himalayan Belt. In: *Tectonophysics and actual problems of the Earth sciences 1*. Inst. of Physics of the Earth, Moscow, pp. 99–109 (in Russian).

Trifonov V.G., Artyushkov E.V., Dodonov A.E., Bachmanov D.M., Mikolaichuk A.V., Vishnyakov F.A., 2008. Pliocene-Quaternary orogeny in the Central Tien Shan. *Russian Geology and Geophysics* 49 (2), 98–112.

Trifonov V.G., Bachmanov D.M., Ali O., Dodonov A.E., Ivanova T.P., Syas'ko A.A., Kachaev A.V., Grib N.N., Imaev V.S., Ali M. and Al-Kafri A.-M., 2012. Cenozoic tectonics and evolution of the Euphrates valley in Syria. In: *Geological development of Anatolia and the Easternmost Mediterranean* / Robertson A.H.F.,

Parlak O. & Ünlügenç (eds). Geological Society, London, Special Publications v. 372; doi 10.1144/SP372.4.

Trifonov V.G., Bachmanov D.M., Simakova A.N., Trikhunkov Ya.I., Ali O., Tesakov A.S., Belyaeva E.V., Lyubin V.P., Veselovsky R.V., Al-Kafri A.-M., 2014. Dating and correlation of the Quaternary fluvial terraces in Syria, applied to tectonic deformation in the region. *Quaternary International* 328-329, 74–93.

Trifonov V.G., Dodonov A.E., Sharkov E.V., Golovin D.I., Chernyshev I.V., Lebedev V.A., Ivanova T.P., Bachmanov D.M., Rukieh M., Ammar O., Minini H., Al Kafri A.-M., Ali O., 2011. New data on the Late Cenozoic basaltic volcanism in Syria, applied to its origin. *J. Volcanol. Geotherm. Res.* 199, 177–192.

Trifonov V.G., Ivanova T.P., Bachmanov D.M., 2010. Vrancea and Hindu Kush areas of mantle earthquakes: comparative tectonic analysis. *Thessaloniki: Aristotle Univ. Sci. Annals of the School of Geology, Spec. vol. 99*, 51–56.

Trifonov V.G., Ivanova T.P., Bachmanov D.M., 2012₁. Evolution of the central part of the Alpine-Himalayan Belt in the Late Cenozoic. *Russian Geology and Geophysics* 53 (3), 289–304.

Trifonov V.G., Ivanova T.P., Bachmanov D.M., 2012₂. Recent mountain building in geodynamic evolution of the central Alpine-Himalayan Belt. *Geotectonics* 46 (5), 315–332.

Trifonov V.G., Karakhanian A.S., 2004. Geodynamics and the history of civilization. *Nauka, Moscow*, 668 p. (in Russian with extended English summary).

Trifonov V.G., Karakhanian A.S., 2008. Dynamics of the Earth and development of the society. *OGI, Moscow*, 436 p. (in Russian).

Trifonov V.G., Lyubin V.P., Belyaeva E.V., Trikhunkov Ya.I., Simakova A.N., Tesakov A.S., Velelovsky R.V., Presnyakov S.L., Bachmanov D.M., Ivanova T.P., Ozhereliev D.V., 2014. Geodynamic and paleogeographic conditions of inhabitation of the earliest hominine in Eurasia (Abarian-Caucasus region). In: *Tectonics of fold belts of Eurasia: similarity, difference, characteristics of mountain building, regional summing. Proceedings of the 46th Tectonic Conference, v. 2. GEOS, Moscow*, pp. 240–246 (in Russian).

Trifonov V.G., Lyubin V.P., Belyaeva E.V., Lebedev V.A., Trikhunkov Ya.I., Tesakov A.S., Simakova A.N., Veselovsky R.V., Latyshev A.V., Presnyakov S.L., Ivanova T.P., Ozhereliev D.V., Bachmanov D.M., Artyushkov S.E., Lyapunov S.M.,

2015. Early Pleistocene of North-West Armenia: stratigraphy, archaeology, and tectonics. *Quaternary International* (*in press*).

Trifonov V.G., Soboleva O.V., Trifonov R.V., Vostrikov G.A., 2002. Recent geodynamics of the Alpine-Himalayan collision belt. GEOS, Moscow, 225 p.

Trifonov V.G., Sokolov S.Yu., 2014. Late Cenozoic tectonic uplift producing mountain building in comparison with mantle structure in the Alpine-Himalayan Belt. *Intern. J. of Geosciences* 5, 497–518; <http://dx.doi.org/10.4236/ijg.2014.55047>.

Trifonov V.G., Trubikhin V.M., Adjamian J., Jallad Z., El Hair Yu., Ayed H., 1991. Levant fault zone in the north-western Syria. *Geotectonics* 25 (2), 145–154.

Trofimov A.K., 1973. Main stages in development of topography in the Central Asian mountains: staged topography of the Central Asian mountains and correlated sediments. In: *Geological evolution of the Tien Shan in Cenozoic*. Ilim, Frunze, pp. 98–127 (in Russian).

Trofimov A.K., Udalov N.F., Utkina N.G., Fortuna A.B., Chediya O.K., Yarovsky V.M., 1976. *Geology of Cenozoic deposits of the Chu Basin and its mountain flanking*. Nauka, Leningrad, 128 p. (in Russian).

Trubitsin V.P., 2005. Tectonics of Floating Continents. *Vestnik (Gerald) of Russian Academy of Sciences*, No. 1, 10–21 (in Russian).

Van der Hilst R.D., Widiyantoro S., Engdahl E.R., 1997. Evidence of deep mantle circulation from global tomography. *Nature* 386, 578–584.

Vine F.J., Matthews D.H., 1963. Magnetic anomalies over oceanic ridges. *Nature* 199, 947–949.

Vinnik L.P., Aleshin I.M., Kaban M.K., Kiselev S.G., Kosarev G.L., Oreshin S.I., Reigber Ch., 2006. Crust and mantle of the Tien Shan from data of receiver function tomography. *Physics of the Earth* 42 (8), 639–651.

Vinnik L.P., Lukk A.A., 1974. Lateral inhomogeneities of the upper mantle beneath Pamirs–Hindu Kush. *Izvestiya of Academy of Sciences of the USSR, Physics of the Earth*, No. 1, 9–22 (in Russian).

Vinnik L.P., Lukk A.A., Nersesov I.L., 1977. Nature of the intermediate seismic zone in the mantle of the Pamir–Hindu Kush. *Tectonophysics* 38, 9–14.

Vinnik L.P., Reigber Ch., Aleshin I.M., Kosarev G.L., Kaban M.K., Oreshin S.I., Roecker S.V., 2004. Receiver function tomography of the central Tien Shan. *Earth Planet. Sci. Lett.* 225, 131–146.

Vostrikov G.A., 1994. Interdependence of the recurrence graph characteristics on seismic flow and earthquake source parameters. GIN of the Russian Academy of Sciences, Moscow, 292 p. (in Russian).

Wang Yu, Zhang X., Jiang Ch., Wei H., Wah J., 2007. Tectonic controls on the late Miocene–Holocene volcanic eruptions of the Tengchong volcanic field along the southeastern margin of the Tibetan plateau. *J. Asian Earth Sci.* 30, 375–389.

Weinstein Y., Navon O., Altherr R., Stein M., 2006. The role of lithospheric mantle heterogeneity in the generation of Plio-Pleistocene alkali basaltic suites from NW Harrat Ash Shaam (Israel). *J. Petrol.* 47, 1017–1050.

Westaway R., 2004. Kinematic consistency between the dead Sea Fault Zone and the Neogene and Quaternary left-lateral faulting in SE Turkey. *Tectonophysics* 391 (1-4), 203–237.

Westaway R., Demir T., Seyrek A., Beck A., 2006. Kinematics of active left-lateral faulting in southeast Turkey from offset Pleistocene river gorges; Improved constraint on the rate and history of relative motion between the Turkish and Arabian plates. *J. Geol. Soc. London* 163, 149–164.

Wilson J.T., 1965. A new class of faults and their bearing on continental drift. *Nature* 207, 343–347.

Yakovlev F.L., 2006. Design of relief of the cover/basement surface, according to estimation of value of fold structure shortening. In: *Regions of active tectonogenesis in recent and old history of the Earth*, vol. 2. GEOS, Moscow, 411–415 (in Russian).

Yakovlev F.L., 2008. First variant of the 3D model of sedimentary cover structure in the North-Western Caucasus, according to the data on fold deformation field. In: *Problems of tectonophysics*. Inst. of Physics of the Earth, Moscow, pp. 335–345 (in Russian).

Yakovlev F.L., 2012. Reconstruction of the balanced structure of the eastern part of Alpine Greater Caucasus using data from quantitative analysis of linear folding – case study. *Bull. of Kamchatka Regional Association “Edu.-Sci. Center”*, *Earth Sci.* 19 (1), 191–214 (in Russian).

Yarmolyuk V.V., Bogatikov O.A., Kovalenko V.I., 2004. Late Cenozoic transcontinental structures and magmatism of the Euro-African segment of the Earth and geodynamics of its formation. *Doklady of Russian Academy of Sciences, Earth Sci.* 395 (2), 183–186.

Yilmaz V., Guner Y., Saroglu F., 1998. Geology of the Quaternary volcanic centers of the East Anatolia. *J. Volcanol. Geotherm. Res.* 85, 173–210.

Yin, A., Nie, S., Craig, P., Harrison, T.M., Ruerson, F.J., Xianglin, Q., Geng, Y., 1998. Late Cenozoic tectonic evolution of the southern Chinese Tien Shan. *Tectonics* 17 (1), 1–27.

Yudakhin F.N., 1983. Geophysical fields, deep-level structure, and seismicity of Tien Shan. *Ilim, Frunze*, 246 p. (in Russian).

Yunga S.L., Yakovlev F.L., 2000. The Pamirs-Tien Shan region. In: *Recent tectonics, geodynamics and seismicity of Northern Eurasia*. Inst. Physics of the Earth, RAS/GEON, Moscow, pp. 431–434 (in Russian).

Yürür M.T., Chorowicz J., 1998. Recent volcanism, tectonics and plate kinematics near the junction of the African, Arabian and Anatolian plates in the eastern Mediterranean. *J. Volcanol. Geotherm. Res.* 85, 1–15.

Zakharov S.A., 1958. Stratostructures of Mesozoic and Cenozoic in the Tadjik Basin. *Academy of Sciences of the Tadjik S.S.R.*, Dushanbe, 228 p. (in Russian).

Zanchi A., Crosta G.B., Darkal A.N., 2002. Paleostress analyses in NW Syria: constraints on the Cenozoic evolution of the northwestern margin of the Arabian plate. *Tectonophysics* 357, 255–278.

Zhang Qingsong, Zhou Yaofei, Lu Xiangshun, Xu Qiuliu, 1991. On the present speed of Tibetan plateau. *Intern. Union for Quaternary Res. 13th Intern. Congr. Abst.* Beijing, p. 423.

Zhao D., 2009. Multiscale seismic tomography and mantle dynamics. *Gondwana Res.* 15, 297–323.

Zhao D., Pirajno F., Dobretsov N. L., Liu L., 2010. Mantle structure and dynamics under East Russia and adjacent regions. *Russian Geology and Geophysics* 51 (9), 925–938.

Zorin Yu.A., Novoselova M.R., Turutanov E.Kh., Kozhevnikov V.M., 1990. Structure of the lithosphere of the Mongolian-Siberian mountainous province. *J. Geodyn.* 11, 327–342.

Zubovich A.V., Trapeznikov Yu.A., Bragin V.D., Mosienko O.I., Shchelochkov G.G., Rybin A.K., Batalev V.Yu., 2001. Deformation field, deep crustal structure, and spatial seismicity distribution in the Tien Shan. *Russian Geology and Geophysics* 42 (10), 1550–1557.

Zubovich A.V., Wang X., Scherba Y.G., Schelochkov G.G., Reilinger R., Reigber C., Mosienko O.I., Molnar P., Michaljow W., Makarov V.I., 2010. GPS velocity field for the Tien Shan and surrounding regions. *Tectonics* 29, 1–23. TC6014.

Zykin V.S., Kazansky A.Y., 1995. Main problems of stratigraphy and paleomagnetism of Cenozoic (Prequaternary) deposits of Chuya depression of Gorny Altai. *Russian Geology & Geophysics* 35, 75–90.

Zykin V.S., Kazansky A.Y., 1996. New data on Cenozoic deposits in the Chuya depression, Gorny Altai: stratigraphy, paleomagnetism, evolution, continental rift tectonics and evolution of sedimentary basins. Russian Academy of Sciences, Novosibirsk, pp. 74–75.